Application of the BCR Fractionation Procedure to Inform the Remediation of Contaminated Soils

Arun Kumar Mudiganti

A thesis submitted in partial fulfilment of the requirements of Sheffield Hallam University for the degree of Doctor of Philosophy

June 2004

Declaration

The work described in this thesis was carried out by the author at the Materials Research Institute and the School of Science and Mathematics, Sheffield Hallam University between October 1999 and June 2004. The author declares that this work has not been submitted for any other degree. The work is original except where acknowledged by reference.

Arun Kumar Mudiganti

Abstract

The potential of the *modified* BCR fractionation (three-step) procedure as an ecological risk assessment tool and to predict the effectiveness of various soil remediation procedures was investigated. Contaminated soil samples were collected from an Industrial Age lead smelting site. Stable isotope analysis for Pb showed that lead contamination in the soil was not due to petroleum. Data obtained from mineralogical techniques (XRD, XRF, ESEM/EDX, FT-IR) and the BCR procedure showed that contaminant metals in the soil were mainly present in reducible and oxidisable forms or associated with Fe/Mn oxyhydroxides and silicates. However, XRD analysis of the residues from each step of the sequential extraction process did not reflect these changes in concentration of the metals.

Batch extraction experiments using pH adjusted deionised water showed that approximately 50% of the total Pb in the soil was extracted in the pH ranges 2-3 and 8-10. This raised questions about the actual fractionation of Pb in the soil, as metal release in the first pH range would have been due to dissolution of calcite while in the latter it would been due to the dissolution of goethite. Batch extraction experiments using magnesium and calcium chloride solutions at pH 5 showed that a higher proportion of Pb was in an ion-exchangeable form than that predicted by the BCR procedure. Batch extractions experiments using ethanoic acid showed that more than 50% of the total lead in soils was extracted into 3M ethanoic acid solutions at pH 5.

In order to understand this phenomenon further, the molarity and pH of the ethanoic acid used in the first step of the *modified* BCR procedure were changed to 3.5M and 5 respectively, and fractionation experiments were conducted. This is a three-step procedure *customised* for the fractionation of metals in soils heavily contaminated with lead. The data suggested that a majority of the Pb in the soil samples was in an ion-exchangeable or weak-acid soluble form. The relatively high dissolution of Pb in comparison with other metals in dilute ethanoic acid at pH 5 suggested that the lead compounds in the soil would have existed as independent mineral phases. This also showed that approximately 80-100% of the metal could be potentially bioavailable and available for extractions using complexing reagents.

In order to test these predictions, phytoextraction and soil washing experiments were conducted. Phytoextraction data showed that all the essential metals were hyperaccumulated and approximately 10-15% of the total Pb in the soil was extracted from the soil. The concentration of bioaccumulated Pb was almost equal to that extracted in the first step of the modified BCR process. This showed that the modified BCR process could effectively predict the bioavailability of non-essential elements.

Soil washing data showed that approximately 70%, 60% and 90% of the total lead in the soil was extracted using citric acid, L-cysteine and EDTA (all three reagents at pH 5) respectively. XRF analysis of the residues from the extractions showed that although there were analysable changes in the concentration of lead, there were no significant changes in the concentration of sulfur and phosphorus in the soil. This provided further evidence for the observation that a majority of the lead in the soil would have existed as independent mineral phases, most likely as PbO, which is ion-exchangeable and weak acid soluble. The data also showed that the *customised* BCR

sequential extraction procedure could effectively predict the concentration of metals desorbed during soil washing. Additionally, column washing experiments using EDTA and ethanoic acid showed that the basic mineral composition of the soils does not alter under the influence of the complexing agents. These experiments also showed that the rate of metal desorption from soil surfaces is not dependent on the soil-solution contact time, rather it depends on metal speciation in soils.

Helianthus annuus plants were grown hydroponically in deionised water and phosphate free nutrient solutions spiked with $Pb(NO_3)_2$ to study the effect of soil mineralogy on biological metal uptake. The data show that a majority of the lead was hyperaccumulated in the roots of the plants as thermodynamically stable chloropyromorphite and Ca pyromorphite. Additional hydroponics experiments were conducted to study the uptake of Au by *H. annuus*. These experiments showed that Au forms nanoparticles on the surface of roots.

Acknowledgements

The author would like to thank Sheffield Hallam University and his supervisor Dr. Philip H. E. Gardiner for providing him with a PhD studentship. The author would like to acknowledge the contribution of Robert Burton, Dr. Stephen Habesch, Paul Slingsby, Dr. Brian Lewis, Stuart Creasey, Dr. Nandu Chaure, Keith Woodhouse, Julian Gillott and Paul Collins in sample preparation and instrumental analysis. The author would also like to thank Peter Styan, Jonathan Melling and Andrew Bradbury for their help. Most importantly, the author would like to thank his parents, sisters and partner Jaina for all their patience, support and understanding.

TABLE OF CONTENTS

LIST OF TABLES

LIST OF FIGURES

Chapter 1 Literature Review

1.1 Introduction

Metal mining and processing activities have rendered large tracts of land all over the world unfit for agriculture or human residence[1]. Remediation of these sites is a complex and challenging problem requiring an understanding of the means of contaminant identification, geochemistry and reduction in potentially adverse affects to human and environmental health. In addition to these technical complexities, socio-economic and legal issues have a major bearing on the approaches to dealing with contaminated sites. Most industrialised countries generally operate 'polluter pays' laws whilst identifying and prosecuting polluters[2]. These laws dictate that if there is reasonable and clear evidence against current or previous landowners or site operators, they have to pay for the restoration or remediation of the site to a standard agreed with the relevant local and environment agencies.

In the United Kingdom, contaminated land comes under the purview of Part IIA, Environment Protection Act, 1990[3]. In broad terms, this act states that a piece of land can be considered contaminated if there is a risk or a possibility of risk of 'significant harm' to human health, 'as a result of substances in, on or under the land' and is identified by the presence of three components: a source, a pathway and a receptor. This regime, which was introduced through the Contaminated Land (England) Regulations 2000 and Contaminated Land (Wales) Regulations 2001, places a duty on local authorities to inspect their areas and identify land that meets the statutory definition of contaminated land. A remediation notice may subsequently be served on appropriate persons to undertake remediation of that land. In certain circumstances, a contaminated site may be classified as a 'special site', in which case the Environment Agency becomes the enforcing authority. In situations where controlled waters are

under risk of pollution or are polluted, the Environment Agency can use powers bestowed under the Water Resources Act 1991 to serve a Works Notice on persons who knowingly permitted the pollution. These Notices are enforced through the Anti-Pollution Works Regulations 1999 SI Number.

It is important that remediation activities do not cause or aggravate pollution; therefore authorisation in the form of a Waste Management Licence (WML) or an Pollution Prevention and Control (PPC) permit is required prior to implementation of these activities (introduced as part of the Waste Management Regulations, 1994)[4]. A WML may be either in the form of a Site Licence or a Mobile Plant Licence (MPL). A Site Licence is similar to that which would be required for a landfill or a waste transfer station and can only be surrendered following the issue of a Certificate of Completion. An MPL is issued for a particular piece(s) of equipment or process(es) that are used for the treatment of certain wastes (including waste soil). The MPL stays with the operator of remediation equipment as it is moved from site to site temporarily, without the need for renewals after the completion of a project.

The Pollution Prevention and Control Regulations 2000 were made under the Pollution Prevention and Control Act 1999. The Regulations came into force on 28th September 2000 and implement the European Community (EC) Directive 96/61/EC on Integrated Pollution Prevention and Control, which was adopted by the Council of the European Union in September 1996. The Regulations apply an integrated environmental approach to the regulation of specified activities (designated as Part A or Part B activities), including some sectors of industry not previously regulated under EPA 1990 e.g., intensive farming of livestock. PPC aims to prevent waste production

and emissions to the environment, and where this is not practicable, to reduce them to acceptable levels.

The principle of 'BAT' (Best Available Technique) is used within PPC and operators must ensure that this standard is achieved at their installations. The Regulations will eventually replace Part 1 of the Environmental Protection Act 1990 (EPA 1990). The main aim of PPC is to achieve a high level of protection of the environment as a whole, by measures that are designed to prevent, or where that is not practicable, reduce emissions of pollutants to air, land and water. A PPC permit includes site-specific controls that are implemented through a site-specific Working Plan, which must be prepared and submitted to the Environment Agency. Additionally, discharges of wastewater are controlled by a discharge consent issued under the Water Resources Act 1991.

The site specific clean up standards required for the PPC permit are agreed with the Environment Agency based on the Soil Guideline Values (SGVs) calculated using the CLEA (Contaminated Land Exposure Assessment) model[3]. The CLEA model replaced earlier work published by the ICRCL (Interdepartmental Committee on the Redevelopment of Contaminated Land) in the guidance note 59/83. The CLEA package is based on human toxicology data that establish levels of unacceptable intake and human exposure based on land use, age, sex, soil and contamination type. SGVs are indicators for "intervention" either in the form of detailed risk assessment or if deemed necessary followed by remediation. They are currently only available for seven metals namely lead, selenium, copper, arsenic, chromium (VI), mercury

(inorganic) and cadmium plus two organics namely phenols and benzo(a)pyrene (representative of PAHs).

1.2 Biological Uptake of Metals from Soil

Various national and international health agencies such as the WHO, US Centre for Disease Control (CDC), International Centre for Cancer Research (IACR), the UK Department of Health have suggested threshold values for metal uptake by human beings through the oral, inhalation and the dermal routes[5]. These thresholds are calculated from experimental studies performed by treating rats, mice, hamsters and monkeys with chemicals at various concentrations and studying their biological response. The technical terminology for these values are reference doses (RfD) and reference concentrations (RfC) in the US for intake via oral and respiratory pathways, while they are called tolerable daily intake (TDI) in the UK. Both values are calculated as mg kg^{-1} body weight per day, assuming an average adult body weight of 70kg and an average daily air intake of $20m^3$. The RfDs, RfCs and TDI assume that there is a certain threshold below which the intake of certain chemicals does not pose any significant human health risks. However, carcinogenic compounds do not have any thresholds and have a potential to cause harm irrespective of their concentrations. In order to take this phenomenon into account, the US EPA uses slope factors, whereby the carcinogenic potency of a compound is calculated relative to the potency of a standard carcinogen such as arsenic. However, the UK DoH does not agree with this approach and believes that certain compounds are carcinogenic at any concentration. Consequently, it recommends the use of index dose (ID), which does not recognise background concentrations of chemicals. The published TDIs and the IDs are inputted into the CLEA model to calculate the soil SGVs for various organic and inorganic compounds.

Metals and metal ions that aid the metabolic activities of organisms are 'essential' (e.g., Na, K, Mg, Ca, Cr (III), Mn, Fe, Co, Ni, Cu, Zn and Mo) and those that inhibit metabolism are called 'toxic' (e.g., Hg^{2+}, CH_3Hg^+, Pb^{2+}, Cd^{2+}, Cr (VI))[11]. Toxic effects depend on the extent to which substances are bound to soil particles or are 'available' to cause harm[6,7]. The bioavailability of metals depends principally on the soil-solution partition coefficients (K_d), which in turn depend principally on the pH of the soil solutions and the speciation of metals on the soil surfaces[11]. The rate of biological metal uptake is mainly dependent on the speciation of the metals in soil solutions as they are distributed in the organisms by different acid-base affinities. In particular free metal concentrations (Cu^{2+}, Zn^{2+}) provide the best guide to both partitioning and bioavailability[8].

One aspect of metal toxicity, but by no means the only one, is the chemical combination of metals and ligands (Lewis acids and bases) in organisms. The cellular bases are almost exclusively sulfur, nitrogen and oxygen donor groups (including H_2O and solute bases e.g., HCO_3^{2-}, HPO_4^{2-}, and OH^-)[8]. The acids are H^+, the essential metal cations and the potentially toxic metals. Among the sulfur-seeking ('soft-soft') B-type metals are Hg, Pb and Tl, as well as the essential protein and enzyme metals Fe, Cu, and Zn. The proton, H^+, has high affinity for all S, N, and O- donors, thus the key role of pH in metal binding in organisms. Mg, Ca, Be, Al, Sn, Ge and the lanthanides are amongst the oxygen-seeking ('hard-hard') metals.

1.3 Behaviour of Metals in Soils

Partition coefficients, as discussed in the previous section, depend on the speciation of metals in soils. Speciation is the "active process of identification and quantification of different defined species forms or phases in which an element occurs in a material". It has also been called the "description of the amounts and kinds of species, forms or phases in which an element occurs in a material"[8]. The species, forms or phases are defined functionally, operationally and as specific chemical compounds or oxidation states of an element[8]. The total concentration of a metal in the soil solution is the sum of the free ion concentration, the concentration of soluble organic and inorganic metal complexes, and the concentration of metals associated with mobile colloidal material.

In situations where metals have been introduced in the environment from human activities, metals are found in five 'pools' as described by Shuman (1991)[9] –

i) dissolved in the soil solution;
ii) occupying exchange sites on inorganic soil constituents;
iii) specifically adsorbed on inorganic soil constituents;
iv) associated with insoluble organic matter;
v) precipitated as pure or mixed solids;

The aqueous fraction, and fractions that are in equilibrium with this fraction i.e. exchangeable fraction, are of primary importance when considering the migration potential of metals associated with soils. Multiphase equilibria must be considered when defining metal behaviour in soils. Metals in soil solution are subject to mass transfer out of the system by leaching to ground water, plant uptake, or volatilisation (for metals and non-metals such as Hg, Se and As). At the same time metals precipitate in chemical reactions with the soil solid phase. The concentration of metals in the soil solution, at any time, is governed by a number of interrelated

processes, including inorganic and organic complexation, oxidation-reduction reactions, precipitation/dissolution reactions, and adsorption/desorption reactions. The ability to predict the concentration of a given metal in the soil solution depends on the accuracy with which multiphase equilibria can be determined or calculated. Several geochemical models such as MINEQL+ and PHREEQC have been developed to study the speciation and multiphase equilibria of metals in the environment.

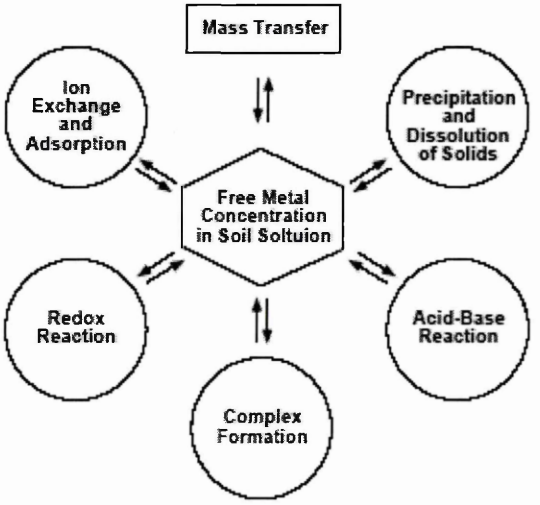

Figure 1: Factors affecting the concentration of free trace metals in soil solutions[10].

Most studies of the behaviour of metals in soils have been carried out under equilibrium conditions. Equilibrium data indicate where reactions are likely to occur under prescribed conditions, but do not indicate the time period involved. The kinetic aspects of oxidation/reduction, precipitation/dissolution, and adsorption/desorption reactions in soil matrices suffers from a lack of published data. Thus the kinetic component, which in many cases is critical to the behaviour of metals in soils, cannot be assessed easily. Without the kinetic component, the current accepted approach is to assume that local equilibrium occurs in the soil profile. Equilibrium

thermodynamics can then be applied not only to predict which precipitation/dissolution, adsorption/desorption, and/or oxidation/reduction reactions are likely to occur under a given set of conditions, but also to estimate the solution composition, i.e. metal concentration in solution, at equilibrium. This approach relies heavily on the accuracy of thermodynamic data that can be found in the literature and also obtained using models such as PHREEQC.

The conditions under which a solid-solution system attains equilibrium can be described using the Gibbs equation: $d\gamma = -RT\ \Gamma\ dC/C$; where γ is the interfacial tension, Γ is the equilibrium concentration of a single metal ion C in dilute solutions, R is the universal gas constant, T is the absolute temperature. This equation suggests that any metal ion that can reduce the interfacial tension, i.e when $d\gamma/dC$ is less than 0, there is a greater concentration of metals in the soil-solution interface than in the bulk solution. Organic solutes generally cause a reduction in the surface tension while inorganic ions cause an increase[11]. Table 1 lists the various forces that dictate the sorption process and the range at which they are effective.

Characteristic Interaction	**Range**
CHEMICAL	
Covalent	Short range
Hydrogen bond	Short range
PHYSICAL	
Ion-Ion	$1/r$
Ion-dipole	$1/r^2$
Dipole-Dipole	
(Coulombic)	$1/r^3$
(Keesom energy)	$1/r^6$
Debye-Induced Dipole	
(Debye energy)	$1/r^6$
Instantaneous Dipole-Induced Dipole	
(London dispersion energy)	$1/r^6$

Table 1: The various forces involved in sorption of metal ions from solution and the range at which they are effective, where r is the ionic radius [5].

1.4 Metal Binding on Soil Surfaces

Accurate analysis of soil-solution partitioning and multiphase equilibria can only be obtained through the analysis of metal binding to soil surfaces[12, 13]. Metal binding takes place through processes such as precipitation, adsorption, surface complexation, chemisorption and ion-exchange[14]. Metals precipitate or co-precipitate onto the soil surfaces when the soil solutions get supersaturated. The precipitation process is not selective or discerning about the nature of the soil surfaces. The mineral nature of the precipitate (crystalline or amorphous) depends on factors such as concentration and speciation of the metals in the soil solution, pH and redox potential of the soil.

When metal ions accumulate on the surface of soil minerals or in the interface between the bulk solution and soil surface, under the influence of physical or chemical forces the process is described as adsorption. Adsorption differs from precipitation in that the metal does not form a new three-dimensional solid phase but is instead associated with the surfaces of existing soil particles. There have been numerous studies of the adsorptive properties of clays and other soil minerals, in particular montmorillonite and kaolinite, and iron and manganese oxides. Jenne (1968)[15] concluded that Fe and Mn oxides are the principal soil surfaces that control the mobility of metals in soils and natural waters. In arid soils, carbonate minerals may immobilise metals by providing an adsorbing and nucleating surface[16].

Surface complexation or binding takes place due to a reduction in the surface energy of particles. This is a process that involves chelation of metals to the functional groups on soil minerals such as goethite (FeOOH), whereby metal ions replace H^+ or OH^- ions due to oxido-reduction processes[17]. Several types of surface complexes can form between a metal and soil surface functional groups and are defined by the extent

of bonding between metal ion and the surface[18]. A number of surface complexation models have been developed that utilise mass law relationships and mass and charge balance equations to describe equilibria between solution species and surface complexes. There are various theoretical descriptions for the structure of the soil-solution interface and location of the surface complexes. One of these models is the Triple Layer Model that assumes that three planes of adsorption exist within the electrical double layer and that the charge at each plane results from the surface complexation of ionic solutes[8].

This model can be visualised three dimensionally as two concentric spheres (inner and outer) of charges surrounding a soil particle. Metal ions are believed to undergo either inner sphere or outer sphere reactions, depending on the affinity of these ions for the surface. Metals in a diffuse ion association or in an outer sphere complex are surrounded by waters of hydration and are not directly bonded to the soil surface. These ions accumulate at the interface of the charged surfaces in response to electrostatic forces. These reactions are rapid and reversible with only a weak dependence on the electronic configuration of the surface group and the adsorbed ion. These two metal-surface interactions have also been called ion exchange reactions because the introduction of other cations into the system, in sufficient concentration causes the replacement or exchange of the original cations. Metals associated with exchange sites may, depending on the environment, be relatively mobile. Exchangeable metals may be the most significant reserve of potentially mobile metals in the soil.

With inner sphere complexation, the metal is bound directly to the soil surface; no waters of hydration are involved. It is distinguished from the exchangeable state by having ionic and/or covalent character to the binding between the metal and the surface. A much higher bonding energy is involved than in the exchange reactions, and the bonding depends on the electronic configuration of both the surface group and the metal. This adsorption mechanism is often termed specific adsorption. The term specific implies that there are differences in the energy of adsorption among cations, such that other ions including major cations, Na, Ca, Mg, do not effectively compete for specific surface sites. Specifically adsorbed metal cations are relatively immobile and unaffected by high concentrations of the major cations due to large differences in their energies of adsorption. Specific adsorption occurs at low concentration of metals in soil solutions. These adsorbed metals are not removed by the input of major cations. With increasing concentration of the metal, the specific sites become saturated and the exchange sites are filled[19]. Metals associated with these non-specific sites are exchangeable with other metal cations and are thus potentially mobile[20].

The most abundant surface functional group involved in surface complexation reactions on oxide surfaces and clay minerals is the hydroxyl group, which is amphoteric and extremely reactive. It is the reactivity of such sites that induces strong pH dependence for sorption of metal ions by mineral surfaces. For example, in the presence of water, the Fe ions located at the surface of an oxide complete their ligand shell with hydroxyl ions so that the surface becomes completely hydroxylated. At the hydroxylated surface or hydrated surface, positive or negative charge is created by an adsorption or desorption of H^+ or OH^-, resulting in a surface potential. Since,

surface charge and surface potential varies with the concentration of H^+ and OH^- ions, they are termed potential determining ions (PDI)[5].

For all pH dependent charged surfaces, whether organic or inorganic, as the pH decreases, the number of negatively charged sites diminishes. Under more acidic conditions, the majority of pH dependent surfaces will be positively charged and under more alkaline conditions, the majority of sites will be negatively charged. The pH at which the net variable charge on the surface is zero is called the *point of zero charge* (PZC)[21]. At the PZC an excess of positive or negative surface charge is balanced by an equivalent amount of anions (A^-) or cations (C^+), respectively, located in the outer part of the electrical double layer. The pH of the PZC of Fe oxides ranges between 7 and 9 without any marked difference between the various mineral forms. An exception to this variable charge phenomena are three layered clays such as montmorillonites and illites, which have a permanent net negative charge due to isomorphic substitution of Al^{3+} for Si^{4+} in the tetrahedral layers and/or substitution of Mg^{2+}, Fe^{2+} for Al^{3+} in the octahedral layers of aluminosilicate clays[6]. This permanent charge arises from the association and dissociation of protons from surface functional groups.

The structural charge developed on either a surface with a permanent charge or a pH dependent charged surface must be balanced by ions of opposite charge at or near the surface. This charge balance is achieved by the acquisition of a cation or anion by ion exchange. Ion exchange can be broadly defined as the 'replacement of one adsorbed, readily exchanged ion by another'[8]. The 'ion exchange capacity of a soil is the number of moles of adsorbed ion charge that can be desorbed from unit mass of soil,

under given conditions of temperature, pressure, soil-solution composition, and soil-solution mass ratio'. The measurement of ion exchange capacity (cation or anion exchange capacity) usually involves the replacement of (native) readily exchangeable ions by a 'standard' cation or anion.

An alternative model of variable-charge surfaces can be proposed in which ions are assumed to adsorb at discrete sites[10]. Charge development on oxide surfaces is then described as chemisorption of an acid, HX, or base, MOH. For example, the adsorption of $CaCl_2$ can be treated as the adsorption of $Ca(OH)_2$ and HCl. For multivalent ion adsorption, however, surface bonding alters surface charge and consequently there is a shift in the PZC. This shift could result from the generation of positive surface charge by the adsorption of positively charged species (e.g., $Mg(OH)_2^0$), or from the greater basicity of adsorbed Mg-OH relative to Fe-OH groups. In effect, the introduction of chemisorbing cations into solution will appear to increase the acidity of the mineral surface, lowering the pH of PZC. Similarly, the addition of anions to solution is expected to have an exactly opposite effect. The chemisorption of ions such a Cu^{2+}, Mg^{2+} and PO_4^{3-} occurs on oxide surfaces by direct coordination to surface groups. In effect, these ions become part of the surface, adsorbing in a non-reversible, largely non-exchangeable manner. They become the potential determining ions (PDI) in addition to H^+ and OH^-. Since they cannot be displaced from the surface by electrolytes such as KNO_3, chemisorbed cations and anions increase the positive and negative surface charges respectively.

1.5 Sorption Isotherms

A sorption isotherm is a mathematical representation of the relationship between the amount of metal sorbed and the equilibrium concentration of the metal (or more correctly, the activity of the free metal) in the soil solution[6]. The simplest and most straightforward isotherm is the Linear isotherm, which says that the accumulation of solutes on the surface of soil particles is directly proportional to the concentration of solutes in solution at a particular constant temperature. This isotherm can be described by the equation $q_e = K_D C_e$, where K_D is the partition coefficient, q_e is the concentration of the solute in solution; C_e is the concentration of the solute on the surface of soils. C_e is expressed as mass per unit mass of soil minerals while q_e is expressed as mass per unit volume of solution. For metals, however, the relationship is seldom linear and other equations with two or more coefficients must be used to describe the data[6].

The equations that are frequently used to describe the curvilinear sorption behaviour of metals in soil are the Langmuir and Freundlich equations[6]. The Langmuir model is a non-linear isotherm which assumes that (i) adsorption is constant and independent of surface coverage; (ii) adsorption occurs only on localised sites, with no interaction between adsorbate molecules; and (iii) adsorption is ultimately limited by the formation of a monomolecular layer of solute on the soil particle surfaces. These conditions are not typically met with metals sorption on soils. The mathematical form of the Langmuir equation is: $\frac{C}{S} = \frac{C}{M} + \frac{1}{Mb}$; where C is the concentration or activity of the free metal in solution; S is the quantity of the metal sorbed by the soil (i.e., mg kg^{-1} soil), M is the maximum sorption capacity of the soil, and b is the

coefficient related to bonding energy. When *C/S* is plotted as a function of *C*, the slope is reciprocal of the sorption capacity, *M*, and the intercept is *1/Mb*.

Another non-linear isotherm that describes metal sorption onto heterogeneous soil surfaces is the Freundlich Isotherm[5]. This model assumes that the surface is comprised of a continuous series of sites, each of which obeys the Langmuir model but has different and constant adsorption energy. The mathematical form of the isotherm can be written as $q = K_d C^{1/n}$; where K_d is the soil-solution partition coefficient, C is the equilibrium concentration of an ion in solution and n is a joint measure of the energies associated with a particular adsorption reaction. Several authors[22,23] have reported non-linear behaviour of metals in soils when using Langmuir and Freundlich equations. This non-linear behaviour has been interpreted to indicate multiple sites of sorption that have different energies of retention. The mechanisms at low concentrations have been attributed to specific adsorption, whereas the mechanisms at higher concentrations have been considered to be exchange reactions or precipitations. Both the Langmuir and Freundlich isotherm expressions have proven valuable in interpreting metal behaviour in soils. These equations were, however developed for modelling gas adsorption on solids. The sorption of metals by soil violates many of the assumptions associated with these equations. Also, it is impossible in a soil system to distinguish between adsorption and precipitation reactions. Adsorption isotherm equations should not be used to indicate adsorption mechanisms without collaborative evidence, but they can be used for an empirical description of the data.

1.6 Procedures Used to Study Metal Fractionation in Soils

As discussed previously, total heavy metal content in soils alone is not a good measure of bioavailability and not a very useful risk assessment tool. The mobility and bioavailability, and hence potential toxicity, of a heavy metal in soil depends on its concentration in soil solution, the nature of its association with other soluble ionic species, and the soil's ability to release the heavy metal from the solid phase to replenish that removed from the plants i.e. for accurate risk assessments[24, 25]. This data can then be subsequently used for the design of effective remediation techniques. A number of models such as MINEQL+ are available to predict the solution phase speciation of heavy metals. The distribution of heavy metals among soil components (solid phase fractionation) is important for assessing the soils potential to supply sufficient micronutrients for plant growth and to retain toxic quantities of heavy metals.

Numerous batch and sequential extraction procedures have been developed for metal fractionation studies. These procedures describe the distribution of metals among the various physico-chemical phases through the application of phase-selective chemical extractions involving multiple extracting agents[26]. The reagents that are commonly used for these procedures are weak acids or bases with good complexing and/or ion exchange capacity. Examples are ethanoic acid, hydroxylamine hydrochloride, citric acid, ammonium ethanoate, EDTA, DTPA and calcium chloride[27,28]. While the extraction procedures cannot be used to identify the actual form of a given metal in soil, they are useful in categorising the metals into several operationally defined geochemical fractions, such as exchangeable, specifically adsorbed, and metals associated with carbonates, organic matter, and/or iron and manganese oxides.

In theory, mild extractants, such as salt solutions, are more likely to extract metals that could be released to the soil solution with input of water than metals associated with stronger binding mechanisms, such as specifically adsorbed or precipitated metals. The Toxicity Characteristic Leaching Procedure (TCLP)[29] is a single extraction procedure, using 0.1M ethanoic acid, developed to simulate the leaching a waste might undergo if disposed of in a municipal landfill. This method is frequently used to determine the leaching potential of cationic metals in landfill situations where, due to microbial degradation of the waste under anaerobic conditions, ethanoic acid is produced. While this procedure is appropriate for demonstrating whether an excavated metal contaminated soil is defined as hazardous for disposal at a landfill, its application for evaluating the mobility of metals under field conditions has been questioned (ref). Production of ethanoic acid does not commonly occur in soils. In certain soil-waste systems, leaching tests using ethanoic acid may be appropriate, but it is not universally representative of the leaching solution for soil-waste systems.

One of the most commonly used sequential extraction procedures is the one developed by Tessier et al.[30], using which metals can be separated into five different fractions – ion-exchangeable, acid soluble, reducible, oxidisable and residual components respectively. The ion-exchangeable fractions can be extracted using acid-base salt solutions such as $MgCl_2$ solutions at pH 7. The acid soluble (generally ethanoic acid) fractions are metals associated with carbonates, clays such as kaolinite and Fe/Mn oxyhydroxides. The reducible fractions consist of metals associated with amorphous or polycrystalline Fe/Mn oxides and can be released using reagents such as hydroxylamine, oxalic acid and dithionite. The oxidisable fractions are metals complexed with humic and fulvic acids and can be released using oxidising agents

such as hydrogen peroxide and sodium hypochlorite. The residual fractions are metals that are trapped in the crystal lattices of clay minerals and silicates and can be extracted using strong acids such as HF, $HClO_4$, HCl, HNO_3 and aqua-regia. Due to several drawbacks associated with the Tessier procedure and its variants, it has not been universally accepted as a standard procedure for fractionation studies[14]. The major areas of concern have been sampling/preservation procedures[31], chemical properties of the target element and sample chemical composition[32], little specificity for the solid phase attacked[33], lack of reference standards for quality control[34], and lack of standardised procedures[35,36]. Although sampling techniques and extraction routines can be standardised to some degree, results from sequential extraction procedures may vary widely in complex matrices such as soils and sediments. Lack of specificity of extractants can result in the mobilisation of elements other than those associated with the mineral fractions of interest.

Tessier et al.[30] presuppose that sequential extraction procedures will conceptually work under ideal equilibrium conditions. However, soils are seldom in equilibrium[29] and consequently, the assumption of equilibrium is often a convenient excuse for simplifying an experimental design, which is typically the case for sequential extraction procedures. As a result, the problem of readsorption of metals has not been addressed satisfactorily by any of the schemes. Metals extracted by one reagent are immediately readsorbed to remaining solid substrates, decreasing the apparent amount of metal extracted in each stage. The readsorbed metals are then released by subsequent stages, leading to an overestimation in those stages[37]. Kheboian and Bauer[38] applied the Tessier method to an artificially spiked soil and found that carbonate bound Pb was significantly readsorbed to iron oxides and oxide bound Cu

to residual silicates, while sulphide-bound Zn was prematurely extracted in the oxide fraction. Rendell et al.[39] found that readsorption of spiked Cu, Pb and Cd in sediments was significant using a variety of extractants and concluded that metals in solution may not adequately represent metals in the fractions attacked. Tipping et al.[40] showed that a hydroxylamine/HNO_3 extraction solution resulted in Pb dissociating from manganese oxides, but the system pH allowed readsorption onto iron oxides in the same matrix. Readsorption problems are exacerbated in sequential extraction schemes due to the lack of specificity of reagents to individual target soil fractions. Roger[41] studied two sequential extraction schemes and concluded that the sequences generally shifted the metals extracted to the residual phase as metals are successively mobilised and readsorbed by the extractions. This results in a tendency to underestimate more mobile forms of metal and to overestimate metals in the more immobile residual phase.

In order to overcome some of these problems, the European Community Standards, Measurement and Testing Programme (formerly BCR) have developed an extraction protocol[13]. This is a three-step procedure that differentiates between (i) 'acid extractable' (0.11M ethanoic acid), (ii) 'reducible' (0.1M hydroxylamine hydrochloride acidified to pH 2.0 with nitric acid), and (iii) 'oxidisable' (1.0M ammonium acetate extraction after oxidation by 8.8M hydrogen peroxide) soil fractions. This protocol emerged out of several years of work and has the advantage of being simpler to perform and to reproduce, as a result of which it is better suited for standardisation. Certified reference soils of known composition can be used to gauge analytical accuracy and completeness of extraction, and to this end, a reference sediment (CRM 601) certified for BCR-extractable contents of selected metals is now

available from the European Commission. Further work is being performed at the BCR for the certification of a reference soil material CRM 483 and more research needs to be performed to justify the use of this procedure for widespread application due to the particular peculiarities of soil matrices[14, 42]. Although the BCR procedure is simpler when compared with other procedures, rigorous validation of extraction results remains difficult. Raksasataya et al.[43] determined that the redistribution of metals was a major problem for the BCR procedure too. However, Ho et al.[44] determined radiochemically that the extent of readsorption in the BCR procedure is less than previously suspected and does not invalidate the results obtained using this method.

1.7 Speciation of Metals in Soil Solutions

Metals species in the soil solutions exist either as free (uncomplexed) metal ions (e.g., Cd^{2+}, Zn^{2+}, Cr^{3+}) in various soluble complexes with inorganic or organic ligands (e.g., $CdSO_4^0$, $ZnCl^+$, $CdCl_3^-$), or associated with mobile inorganic or organic colloidal material[45]. Common inorganic ligands are SO_4^{2-}, Cl^-, OH^-, PO_4^{3-}, NO_3^- and CO_3^{2-}. Soil organic ligands include low molecular weight aliphatic, aromatic, and amino acids and soluble constituents of fulvic acids. Formation constants for various metal complexes are available in the literature[46]. Organic complexation of metals in soil is not as well defined as inorganic complexation because of the difficulty of identifying a large number of organic ligands that may be present in soils. The presence of complex species in the soil solution can significantly affect the transport of metals through the soil matrix relative to the free metal ion. With complexation, the resulting metal species may be positively or negatively charged or be electrically neutral (e.g. $CdCl_3^-$, $CdCl^+$, $CdCl_2^0$). The metal complex may be only weakly adsorbed or more strongly adsorbed to soil surfaces relative to the free metal ion. The free metal ion is,

in general, the most bioavailable and toxic form of the metal. Several elements of environmental concern exist in soils in more than one oxidation state: As(V) and As(III), Se(VI) and Se(IV), Cr(VI) and Cr(III), Hg(II) and Hg(I). The oxidation state of these metals determines their relative mobility, bioavailability and toxicity. For example, hexavalent Cr is relatively mobile in soils, being only weakly sorbed by soils. Hexavalent Cr is also extremely toxic and a known carcinogen. Trivalent Cr, on the other hand, is relatively immobile in soil, being strongly sorbed by soils and readily forming insoluble precipitates, and it is of low toxicity.

Atomic absorption spectrophotometers (AA) and inductively coupled plasma emission spectrometers (ICP) are commonly used to determine the metal concentration in soil solutions. Both techniques measure the total metal concentration in the solution without distinguishing metal speciation or oxidation state. Free metal, complexed metal ion concentrations and concentration of metals in different oxidation states can be determined using ion selective electrodes, polarography, colorimetric procedures, gas chromatography-ICP-AES, and high performance liquid chromatography-ICP-AES[47]. While these methods are necessary for accurate measurements of metal speciation and oxidation state, commercial laboratories do not routinely perform these methods. Metal concentrations determined by AA or ICP are often used as inputs into thermodynamic computer programs such as MINEQL+. Output consists of an estimation of the concentration of free metals and complexed metals at equilibrium for the specified conditions.

1.8 Desorption of Contaminants from Soil Surfaces

Although adsorption and desorption together establish an adsorption equilibrium, desorption has received relatively little experimental attention. Chemical desorption from soil and sediment is of central importance to most environmental concerns. Desorption affects chemical fate, toxicity, and associated risks to human and aquatic life as well as the efficiency of most remediation technologies. Desorption is commonly modelled as a reversible partition process in fate, risk and remediation models[48]. However, the process of metal sorption to soil surfaces is seldom reversible. Numerous laboratory experiments have demonstrated that sorption of organic and inorganic compounds is not a fully reversible process (i.e. sorption and desorption often exhibit hysteresis)[49]. Hysteresis is a phenomenon that may be observed during desorption studies, wherein the adsorption and desorption curves may not be analogues. Assuming the adsorption pattern is linear and uniform with respect to the concentration of ions in solution and solid, desorption pattern may be logarithmic and non-uniform. The contaminants that show hysteresis may be more tightly held during desorption than during adsorption (or K_d during desorption is larger than K_d during adsorption i.e. it is not in equilibrium)[10]. Lack of reversibility of sorption results in a failure to predict the long-term release of contaminants to the environment. Even with the application of some of the most advanced remediation technologies (physically, chemically, and/or biologically enhanced), it is often observed that a small fraction of the sorbed contaminant remains in the soil or sediment. Knowledge and prediction of desorption is necessary for designing more effective remediation schemes. If it could be shown that pollutants would not be released from soils and sediments in any significant concentrations (i.e for risk assessment), either abiotically or via biological means, they would be of little

practical concern and could be safely left in place. As a result, the impact on remediation costs would be enormous.

In addition to irreversible adsorption, several other mechanisms have also been proposed to explain the observed incomplete desorption. For several classes of organic and inorganic compounds, chemisorption prevents the release of chemicals from sediments and soils[50]. Heterogeneous adsorption sites with varied release of chemicals have been postulated to explain the continuous release of chemicals, whereby a fraction of the chemical is assumed to adsorb to sites with high adsorption energy or specificity. Heterogeneous adsorption isotherms often deviate significantly from linearity.

The other common phenomenon noticed during column washing experiments that causes deviations from ideality is physical non-equilibrium. When contaminants in a column packed with soil are washed with a solution containing chemicals, different concentrations in a cross-section of the column arise when the flow sweeps the solutes past stagnant zones. When diffusion into the stagnant zone is unable to equalise concentration gradients introduced by advective flow, the process is said to be in physical non-equilibrium. It may happen in column experiments when flow velocity is high and not all pores are penetrated with equal speed, and also in batch experiments when homogenisation is inadequate and time for the chemical to reach all the pores has been too short. Physical non-equilibrium is thus a result of immobile water that exists in dead-end pores or micropores in aggregated parts of the soil[10].

1.9 Remediation Techniques

The objective of any soil remediation project is to remove the source-pathway-receptor link, as identified by a suitable risk assessment procedure. This can be achieved either through source removal, installation of a barrier between the source and the receptor, or in extreme cases relocation of the receptor[51]. Under the Part II A regime (Environment Protection Act 1990, UK), having established the appropriate persons for remediating of a contaminated site, the relevant enforcing authorities must serve notice of these facts to the owner or occupier of the land and any other appropriate person(s). The enforcing authority cannot then take any further action for three months, unless there is imminent danger of harm or pollution being caused[23]. During this period the appropriate person may seek to convince the authority that he will undertake the work voluntarily; or he may seek to demonstrate it would not be reasonable to serve a remediation notice, given the costs and potential harm involved. Failing such actions by the end of the period, the enforcing authority will then serve a remediation notice, specifying the work required, and the date by which it should be completed. Failure to comply with such a notice is a criminal offence, punishable by daily fines as long as the work remains outstanding. Alternatively, the enforcing authority can undertake the work itself and reclaim the costs from the person on whom the notice was served.

The procedure of choice principally depends on the prevailing legislative guidance and the directives provided by the Environment Agency. The various contaminated soil treatment techniques and indicative costs are set out in Table 2. In addition to these direct remediation costs, there may also be indirect expenditure such as the cost of site specific method statement design and related discussions as required by the Client and the local Environment Agency, the costs of applying for a WML, MPL and

the cost of geotechnical site surveys before and after the use of a remediation procedure[4, 23]. Additionally, depending on the extent of contamination, the geology of the area, extra costs are incurred for example for continuous groundwater monitoring for several years after the completion of the remediation activities at the site. Additional costs are more often than not incurred whilst conducting ecological surveys at a site, which are part of a planning application for a site redevelopment. Rare species of birds, bats, newts, owls, snakes, deer and fowl have to be protected under the Wildlife Conservation Act, 1981. In situations where there is a good likelihood of the breeding and feeding grounds of these animals being disturbed, alternative sanctuaries have to be provided or constructed. These costs are generally included in a project tender notice and generally paid for by the polluter or the appointed client representative.

Treatment Technique	Application	Indicative Cost
Off-site Removal	Can be used for most contaminants depending on the consent conditions of the ultimate disposal route.	
Landfill	The most common treatment of contaminated land, but may simply shift the problem to another location.	£6-£32/tonne, with 'special waste' being at the more expensive end. (N.B. exempt from landfill tax, if remediation is voluntary).
Incineration		£150-£1500/tonne
Vitrification		£150-£300/tonne
Destructive Treatments	Either on or off-site. Do not remove all contaminants and difficult to predict effects accurately.	
Biological methods	Suitable for organic contaminants and treatment of excavated material.	£10-£70/tonne
Chemical methods (including stabilisation/solidification)	Used to treat excavated material and a wide range of organic and inorganic contaminants.	£40-£100/tonne
Physical methods such as vacuum extraction.	Used for a wide range of organic and inorganic contaminants. Vacuum extraction removes in situ low molecular weight contaminants.	£1000,000-£200,000/hectare
Barrier Methods	Physically seal in the contaminated material. Prone to failure, so restored site will have limited end uses. Can be used for a wide variety of contaminants, but long term effects of some, such as acids and organic solvents, on barrier permeability is yet to be fully assessed.	
Cover systems		Landscaped clay: £15-£25/m^2; granular sub-bases: £12-£20/m^2; costs are dependent on the final use and may be up to £100/m^2.
Vertical Barriers	Cost effective where a natural horizontal seal such as clay exists at a shallow depth (<12m).	Related to overall size and depth. A slurry wall vertical barrier 0.6m thick to a depth of 8m would cost about £55/m^2.

Table 2: Methods and costs of treatment of contaminated land

The so called 'dig and dump' methods that involve the removal of source by excavation followed by disposal in a licensed landfill have been and continue to be the cheapest form of remediation for metal contaminated soils[52]. The excavated areas are generally lined with a geotechnical impermeable membrane followed by backfilling with topsoil or engineering fill depending on the intended end-use of the site. This procedure is currently cheap because of the relatively large number of landfill sites (approximately 250) in the United Kingdom.

The European Landfill Regulations 2000 that is due to come into force in July 2004, outlaw the disposal of contaminated material to landfill without pre-treatment[53]. In addition, the regulations will result in the closure of all but a couple of dozen licensed landfill sites. Consequently, the cost of disposal of contaminated soils to landfill sites is expected to be prohibitively expensive[54]. In situations where the local environmental authorities are amenable to the idea and where the contamination is limited to a few hot spots, clean soil can be imported and mixed with contaminated soil (soil mixing), resulting in a reduction of the average concentration of the soil to regulatory levels. This is a high-risk solution because of potential contaminant mobilisation due to changes in soil conditions such as pH, redox potential, species transformation etc., which increases the likelihood of prosecution of individuals or organisations under the 'polluter pays' laws.

As a result of these problems associated with landfilling and soil mixing, industrialists and researchers are looking at large scale applications of proven physico-chemical and biological techniques that can be applied in-situ, ex-situ or on-site.

1.10 Electrokinetic Techniques

A potentially cheap and effective technique for the removal of metals from soil surfaces and pores is electrokinetic remediation. This procedure involves the application of a low level dc current (which depends on the soil type) across a soil cross-section to desorb metals from soil surfaces. The basic principle of this procedure is that the surface of a soil particle is separated from the viscous solution by an imaginary elastic layer known as the shear or slipping plane (the electric potential across this plane is known as zeta potential). Electric potential is applied using inert electrodes, generally made of graphite, activated titanium and ceramic, across the shear or the slipping plane[55]. Electrolysis of water produces hydrogen ions in the anode compartment that causes an acid front to migrate through the soil cell, resulting in the desorption of metals from soil surfaces. The zeta potential of soil particles under standard conditions is negative but increases with acidity, ionic strength or hydrolysis of cations results in a positive potential leading to a reduction in fluid flow towards the cathode and an increase towards the anode causing electro-osmosis or ionic migration of metal ions in soil. Enhancing agents such as water, EDTA, ethanoic, hydrochloric and nitric acids are added to the soil to aid the desorption of metals from the soil particles.

The advantages of this process are its applicability to fine soils (clays and silts), low operating cost (US \$50-200 m^{-3}), and the potential for extracting a wide range of contaminants at varying concentrations[56]. It has been applied for the treatment of kaolinite, bentonite, sandy soils contaminated with elements such as As, Cd, Co, Cr, Cs, Hg, Ni, Pb, Sn, Zn, Sr, U and Cs[57]. Pilot scale studies at a lead contaminated site in Hong Kong reported a reduction in Pb concentration from 4500 to 300 mg kg^{-1} in 30 weeks. Field demonstration of in-situ electrokinetic remediation at a site

composed of alluvium and fine to coarse grained sand and gravel contaminated with 200mg kg^{-1} Cr, showed a reduction in the extractable metal fraction from 28 to 5mg kg^{-1} after 700 hours of operation[58].

This technology although effective, suffers from severe limitations due to the very nature of the electrical conduction. In order for the procedure to be effective the soil solution has to behave like a conductor of electricity with as low a resistance as practicably possible[59]. This is difficult to achieve in contaminated soils, because they are generally made-ground with a variety of objects such as bricks, rocks, ash and clinker of varying fractions and composition. Furthermore, the soil cells have to be isolated from underlying aquifers and water bodies to prevent any leachate from reaching them. Additionally, the question of what to do with the leachate subsequent after application of the process remains unresolved. Consequently, it is difficult to obtain a mobile plant licence (MPL), IPPC authorisation or a Waste Management Licence (WML) from the Environment Agency for this process.

1.11 Stabilisation and Solidification

Stabilisation/solidification (S/S) is a remediation technology that relies on the reaction between a binder and the soil matrix, often in the presence of water to reduce the mobility of contaminants[60]. Stabilisation involves the addition of reagents to a contaminated material (e.g., soil or sludge) to produce more chemically stable contaminants. Solidification involves the addition of reagents to a contaminated material to change the physical state of the material, in order to encapsulate the materials and reduce access by external agents. These procedures effectively 'lock' the metal contaminants in soils through changes in physical state of the contaminated material e.g., dewatering, and through transformations in the chemical state of the

contaminants, thereby reducing the mobility and availability of contaminants to potential receptors. S/S is an established remediation and treatment technology in the USA and some EU member countries such as UK, Spain, France and Germany.

Stabilisation followed by solidification of soils using lime and cement is widely used in the construction industry[60]. Hydration of cements results in the formation of semicrystalline calcium hydrosilicate (CSH), calcite and hydrogarnets that bind metals by ion exchange and coordinate bonding. Metals in soils are reduced to insoluble carbonates, hydroxides and phosphates[61,62]. Cement pastes have a high pH, low solubility of their hydration products, good specific surface area and microporosity[63]. Zeolites hydrated from alkali slag cements can also immobilise metals. These are crystalline, hydrated aluminosilicates of alkali and alkaline earth metal ions and have a cage like structure that provides a very high cation exchange capacity. Clinopolite, chabazite and phillipsite are natural zeolites that have been widely used in industrial filters for the removal of ions and molecules from various solution and gas mixtures[64]. Metal adsorption can be enhanced by the addition of alumina that precipitates in the form of partially neutralised hydroxide layers on mineral surfaces and in the interstitial spaces of soil particles. Clay minerals coated with aluminium hydroxides e.g., Al-montmorillonite and Al_{13}-montmorillonite have been observed to specifically adsorb Ni, Cu and Zn, with an increase in binding strength with age[32].

The rate of solidification can be enhanced using machinery such as filter presses, hydrocyclones, rotary driers or standard heavy rollers, with the choice of equipment being determined by project requirements[30, 65].

The effectiveness of stabilisation/solidification procedures depends on several factors, which include choice of an appropriate chemical formulation; effective contact between the contaminants and the treatment reagents, which can be achieved by ensuring a high degree of chemical and physical consistency of the feedstock[30, 66] and the use of appropriate mixing equipment; control over external factors, such as temperature and humidity and the degree of mixing after gel formation, since these affect the setting and strength development processes. Stabilised contaminants may be remobilised if the physical and chemical nature of the treated product alters in response to changes in the external environment, such as exposure to an acidic discharge that can result in the release of free metal ions[67, 68]. The long-term durability of the product is influenced by the absence of substances that inhibit the stabilisation/solidification processes (for example excess sulphate and chloride attacks cement, which prevents it from setting)[69].

1.12 Soil Washing

This is a remediation approach in which water and complexing agents are used to remove metal ions bound to the surface of soil particles. Metal species in contaminated soil can be mobilised by exploiting the chelating behaviour of complexing agents such as EDTA and citric acid[70]. A coordination compound, or complex, is formed when a Lewis base (ligand or donor) is attached to a Lewis acid (acceptor) by means of a 'lone-pair' of electrons. The choice of a complexing agent for soil washing depends on its affinity for binding heavy and transition metals[30, 39].

Ligands are classified according to the number of donor atoms that they contain and are known as uni-, bi-, tri-, tetra, penta-, and hexa-dentate accordingly, as the number is 1, 2, 3, 4, 5, 6. Unidentate ligands may be simple monatomic ions such as halide

ions, or polyatomic ions or molecules that contain a donor atom from Group 14 or 15, or even 16 (e.g., CN^-). In many cases, where two or more atoms with unshared pairs of electrons are present in the same ion or molecule, and if their spatial properties are favourable (i.e., if they are not too close together or far apart), they may coordinate to the same metal atom or ion to form a ring e.g., carbonate (CO_3^{2-}) and oxalate ($C_2O_4^{2-}$) ions. The phenomenon of ring formation by a ligand in a complex is called chelation and the ring formation is called a chelate ring. Bidentate ligands form chelate rings while tridentate ligand forms two fused rings. The formation of fused chelate rings results in complexes that are more stable than those containing rings that are not fused. A good comparison is $[Cu(gly)_2]$ ($K_{sp} = 5.6 \times 10^{-16}$) and $[Zn(gly)_2]$ ($K_{sp} = 1.1 \times 10^{-10}$) with $[Cu(edta)]^{2-}$ ($K_{sp} = 1.38 \times 10^{-19}$) and $[Zn(edta)]^{2-}$ ($K_{sp} = 2.63 \times 10^{-17}$). The complexing agents in these cases are amino acids that form 5-membered chelate rings, but with glycine no fused rings are formed while EDTA forms five fused rings if all its possible donor atoms coordinate [30, 39].

Complexing agents such as EDTA and NTA are very popular because of their ability to form stable metal complexes. The dissociation constant of a complex is a measure of its thermodynamic stability ($\Delta G° = -2.303RT \log K$). This stability varies widely, but in general metals with higher oxidation state form stronger complexes. The effectiveness of a complexing agent used in soil washing is dependent mainly on metal fractionation and physical properties of soils. Porosity resulting from clay and silt content in the soil have a major role to play in determining the degree of contact between the solution and the soil particles [30, 39].

Other properties affecting the effectiveness of the washing process are pH and ionic strength. The degree of dissociation of a complexing agent depends on the soil and solution pH, while the degree of displacement of metal ions from mineral surfaces depends on the surface charge and a shift in the PZC (point of zero charge). Any alteration of PZC in the presence of complexing agents causes the dissolution of minerals. Several bench scale tests performed by various authors showed that chelants such as EDTA, NTA, DcyTA and PDA to be effective in extracting most heavy and transition metals for most soil types over the entire pH range[39]. Column washing studies show that the time taken to leach out 85% of metals using EDTA from soils contaminated with approximately 4000mg kg^{-1} Pb and 2500mg kg^{-1} Zn was less than an hour with flow rate having no significant effect on the extraction[71].

Soil washing techniques utilise machinery from the mining industry and exploit the fact that the majority of metal contaminants are often sorbed to the fine fractions (<60μm) of soils i.e., clays, silt and metal oxides. Separating the fine from the coarse fractions using methods such as density fractionation, centrifugation, power screening, hydrocyclones, Wilfley table, spiral and jig reduces the total volume of the contaminated material that requires treatment[36]. The remaining coarse fraction (>0.063m) is normally relatively clean and is often reused as 'inert' backfill. In situations where the contaminant levels in the 'coarse' materials is found to be above the recommended limits, a process called attrition scrubbing can be used. This method uses high-energy mixers to effect mechanical scrubbing on slurried soil during which the coatings or films on individual grains are removed, thus releasing metals. The material that is untreatable using soil washing can be either shipped to a

controlled landfill or treated further by a variety of processes, which immobilise the contaminants[72].

The first large scale soil washing operation was conducted in New Jersey where 19200 tonnes of soil and sludges contaminated with 11300, 16300, 389 and 11100 mg kg^{-1} of Cr, Cu, Pb and Ni were transported and treated[36]. The dried soil and sludge had a total moisture content of 15% and a pH of 6.5. The washing system consisted of a series of hydrocyclones, conditioners and froth flotation cells. A dry waste volume reduction of 90% was achieved in four months at an estimated cost of US250m^{-3}$ and all the clean-up goals were met to the US Federal regulatory requirements. Full-scale in-situ soil washing has also been applied at a site in Oregon where soil contaminated with 60000 mg kg^{-1} of Cr was treated using water, with the leachate being collected in infiltration basins and trenches[41]. The average Cr(VI) concentration in the soil plume decreased from 1923 to 207 mg L^{-1}.

The environmental firms Davy International (Environmental Division), UK and Kommunekemi, Denmark have developed a two-step treatment technology that uses ex-situ soil washing using acidic and alkaline reagents followed by metal adsorption by activated charcoal or cation resins in direct contact with soil slurry[36]. Metal ions are subsequently recovered from the activated charcoal or ion exchange resin. A bench scale test performed on contaminated soil from a wood preservation site caused a reduction in concentration of Cu, Cr, Zn and As from 360, 621, 1668 and 1204 to 22, 64, 68 and 112 mg kg^{-1} respectively[41].

A large scale portable soil washing and vacuum distillation plant known as the Harbauer technology, consisting of soil washing that preconcentrated mercury in a fine fraction followed by vacuum distillation at 350-450°C was tested at Marktredwitz, Germany[36]. The site contained 57000m^3 of soil contaminated with 5000mg kg^{-1} of Hg along with an assortment of solvents and chemical waste. The aim of the project was to establish whether the treatment process reduced the contamination to landfill limits. Vacuum distillation volatilised the Hg in the soil (with a majority of the Hg in the efflux gas stream being scrubbed out using a mercury scrubber), after which the treated fine fractions (100μm-2mm) containing 11-31mg kg^{-1} of Hg were mixed with coarse soil (2-60mm) containing less than 5mg kg^{-1} of Hg and disposed of in a designated landfill. 15000 tonnes of soil were treated in the first year at a rate of 300 tonnes per day. Hg concentration in the soil was reduced from 1900 to 10mg kg^{-1} at an estimated cost of US$ 320 m^{-3}.

Metal laden wash solutions can be treated using a variety of methods to recover the metals and reagents or to protect the environment from any adverse side effects resulting from the products of the soil washing procedures[39]. Effluents can be potentially treated by the creation of permeable reactive barriers[73]. 'A permeable reactive barrier is an engineered treatment zone of reactive material(s) that is placed in the sub-surface in order to remediate contaminated fluids as they flow through it. A PRB has a negligible overall effect on bulk fluid flow rates in the sub-surface strata, which is typically achieved by the construction of a permeable reactive zone, or by construction of a permeable reactive 'cell' bound by low permeability barriers that direct the contaminant towards the zone or reactive media'. A total of 70, 20 and 5 barriers have been constructed in the USA, EU and the UK respectively[62]. These

barriers are constructed using zero-valent iron, iron, furnace slag, zeolites, pillared and modified clays etc., to treat a variety of organic and inorganic contaminants.

The metal laden liquids can also be treated using electrokinetic and redox techniques. Allen et al.[74], reported a 95% recovery of Cu and Pb bound to EDTA using electrolysis. Reagents such as EDTA can be recycled by substituting metal cations with Fe^{3+} at low pH, which is followed by reductive precipitation of Fe^{3+} at high pH using NaOH. Bacteria such as *Pseudomonas fluorescens* and *Azotobacter vinelandii* that enzymatically degrade citric acid complexed with Ni and Fe complexes can also be used to degrade metal-chelate complexes. Plants such as *Phragmites, Agrostis stolonifera, Cirisium arvense, Rumex acetosa, Pulicaria dysentrica, Eichhornia crassipes, Ceriodaphnia dubia, Pimephales promelas* growing in artificial wetlands have the ability to degrade metal laden wash solutions and accumulate substantial concentrations of heavy metals in their biomass[75,76,77,78,79]. Lytle et al.,[80] reported that *Eichhornia crassipes* (water hyacinth) has the potential for in-situ detoxification of Cr(VI) contaminated waste streams. This plant has a high biomass accumulation (106-165 t ha^{-1} yr^{-1}) and is very easy to harvest. They observed significant accumulation of Cr(III) in the plant leaves suggesting that there was reduction of Cr(VI) after uptake by the plant roots.

1.13 Bioremediation

Bioremediation of metal contaminated soil has become a topic of extensive research in recent years because of the environmental problems associated with conventional remediation techniques such as soil washing[81]. It has the ability to preserve or in some cases enhance the properties of soil because it takes advantage of the metabolic processes of living organisms to extract, stabilise or immobilise metal contaminants in

soil. Microorganisms such as *Geobacter metallireducens* and *Shewanella putrefaciens* obtain energy for growth on organic matter using Fe^{3+} as an oxidant[82]. Some bacteria such as *Aquaspirillum magnetotacticum* transform extracellular Fe to the mixed valence iron oxide mineral magnetite (Fe_3O_4). Dissimilatory Fe reducing bacteria can accumulate magnetite as an extracellular product (biomineralisation).

The principal methods of bioremediation are land farming (mixing the top soil with microbes and then turning over at periodic intervals); composting (applicable to metals in organic form or associated with organics); bioreactors (soil in the form of slurry and degradation using aerobic and anaerobic bacteria); bioventing (stimulate the growth of anaerobic bacteria by drawing oxygen out of the soil); bioaugmentation (encouraging the growth of native microorganisms by the addition of nutrients to soil); bioleaching (leaching metals from piles using reducing bacteria)[83, 84]. The factors that affect the growth of bacteria in soil are energy sources (electron donors), electron acceptors, nutrients, pH, temperature and inhibitory substrates or metabolites. The microbial population is highest in the topsoil where there is the greatest accumulation of organic matter in the rhizosphere of plants. With increasing depth the population of anaerobic bacteria, which are generally named as heterotrophs, increases. Heterotrophic soil microbes utilise soil minerals for their metabolism unlike autotrophs that produce energy using sunlight. They produce organic acids (instead of sucrose as in autotrophs) that can mobilise and solubilise metals at high pH (e.g., *Thiobacilli* at pH 5.5)[85].

The bioleaching of metal sulphides is caused by heterotrophic bacteria such as *Thiobacillus ferrooxidans, Leptosporium ferrooxidans, Thiobacillus thiooxidans,*

Metallogenium, Acidianus sulpholobus spp[86]. The dissolution of metal sulphides can occur directly or indirectly. In the direct mechanism metal ions are released when the sulfur on the metal ions is converted to sulphates by bacterial enzyme action. In the indirect mechanism the metal dissolution takes place by the oxidation of Fe^{3+} ions releasing Fe^{2+} and sulfur ions. This process is one of the major causes of acid mine drainage and related phenomena. Bioleaching takes place mainly due to acid production from bacterial metabolism, which results in lowering of pH and consequent metal mobilisation. Strains of *Thiobacillus ferroxidans* and *Thiobacillus thiooxidans* have been reported to extract >50% of As, Cd, Co, Cu, Ni, V, Zn, B and Be. *T. ferrooxidans* does not oxidise FeS_2, MoS_2 without the presence of Fe^{2+} or Fe^{3+} ions, whereas, leaching of sulphides like ZnS, CdS, NiS, CoS, CuS or Cu_2S is related to their solubility products. In the absence of Fe ions *T. ferroxidans* acts in the same manner as *T. thioxidans* reducing metal ions by the oxidation of sulfur[87].

Microbial polysaccharides produced from bacteria such as *Methylobacterium organophilum* and *Trichoderma harzianum* have been reported to form complexes with heavy metals and immobilise them[88]. Diels et al., [89] reported a large decrease in the bioavailability of Cd, Zn, and Pb due to adsorption on bacterial cell walls. Siderophores are short chain Fe^{3+} specific ligands that are synthesised by bacteria and fungi under conditions of Fe stress. Trihydroxamate siderophores (e.g., desferrioxamine B) are produced in fungi where the three hydroxamate groups are complexed to Fe^{3+}. The concentration of siderophores is high in the rhizospheres of plants and in organic rich soils[90]. Furthermore, the addition of Fe(III) and the presence of extra-cellular polymers (EPS) secreted by bacteria also play an important role in the bioleaching of metal sulphides. For the bacterial degradation of metal

sulphides, the presence of EPS is indispensable[91]. Such films have been observed associated with the cells of *T. ferroxidans* growing on pyrite. During pyrite dissolution, cells of *T. ferroxidans* attach to the mineral surface by means of excreted exopolymeric substances (lipopolysaccharides), such as glucuronic acid subunits of the carbohydrate polymer, and oxidise the mineral resulting in the production of sulfuric acid[92].

Metals can be sorbed on to microbial cell walls and retained by biosorption. Authors have reported the adsorption of Zn onto the cell walls of *Rhizopus arrhizus* using fungal chitin and chitosan[93]. Freeze dried biomass of white-rot fungi (*Phanerochaete chryosporium*) has been found to adsorb Cd^{2+}. Dry *Phanerochaete chryosporium* sorbed mercury and alkyl mercury species in the following order: CH_3HgCl > C_2H_5HgCl > Hg(II) (79, 67 and 61 mg g^{-1} dry wts respectively). Immobilised *Saccharomyces cerevisiae* has been reported to accumulate Hg>Zn>Pb>Cd>Co>Ni>Cu. *Aspergillus niger* mycelium when chemically modified with carboxy or ethyldiamino groups increased Ni biosorption from 70 – 1060 mmol kg^{-1}. Higher extraction of Pb, Cd and Cu has been reported using *A. niger* when compared with F-400 activated charcoal. Metal binding in microorganisms can also be increased by gene modification. When the gene sequences coding for histopolypeptides and cystopolypeptides were fused with the sequence for *LamB* protein in *Escherichia coli*, binding of Cd^{2+}, Cu^{2+} and Hg^{2+} increased by several magnitudes[68]. Chen et al.,[94] reported a four hundred fold increase in Hg^{2+} adsorption from soil using a modified *E. coli* strain expressing for Hg^{2+} transporters and metallothioneins.

Bioremediation of metal contaminated soils is still in its infancy and there have not been any credible reports of this procedure being applied for the restoration of a 'real' site.

1.14 Phytoremediation

Phytoremediation is the most widely investigated and applied biological technique for the remediation of metal contaminated soils[74]. It is a process that exploits the metabolic and physiological mechanisms of plants to stabilise and extract heavy metals in soil[95]. The uptake of trace metals in plant roots takes place due to processes that include advection or diffusion of the metal from the bulk solution to the roots, diffusion through the solution boundary and the protective layers on the surface of roots (e.g., mucus, cell wall, casparian strips etc.), sorption or surface complexation of metals at binding sites on the cell surfaces, uptake (transport) of the metal through the cell membrane on the surface[96]. Any of these steps has the potential to be the rate limiting process, depending on the plant, the nature and speciation of the accumulated element, and the properties of the medium including pH, mineral content, conductivity, temperature etc[97].

Phytoremediation is a generic name given to three processes, namely, phytoextraction, phytostabilisation and phytovolatilisation[98]. Phytoextraction is a phenomenon involving the extraction and accumulation of pollutants by plants. Phytostabilisation is a phenomenon that reduces the mobility of metals in soil either through chemical transformation of metals in the rhizosphere of plants or through changes in physico-chemical properties of the soil e.g., increase in organic matter content etc. In phytovolatilisation contaminants are lost from the plant biomass as a result of evapo-transpiration. This process is principally applicable to organic and

organometallic compounds. From an environmental pollution viewpoint phytoextraction is perhaps the technique of choice because this process removes the contaminants from the soil and accumulates them in the plants' biomass, which can then be removed for further processing.

Baker[99] classified plants as hyperaccumulators, indicators and excluders on the basis of their capacity to accumulate metals. Hyperaccumulators (e.g., *Thlaspi spp., Alyssum spp., Chenopodium spp., Utrica spp.* etc.) are plants that accumulate metals in their biomass several thousand times relative to the concentration of metals in soil[100]. About 400 species of hyperaccumulating plants have been identified in Europe, USA, Australia and New Zealand[101]. Most hyperaccumulators are contaminant specific because their root surfaces are specifically evolved to absorb elemental nutrients by the secretion of high affinity chemical receptors known as phytochelatins[102]. Indicator species are plants that accumulate metals at concentrations similar to those of the metals in soil. Excluders are plants that actively exclude heavy metals from their biomass.

Extraction by plants such as legumes is aided by symbiotic mycorrhizae in the roots. These mycorrhizae increase the surface area of absorption of roots for nutrient uptake[103]. These organisms have also been reported in the roots of plants growing in sites contaminated with heavy metals. Arbuscular endomycorrhizal infection has been reported to increase by a factor of three in prairie grasses growing on sites contaminated with iron ore[104]. Ectomycorrhizae protect the host plant from toxicity by accumulating metals in their cell walls. Metals are biosorbed on cell wall chitin, and cellulose derivatives[105]. Cu and Zn were found to be immobilised by extracellular

fungal slime resulting in metal-phosphate bonds[106]. Raman et al.,[107] isolated *Glomus* and *Gigaspora* spp., mycorrhizae in fourteen species of plants growing in mangenite contaminated sites in India. Fungal spores of *Glomus aggregatum*, *G. fasciculatum* and *Entrophosphora* spp. were isolated in plants growing around a calamine (ZnO) mine in Poland. Turnau[108] showed that Zn was concentrated as crystals (of Zn compounds) in the fungal mycelial body.

Phytoremediation was first applied to artificial wetlands using reed beds and floating plant systems for the treatment of contaminated soil and water[109]. The most popular plants for phytoremediation are those belonging to the Brassica and Helianthus families (e.g., Indian Mustard and Sunflowers). Good hyperaccumulators such as *Thlaspi* (Alpine pennycress) and *Alyssum* spp., belong to the Brassica family. *Brassica juncea* (Indian Mustard) can accumulate Cd^{2+}, Ni^{2+}, Pb^{2+} and Sr^{2+} into root tissues at levels five hundred times more than that in the growth medium[110]. *Helianthus annuus* roots were reported to concentrate uranium 30,000 times that available in solution. Similarly, tobacco roots exposed to low concentrations (1-5μg ml^{-1}) of ionic mercury (Hg^{2+}) in solution accumulated the metal a 100-fold in a few hours. These plants are preferred, because unlike for hyperaccumulators there is extensive information available on their agronomy, pest control, breeding capacity and physiology [111].

Metal removal is a function of the metal concentration in the shoots and the total biomass[112]. Biomass increase can be accomplished through intensive cultivation that facilitates rapid plant establishment and growth. Oil seed Brassicas have been known to produce 18 tons of dry biomass per hectare in approximately 2.5 months of

cultivation and growth rates in excess of 200 kg per hectare of dry matter per day under agricultural conditions[113]. *Brassica juncea* (Indian Mustard), *Brassica rapa* and *Brassica napus* (radish) have been reported to accumulate far higher concentrations of Cd, Cu and Zn than *T. caruslescens* as a result of higher biomass accumulation into the former[114]. *Helianthus annuus*, *Beta vulgaris* (sugar beet) and *Spinacea olaracea* (Perpetual spinach) have been reported to accumulate greater amounts of metals than *B. juncea* because of significantly greater biomass accumulation[90]. Low uptake rates in contaminated soil can be improved by using a mixed cropping regime, in which plants of different species are grown simultaneously until they reach the end of the exponential phase of their growth cycle[90].

The factors that affect metal uptake by plants are bioavailability (as a function of soil conditions such as pH and redox potential), nutrient status and phenotype. Willey et al.,[115] showed that uptake by plants is lower for medium to heavily contaminated soils compared to marginal ones. This is due to the saturation (and/or destruction) of the active physiological mechanisms such as transporters in plants[116,117,118,119]. Two related sub-families of zinc transport proteins (ZIP) have been reported to be involved in the transport of Zn^{2+} and Fe^{2+}, as shown in an increased expression of ZIP1 and ZIP3 genes in plant roots starved of zinc[120]. A four-fold increase in Fe content was observed when the roots of tobacco (*Nicotiana tabacum*) plants were transformed with ferric reductase coding sequences FRE1 and FRE2[121,122].

Apart from transporters and translocaters, plants also possess metal sinks known as metallothioneins and phytochelatins[123,124]. These are cysteine rich peptides that are responsible for storing sulphide reducible metals.[125] These peptides are used by

plants and fungi for detoxification and are enzymatically synthesised from glutathione in the presence of metal ions by an enzyme called glutathione synthase. Phytochelatins have been reported to occur in large amounts in *B. juncea* plants growing in cadmium contaminated soil[126]. Plants growing around mines have been reported to produce 10-100 times greater concentration of phytochelatins in their roots compared to their leaves[127]. Metal detoxification in plants probably occurs because phytochelatins have the ability to bind inorganic sulphide resulting in the formation of a stable metal-phytochelatin complex. Metallothioneins are thought to chaperone nutrient metals to various necessary roles in plants[128]. Plant metallothionein-like genes have been isolated from several plant species such as maize, soybean, rice, wheat and radish (*Brassica napus*)[129]. When *P. sativum* metallothionein-like gene was expressed in *Arabidopsis thalliana*, increases in Cu accumulation of several fold were reported[130].

Uptake and resistance to phytotoxicity can also be increased by genetic engineering of plants with the introduction of metallothionein and the bacterial iron reductase gene *merA* into high biomass accumulating plants[131]. This increases the metal tolerance of plants that helps them to survive in heavily contaminated soils. Mutagenised *merA* sequence (*merApe9*) when transformed to *A. thalliana*, resulted in a three fold increase in Hg^0 uptake compared with control plants[132]. Introduction of the *merB* gene resulted in an increased conversion of organic mercury (methyl mercury) to less harmful divalent mercury (Hg^{2+}). Tobacco (*Nicotiana tabacum*) and yellow poplar (*Liriodendron tulipfera*) were genetically transformed by the introduction of *merA* and *merB* genes that increased their capacity to tolerate Hg in addition to increased

uptake. These modified plants also phytovolatilised mercury after uptake, as a result of transpiration (i.e., loss of water through plant leaves (stomata)).

The solubility and transport of many heavy metals into roots is increased under acidic conditions in soils. Plant roots under times of phosphorus stress secrete citric acid and malic acid, which lower the soil pH thereby increasing the availability of metals in the rhizosphere. These acids also act as substrates for bacteria, which in turn reduce metal ions thereby enhancing their uptake by plants. Complexing agents such as EDTA or DTPA when added to soil increase the availability of metals to plants[133]. Cunningham et al.,[134] demonstrated that plants grown in soils amended with EDTA and ethanoic acid accumulated 56 times more lead than those grown in untreated soils. A 140 fold increase in the accumulation of Pb was observed in the shoots of *Pisum sativum* (pea) growing in soils amended with chelating agents such as EDTA and DTPA.

Phytoremediation has several advantages over other techniques and these include low input and manpower costs[135]. Site disruption is minimal and the whole process is socially acceptable and aesthetically pleasing. Commonly available agricultural techniques and equipment can be utilised for planning, maintenance and harvest of the crops. Most of the plants that can be utilised for phytoremediation have well-known life cycles, breeding practices and pest control procedures. The harvested biomass could be easily incinerated either on-site or off-site resulting in further waste volume reduction. A major drawback of phytoremediation is the relatively long time taken to be effective compared with other physico-chemical techniques. Furthermore, phytoremediation is mainly applicable to marginally and surface contaminated soils

because metal uptake by plants decreases with increasing concentration and depth. Therefore, in order to increase metal tolerance and uptake, substantial research is required particularly in the field of genetic modification to produce high biomass accumulating plants. More research into the engineering aspects of phytoremediation is required so that current and future technologies are effective.

1.15 Analytical Techniques

The efficiency of environmental risk assessment and remediation procedures depends on the accuracy of analytical data. The choice of an analytical technique depends on the nature of the analyte e.g., soil, water, gas etc. Techniques such as atomic absorption spectroscopy (AAS), inductively coupled plasma atomic emission Spectroscopy (ICP-AES), inductively coupled plasma mass spectrometry (ICP-MS) are used for the analysis of metal content in solutions[136]. This is done after the solubilisation of metals from soil using solutions such as hot acids, water and complexing agents. These techniques on their own, measure the total metal concentration in the solution without distinguishing between free metal ions, complexed metal ions and metals in different oxidation states. Speciation of metals in solutions can be determined using ion selective electrodes, polarography, colorimetric procedures, gas chromatography (GC) and high performance liquid chromatography (HPLC) coupled with AA, ICP-AES or ICP-MS.

Direct speciation analysis of metals in soils can be performed using non-destructive techniques such as X-ray diffraction (XRD), environmental scanning electron microscopy (ESEM) and energy dispersive X-ray spectroscopy (EDX), and Fourier transform infra-red spectroscopy (FT-IR)[137]. These techniques have the advantage of being able to 'see' soil compounds using X-ray or infra-red radiation without

changing the chemical properties and the structure of the soil in a significant way. The data obtained from these techniques are compared with published databases of minerals and compounds. These techniques although very effective and routinely used to study the structure of soils, suffer from drawbacks such as sensitivity to moisture, particle size and cost.

1.16 Sample Homogenisation

Solid samples (soil and plant) are generally too heterogeneous to satisfy the needs of instrumental analysis. Therefore, preliminary treatments are required to obtain a more representative sub-sample with a finer particle size[138]. Prior to the further steps, samples are dried at ambient temperature or in a laboratory oven (usually 75°C for Hg, 105°C for other elements). For some types of samples (generally plant samples), lyophilisation procedures (drying by freezing) are increasingly being used. These procedures allow the preservation of the initial sample texture and/or facilitating subsequent grinding. Dry solid samples such as soils and sediments, may be ground (dry or wet) manually (mortars) or mechanically (ball, hammer, roll and disk mills or grinders) made from steel, agate, boron or tungsten carbides, corundum. Homogenisation of other types of solid samples (plant tissues) is generally performed using various types of mixers[139]. Fresh organic samples are generally homogenised, by grinding after freezing in liquid nitrogen.

1.17 Sample Mineralisation and Metal Dissolution

Samples of organic or mixed nature are often subject to two distinct steps, mineralisation and dissolution, which often take place simultaneously. Samples of purely inorganic composition are simply dissolved. The composition of environmental samples varies from purely inorganic (e.g., fly ash) to purely organic

(e.g., fats), but generally, they are an intermediate combination of the extremes. This means total dissolution of samples cannot be achieved in one step using a single reagent[114]. In practice, the necessary number of steps and reagents is dictated by the matrix composition. Therefore, depending on the nature of the sample, appropriate digestion methods must be chosen.

1.18 Dry Ashing

In dry ashing procedures, the organic matter is decomposed at high temperature (450-500°C) and the resultant ash is dissolved in a strong acid. In most modern wet procedures, various combinations and proportions of strong acids with hydrogen peroxide ensure the mineralisation and dissolution of the ashed sample. The biggest advantage of dry ashing procedures is the possibility of treating relatively large quantities of sample and dissolving the resulting ash in a small volume of acid (generally nitric or hydrochloric). This procedure permits the preconcentration of trace elements in the final solution, which is useful when very low analyte concentrations are to be determined[113]. Additionally, the resulting ash is completely free of organic matter, which may interfere with certain determinations. Furthermore, the sample matrix is largely simplified and the resulting solutions are of acceptable characteristics (clear, colourless and odourless). In spite of these advantages dry ashing can lead to loss of volatile elements such as mercury, arsenic and selenium.

1.19 Wet Digestions

For the determination of total elemental content in soils and sediments, the majority of wet digestion procedures involve the use of six reagents. Nitric acid, sulfuric acid, perchloric acid and hydrogen peroxide cause the oxidation of organic matter, while hydrochloric and hydrofluoric acids ensure the dissolution of inorganic compounds.

Sulfuric acid is the main component of an efficient mixture of nitric acid, sulfuric acid, hydrogen peroxide used to digest soil and sediment samples[113, 114]. However, sulfuric acid is not commonly used due to its tendency to form insoluble metal sulphates. Hydrofluoric acid and perchloric acid due to their extreme reactivity are not commonly used in laboratories for the solubilisation of metals in soils, due to safety reasons. Aqua-regia, a mixture of three parts HCl and one part HNO_3 is most commonly used for the dissolution of metals in soils and sediments. Although this mixture does not dissolve silica, it does cause the solubilisation of most metals in soils.

1.20 Digestion Procedures

The choice of a digestion procedure depends on the contaminant and the sample matrix. The mineralisation and dissolution of organic samples is generally not problematic. Most wet digestion procedures utilise a single acid (usually nitric) or a mixture of acids and other oxidants (usually nitric acid and hydrogen peroxide). The mineralisation is performed in open or close systems[113, 114, 140]. Traditionally, open systems (digestions at atmospheric pressure) employ any vessel, usually in glass or PTFE (beaker, conical flask), with or without a refluxing condenser and heated using a conventional source (Bunsen, hot plate, sand bath etc.). A previously dried or fresh sample is weighed into a mineralisation vessel and reagents are added. The mixture is heated to boiling, which is maintained for the time necessary for sample decomposition and dissolution to occur. After cooling, the resulting solution is quantitatively transferred in to a calibrated flask and made up to volume. If an insoluble residue remains after this procedure, it may be necessary to remove this by filtration or centrifugation. Open systems have developed into mineralisation ramps composed of several vessels equipped with reflux condensers to limit possible

volatilisation losses of some analytes but also to avoid the evaporation of reactive mixtures[117]. Open systems heated by microwave energy are also currently available in manual and automated modes.

Closed systems (pressurised acid digestions) are mainly represented by various models of PTFE-lined digestion bombs with or without a robust stainless steel body or by high-pressure quartz vessels. Digestions performed in such devices benefit from the synergistic effects of temperature and pressure. These techniques are generally more efficient than conventional wet digestions in open systems because the loss of volatile elements is avoided and the decomposition of more difficult samples is facilitated. The factors limiting pressure bombs are the small amount of organic matter that can be treated (0.1-0.2g) and the fact that only nitric acid can be used for the process.

1.21 Elemental and Mineralogical Determination

Qualitative and quantitative information on metals in soils can be determined using techniques such as X-ray fluorescence (XRF) spectroscopy, X-ray diffraction (XRD) spectroscopy, inductively coupled atomic emission spectroscopy (ICP-AES) and inductively coupled mass spectrometry (ICP-MS).

X-ray fluorescence (XRF) Spectroscopy

XRF is a spectroscopic technique that is used to obtain qualitative or quantitative information on the elemental composition of a sample[141]. When a sample is irradiated with very high energy photons (from 5 to 60 keV), X-ray photoluminescence, which is characteristic of the elements present in the sample is produced. There are two kinds of XRF instruments – wavelength dispersive and energy dispersive (Figure 2).

The characteristics of the emission spectrum do not depend on the chemical state of the elements in the sample. This non-destructive analysis technique can be used for all elements in solid or liquid samples.

It is important to correct for matrix effects to prevent reduction in spectral peak intensities due to absorption effects. This can be achieved by heating the sample with a fusion reagent or fusion mixture such as borax to form a fused sample. The molten fused sample is poured on to a cold, flat surface to produce a glass, which can be analysed directly by XRF, or it may be cooled, ground and analysed thereafter. To facilitate grinding the hot brittle solid can be shattered by dropping it into cold water, or some other liquid that does not dissolve the glass. The solid fused samples can be loaded directly onto a sample holder and analysed.

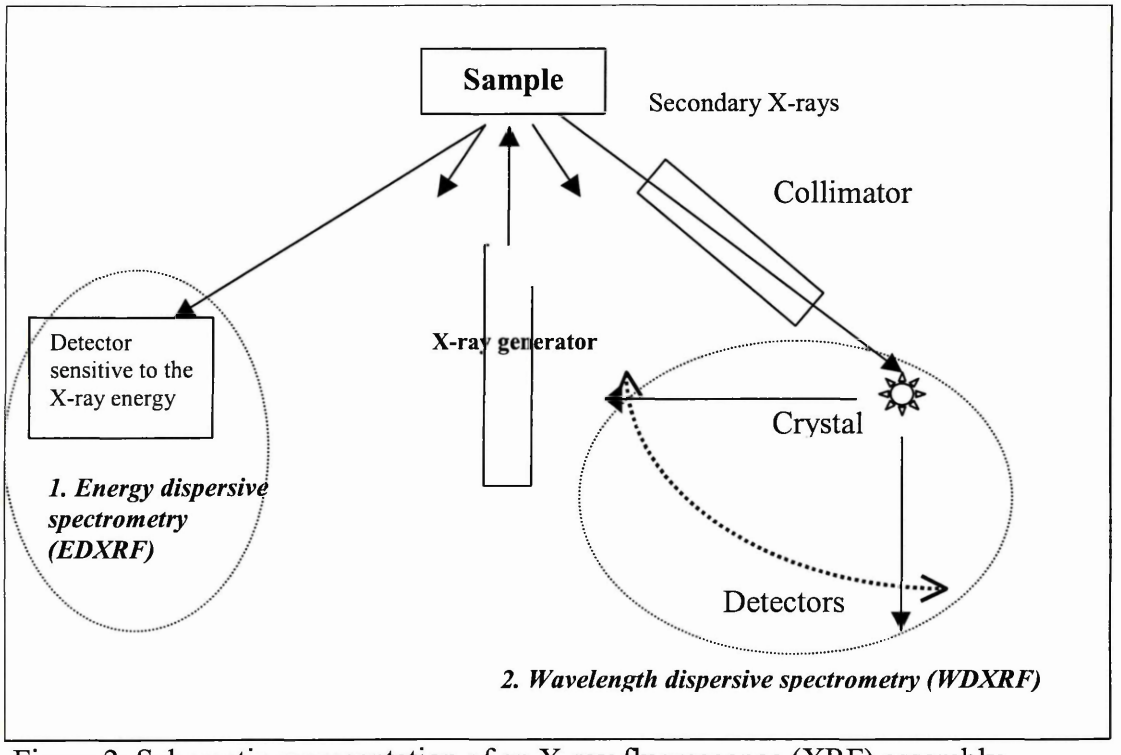

Figure 2: Schematic representation of an X-ray fluorescence (XRF) assembly.

Serious absorption effects arising from matrix interferences can also be reduced by matrix dilution. The samples are diluted with a material that has a low absorption, such as powdered starch etc. The concentration, and therefore the effect of the interfering matrix elements is reduced. However, the most practical way of applying matrix correction is with an internal standard. The internal standard technique is only valid if the matrix elements affect the reference line and analytical line in exactly the same way. If either the reference peak or the analytical peak is selectively absorbed or enhanced by a matrix element, the internal standard peak to analytical peak intensity ratio is not a true measure of the concentration of the element being determined.

Matrix effects such as absorption and enhancement are often negligible when thin samples are used for analyses. A thin sample is defined as one in which the total mass per unit area, m, is given by

$$m \leq \frac{0.1}{\mu}$$

where μ is the effective mass absorption coefficient. Thin samples are prepared by pressing the analyte samples into a pellet, usually under a pressure of 10-20 tons/cm^2. Prior to pelleting, an inorganic powder has to be mixed with a binder that may be an electrical conductor[142]. For XRF analysis, a low or high absorber is sometimes employed. For some purposes, for example when only a small amount of material is available, the pellet may be backed by the pure binder (such as cellulose) or other metal, with only one face of the pellet being composed of the sample/binder mixture[143].

If proper sample preparation procedures are followed quantitative data obtained using this technique can be as accurate as those from wet techniques. However, XRF cannot detect elements whose concentration in the soil is less than 1%w/w. This method is useful for the analysis of metals such as rare earths that lack reliable wet chemical methods. It generally serves as a complementary method to optical emission spectroscopy, particularly for major constituents. Furthermore, it can also be used for the analysis of non-metallic specimens because the sample need not be an electrical conductor.

X-ray Diffraction

X-ray diffraction is a versatile non-destructive technique for the identification and quantitative determination of the various crystalline forms, known as 'phases' of compounds present in powdered and solid samples. Soil minerals are usually studied using the powder diffraction method. Homogenised, thinly ground powder samples (<50μm) are loaded onto a sample holder and analysed under a fixed X-ray beam for a fixed period of time[144]. A plot of diffracted X-ray intensity versus twice the diffraction angle i.e. 2θ-is obtained. The relationship between the wavelength of the radiation λ, the angle θ between the incident beam of radiation and the parallel planes of atoms causing the diffraction and the spacing d between these planes is called Bragg's law. This law is expressed in a mathematical form as $2d\sin\theta = n\lambda$. Identification is achieved by comparing the X-ray diffraction pattern or 'diffractogram' obtained from an unknown sample with an internationally recognised database such as JPDS database containing reference patterns for more than 70,000 phases.

The essential feature of the diffraction of waves of any wavelength is that the distance between scattering centres be about the same as the wavelength of the waves being scattered. The dimensions of X-rays and the structural spacings of crystals are both about 10^{-8} cm. X-rays are scattered by the electrons around the nuclei of the atoms composing a unit cell. This scattering is modified in three ways –

1) by the way in which electrons of a particular atom are distributed within the field of influence of that atom.

2) by the thermal vibrations that tend to blur the atoms as scattering centers as temperature increases.

3) by the way atoms are arranged within the unit cell.

Each scattering centre contributes a diffracted beam that can be represented by a vector. Atoms, unit cells, or crystallites (very small crystals) can be treated as scattering centres. All the vectors from scattering centres within an optically coherent domain must be summed into a single vector, and then the vectors from each domain must be summed. This will result in a diffracted beam with a specific amplitude and phase, which allows the calculation of its intensity and its comparison to experimental results.

Once a mineral phase has been identified based on its diffraction peaks, additional information is obtained from diffraction peak widths. Well crystallised minerals of sand and silt size give sharp diffraction lines whose widths are determined only by broadening caused by the X-ray diffractometer itself. Clay-sized particles show broader lines caused by diffraction effects from the small particles. The smaller the

particles are, the broader the diffraction lines. X-ray line width and particle size are related by the Scherrer equation:

$$L_{hkl} = \frac{(K\lambda)}{(\beta \cos\theta)}$$

where L_{hkl} is the mean crystalline dimension perpendicular to the diffracting planes with Miller indices, *(hkl)*, K is a constant equal to 0.9, λ is the x-ray wavlength, β is the width (in radians) at one half peak height corrected for instrumental broadening, and θ is the diffraction line position. In addition, L_{hkl} measures the size of the coherently diffracting domains within the crystals. If the crystals consist of several coherently diffracting domains, then L_{hkl} will be smaller than the actual physical size of the crystals observed by electron microscopy.

Elemental Analysis using Atomic Emission Spectrometry

Atoms when excited at high temperatures emit characteristic radiation[145]. This radiation can be used to obtain quantitative and qualitative information about elements using the atomic spectrum emitted by a sample. The wavelength at which a peak is obtained in the spectrum identifies the element, whereas the intensity of the peak quantifies its concentration. The principal components of optical emission spectrophotometers are (1) the sampling device and source, (2) the spectrometer and (3) the detector and the readout device. The choice of sampling device and source depends on sample type and the analytical data desired. Excitation and ionisation of atoms can be obtained using sparks, electric arcs and inert-gas plasmas.

Nowadays, inert-gas (argon or helium) plasma based sources are preferred over electric discharge sources because of their greater accuracy, sensitivity and precision

for a larger number of elements. These advantages arise from higher plasma temperatures (6000 –10000 K) that result in greater ionisation efficiencies of atoms, especially those in solutions. The inductively coupled plasma (ICP) torch is a device that is sustained by induction from a high-frequency magnetic field. Initially, argon gas flows through a 25mm quartz tube, which is surrounded at the tip by an induction coil. An ac current flows through the coil at a frequency of around 30MHz and power levels of about 2kW.

The argon gas stream that enters the coil is initially seeded with free electrons from a Tesla discharge coil. These seed electrons interact with the magnetic field of the coil and gain sufficient energy to ionise argon atoms by collisional excitation. Ions and electrons resulting from the initial Tesla spark are accelerated by the magnetic field in a circular flow perpendicular to the stream that emerges from the tip. Reversal of the direction of the current in the induction coil reverses the direction of the magnetic field applied to the mixture of atoms, ions and electrons. The fast moving cations and electrons, known as the eddy current, collide with more argon atoms to produce further ionisation and intense thermal energy. A flame shaped plasma forms near the top of the torch (Figure 3).

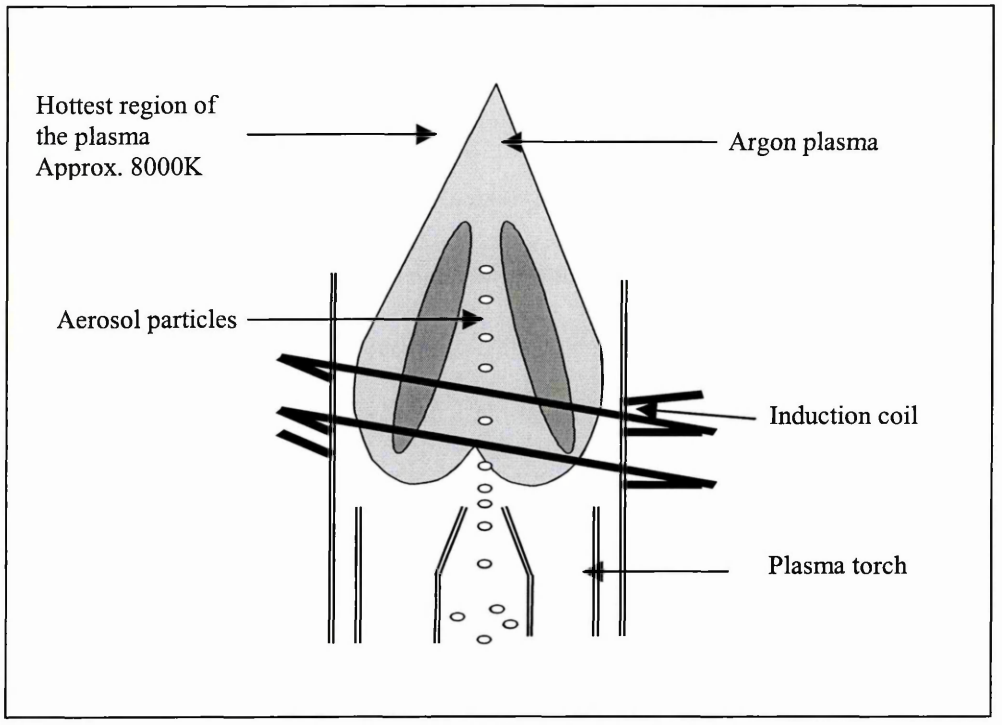

Figure 3: Schematic configuration of an ICP-AES torch.

The excitation and emission zones in the ICP are spatially separated, as a result of which there is a relatively simple background spectrum that consists of argon lines and some weak band emission from OH, NO, NH, and CN molecules. This low background, combined with a high signal to noise ratio of analyte emission, results in low detection limits, typically in the ng L^{-1} range. There is a well-defined boundary between the tail that contains the analyte and the current carrying portion of the inert plasma, which results in minimal interelemental and matrix interferences. The high temperatures in the plasma ensure the complete breakdown of chemical compounds and stop the formation of other interfering compounds.

The accuracy and precision of the ICP-AES system in analysing liquid samples, however, depends greatly on the sample introduction procedures. ICP systems suffer

from drawbacks such as low transport efficiency, low washout rate due to low gas and liquid flow rates (approximately 1L min^{-1} and 1mL min^{-1} respectively). The broad linear range of ICP increases the problems of low washout, up to five orders of magnitude i.e. it is possible that a concentrated sample of 2000μg mL^{-1} could be followed by one containing 0.1μg mL^{-1} of analyte. As a result of these problems, there are certain practical factors that dictate the analytical precision of an ICP system: (1) a maximum sample drop size that can be introduced into the atomizer, (2) rate of solvent flow that must fall within a specific range of values

Particle size is generally controlled in ICP systems using pneumatic nebulisers[152]. The most commonly used nebulisers are cross-flow and Babington nebulisers. In cross-flow nebulisers the liquid sample is sprayed at right angles to the argon gas stream that results in the formation of an aerosol. Babington nebulisers use a spherical surface with small holes arranged in a circular manner. The liquid that flows over the outer surface of the sphere is nebulized by gas flowing from within the sphere through the small holes. Both these nebulisers are inherently blockage free because of their design and operation. They are used with samples containing suspended particles or when it is not convenient to totally dissolve the sample with acids or other reagents. They are also useful when the viscosity of the samples varies widely. When using these devices it should be remembered that transporting the analyte to the plasma or flame does not ensure a proportional supply of atoms or ions. Analyses should be verified with standard reference materials wherever possible.

Detection systems used for multielemental analysis are either sequential or simultaneous. In the former system, dispersed radiation is transmitted sequentially to

a single detector. This is achieved using scanning monochromators or rotating filters. Simultaneous or parallel systems are multichannel with one or more detectors for each analyte element. Figure 4 is a schematic of a standard ICP-AES setup.

Interference effects in the ICP-AES, associated with the presence of matrix elements can be classified as either spectral or non-spectral. If accuracy of data is to be maintained it is important to characterise and quantify the effects so that appropriate corrective measures can be undertaken. Interference effects are potentially most deleterious when analyses are performed close to the limit of detection.

Spectral interferences arise when unwanted (i.e. non-analyte) radiation strikes the detector and contributes to the overall net line intensity. Sources of spectral interferences include direct line overlap (e.g. Ti 228.618 nm on Co 228.616 nm), ion-atom recombination continuum emission (e.g., Al), molecular band emission (e.g. OH at Al 309.271 nm) and stray light. Direct line overlap may be avoided by selecting an alternative interference-free wavelength. Interferences due to plasma background emission again can be avoided by selection of an alternative line or minimised through background correction. A wavelength scan in the region(s) of interest can help to clarify the nature of the problem (wavelength scans are also of value for checking the purity of stock solutions). If spectral interferences are found to be significant and cannot be avoided, such effects should be quantified and corrected for in the calibration scheme. Analysis of quality control standards or in-house synthetic solutions (containing appropriate levels of interfering elements) may be used to test the effectiveness of the correction procedures.

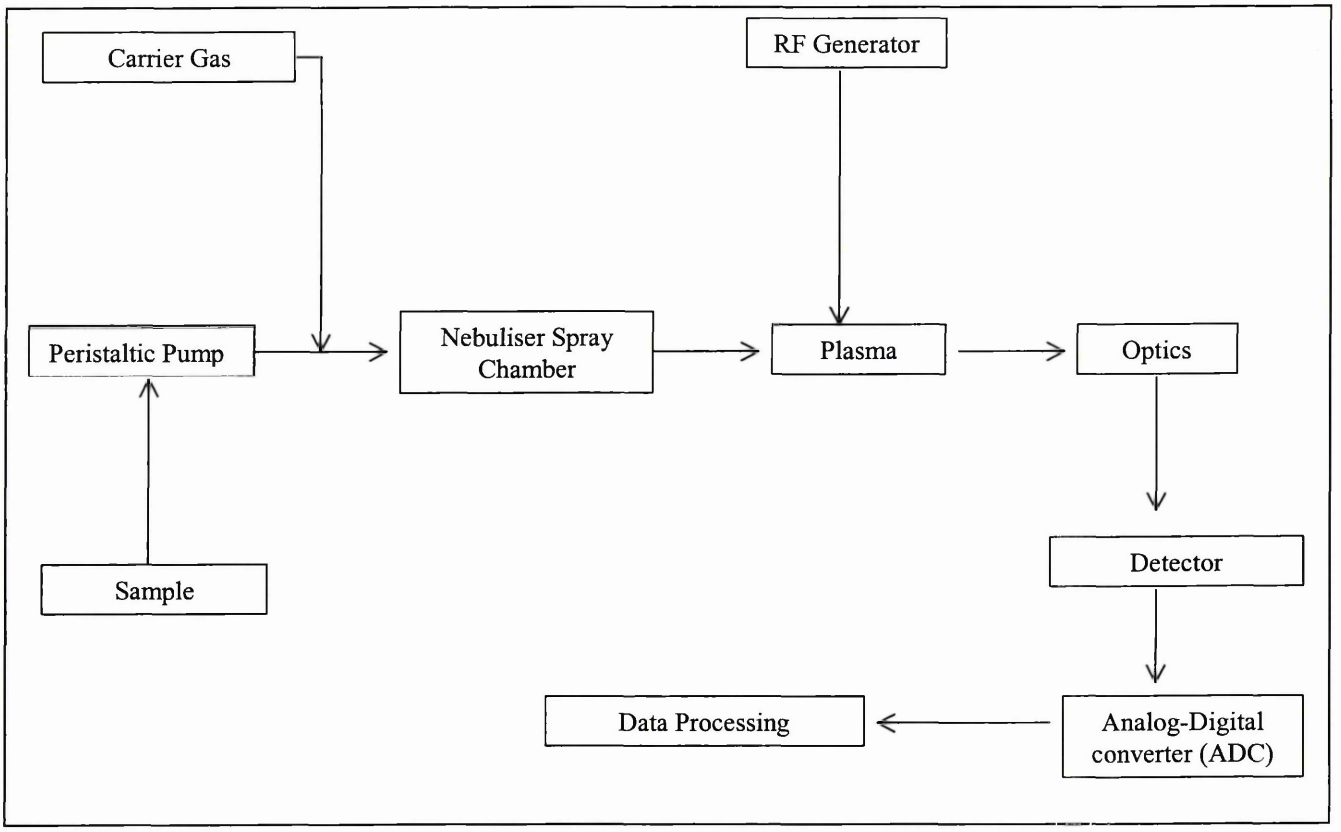

Figure 4: Schematic of a typical ICP-AES system.

Inductively Coupled Plasma Mass Spectrometry (ICP-MS)

Elemental analysis using ICP-MS is performed through the detection of metal ions in the solutions[146]. Sample introduction into the ICP unit takes place by conventional ICP sample introduction methods, which include nebulization, hydride generation, and electrothermal vaporization. The mass spectra are much simpler than the corresponding optical spectra and lower detection limits are attained. The spectra are used for qualitative analysis and quantitative deductions. Positive metal ions are directed through a sampling cone, which then interface with the plasma, then a second cone under vacuum direct them into the ion lens. The ions produced are extracted from the plasma into the mass spectrometer region which is held at high vacuum (typically 10^{-4} Pa). The vacuum is maintained by differential pumping i.e., the analyte

ions are extracted through a pair of orifices, known as the sampling and skimmer cones.

The ion beam in subsequently focused by the lens into a mass analyser, typically a quadrupole in ICP-MS instruments, which is also subject to a vacuum. Specific electrical fields are manipulated in the quadrupole to produce a stable trajectory for ions that have a particular mass to charge (m/z) ratio. Other ions with a different m/z ratio do not have stable trajectories for the applied field and therefore are not detected. Adjustment of the AC and DC potentials applied to the quadrupole during a mass scan provides the stable trajectories necessary for the sequential detection of ions with different m/z values.

Spectroscopic interferences in ICP-MS occur due to isobaric ions, adduct and refractory oxide ions and doubly charged ions. For quadropole analysis, isobaric interference occurs when two elements have isotopes that differ in mass by less than one unit. For example $^{40}Ar^{+}$ overlaps the peak of $^{40}Ca^{+}$ making it necessary to use the second most abundant isotope of calcium, $^{44}Ca^{+}$ during analysis. The analytes of interest and their isotope in a multi-element analysis should be chosen to avoid isobaric interference. If possible the most abundant isotope for each analyte should be chosen to provide the most sensitive analysis. Most elements have several isotopes, one of which should be free from interference. However the abundance of the isotope chosen may be significantly less, as in the case for calcium above ($^{40}Ca^{+}$ 97%, $^{44}Ca^{+}$ 2.1% abundance). Consequently sensitivity is compromised, therefore, integration time, the time allowed for the acquisition and detection of the species must be increased[152].

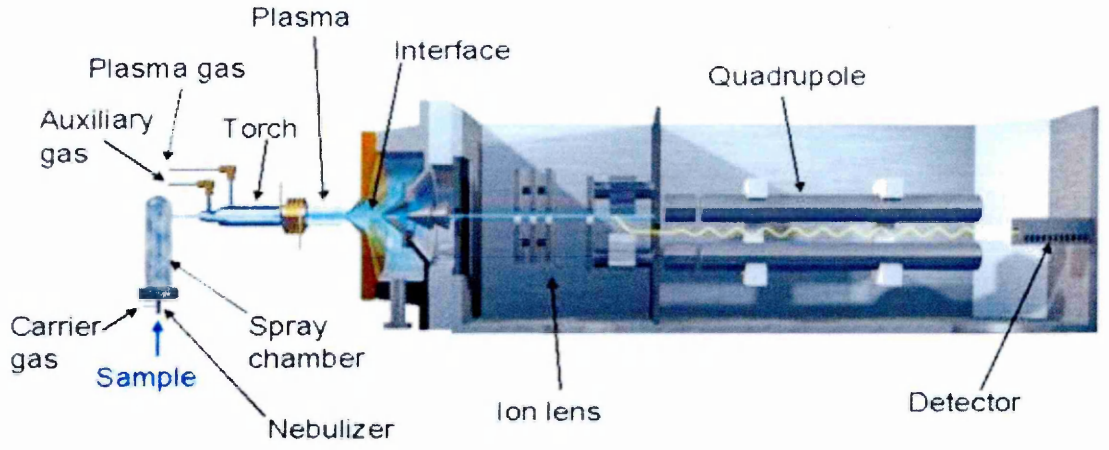

Figure 5: Schematic representation of the HP4500 set-up (reproduced from the Agilent technical library[147]).

Interaction between species in the plasma, matrix or space between the interface of the instrumental components can result in molecular ions that can overlap with the analytes of interest. The most serious interfering species are molecular oxides and hydroxides due to the availability of oxygen species from dissociation of aqueous solvents. In particular isotopes of argon and calcium oxides and hydroxides have masses that are congruent with isotopes of Fe, Ni, Co and Cu. Manipulation and optimisation of the operating conditions can reduce the magnitude of the population of oxide species. Recent developments utilise collision cells to break up molecular ions. The cell, which contains a gas, is positioned between the ion lens and the mass analyser. The ion beam is focussed to enter the collision cell where it is transmitted through the cell by a second quadrupole. Collisions in the cell effectively remove the molecular ions prior to entering the mass analyser.

By careful manipulation of the energy supplied in creating the plasma, singly charged ions are preferentially produced. Doubly charged species effectively reduce by half

the detected mass, hence there is a necessity to avoid their formation. The average ionisation energy of the atmospheric pressure argon ICP is dominated by the first ionisation potential of argon at approximately 15.7 eV (i.e. the ionisation capacity of the plasma). Most elements have first ionisation potentials below that of argon, therefore they too will be ionised. Also, most elements have second ionisation potentials greater than 15 eV, consequently singly charged ions are preferentially produced. There are exceptions such as the alkali earth metals Ca and Mg along with several other elements which all have second ionisation potentials below 15.7 eV, as a result of which there is spectral overlap between these species and adduct or oxide ions.

High concentrations of matrix constituents can cause a suppression of signal for the analytes of interest. The effect is dependent upon the total amount of matrix constituent rather than its proportional composition with the analyte species. High dissolved solid content in the sample can induce suppression of the analyte signal as a function of analysis time. The suppression or 'drift' problem is associated with the build-up of salts on the orifice of the interface sampling cone. As the salts accumulate the effective diameter of the cone's orifice is progressively reduced and the transmission of ions into mass analyser is correspondingly affected. Consequently, the ion signal at the detector will record a gradual decrease in the analytes as the analysis time progresses. Dilution of the sample is the simplest solution to the problem of drift. Another approach that can be used to correct for the instrument drift is the addition of an internal standard to the samples and standards.

Fourier Transform Infrared Spectroscopy (FT-IR)

FT-IR can be used to study the properties of soil minerals in-situ. Infrared radiation is electromagnetic radiation with a wavelength between 10^{-3} and 10^{-6}m respectively[148]. In infrared spectroscopy the number of waves per cm, called wavenumber (cm^{-1}) is commonly used. The infrared region is divided into three parts e.g., near-infrared = 0.78-3μm, middle-infrared = 2-15μm and far-infrared = 15-300μm. When a molecule is irradiated with near infrared light it can absorb radiation if the radiation has the same energy as the vibrational or rotational transitions of the molecule. In the far-infrared region mainly rotational energy is absorbed and these are responsible for the observed transitions. In the middle infrared region rotational as well as vibrational changes in the molecules give rise to the bands in the spectrum. In the near infra-red region mainly multiples of the vibrational energy (overtones) are absorbed. Rotational transitions have only weak energies about a hundredth those of the vibrational. They can only be observed with highly sensitive grating instruments.

Most vibrations of minerals are found in the 250 to 4000 cm^{-1} region (40 to 2.5μm). It requires three coordinates to describe the position of an atom in space. The atom has three degrees of freedom. A system of N free moving atoms has 3N degrees of freedom. For its rotational and transitional movements, three degrees of freedom of each are needed. Thus 3N-6 degrees of freedom are left to describe the vibrations of the molecule. These vibrations are called the normal or fundamental vibrations. But only a non-linear molecule e.g., H_2O, has 3N-6 vibrations. For a linear molecule, e.g., CO_2, only two rotational coordinates are needed, thus 3N-5 vibrations are possible. Stretching vibrations are those where the changes of the atomic distances occur mainly along the chemical bond connecting the atoms. They give a periodic

extension and contraction of the chemical bond. Vibrations other than stretching are called deformation vibrations. They give a periodic bending of the molecule. Deformations are of lower energy because the stretching forces are larger than the bending forces.

The components of a standard FT-IR are a beam splitter and two mirrors, one fixed in position, while the other is scanned back[149]. The collimated monochromatic radiation incident on an ideal beam splitter is divided into two equal beams, such that 50% is transmitted to one of the mirrors while 50% is reflected to the other mirror. These two beams are then reflected back and returned to the beam-splitter, where they are recombined and 50% sent through the sample to the detector. The remaining 50% is essentially lost as it is sent back towards the source. Because the moving mirror is scanned, the optical difference between the two recombined beams will be varied. When the path difference is an integral number of wavelengths, then the beams will be in phase and constructive interference will occur between the recombined beams.

Destructive interference occurs when the path difference is $\lambda/2$, i.e. when the moving mirror has moved a distance equivalent to $\lambda/4$ from the in phase position[150]. These differences in optical path are often referred to as optical retardation. If the moving mirror is scanned at constant velocity, the detector will measure a sinusoidally varying signal as the beams move in and out of phase. The intensity measured is therefore a function of the moving mirror displacement. As the moving mirror travels away from the position of zero path difference between the two recombined beams, the intensity of radiation reaching the detector varies as a cosine function of the optical retardation is expressed in the form –

$I(\delta) = B(\nu)\cos(2\pi\delta/\lambda) = B(\nu)\cos(2\pi\delta\nu)$, where $I(\delta)$ = the intensity of radiation at the detector, δ = the optical retardation, $B(\nu)$ = the single-beam spectrum intensity at wavenumber ν.

The single beam spectrum is then calculated by computing the cosine Fourier transform of $I(\delta)$. The combination of the monochromatic source of wavelength λ (the spectrum) and the cosine function (its interferogram) are known as a Fourier transform pair. For a polychromatic source (i.e. broadband infrared source) the interferogram represents the summation of all the individual cosine waves corresponding to each of the wavelengths in the source. These will only be in phase at the position of zero path difference. Hence, the strong interferogram centre-burst is normally observed.

When the particle size is larger than the wavelength of the incident rays, in this case 2.5-25μm, they will act as mirrors and thus influence the intensity of the IR bands by reflection. A decrease of the intensity of the transmitted rays may also be caused by Tyndall scattering of the rays by particles 10-15 times smaller than the wavelength. Hollow microcavities which have lost their water by heating, as in heated quartz, microdiscontinuities (crystal defects) and small local inhomogeneities of the refraction index in fluids due to fluctuations of density or concentration of the molecules, caused by thermal motions, are other sources of scattering. Scattering is a function of particle size, refractive index and wavelength.

When an absorption band is approached from the long-wavelength side, the refractive index of the sample increases until a maximum is reached. Thereafter it decreases

very sharply. As the amount of scattered radiation is proportional to the second power of the difference in refractive index of the particles and the embedded medium, the band will be asymmetric. The transmission is higher at the high frequency side of the band and the maximum is shifted to longer wavelengths. This effect called after Christiansen, its discoverer, decreases when particle size decreases to a diameter very small compared to the wavelength of the light.

The most commonly used sample preparation technique for solid materials is the pellet method. The sample is mixed in agate mortar with ethanol and an excess of KBr (1:200 to 1:700) of analytical quality for IR spectroscopy. After drying the mixture at 120°C, it is pressed in a die for ½ to 1 min at ~10 ton cm^{-2} under simultaneous suction of ~ 0.1 mm Hg (to remove entrapped air) into a transparent pellet of 13 or 20mm diameter and ~1 mm thickness and again dried for 1h at 120°C to remove the last traces of absorbed H_2O. A reference pellet of only the matrix is also made.

Environmental Scanning Electron Microscopy (ESEM)

The advent of the scanning electron microscope (SEM) in the late 1940s has facilitated the three dimensional visualisation of samples although the use of SEM as a commercialised instrument did not occur until 1965. All samples at this time were observed and analysed under vacuum. The ESEM may be seen as a natural extension of the SEM. The former incorporates all the conventional functions of the latter and in addition opens new ways of examining any sample, wet or dry, insulating or conducting[151]. Analysis of wet samples is important because it allows the user to observe samples without any pre-treatment, as a result of which the distribution of metals can be observed in their natural state. Elimination of sample preparation and

high vacuum constraints of the sample environment has opened up a host of applications for the ESEM. These include wet, oily, dirty, non-conductive samples that may be examined in their natural state without modification or preparation. The result is high resolution imaging of samples of any composition in a gaseous environment, at pressures as high as 50 Torr and temperatures as high as 1500°C. What makes this technique particularly useful is that the interaction of the electron beam with the sample generates a variety of signals, some of which are X-rays, that are characteristic of the sample and inorganic atoms bound to its surface.

The interaction of the electron beam with the sample produces X-rays. The lack of charging artefacts in the ESEM has direct benefits for X-ray analysis[152]. Because of its poor spatial resolution, the X-ray signal is more often used for analysis than imaging. It eliminates the interference normally associated with sample coatings and permits analysis at higher accelerating voltages or non-conductive samples. Another important factor to make X-ray analysis easier and more accurate is the necessity to consider what excitation energy is required to detect a particular element line. Generally the simple well-separated peaks are the lowest order peaks, K lines are simpler than L lines, which are simpler than M lines. Efficient X-ray excitation, usually requires a beam voltage two or three times the energy of the line of interest. Low beam energies are often used in the conventional SEM to reduce charging but also make X-ray analysis very difficult.

However ESEM has its problems such as the presence of skirt electrons that can further degrade X-ray spatial resolution. Electrons scattered out of the beam by gas molecules form a skirt. Displacement of a scattered electron from its original

destination on the sample on the sample is a function of – (a) scattering angle (b) remaining distance to the sample from the scattering site. Each successive scattering event increases the potential range of displacement. The size of the resulting electron skirt depends on the – (a) Beam gas path length (b) Sample chamber pressure. These potential problems can be overcome by – (a) minimising the path length that reduces the likely displacement from any one scattering event (b) minimising the chamber pressure also reduces the scattering probability. There is one other source of X-ray background of which the operator must be aware. Beam electrons can also excite X-ray from the chamber gas. These occur as a low-level characteristic of the gas composition. Again, minimising gas path length and pressure reduces this signal. Therefore gas choice may be an issue, depending on the elements within the sample matrix.

1.22 Sampling Locations for the Soils Used in this Thesis

The soil samples for this study were obtained from Oldhay, Totley, Sheffield. Maps from the early 1890s and a current map of the area with sampling points marked on them have been included in Appendix 1. The sampling points were chosen on the basis of historical evidence suggesting intense industrial activity in this area from the early medieval to late industrial revolution times. Lead ore was mined in the Peak District and transported to the Sheaf Valley for smelting[153]. There were ten smelting mills at Dore, Ecclesall, Norton and Totley from the late 16th to the middle of 18th century, for which there are historical records that confirm that several of these were involved in lead smelting. Numerous brooks criss-crossing the area would have been ideal for generating water power used during the early industrial revolution, for example in the 17th century there appear to have been a number of lead smelting mills located on Totley and Oldhay brooks which are tributaries of the River Sheaf.

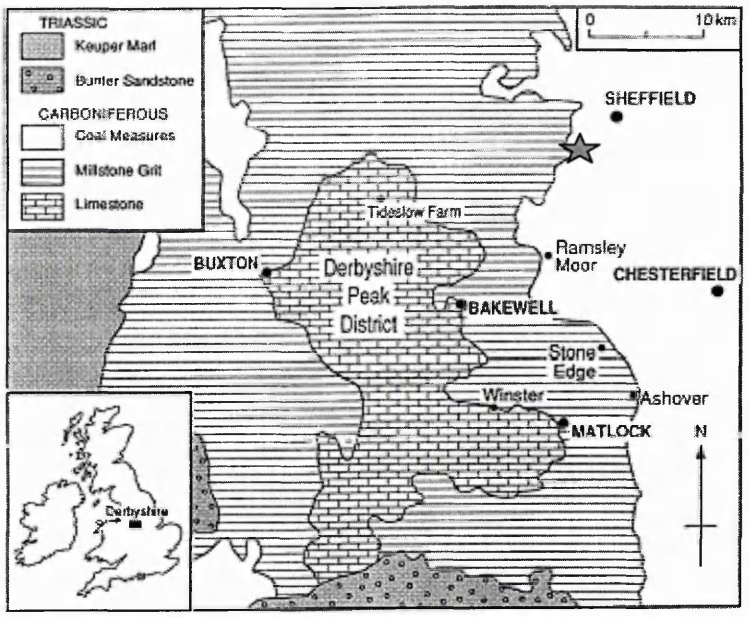

Figure 6 – Map of the sample collection area[153]. ★Approximate location of the Old Hay. Appendix 1 contains detailed maps of this area.

A well-documented smelter was one located at Old Hay, which was built and operated by the Earl of Shrewsbury from 1585. It changed ownership several times, but continued to smelt lead until 1805 when it ceased operation. Thereafter it was used for various other industrial activities such as a metal grinding mill etc[154]. Sparham[155] conducted a line transect survey of lead and zinc contamination in the area from Cordwell Valley to Totley. The average concentration of lead at the Old Hay site ranged between 2000-10000 mg kg^{-1} while zinc levels were 200-900 mg kg^{-1}. Estimates of background or natural levels of lead have been estimated to be approximately 30-300 mg kg^{-1}.

From a geological perspective the principal minerals of lead, copper and zinc found in the Peak District are Galena (PbS), Cerussite ($PbCO_3$), Sphalerite (ZnS) and Chalcopyrite (CuS)[156]. The main area of deposits for these minerals lies north-west to south-east of the site, immediately beneath the 'toadstone' horizons of limestone. Galena is found in the form of veins in the carboniferous limestone. Hence it can be

reasoned that any surface contamination of soil in this area with lead, zinc or copper may be assumed to have come from anthropogenic sources. In order to gain further confirmation as to the true origin of the lead contaminant, isotopic ratio (^{206}Pb:^{207}Pb) studies were conducted.

1.23 Aims and Objectives of the Thesis

The principal aim of this project is to ascertain the potential of the BCR sequential extraction procedure as a risk assessment tool and as a tool to predict and suggest remediation techniques for heavy metal contaminated soils. The first objective is to apply the BCR procedure for the study of metal fractionation in contaminated soils from a former lead smelting site, assuming that these soils were representative soils from a typical industrially contaminated site. The second objective is to use mineralogical techniques such as X-ray techniques and electron microscopy to study the accuracy of the data obtained using the BCR procedure. The third objective is to use data obtained from the BCR technique to design and execute soil washing and phytoremediation experiments. The data obtained from the remediation procedures will be compared with those obtained using the BCR procedure.

Chapter 2 Materials and Methods

2.1 Sample Collection and Preparation

Soil samples were collected from three locations (labelled C1, C2 and B1; see Figure 4, Appendix 1) in the Oldhay area. The sampling locations C1 and C2 were chosen because this area has a history of water-powered lead smelting before and during the Industrial Age[156]. Sample B1 was collected to provide data on the background concentration of metals in soils in this area. This location was not expected to have any previous history of major metal smelting operations because of the distance and height from the river.

The collected samples were taken to the laboratory where they were coned and quartered to give approximately 100g sub-samples. Larger objects such as stones and pebbles were removed and the samples were then thoroughly mixed and air-dried at 30°C for two weeks in a ventilated soil drying room to remove moisture. The air-dried samples were sieved through a 2mm sieve and then ground using a pestle and mortar to a fine powder capable of passing through a 100μm sieve.

2.2 Glassware and Reagents

All glassware used in the experiments were first thoroughly washed in a washing machine using a non-cationic surfactant washing powder, followed by thorough rinsing using tap water and deionised water. The washed glassware was soaked in 5% v/v nitric acid for a minimum of 24 hours, and rinsed with deionised water before use. Aqueous solutions were prepared with double-distilled deionised water. All reagents were of Aristar grade (BDH, UK) unless stated otherwise. All the salts were of high purity (w/w assay 99%) unless otherwise stated. The standards used for ICP-AES calibration, were of Aristar grade and were stored in a cold room at 4°C until required.

2.3 Safe Working Practices

To prevent accidents, injury to persons and harm to the environment, strict safe working practices were adopted. Prior to the commencement of every new set of experiments, a set of COSHH forms were completed and sent to the Departmental Safety Officer. Experiments were commenced subsequent to incorporation of the Safety Officer's recommendations and approval.

Prior to sample collection, it was ensured that the weather conditions were suitable i.e. no snow/ice, excessive wind or rain. Hard hat, Wellington boots, safety gloves and high-visibility vests were obtained from the Departmental store and put on during sampling. Proper precautions were taken during sampling, avoiding holes, river banks and steep inclines etc.

During the course of sample preparation, gloves, dust masks and laboratory coats were worn. The waste materials from the sample preparation were carefully enclosed in plastic containers and handed over to the Safety Technician for disposal. All sample drying was performed in a well-ventilated clean soil drying room.

Metal extractions using acids and reagents were performed in a fume hood fitted with an automatic alarm system. Acid resistant gloves, laboratory coat and safety goggles were worn for protection. The extractants were carefully decanted into other containers in the confines of the fume hood. Waste materials were transferred to special containers earmarked for waste. These waste containers when full were handed over to the Safety Technician who took steps to ensure their safe disposal.

Reactive chemicals such as hydrogen peroxide were stored in a refrigerator when not in use. Strong acids and organic chemicals were stored in a separate reagent cupboard fitted with a fume extraction system. All acids and liquid chemicals were stored in Winchester bottles and were transported in Winchester bottle holders to prevent spillage during accidents.

The University Electrician for electrical safety routinely checked all analytical electrical equipment and instrumentation. Routine maintenance of the instruments was carried out suitably trained competent technical staff. All gases for the instruments were stored in a well-ventilated, climate controlled alarmed storage room. The gas supply tubes had suitable valves and systems to cut the supply in case of emergencies.

2.4 pH Measurements

The pH of the three soils was measured using the British Standard BS 1377: Part 3:1990[157]. An initial sample was obtained and allowed to air-dry by spreading out on a tray exposed to air at room temperature. The samples were sieved on a 2mm sieve. Stones were rejected, ensuring that no fine material adhered to them, by brushing. The mass of the 2mm sample was recorded to the nearest 0.1%. Throughout these and subsequent operations, it was ensured that there was no loss of fines. 30 ± 0.1g of soil was weighed out and transferred to a 100mL beaker. 75mL of deionised water was added to the beaker and the suspension stirred for a few minutes. The beaker was covered with a watch glass and allowed to stand for 8h.

A pH meter was calibrated using buffer solutions (Aristar grade, BDH, UK) at pH 4.0, 7.0 and 9.2 and values for the soil solutions were recorded. The electrode was washed

with deionised water and immersed in the soil suspension. Three replicate readings of the suspension pH were taken. The electrode was removed from the suspension and washed with distilled water. The calibration of the pH meter was rechecked against one of the buffer solutions prior to analysis of the next sample.

2.5 Determination of the organic matter content

The percentage by dry mass of organic matter in the three soil samples was determined by ashing in an electric muffle furnace at 440 ± 25°C (BS 1377)[157]. 10g of each soil sample were carefully weighed out into clean heat resistant ceramic crucibles. The crucibles were transferred to a muffle furnace preheated to 450°C and left for 8 hours. At the end of the cooling period the crucibles were carefully removed from the furnace and allowed to cool. The cooled samples were carefully weighed and the mass difference noted. The total organic content was calculated using the following formula –

$\%LOI = (m_3 - m_4)/(m_3 - m_c) \times 100$

Where m_3 is the original dry mass of sample (in g);

m_4 is the mass of the crucible and the specimen after ignition (in g);

m_c is the mass of the crucible (in g).

2.6 Determination of Moisture Content

A clean, dry glass 100mL beaker was weighed to the nearest 0.1g. A sample of 300g of soil was taken, crumbled and placed loosely in the container and the lid replaced. The container with its contents was then weighed and the mass recorded. The lid was removed and the container with its contents was placed in an oven and dried at 105°C overnight. After drying, the lid was replaced and the sample was allowed to cool. The container and its contents were weighed to the nearest 0.1g. The following

formula was used to calculate the moisture content W, as a percentage of the dry soil mass–

$W = (m_2 - m_3)/(m_3 - m_1) \times 100(\%)$

Where m_1 is the mass of the container (in g); m_2 is the combined mass of the container and wet soil (in g); m_3 is the mass of container and dry soil (in g).

2.7 Density Fractionation Studies

Density fractionation i.e. separation of 'light' (clay) and 'heavy' (quartz) fractions, studies were conducted using a technique described by Cotter-Howells[158]. 5g samples of the 100μm fraction of the soil were transferred to four clean 50mL centrifuge tubes. 40mL of di-iodomethane (s.g. = 3.32) (BDH, UK) was added to the tubes and the sample shaken over a vibrating shaker, with only enough power to thoroughly homogenise the mix. This method yields two fractions of low and high density. The tubes were subsequently transferred to a bench-top centrifuge and centrifuged for 40 minutes at 1000rpm. The supernatant ('light' fraction) from each tube was transferred to clean 50mL centrifuge tubes and dried under pressurised nitrogen. The sediment ('heavy' fraction) was dried out using the same procedure. The masses of the resulting high and low density fractions were recorded and the concentrations of the major elements and minerals determined using ICP-AES and XRF.

2.8 Acid Solubilisation of Soil Metals

Soil samples of various particle sizes were homogenised using a pestle and mortar followed by drying overnight in a hot-air oven at 105°C. The dry ground samples were transferred to dark brown glass bottles and stored in a cold room at 4°C. A representative air-dried soil sample (0.2g <500μm) was transferred to a suitable glass beaker, to which aqua-regia (24mL, 1:3 conc. HCl/HNO_3) was added. The beaker

was covered with a watch glass and then the mixture was heated at 40°C for approximately 30 minutes on a hotplate to digest the organic component and then gently boiled for a further 75 minutes with the temperature increased gradually to 95°C.

On completion, the digest was allowed to cool, filtered using Whatmans No. 541 filter papers into volumetric flasks and made up to 50mL with deionised water. All the sample digestions were carried out in triplicate. The optimum mass for the digestions were determined by digesting 0.1, 0.2 and 0.3g of sample in 12, 24, and 36mL of aqua-regia. Optimum extraction time was established by digesting a fixed mass of sample (0.2g) in aqua-regia (24mL) for 1, 1.5, 2 and 2.5hrs.

2.9 Stable Lead Isotope Studies

In order to establish the origin of the lead contamination the isotopic ratio (^{206}Pb:^{207}Pb) studies were measured using the HP4500A ICP-MS[159]. These two isotopes were chosen because they can be measured most accurately[159]. The aqua-regia digest solutions for the soils were used for this analysis. The instrument software has in-built routines for the analysis of chosen isotopes.

2.10 Modified BCR 601 Sequential Extraction Procedure

Sequential extraction experiments were performed according to the Modified BCR 601 protocol described by Rauret et al[160]. This is a procedure developed by the European Commission's Standards, Measurements and Testing Programme (formerly BCR). This procedure was developed to harmonise the protocols for the fractionation of metals in sediments and soils, so that the results obtained from different laboratories are comparable[161]. A certified material CRM 483, which is a sewage

sludge amended heavy metal contaminated soil, has been developed to be used as a quality control tool[162].

Soil samples from the sampling points C1, C2 and B1 were sieved, dried and stored in darkened bottles. Known amounts of each of these soil samples were weighed and transferred to 50mL centrifuge tube using a plastic spatula. A known volume of the specified reagents were added to the tube and capped. The tubes were then shaken on a vibrating shaker for 10min and uncapped to release gases resulting from the reactions between the solutions and the soil minerals. The tubes were capped again and agitated further using the orbital shaker.

A Heidolph Unimax 1010 was modified by attaching a basket at the top, such that when the tubes with solution were placed flat on their sides in the basket, the orbital rotations of the shaking platform, caused an end-over-end movement of the solution in the tubes. This resulted in good soil-solution contact.

Step 1: 0.11M of ethanoic acid was prepared by diluting in a volumetric flask a stock solution of 16.5M (Aristar grade (99%w/v), BDH, UK). The solutions were shaken end-over-end manually ensuring optimum mixing of the solutions. 40ml of this solution was pipetted into a 50mL polypropylene tube containing 1g of soil dried for 2h at 105°C. The soil-solution mixture was agitated for 16 hours at ambient temperature (approx 20°C) on the modified Heidolph Unimax 1010 orbital shaker at 150 rpm. The extract was separated from the soil by centrifugation at 2500 rpm for 20 min. The supernatant was immediately decanted, filtered using a Whatman No. 541 filter paper and made up to 50mL in a volumetric flask with deionised water.

The solutions were analysed immediately on the ICP-AES and the ICP-MS after diluting the samples ten times to reduce the high organic content in the solution, mainly due to the ethanoic acid. In case of a delay in analysis, the samples were stored in clean, dry polyethylene bottles at 4°C in a cold room. The soil residue was washed with 20mL deionised water by shaking for 15 min followed by centrifugation at 2500 rpm for 20 min. The washings were discarded and the sediment stored at 4°C for the next step of the process.

Step 2: 0.5M of hydroxylamine hydrochloride was prepared by dissolving an appropriate quantity of the dry salt (Aristar grade, BDH, UK) in deionised water in a 250mL beaker. The solution was adjusted to pH 2 by adding drops of 2M nitric acid solution. The solution was transferred to a 250mL volumetric flask, which was capped and shaken end-over-end manually for 5mins and uncapped to release excess gases in the solution. The contents of the volumetric flask were made up to volume using deionised water. A 40 mL volume of this solution was added to the residue from step 1 and the soil extractions performed as described for the samples in step 1.

Step 3: A water bath was filled and the water allowed to reach a temperature of 60°C. A 10 mL volume of 30% w/v hydrogen peroxide (Aristar grade, BDH, UK) was added in small aliquots to the residue from step 2 in centrifuge tubes. The centrifuged tubes were covered with watch glasses and the soil was allowed to digest at room temperature for 1h in a fume hood. The soil in the tubes was agitated gently with a clean glass rod at regular intervals to optimise the contact between the soil and the solution. The tubes were then transferred to the water bath and allowed to stand in a test tube stand. The temperature of the water was slowly increased to 85°C and the

digestions were allowed to continue until the solution volume reduced to 1-2mL. A further 10mL of solution was added to the tube and the procedure repeated until the solution volume reduced to 1-2mL again. The sample was allowed to cool in the fume hood.

A 1M ammonium acetate solution was prepared by weighing out a known mass of the salt (Aristar grade, BDH, UK) into a 250mL beaker. The pH of the solution was adjusted to 2.0 using 2M nitric acid. The solution was then transferred to a volumetric flask and made to volume using deionised water. 40mL of this solution was added to the cooled moist residue and shaken gently end-over-end and allowed to stand for a few minutes with the cap of the centrifuge tube taken off to remove the excess gases. The sample was shaken for 16h, centrifuged and the extract separated as described in Step 1.

Residual Digestion – The residue from step 3 was washed with deionised water, centrifuged for 10min at 2500 rpm and the washings discarded. The residue was then dried overnight at 105°C and the weight noted. They were then transferred to a 125mL beaker and 24mL of aqua-regia added to the solution and boiled on a hotplate with the temperature being increased slowly from 40° - 120°C. At the end of 2h, the heat was turned down slowly to allow a gradual cooling. Upon cooling the solutions in the beakers were filtered into 50mL volumetric flasks and analysed for metals using the ICP-AES. All the above steps were repeated for the extraction of metals from the Reference Material CRM 601, as a quality assurance step.

2.11 X-ray Fluorescence (XRF) Analysis of Soil

A wavelength dispersive PW2400 X-ray fluorescence spectrometer (Philips, Eindhoven, The Netherlands) was used for quantitative bulk analysis of inorganics in the various soil fractions. Samples were dried overnight in a fan oven at 105°C to remove residual moisture in the samples. This was followed by an immediate, thorough homogenisation using a pestle and mortar. A known amount of each sample was then carefully weighed out into aluminium foil cups, using a top-pan balance accurate to 0.001g. The samples in the cups were then converted into 23.0mm x 3.5mm circular pellets using a hydraulic press at 20 tons/cm^2. The pellets were then placed in the XRF sample holder and metal analysis was performed on the XRF instrument running in a sequential mode. Loss on ignition (LOI) of the soil metals was analysed by heat fusing the soil at 1050°C, pressing the sample into a pellet followed by analysis on the XRF.

2.12 X-ray Diffraction (XRD) Analysis of Soil

Speciation analysis of the soil minerals was performed using a PW 1710 X-ray diffraction instrument (Philips, Eindhoven, The Netherlands) fitted with a chromium X-ray tube. The 100μm fraction of the soil was thoroughly ground and passed through a 60μm mesh size plastic sieve. The 60μm fraction was collected and dried overnight in a fan oven to remove residual moisture from the soil. This was followed by an immediate, thorough homogenisation using a pestle and mortar. Samples were then transferred to an XRD powder holder. Analyses was performed for 8h at a scan step size of 0.020° 2θ per second with 10 second scan time per step using 40kV generator potential and 25 mAmp tube current. Peak matching was performed using Xpert-Draw JCPDS software database[163].

2.13 Fourier Transform Infra-Red (FT-IR) Analysis of Soil

Fourier Transform Infra-red analysis, used to identify the clay type, was performed using a Mattson Polaris FT-IR (Mattson Instruments, Manchester, United Kingdom) fitted with a Greasby-Specac Diffuse Reflectance sample cell with the detector cooled to –196°C with dry air purging of the sample holder area[123]. This technique is widely used for powder mineral analysis because of the sensitivity of the method over normal transmission IR. The sample for analysis was prepared by grinding a 5% w/w sample/KBr mixture and transferred to a powder holder, and purged with dry air for 45 minutes before each spectrum was taken. The instrument was set to collect 100 spectra at $4cm^{-1}$ resolution.

2.14 Environmental Scanning Electron Microscopy (ESEM)/Energy Dispersive X-ray Spectroscopy (EDX)

The soil samples were imaged and elemental distribution on the particle surfaces was studied using a FEI-Philips XL30 environmental scanning electron microscope (ESEM-FEG, FEI) (Philips, Eindhoven, The Netherlands) running in the wet mode, coupled to an ISIS 300 EDX analyser (Oxford Instruments, High Wycombe, UK) using a Pentajet ATW detector. A small quantity of the sample was transferred to the ESEM sample stub and carefully placed in the analysis chamber. Images were acquired using the secondary electrons and ESEM images and EDX spectra for the area acquired. The areas of interest were also mapped for various elements using the EDX and the associated proprietary software.

2.15 Batch Extractions using Deionised Water

These experiments were performed to study the extraction patterns of metals in deionised water in the pH range 2-12. In order to prepare water solutions of varying pH, dilute hydrochloric acid (10%) and/or dilute ammonium hydroxide (10%)

solutions were added drop-wise to 200mL deionised water in a beaker and the pH adjusted to the required value. Soil samples (C1) of 1g masses were carefully weighed out into 125mL conical flasks. Solutions in the volume range 10 to 100mL at pH 2 were added to 125mL flat-bottomed polyethylene conical flasks, at increments of 10mL. The soil-solution mixture was agitated for 16 hours at ambient temperature (approx 20°C) on the modified Heidolph Unimax 1010 orbital shaker at 150 rpm. The extract was separated from the soil by centrifugation at 2500 rpm for 20 min.

The supernatant was immediately decanted, filtered using a Whatman No. 541 filter paper and made up to 50mL in a volumetric flask with deionised water. The conical flasks were thoroughly rinsed with deionised water and the filtrate added to the filtered solution in the volumetric flask. The extraction procedure was repeated using solutions in the pH range 3 –12, at the optimised volume. All the solutions were immediately acidified using 5% HCl to prevent microbial growth. The samples were analysed immediately on the ICP-AES and/or the ICP-MS; otherwise, they were stored in polyethylene bottles in a cold room at 4°C. The accuracy and precision of the analysis was checked using the reference material GBW07411 and by replicate analysis after every eight samples.

2.16 Soil Washing using Calcium Chloride and Magnesium Chloride

1M stock solutions were prepared by dissolving appropriate quantities of the dry $MgCl_2$ or $CaCl_2$ salts. The $CaCl_2$ solution was diluted to 0.1M using deionised water. The pH of these solutions was adjusted to 5.4±0.2 using 5% v/v HCl. Soil samples (C1) weighing 1g each were carefully weighed out into 125mL polyethylene conical

flasks. 40mL of solution ($CaCl_2$ or $MgCl_2$) was added to each of the tubes. The soil-solution mixture was agitated for 16 hours at ambient temperature (approx 20°C) on the modified Heidolph Unimax 1010 orbital shaker at 150 rpm. The extract was separated from the soil by centrifugation at 2500rpm for 20 min. The supernatant was immediately decanted, filtered using Whatman No. 541 filter paper and made up to 50mL in a volumetric flask with deionised water. The extract samples were then analysed immediately on the ICP-AES and/or the ICP-MS; otherwise, they were stored in polyethylene bottles in a cold room at 4°C. The samples were diluted 100 times prior to analysis using the ICP-AES or the ICP-MS to prevent matrix interferences arising from excessive Ca and Mg in the solutions.

2.17 Soil Washing using Ethanoic acid

The molarity for optimum extractions of metals was observed by performing batch extractions using ethanoic acid solutions in the concentration range 0.001-6M. A stock solution of 10M ethanoic acid was prepared by diluting an appropriate volume of Aristar grade ethanoic acid. The stock solution was progressively diluted to produce ethanoic acid of the required molarity (0.001-10M). The pH of the solution was adjusted to 2.8 ± 0.2 using 0.01M hydrochloric acid. Soil samples (C1) weighing 1g were transferred to 50mL polyethylene centrifuge tubes and 40mL ethanoic acid solutions of different molarities were added to each of the tubes. The soil-solution mixture was agitated for 16 hours at ambient temperature (approx 20°C) on the modified Heidolph Unimax 1010 orbital shaker at 150 rpm. The extract was separated from the soil by centrifugation at 2500 rpm for 20 min. The supernatant was immediately decanted, filtered using a Whatman No. 541 filter paper and made up to 50mL in a volumetric flask with deionised water.

The volume at which optimum metal extractions took place using ethanoic acid at the optimised molarity was deduced by performing batch extractions in the volume range 10-100mL. Soil samples (C1) weighing 1g were transferred to 125mL polyethylene conical flasks and ethanoic acid solutions of different volumes (10 –100mL at increments of 10mL) were added to each of the tubes. The remainder of the extraction and sample preparation process was similar to that used for the molarity optimisations.

The pH at which optimum metal extractions took place using the ethanoic acid solutions (at the optimised molarity and volume) was deduced by performing batch extractions in the pH range 2-10. The pH of the ethanoic acid solutions was adjusted using dilute HCl or NH_4OH. Soil samples (C1) weighing 1g were transferred to 125mL polyethylene conical flasks and ethanoic acid solutions were added to each of the tubes. The remainder of the extraction and sample preparation process was similar to that used for the molarity and volume optimisations. The solutions were analysed immediately on the ICP-AES and the ICP-MS after diluting the samples ten times to off-set the high organic content in the solution, mainly due to the ethanoic acid. In case of a delay in analysis, the samples were stored in clean, dry polyethylene bottles at 4°C in a cold room.

2.18 Soil Washing using Complexing Agents

Batch extraction experiments were conducted to study the molarity, volume and pH at for optimum metal extractions using EDTA, citric acid and L-cysteine[164]. These solutions were prepared by dissolving an appropriate quantity of the Na-EDTA, Na-citrate and L-cysteine salts (Aristar grade, Merck, UK) in deionised water. The molarity for optimum extractions of metals using these reagents was observed by

performing batch extractions using these solutions in the concentration range 0.001-1M. The volume at which optimum metal extractions took place using these reagents (at the optimised molarity) was deduced by performing batch extractions in the volume range 10-100mL. The pH at which optimum metal extractions took place using the three reagents (at the optimised molarity and volume) was deduced by performing batch extractions in the pH range 2-10. The extraction, sample preparation and analysis procedures were similar to those discussed previously for ethanoic acid.

2.19 XRF Analysis of the Residual Soils from the Batch Extractions

The residual soils from batch extractions using each of the reagents were air dried at 105°C, thoroughly ground, pelletised and analysed for changes in bulk mineral composition using XRF.

2.20 Customisation of the modified BCR 601 Sequential Extraction Procedure

Step 1: Ethanoic acid (40mL, 3.5M, pH 5) was transferred by pipette to the sample tube containing 1g of soil. The soil/solution mixture was agitated for 16h at ambient temperature (approx. 20°C) on a Heidolph Unimax 1010 mechanical shaker at 150rpm. At the end of the shake time, the sample tubes were centrifuged at 3000rpm for 20mins. The supernatant was immediately decanted and made to volume (50mL) with distilled water and subsequently analysed by ICP-AES. The sample residue from Step 1 was washed with 20mL of deionised water with shaking for 15 minutes. The washings were discarded after centrifuging at 3000rpm for 15mins.

Step 2: 60mL of 0.5M hydroxylamine hydrochloride (adjusted to pH 2 with 25mL of 2M nitric acid) was added to the sample residue from step 1, and after extraction, analysis was performed as described in Step 1.

Step 3: Hydrogen peroxide (30%) was added slowly to the residue from step 2 and allowed to digest at room temperature for 1 hour with occasional manual shaking. The digestion was continued in a water bath (85°C) for 1 hour after which time the sample tube cap was removed and the volume reduced to approximately 3mL. A second aliquot of hydrogen peroxide was added and the procedure repeated (minus the room temperature digestion period) and the volume reduced to approximately 1mL on completion. Ammonium acetate (50mL, 1mol L^{-1}) adjusted to pH 5 with concentrated nitric acid was added to the residue followed by extraction and analysis as described above. The residue after the sequential extraction steps was subjected to an aqua-regia digest as previously described.

2.21 XRD of the residue from the Sequential Extraction Process

The residue from each step of the sequential extraction process was dried at 105°C, ground thoroughly and analysed using XRD for changes in speciation of the metals as a result of the treatments.

2.22 Column washing studies

These experiments were carried out by packing 50g of soil (2mm fraction) into a Pharmacia76/40 chromatographic preparative column with cellulose filters (schematic of the experimental in Figure 7) [165]. The columns were packed manually and flushed with deionised water (pH 7) using a peristaltic pump. The optimum pump speed (the speed at which there were no blockings or leakages) was observed to be 2.5mL min^{-1}.

The washing experiments were performed by pumping EDTA (at the optimum molarity and pH) at a rate of 2.5mL min^{-1} through the columns and 25mL aliquots (71 were collected). The aliquots were continuously collected over a period of 10h without any breaks. Each aliquot was analysed for pH and stored in a temperature controlled cold room at 4°C. The samples were diluted twenty five times in 25mL volumetric flasks and analysed using the ICP-AES. The experiments were repeated using 1.75M and 0.11M ethanoic acid at pH 5±0.2 and 2.8±0.2 respectively.

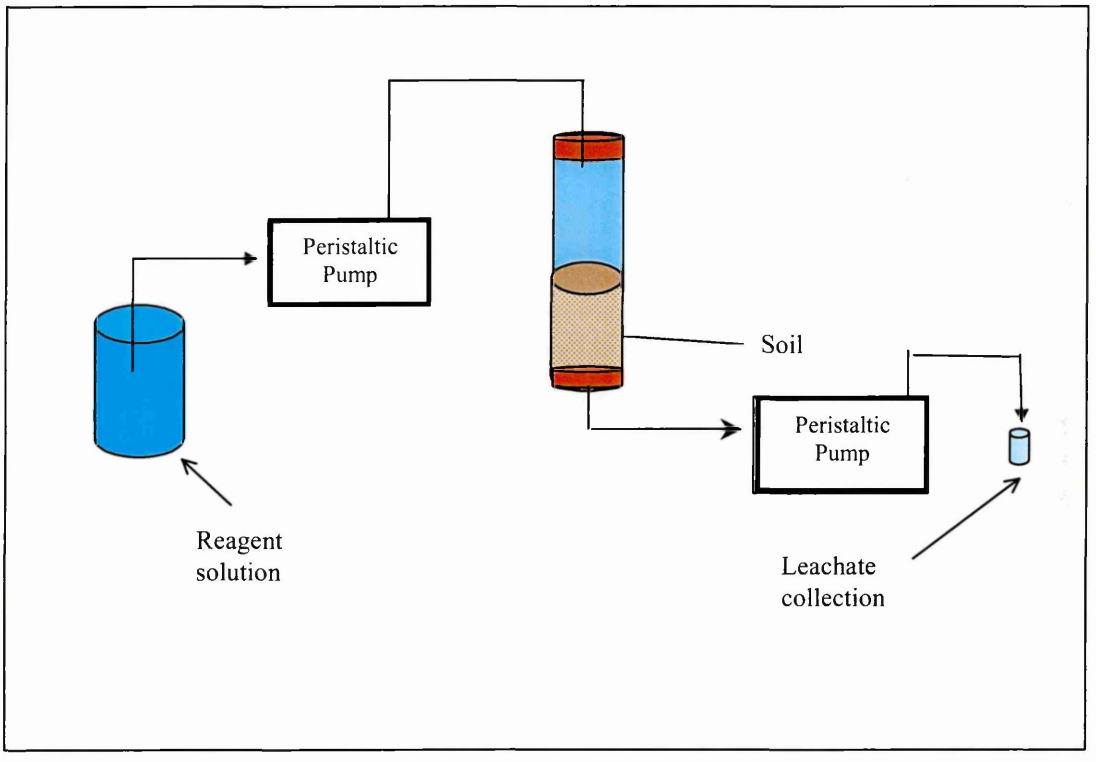

Figure 7 – Experimental set-up for the column washing studies (column diameter: 40mm; column length – 40cm).

2.23 Phytoextraction of Metals from the Soils

Helianthus annuus (sunflower) *var.* Dwarf Yellow seeds were obtained from Moles Seeds (Turkey Cock Lane, Colchester, Essex). The seeds were planted in seed trays, using GEM multipurpose compost and then germinated in a climate-controlled greenhouse for 21 days. The seedlings were transplanted to 4" x 6" plant pots filled

with contaminated soils C1, C2 and B1. The first crop (H1) from each soil was harvested 4 weeks after transplantation, second (H2) and third (H3) crops were harvested after 6 and 8 weeks respectively after transplantation. The soil was kept moist at all times by regularly watering with tap water, which was analysed for metal content. The harvested plants were thoroughly washed under deionised water to remove soil attached to the roots and separated into root, shoot and leaves. Each part of the plant was freeze dried for approximately 20hours.

The dry mass of each part of the plant was obtained on removal from the freeze drier. Each section of the plant was ground using a clean (acid-washed), dry pestle and mortar and then individually digested in concentrated nitric acid by gentle boiling on a hot plate for 30 minutes. The resultant digest was made up to volume in volumetric flasks and analysed by an Agilent 4500 ICP-MS for metal content.

2.24 Phytoextractions by Plants Growing in Hydroponics Solutions

Helianthus annuus var. Russian Giant (Thomson & Morgan Seeds, Ipswich, UK) seeds were sown in nutrient rich rock wool and allowed to germinate in a propagator located in a climate controlled greenhouse (20°C, 12h light). After the complete emergence of the first set of cotyledons, the seeds were transferred to a hydroponics nutrient solution (Nutravita®, Aquaculture Ltd., Sheffield, UK). Table 3 lists the concentration of nutrients in the Nutravita solutions. The solution consisted of two parts – A and B, 4 mL of each of which was dissolved in 1 litre of deionised water and the pH adjusted to 5.4 ± 0.2 in 500 mL polyethylene bottles. The seedlings were allowed to grow in solution for a period of six weeks, with the nutrients replenished every two days to keep the pH and nutrient content stable.

Nutrient	Part A (% composition)	Part B (% composition)
Nitrogen (total)	5.13	5.13
Nitrate nitrogen	4.75	4.38
Ammoniacal nitrogen	0.38	0.38
Nitric nitrogen	0	0.38
Potassium (K_2O)	7.8	7.8
Phosphorus (P_2O_5)	2.6	2.6
Calcium	3.63	2.63
Magnesium (MgO)	1.7	1.25
Boron	0.0087	0.0087
Copper	0.002	0.002
Iron	0.068	0.068
Manganese	0.0145	0.0145
Molybdenum	0.0013	0.0013
Zinc	0.0098	0.0098
Cobalt	0.0013	0.0013
Nickel	0.0013	0.0013

Table 3: Composition of Nutravita hydroponics nutrient solutions.

A first set of experiments were conducted using solutions spiked with 1000 mg L^{-1} Pb^{2+}, which were prepared by dissolving 1.64mg L^{-1} $Pb(NO_3)_2$ (Merck UK Ltd) solution in double distilled deionised water. A second set of experiments were performed using 10, 100 and 1000mg L^{-1} Pb^{2+} spiked solutions, which were prepared by dissolving an equivalent amount of lead salt in nutrient solutions without any PO_4^{3-} content (Aquaculture Ltd., Sheffield, UK). The stock 1000mg L^{-1} solutions (containing nutrients) were diluted to produce 100 and 10 mg L^{-1} solutions. The pH of the solution was adjusted to 5.6 ± 0.2 with NH_4OH. The plants were transferred to polyethylene bottles containing the solutions. An equivalent number of control plants were allowed to grow in unspiked deionised water and nutrient solutions for the same period of time. At the end of the scheduled growth period, the plants were removed from solutions, thoroughly washed with dilute HCl and deionised water, separated into root, stem and leaves and freeze-dried overnight. The dry biomass was ground in clean pestle and mortars and stored in sample tubes in a dessicator. Each section of

the plant was then individually digested in concentrated nitric acid by gentle boiling on a hot plate for 30 minutes. The resultant digest was made up to volume in volumetric flasks and analysed using the ICP-MS for metal content.

Wavelength dispersive X-ray fluorescence (Philips) analysis of the root samples from hydroponics experiments was conducted and the results compared. X-ray diffraction analysis of the samples was conducted using a Philips 1710 powder diffractometer and the peaks matched with a JCPDS database. A known amount of the sample 0.002g was ground in 200 mg of KBr and pressed into a disc, followed by FT-IR analysis using a Galaxy 4020 series FT-IR spectrometer. The samples were also analysed using a FEI-Philips XL30 environmental scanning electron microscope (ESEM-FEG, FEI, Eindhoven, Netherlands) coupled with an ISIS 300 EDX analyser (Oxford Instruments, High Wycombe, UK) using a Pentajet SATW detector.

2.25 Protocols for Analyses using ICP-AES and ICP-MS

Analyses of metals in the extractants were performed using a Spectro Instruments ICP-AES, when the concentration of metals in solution was in the concentration range 2-200 mg L^{-1}. The ICP-AES was calibrated using 0, 1, 10, 100, 250, 500mg L^{-1} multielemental calibration solutions. These solutions were prepared from stock solutions of each of the elements (Aristar grade, Merck, UK) by batch dilutions of 1000mg L^{-1} stock solutions. When the concentrations of the metals were too close to the instrumental detection limits (i.e. less than ten times the lower limit of detection), the solutions were analysed using the HP4500 ICP-MS. The ICP-MS was calibrated using 0, 1, 10, 100, 500 and 1000 μg L^{-1} multielemental calibration solutions. These

solutions were prepared by batch dilutions of 1000μg L^{-1} solutions. The operating conditions for these two instruments are described in Table 4.

Instrument		**ICP-AES**	**ICP-MS**
Model		Spectro	Agilent 4500a
Power		1220 W	1200W
Torch		Three piece	Fassel
Spray chamber		Cyclonic	Cyclonic
Nebuliser		Cross flow	Babington
Sample introduction		Peristaltic	Peristaltic
Solution uptake		0.8 mL min^{-1}	0.8 mL min^{-1}
Nebuliser gas flow rate		1.0 L min^{-1}	1.0 L min^{-1}
Nebuliser gas pressure		234 kPa	234kPa
No of sweeps per replicate		1	1
No of replicates		5	5
Emission wavelengths (nm)			m/z
Pb	220.351		^{208}Pb
Hg	253.852		^{198}Hg
Cd	226.502		^{111}Cd
Cu	324.754		^{63}Cu
Zn	213.856		^{64}Zn
Cr	267.716		^{53}Cr
Mn	257.610		^{55}Mn

Table 4 – Operating conditions for the analysis of metals using the ICP-AES and ICP-MS.

Procedural blanks were analysed to study the contribution of reagents and glassware to contamination. One instrument blank (deionised water) was analysed for every 10 samples. Contributions from the matrices into which the analytes were extracted were ascertained by analysing blank matrix samples. Calibration standards were prepared in the same matrices as the reagents used for the extractions, in order to compensate for matrix interferences. Known standards were run on both ICP-AES and the ICP-MS instruments after every 10 and 8 samples respectively in order to check for instrumental drift. Recalibration was carried out if the results differed by more than 10%. Additionally, calibration standards were analysed after each recalibration to assess 'memory' effects. The quality of these analysis procedures was checked using the reference materials GBW07411 (LGC Ltd., Teddington, UK).

2.26 Analysis of Metal Speciation in Solutions using the PHREEQC and MINEQL+ Geochemical Models

Geochemical software packages can be used to simulate chemical equilibrium in solutions and use the data to predict metal speciation in solutions (see Table 5). Some of the most widely used packages are PHREEQC and MINEQL+. PHREEQC is a modelling software used for simulating chemical reactions and transport processes in natural and polluted waters[166]. The programme is based on equilibrium chemistry of aqueous solutions interacting with minerals, gases, solid solutions, exchangers and sorption surfaces, and includes the capability to model kinetic reactions with rate equations that are specified by the user[167]. This package uses three databases as backend data warehouses for the simulations. Surface complexation constants for two of the databases distributed with the programme (PHREEQC.DAT and WATEQ4F.DAT) were taken from Dzombak and Morel[168]. Surface complexation constants for an additional database, MINETEQ.DAT, distributed with the programme were taken from MINETEQA2. Ion exchange reactions are modelled using the Gaines-Thomas convention and equilibrium constants derived from Appelo and Postma[169] were included in two of the databases distributed with the programme.

MINEQL+ is a chemical equilibrium modelling system that can be used to perform calculations on low temperature (0-50°C), low to moderate (<0.5M) aqueous solutions[170]. MINEQL+ is a data driven program that can be used by selecting chemical components from a menu, scanning the thermodynamic database and running the calculations. However, MINEQL+ also provides tools that allow the user to take control of the reaction data, create a thermodynamic database, perform synthetic titrations and automatically process multiple samples (such as field data). MINEQL+ uses a thermodynamic database that contains the entire USEPA

MINTEQA2 database plus data for chemical components that the EPA did not include, so all calculations produce results compatible with EPA specifications.

Model	Features
PHREEQC	Fast convergence on carbonate problems; efficient and modular program
EQ3	Fast convergence; mineral equilibrium fixes component concentration; EQ6 has path finding ability; bulk program; large database
GEOCHEM	Database with many species of interest for soil science
MINEQL+	Large database, aimed at complexing of heavy metals; fancy models for adsorption on soil surfaces
ConSim	Derives remedial targets for soils based on assessment of risk to controlled waters.
MODFLOW	Describes the three dimensional flow of contaminant plumes

Table 5: Available geochemical computer models[169].

Chapter 3 Metal Fractionation Studies

3.1 Introduction

As discussed previously, the retention of metals in contaminated soils occurs as a result of precipitation onto primary (silicates) or secondary minerals (oxides, carbonates) or complexation with soil ligands or oxyhydroxides[171]. Metals can also exist as independent minerals at heavily contaminated sites e.g., as HgS (cinnabar), CdS, $CdCO_3$, PbO etc. Metals in soil can be mobilised through a variety of processes, mainly as a result of changes in soil conditions. A decrease in the pH of the soil solution (acidification) causes metal mobilisation through cation exchange, hydrolysis and dissolution of minerals such as carbonates. Conversely, increase in pH to alkaline levels results in mobilisation of anionic elements such as Cr, As and Se. Strongly oxidising conditions may cause the dissolution of metal sulphides, while strongly reducing conditions may cause dissolution of iron and manganese oxyhydroxides. Metals can also be leached out as a result of an increase in concentration of organic ligands such as EDTA and citric acid.

Metal leaching due to these mechanisms results in a potential risk of contamination to controlled waters. Therefore, any risk assessment procedure used to understand the contamination risk to controlled waters should have the ability to predict the impact of environmental changes (pH, redox conditions etc.) on metal mobility in soil solutions. The Environment Agency and the Scottish Environment Protection Agency (SEPA) have recognised the need to "develop a standardised, practical and reasonable approach to soil and groundwater remediation for the protection of water resources that can be applied on a site-by-site basis" and is consistent with current legislation and guidance[172]. The method for identifying these potential remedial standards is

based on a risk assessment approach that involves the use of a 'source-pathway-receptor' analysis.

The Environment Agency in the document R&D 20 recommends the application of the NRA leach test for Tier 1 analysis of a four tiered analysis protocol for risk assessment[173]. The four-tiered approach was introduced in 1999 to provide a logical and verifiable framework for the assessment of potential risk of significant harm to controlled waters as a consequence of contaminated soil. The first tier assesses risk based on metal mobility in soils, which is measured using the NRA leach test and published metal specific K_d values. The second tier takes into account dilution and dispersion effects along with data from Tier 1 analysis. The third and fourth tiers take into account natural attenuation and biodegradation of contaminants along with the data from the first two tiers. In practice, it is very difficult to quantify the effects of dilution, dispersion, natural attenuation and biodegradation on contaminant mobility. As a result, most practitioners simply use data from Tier 1 analysis for the assessment of risk to controlled waters.

The NRA leach test used for Tier 1 analysis involves the agitation of a mass of contaminated soil with a volume of water (eluate) and measurement of the concentration of contaminants in the eluate. Test parameters such as the mass of soil, the volume of eluate, the period of agitation, preparation (crushing) of soil, and environmental controls such as pH and temperature can be set as deemed fit by the analyst. This lack of standardisation has severely limited the application of this procedure as a credible risk assessment tool[174]. Another drawback of the NRA leach

test is that it does not predict the effect of changes in soil conditions on metal mobility nor does it provide any information on the fractionation of metals.

However, sequential extraction procedures have been developed that can provide clues about the effect of changes in environmental conditions on the mobility of metals in soils[175]. These procedures involve the use of a series of soil fraction/phase specific leaching agents to study the binding of metals to soil minerals[176]. Several authors have used data obtained through the application of Tessier procedure for the prediction of metal leachability and bioavailability[177]. Accurate information on metal fractionation and the risks posed by soil contamination is critical to the design of efficient procedures for the remediation of contaminated soils. Another approach for the study of metal fractionation is the modified BCR procedure[178]. This procedure was originally developed for the study of metal fractionation in sediments. However, it is gaining increasing popularity as a tool to study metal fractionation in soils. It is a three-stage procedure that involves the use of 0.11M acetic acid, 0.5M hydroxylamine hydrochloride (pH ~ 2.2), boiling soil samples in 66%v/v H_2O_2 and 1M (pH ~ 2.2) ammonium acetate. The first stage extracts metals that are ion-exchangeable, and those bound to carbonates and kaolinites (1:1 clays)[179]. The second stage extracts metals bound to phases that are reducible i.e. those bound to iron and manganese oxides and 2:1 clays such as illites and smectites. The third stage extracts the oxidisable fraction of the metals i.e. fraction bound to humic and fulvic acids in the soil.

The author investigated the applicability of the modified BCR procedure as a potential risk assessment tool and as a precursor to the application of procedures such as soil

washing and phytoextraction for the remediation of soils. Mineralogical techniques, such as XRF, ESEM/EDX and XRD along with the modified BCR procedure were used for an in-depth analysis of the distribution of metals in soils. This data was used to evaluate potential remediation strategies for the soil, which included soil washing and phytoremediation.

3.2 Results and Analysis

The pH of the soils C1, C2, and B1 was 5.9, 5.6 and 5.6 respectively. The moisture content of the three soils was 39%, 32% and 33% (w/w) respectively. The total organic content of the three soils was 2%, 3% and 3% (w/w) respectively. It is noteworthy that during sampling and preparation, several slag particles were found in and removed from all three soils. These slag particles had the potential to overestimate the concentration of metals actually bound to the soil particles. Therefore the soil samples were sieved and fractions with a particle size of $\leq 100\mu m$ were collected and used for further analysis.

3.2.1 Pseudo-total digestions

The digestion time for optimum extraction of Pb, Zn, Mn, Mg and Cu was observed to be two hours. Data obtained from the analysis of the digested samples are presented in Table 6. They show that the mean concentration of Pb in the soil samples C1, C2 and B1 was 8100±445, 1550±121, 1020±130 mg kg^{-1} respectively. This suggests that the soil might have been contaminated with Pb, as the threshold soil guideline value (SGV) for Pb in the CLEA guidance document CLR 7 is 750mg kg^{-1} for residential gardens and allotments[180]. The concentration of all the other measurable trace elements (Cr, Cu, Mn, Cd and Zn) was below the CLEA and ICRCL recommended

levels[181,182,183]. The completeness of the digestion procedure and the accuracy of the analysis procedure were confirmed using the reference material NCSDC7703. One tailed student t-test (with unequal variance) showed that there is no significant difference between the obtained and certified values.

Soil	Cu	Al	Mg	Cr	Mn	Pb	Zn
B1 Conc (mg/kg)	25±1	12500 ± 805	1060 ± 176	14.8 ± 1.4	189 ± 10	1020 ± 130	95 ± 6
C2 Conc (mg/kg)	19.0 ± 1.3	10800 ± 376	1170 ± 37	17.3 ± 1.0	489 ± 28	1550 ± 121	107 ± 15
C1 Conc (mg/kg)	41 ± 1	15800 ± 799	2350 ± 165	28.4 ± 2.9	493 ± 47	9000 ± 445	371 ± 28
NCSDC77303 (mg/kg) **Certified values**	65±5	-	-	20±5	9700±600	2700±100	3800±300
NCSDC77303 (mg/kg) **Obtained values**	67±3	-	-	19.6±1.3	9700±224	2650±61	4000±108

Table 6: Results from the digestion of soil in aqua-regia, followed by multielemental analysis of the solutions using ICP-AES and ICP-MS.

3.2.2 XRF analysis

The mineralogical composition (%w/w) of the soil sample C1 was analysed using the XRF. The purpose of this analysis was to complement the data obtained from the pseudo-total digestions and to study the distribution of metals in the different fractions. Four fractions of the soil sample C1 were analysed i.e. the 2mm, 100μm, 'light', 'heavy' fractions (data presented in Table 7). The 2mm fraction is composed of particles that are ≤ 2mm in diameter. The 100μm fraction was composed of particles that were ≤100μm in diameter. The 2mm fraction was also separated into 'light' and 'heavy' fractions based on density (using diiodomethane).

The total LOI (loss on ignition) of the soil mass (2mm fraction) was approximately 16.4%. The molecular ratios of SiO_2:Al_2O_3 was >2, indicating the presence of naturally abundant fire clays in the soil[184]. These are clays that are dominated by

kaolinite and illite with alumina contents varying between 25% and 40%. The presence of sulfur (1.1%) and without any variations in concentration between the different fractions suggested the presence of metal sulphates in the soil [11]. Similarly, the presence of phosphorus (0.9%) in the soil suggested the possible presence of metal phosphates in the soil[11].

The data show that the average concentration of Pb in the 2mm, 100μm fractions was 5200 and 7100mg kg^{-1} respectively. The concentrations of Pb, Ca, Fe and Zn in the 100μm fraction were approximately in the same range as those observed from the wet digestions. The higher concentration of the metals observed in the 100μm fraction was probably due to the dilution of clays and metal oxides in the 2mm soil fraction by quartz, as metals are generally concentrated in fines such as clay and silt. Evidence for this preferential desorption comes from analysis of the 'light' (clay) and 'heavy' (quartz) fractions from the density fraction studies. The mean concentration of Pb in the 'light' and 'heavy' fractions was observed to be 12200 and 3900mg kg^{-1} respectively.

Mineral	% Composition (w/w)	% Composition (w/w)	% Composition (w/w)	% Composition (w/w)
	2 mm fraction	100 μm fraction	Clay (light)	Quartz (heavy)
Na_2O	0.4	0.4	0.4	0.7
MgO	1.0	1.1	1.2	0.4
Al_2O_3	19.1	20.4	23.6	9.8
SiO_2	64.9	61.0	53.7	75.2
P_2O_5	0.8	0.7	0.9	0.3
SO_3	1.1	1	1.1	0.9
K_2O	2	2.1	2.4	2.0
CaO	1.5	2.2	2.0	1.3
Mn_3O_4	0.1	0.1	0.2	0.1
Fe_2O_3	6.7	7.9	11.1	6.1
ZnO	0.04	0.04	0.1	0.04
PbO	0.5	0.8	1.2	0.4

Table 7: Mineral composition of the soil C1 as analysed using XRF.

3.2.3 X-ray Diffraction Analysis

XRD analysis of 100μm, light and heavy fractions of the sample C1 was performed to study the nature and speciation of minerals in the samples (data presented in Figure 8 and Table 8). The 2mm fraction was not analysed, as the presence of large quantities of quartz in the samples results in the masking of other crystalline mineral peaks by quartz peaks in the XRD spectrum [11]. This phenomenon was confirmed in the XRD spectra of the three samples, which show that the spectra for the 'heavy' and 100μm fractions consisted of quartz peaks of greater intensity than those observed in the spectra for the 'light' fraction in the 30-45°2-theta range. The identity of these peaks was confirmed from the JCPDS database (Table 8)[185]. This database lists the identity of crystalline compounds based on the relative position of their respective peaks in an XRD spectrum.

Crystalline iron compounds were present principally in the form of goethite (FeOOH) and iron phosphates. Crystalline calcium compounds were present principally as phosphates ($Ca_2P_2O_7$), hydroxyapatite ($Ca_{2.5}Pb_{7.5}(OH)_2(PO_4)_6$) and calcium lead silicates ($Ca_2Pb_3Si_3O_{11}$), which may have been part of the lead slag in the soil. Relatively intense peaks were observed for the clays, illite ($K(Al, Fe)_2AlSi_3O_{10}(OH)_2.H_2O$), kaolinite ($Al_2Si_2O_5(OH)_4$) and muscovite ($KAl_2Si_3Al_{10}(OH)_2$). Crystalline lead compounds were present principally as lanarkite ($Pb_2(SO_4)O$), other lead sulphates (such as $Pb(S_2O_3)$), carbonates (Pb_2OCO_3), pyrophosphates ($Pb_2P_2O_7$) and silicates ($Ca_2Pb_3Si_3O_{11}$). All the other metal compounds were undetectable because of their low concentration, as the minimum detection limit (MDL) for the XRD was approximately 0.25%.

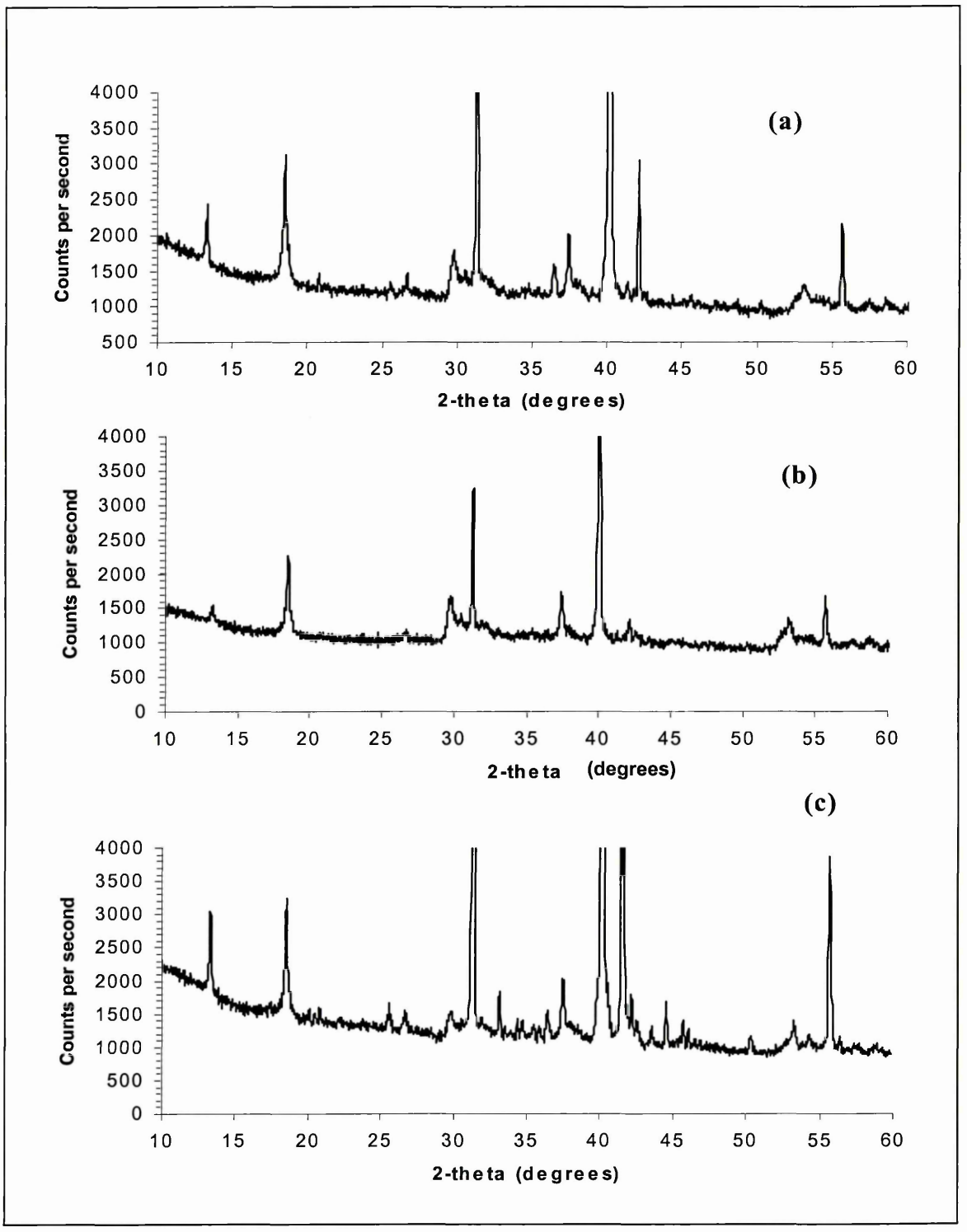

Figure 8: XRD spectra for (a) 100 μm, (b) 'light' clay and (c) 'heavy' quartz fractions of sample C1 (see Table 8 for peak assignments).

Peak (°2θ)	Possible Mineral Species
13	Quartz [SiO_2], Goethite [FeO(OH)], illite [$Al_2Si_2O_5(OH)_4$], Lanarkite [$Pb_e(SO_4)O$], Lead sulfur chloride[$Pb_7S_2Cl_{10}$], Lead oxide carbonate [Pb_2OCO_3]
18	Quartz, Goethite [FeO(OH)], Lead silicate [$Pb_3Si_2O_7$], Kaolinite-1Md [$Al_2Si_2O_5(OH)_4$], Lanarkite [$Pb_2(SO_4)O$], Lead oxide carbonate [Pb_2OCO_3], Lanarkite, lead sulfur chloride, lead oxide carbonate.
21	Quartz
26	Quartz
27	Quartz, Goethite [FeO(OH)], Lead silicate [$Pb_3Si_2O_7$], Calcium lead silicate [$Ca_2Pb_3Si_3O_{11}$],
30	Quartz, Goethite [FeO(OH)], Lead silicate [$Pb_3Si_2O_7$], Lead sulphate [$Pb(S_2O_3)$]
32	Quartz, Lead oxide carbonate [Pb_2OCO_3], Goethite [FeO(OH)], Lead silicate [$Pb_3Si_2O_7$], Calcium lead silicate [$Ca_2Pb_3Si_3O_{11}$], lead sulphate [$Pb(S_2O_3)$]
37	Quartz, Kaolinite-1Md [$Al_2Si_2O_5(OH)_4$], Goethite [FeO(OH)], Lead silicate [$Pb_3Si_2O_7$], lead sulphate [$Pb(S_2O_3)$]
38	Quartz, Kaolinite [$Al_4(OH)_8(Si_4O_{10})$], Lanarkite [$Pb_2(SO_4)O$], Lead oxide carbonate [Pb_2OCO_3], Goethite [FeO(OH)], Calcium lead silicate [$Ca_2Pb_3Si_3O_{11}$]
40	Lanarkite [$Pb_2(SO_4)O$], Quartz [SiO_2], Kaolinite-1A [$Al_2Si_2O_5(OH)_4$], Lead oxide carbonate [Pb_2CO_4], Illite [$K(Al, Fe)_2AlSi_3O_{10}(OH)_2!H_2O$] Hydroxylapatite [$Ca_{2.5}Pb_{7.5}(OH)_2(PO_4)_6$, Calcium Phosphate [$Ca_2P_2O_7$], Goethite [FeO(OH)], Calcium lead silicate [$Ca_2Pb_3Si_3O_{11}$], Muscovite [$KAl_2Si_3Al_{10}(OH)_2$]
42	Quartz [SiO_2], Lead phosphate [$Pb_2P_2O_7$], Iron lead phosphate [$Fe_2Pb_3(PO_4)_4$], Lanarkite [$Pb_2(SO_4)O$], Lead oxide carbonate [Pb_2OCO_3], Goethite [FeO(OH)], Calcium lead silicate [$Ca_2Pb_3Si_3O_{11}$]
45	Goethite [FeO(OH)], Lead silicate [$Pb_3Si_2O_7$], Calcium lead silicate [$Ca_2Pb_3Si_3O_{11}$], Iron phosphate [$Fe_7(P_2O_7)_4$]
52	Pyrophosphite [$K_2CaP_2O_7$], Lanarkite [$Pb_2(SO_4)O$], Lead oxide carbonate [Pb_2OCO_3], Quartz
56	Quartz, Lanarkite [$Pb_2(SO_4)O$], Lead oxide carbonate [Pb_2OCO_3]
60	Lanarkite [$Pb_2(SO_4)O$], Lead oxide carbonate [Pb_2OCO_3], Goethite [FeO(OH)], Lead silicate [$Pb_3Si_2O_7$], Calcium lead silicate [$Ca_2Pb_3Si_3O_{11}$]

Table 8: Possible mineral species in the soil sample C1. Peak assignments for the spectra in Figure 8 (data from the JCPDS database).

3.2.4 FT-IR Analysis

These analyses were performed to complement the data obtained from XRD analysis. FT-IR analysis of the 'light' and 'heavy' quartz fractions confirms the presence of kaolinite (Sheffield Fire Clay)[186]. Strong stretch and bend frequencies characteristic of this clay are seen at various wavenumbers (cm^{-1}) as shown in Table 9 and Figure 9. The presence of iron oxides and hydroxides (such as goethite) is also suggested from the –OH stretch frequencies at 797 and 697 cm^{-1}. The stronger stretch and bend frequencies in the 'light' fraction of the soil suggests the presence of clays, iron oxides and hydroxides in this fraction.

Wavenumber (cm^{-1})	Assignment	Mineral
3698	Al---O-H stretch	Kaolinite (Fire Clay, Sheffield, England)
3622	Al—O-H stretch	Kaolinite (Fire Clay, Sheffield, England)
1106	Si-O stretch	Kaolinite
1031	Si-O-Si bend	Kaolinite
1011	Si-O-Si bend	Kaolinite
797	-OH stretch	Kaolinite
697	-OH stretch	Kaolinite
478	Si-O bend	Quartz/Clay
538	Si-O bend	Quartz/Clay

Table 9: FT-IR peak assignments for the analysis performed on the soil samples (peak data obtained from Beutelspacher and van der Marel[186]).

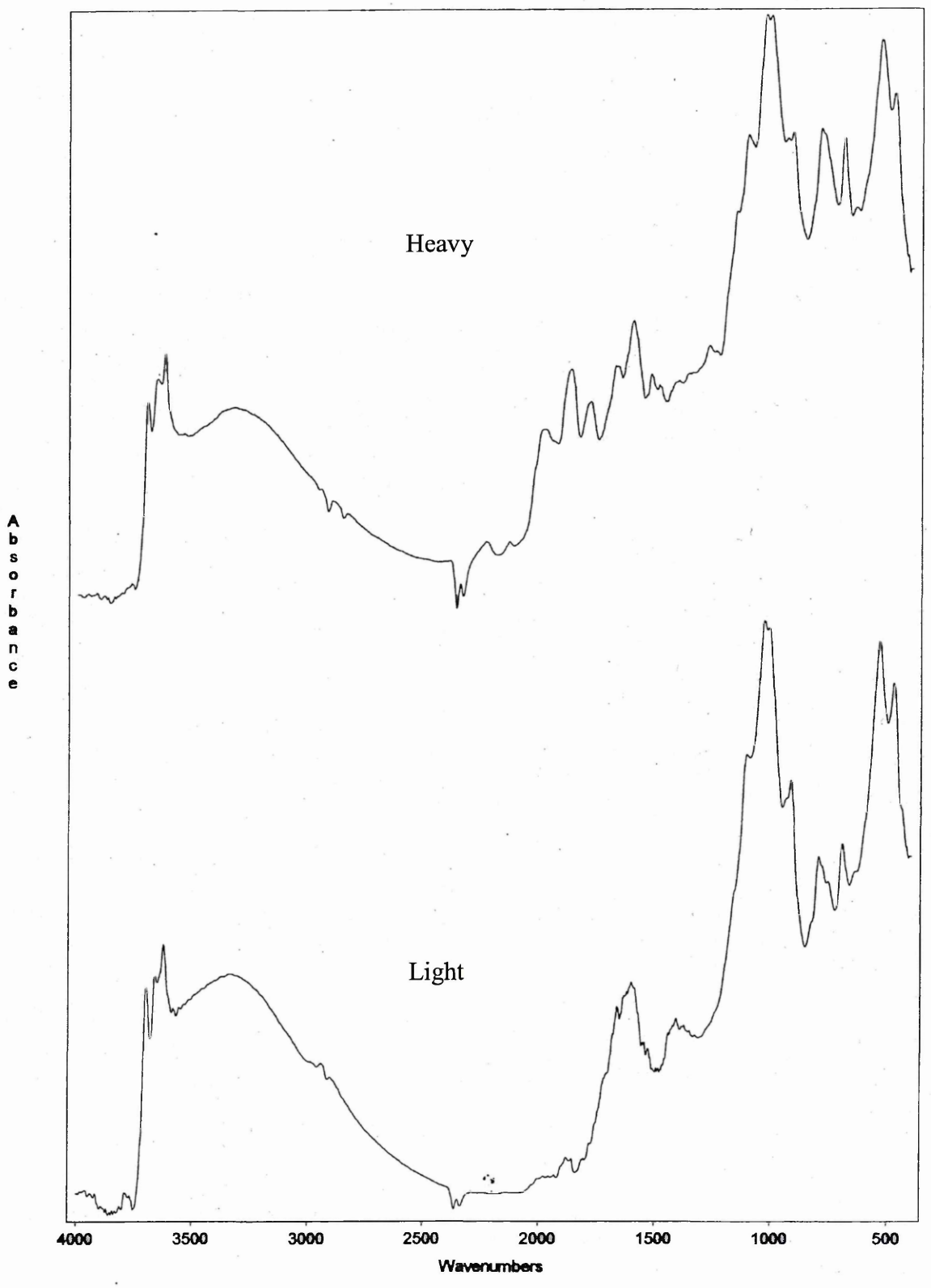

Figure 9: FT-IR absorption spectrum for the light and heavy fractions of the soil.

3.2.5 ESEM/EDX Analysis

These analyses were performed to study the distribution of various metals in the soil matrix. Only the 'light' fraction was analysed to reduce excessive interference from quartz in the bulk sample. The elemental maps in the Figs. 10(ii-vi) correspond to the areas in the secondary electron image in Figure 10(i). Each square displays the spatial distribution of one element, with areas with the highest concentration of a particular element represented in white (with the darker areas signifying low or negligible concentration). Since the background has been subtracted from each element map, pixel per pixel, these maps represent the net intensities of the signals recorded in the energy windows characteristic of the specified elements. The intensity of each peak is related to the presence of the specified element and its relative concentration.

Good overlap was observed between the distribution pattern of Pb and Fe, Pb and Al, while there was low overlap between the Pb and Si distribution. This suggests that the majority of Pb in the soil might have been bound to clays and iron oxides. Other elements were undetectable using the EDX as the concentration of these elements was below the method detection limit of the instrument.

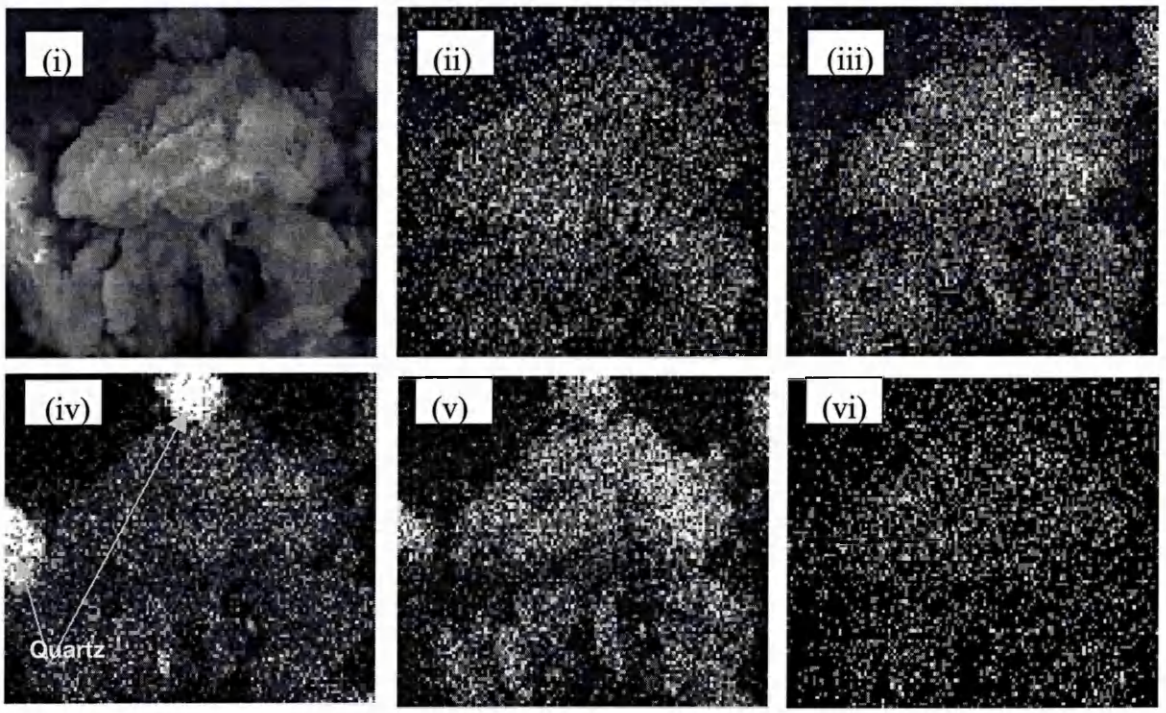

Figure 10: ESEM/EDX map of the **100μm** fraction of the soil. (i) Secondary electron image of the sample, (ii) Fe (iii) Al (iv) Si (v) oxygen and (vi) Pb map respectively.

3.2.6 Stable Isotope Analysis

Stable isotope analysis was performed to ascertain the true origin of lead in the soil samples i.e. natural abundance, industrial activities (such as lead smelting) or petroleum. These showed that the ratio of $^{206}Pb/^{207}Pb$ in the samples C1, C2 and B1 was 1.213±0.008, 1.229±0.009 and 1.223±0.009 respectively. Whitehead et al.[159] studied vertical migration of Pb through fractured sandstone beneath a medieval 'bole type' smelting site east of Bakewell in the Peak District National Park, Derbyshire, UK, using Pb isotope tracing. These studies showed that $^{206}Pb/^{207}Pb$ isotopic ratio of surface slag samples was in the range 1.1802-1.1820, whilst the background $^{206}Pb/^{207}Pb$ ratio was 1.1670 ± 0.003. One-tailed student t-test with unequal variance (95% significance) showed that there is a significant difference between the $^{206}Pb/^{207}Pb$ values published by Whitehead et al., and those obtained in this study.

This difference of approximately 0.03 units between the obtained and published values may be the result of differing instrumental precision. Whitehead et al.[159] used a thermal ionisation mass spectrometer while the data presented in this study was obtained using a quadropole ICP-MS. Whitehead et al.[159] estimated the precision of the thermal ionisation mass spectrometer in deriving the $^{206}Pb/^{207}Pb$ as 0.03%, whilst the estimated precision of the quadropole was in the range 0.65 – 1.07%. However, it is noteworthy that there is a significant difference between the published isotopic ratios of background Pb (i.e. isotopic ratio of Pb in uncontaminated sandstone) and those obtained in this study. This suggests that the Pb in the soil samples used for this study was not due to natural abundance. The data also show that the Pb in the samples was not from petroleum, as the $^{206}Pb/^{207}Pb$ ratios of Pb in UK petrol was approximately 1.065 ± 0.003[159(a)].

3.2.7 Sequential Extractions using the Modified BCR Procedure

The BCR sequential extraction procedure was applied to the samples C1, C2 and B1 to study the fractionation of metals. The results from these experiments are presented in Tables 10-12. Each extraction was repeated five times to ensure reproducibility of the results.

It is noteworthy that there were problems with the H_2O_2 section of the third step due to the intensely oxidising nature of the reagent. During initial sample preparation trials, there were large sample losses due to the samples boiling over. This problem recurred even when the reagent was added to the samples after the centrifuge tubes were taken out of the water bath. In order to prevent sample losses, the reagent was added to the samples with the centrifuge tubes placed in a container filled with

crushed ice. The centrifuge tubes were placed in the water bath after the initial vigorous reaction after the addition of H_2O_2 had dissipated.

	Step1	Step2	Step3	Residual	Sum	Total*	% Recovery
Cd	<0.07	<0.07	13.2 ± 1.0	51 ± 3	64	64 ± 32	100
Cr	<0.05	135 ± 5	4 ± 0.6	15 ± 3	154	152 ± 19	101
Cu	25 ± 6	25±1	9 ± 2	20 ± 2	79	76 ± 4	104
Ca	2310 ± 150	1100 ± 35	386 ± 116	124 ± 20	3920	3460 ± 416	114
Al	211 ± 26	785 ± 45	315 ± 90	2750 ± 478	4050	4930 ± 418	82
Mg	261 ± 22	81 ± 4	119 ± 31	490 ± 90	951	902 ± 58	106
Fe	52 ± 9	4430 ± 68	114 ± 35	9560 ± 1300	14100	18900 ± 2351	75
Mn	177 ± 8	206 ± 6	13 ± 3	55 ± 7	451	415 ± 30	109
Pb	1030 ± 43	4440 ± 56	130 ± 3	707 ± 8	6310	6360 ± 74	99
Zn	45 ± 3	52 ± 3	22 ± 1	63 ± 3	182	182 ± 12	100

Table 10 - Data from sequential extraction of metals from the contaminated soil C1. All values are in mg kg^{-1} air-dried soil. Sum - sum of the concentration of metals extracted in the four steps of the sequential extraction procedure; Pseudo-total – concentration of metal extracted in total digestion of the soil in aqua-regia; % recovery – ratio of sequential extractable to total digestible. Each extraction was repeated five times.

	Step1	Step2	Step3	Residual	Sum	Total	% Recovery
Cd	66 ± 9	<0.07	20 ± 4	158	178	171 ± 13	104
Cr	<0.05	4 ± 0.4	13 ± 0.8	70	86.8	79 ± 35	110
Cu	1.6±0.1	1.5±0.1	17.3±0.4	27	47.2	40 ± 0.5	118
Ca	1640±37	760 ± 26	163 ± 8	23	2590	2500 ± 23	103
Al	93 ± 1	464 ± 10	1730±15	2580	4870	4710 ± 48	103
Mg	163± 4	42 ± 2	186 ± 7	370	761	755 ± 6	101
Fe	9 ± 0.1	1820±90	2770±48	16410	21000	21600±168	97
Mn	82 ± 2	244 ± 11	63 ± 1	129	518	511 ± 4	101
Pb	121 ± 12	897 ± 42	477 ± 5	429	1920	1680 ± 31	115
Zn	15 ± 1	12 ± 1	27 ± 1	65	119	103 ± 12	116

Table 11 - Sequential extraction of metals in soil C2. All values are in mg kg^{-1}. Each extraction was repeated five times.

	Step1	Step2	Step3	Residual	Sum	Total	% Recovery
Cd	42 ± 5	8 ± 1	49 ± 2	148 ± 43	197	110 ± 18	179
Cr	<0.0489	5 ± 1	13 ± 0.5	79 ± 6	97	106 ± 6	91
Cu	2.3 ± 0.1	1.8±0.1	26 ± 1	28 ± 0.2	58	46 ± 1	126
Ca	1860 ± 53	697±103	315±95	62 ± 15	2930	2280 ± 15	129
Al	80 ± 5	383 ± 8	1630 ± 53	2950 ± 146	5040	4070 ± 38	124
Mg	97 ± 2	27 ± 5	111± 5	345 ± 22	580	498 ± 5	117
Fe	17.5 ± 2.5	2520±3	2920 ± 23	15700±736	21200	20100±100	105
Mn	60 ±1	59 ± 3	47 ± 2	69 ± 2	235	206 ± 6	114
Pb	95 ± 10	447 ± 18	359 ± 31	204 ± 3	1100	1010 ± 23	109
Zn	18.5 ± 1	6 ± 0.6	28 ± 0.7	67 ± 2	119	95 ± 6	125

Table 12 - Sequential extraction of metals in soil B1. All values are in mg kg^{-1}. Each extraction was repeated five times.

Lead

Approximately 16% (1030mg kg^{-1}), 66% (4440mg kg^{-1}), and 2% (130mg kg^{-1}) of the total Pb in **sample C1** was extracted in step one (ethanoic acid), step two (hydroxylamine hydrochloride) and step 3 (hydrogen peroxide and ammonium acetate) respectively. 84% of the total lead in the soil was extracted in the first three steps. The residual lead (~16%) in the soil was extracted by total digestion of the residue from step 3 in aqua-regia. The reproducibility of the extraction process was generally good with the RSD in the data from all three steps being <10%. The data show that the Pb desorption pattern from the soil surfaces to be as follows: reducible>ion exchangeable/weak acid soluble > residual >oxidisable. (**Possible fractionation:** Reducible – metals bound to Fe/Mn oxides and oxyhydroxides, 2:2 clays; ion-exchangeable/weak acid soluble – metals bound to Ca/Mg carbonates, 1:1 clays; residual – metals associated with silicates; oxidisable – metals complexed with organic matter).

Approximately 6% (121mg kg^{-1}), 47% (897mg kg^{-1}), and 25% (477 mg kg^{-1}) of the total Pb in **sample C2** was extracted in steps one, two and three respectively. 78% of the total Pb in the soil was extracted in the first three steps. The residual lead (~22%) in the soil was extracted by pseudo-total digestion of the residue from step 3 in aqua-regia. The reproducibility of the extraction process was good with the RSD in the data from all three steps being ≤10%. The data show that the Pb desorption pattern from the soil surfaces to be as follows: reducible >oxidisable > residual >ion-exchangeable/weak acid soluble.

Approximately 9% (95mg kg^{-1}), 40% (447mg kg^{-1}), 32% (359mg kg^{-1}) of the total Pb in **sample B1** was extracted in steps one, two and three respectively. 81% of the total lead in the soil was extracted in the first three steps. The residual lead (~19%) was extracted by pseudo-total digestion of the residue from step 3 in aqua-regia. The reproducibility of the extraction process was good with the RSD for the three steps being ≤10%. The data show that the Pb desorption pattern from the soil surfaces to be as follows: reducible>oxidisable>residual>ion-exchangeable.

Zinc

Approximately 25% (45mg kg^{-1}), 29% (52mg kg^{-1}) and 12% (22mg kg^{-1}) of the total Zn in the **sample C1** was extracted in steps one, two and three respectively. 66% of the total Zn in the soil was extracted in the first three steps. The remainder of the zinc in the soil (35%) was extracted in aqua-regia digests of the residue from step 3. The reproducibility of all three steps was good, with the RSD being <10%. The data show that the Zn desorption pattern from the soil surfaces to be as follows: reducible>ion-exchangeable>residual>oxidisable.

Approximately 13% (15mg kg^{-1}), 10% (12mg kg^{-1}) and 23% (27mg kg^{-1}) of the total Zn in the **sample C2** was extracted in steps one, two and three respectively. 46% of the total Zn was extracted in the first three steps. The remainder of the zinc in the soil (54%) was extracted in aqua-regia digests of the residue from step 3. The data show that the Zn desorption pattern from the soil surfaces to be as follows: residual>oxidisable>ion-exchangeable>reducible.

Approximately 19.5% (18.5mg kg^{-1}), 6.3% (6mg kg^{-1}) and 30% (28mg kg^{-1}) of the total Zn in the **sample B1** was extracted in steps one, two and three respectively.

55.8% of the total Zn was extracted in the first three steps. The remainder of the zinc in the soil (44.2%) was extracted in aqua-regia digests of the residue from step 3. The data show that the Zn desorption pattern from the soil surfaces to be as follows: residual>oxidisable>ion-exchangeable>reducible.

Copper

Approximately 33% (25mg kg^{-1}), 33% (25mg kg^{-1}) and 11% (9mg kg^{-1}) of the total Cu in the **sample C1** was extracted in steps one, two and three respectively. 77% of the total Cu was extracted in the first three steps. The remainder of Cu in the soil (23%) was extracted in aqua-regia digests of the residue from step 3 of the residue from step 3. The reproducibility of Cu extractions using the procedure was poor, as the RSDs for steps 1, 2 and 3 were 25%, 20% and 22%. The data show that the Cu desorption pattern from the soil surfaces to be as follows: ion-exchangeable = reducible>residual>oxidisable.

Approximately 4% (1.6mg kg^{-1}), 4% (1.5mg kg^{-1}) and 43% (17.3mg kg^{-1}) of the total Cu in the **sample C2** was extracted in steps one, two and three respectively. 51% of the total Cu was extracted in the first three steps. The remainder of Cu in the soil (49%) was extracted in aqua-regia digests of the residue from step 3. The procedure showed good reproducibility as the RSDs for steps 1, 2 and 3 were below 10%. The data show that the Cu desorption pattern from the soil surfaces to be as follows: residual>oxidisable>reducible = ion-exchangeable.

Approximately 5% (2.3mg kg^{-1}), 4% (1.8mg kg^{-1}) and 57% (26mg kg^{-1}) of the total Cu in the **sample B1** was extracted in steps one, two and three respectively. 66% of the total Cu was extracted in the first three steps. The remainder of Cu in the soil

(34%) was extracted in aqua-regia digests of the residue from step 3. The procedure showed good reproducibility as the RSDs for steps 1, 2 and 3 were below 10%. The data show that the Cu desorption pattern from the soil surfaces to be as follows: oxidisable>residual>ion-exchangeable> reducible.

Cadmium

The concentration of Cd extracted from **sample C1** in steps 1 and 2 was below ICP-AES limits of detection (<0.07mg kg^{-1}). Approximately, 20% of the total Cd was extracted in step 3, while the remainder (80%) was extracted in aqua-regia digests of the residue from step 3. The data show that the Cd desorption pattern from the soil surfaces to be as follows: residual>oxidisable>ion-exchangeable = reducible.

Approximately 39% (66mg kg^{-1}) and 12% (20mg kg^{-1}) of the total Cd in **sample C2** was extracted in steps one and three respectively. The concentration of Cd extracted in step 2 was below ICP-AES limits of detection. The remaining 51% of the total Cd in the soil was extracted in aqua-regia digests of the residue from step 3. Reproducibility of the extractions was poor as the RSDs for steps 1 and 3 were 13.6% and 20% respectively. The data show that the Cd desorption pattern from the soil surfaces to be as follows: residual>ion-exchangeable>reducible>oxidisable.

Approximately 21% (42mg kg^{-1}), 4% (8mg kg^{-1}) and 25% (49mg kg^{-1}) of the total Cd in **sample B1** was extracted in steps one, two and three respectively. 50% of the total Cd in the soil was extracted in the first three steps. The remainder of the Cd in the soil (50%) was extracted in aqua-regia digests of the residue from step 3. The procedure showed moderate reproducibility with the RSDs for steps 1, 2 and 3 being

12%, 12.5% and 4% respectively. The data show that the Cd desorption pattern from the soil surfaces to be as follows: residual>oxidisable>ion-exchangeable>reducible.

Chromium

Approximately 89% (135mg kg^{-1}) and 2.5% (4mg kg^{-1}) of the total Cr in **sample C1** were extracted in steps 2 and 3 respectively. The concentration of Cr extracted in step one was below ICP-AES limits of detection (<0.05mg kg^{-1}). The remainder of the Cr (8.5%) in the soil was extracted in the aqua-regia digests of the residue from step 3. The data show that the Cr desorption pattern from the soil surfaces to be as follows: reducible>residual>oxidisable>ion-exchangeable.

Approximately 1.7% (4mg kg^{-1}) and 15% (13mg kg^{-1}) of the total Cr in **sample C2** was extracted in steps 2 and 3 respectively. The concentration of Cr extracted in step one was below ICP-AES limits of detection (<0.05mg kg^{-1}). The remainder of the Cr (84%) in the soil was extracted in the aqua-regia digests of the residue from step 3. The data show that the Cr desorption pattern from the soil surfaces to be as follows: residual>oxidisable>ion-exchangeable>reducible.

Approximately 4.7% (4mg kg^{-1}) and 12.3% (13mg kg^{-1}) of the total Cr in **sample B1** was extracted in steps 2 and 3 respectively. The concentration of Cr extracted in step one was below ICP-AES limits of detection (<0.05mg kg^{-1}). The remainder of the Cd (83%) in the soil was extracted in the aqua-regia digests of the residue from step 3. The data show that the Cr desorption pattern from the soil surfaces to be as follows: residual>oxidisable>ion-exchangeable>reducible.

Manganese

Approximately 39% (177mg kg^{-1}), 46% (206mg kg^{-1}) and 3% (13mg kg^{-1}) of the total Mn in **sample C1** was extracted in the steps one, two and three respectively. The remaining Mn (12%) in the soil was extracted in aqua-regia digests of the residue from step 3. The data show that the Mn desorption pattern from the soil surfaces to be as follows: reducible>ion-exchangeable>residual>oxidisable. This data provides evidence about the phase selectivity of hydroxylamine hydrochloride, showing that this reagent may indeed be specific to the Mn oxides and hydroxides.

Approximately 16% (82mg kg^{-1}), 47% (244mg kg^{-1}), and 12% (63mg kg^{-1}) of the total Mn in sample C2 was extracted in aqua regia digests from step 3. The remaining Mn (25%) in the soil was extracted in steps one, two and three respectively. The data show that the Mn desorption pattern from the soil surfaces to be as follows: reducible>residual> ion-exchangeable>oxidisable. This data provides evidence about the phase selectivity of hydroxylamine hydrochloride, showing that this reagent may indeed be specific to the Mn oxides and hydroxides.

Approximately 26% (60mg kg^{-1}), 26% (59mg kg^{-1}), 23% (47mg kg^{-1}) of the total Mn in the sample B1 was extracted in steps one, two and three respectively. The remaining Mn (25%) in the soil was extracted in aqua regia digests of the residue from step 3. One-tailed Student t-test showed that there is no significant difference between the concentrations of Mn extracted in steps 1 and 2 from sample B1. The data show that the Mn desorption pattern from the soil surfaces to be as follows: reducible = ion-exchangeable>residual>oxidisable. This data raises doubts about the phase selectivity of hydroxylamine hydrochloride, as there is no significant difference between the concentration of Mn extracted in steps 1 and 2.

Iron

Approximately 0.4% (52mg kg^{-1}), 31% (4430mg kg^{-1}), 0.8 (114mg kg^{-1}), 68% (9558mg kg^{-1}) of the total aqua-regia soluble Fe in the **sample C1** was extracted in steps one, two, three and residual digestion respectively. 75% of the total aqua-regia soluble Fe was mobilised during the sequential extraction process. The actual concentration of Fe in the soil was approximately 67,000mg kg^{-1}, as shown by the XRF analysis. The data show that the Fe desorption pattern from the soil surfaces to be as follows: residual>reducible>oxidisable>ion-exchangeable.

Approximately 0.04% (9mg kg^{-1}), 9% (1820mg kg^{-1}), 13% (2770mg kg^{-1}) and 75% (16412mg kg^{-1}) of the total aqua regia soluble Fe in the **sample C2** was extracted in steps one, two, three and residual digestion respectively. 97% of the total aqua-regia soluble Fe was mobilised during the sequential extraction process. One tailed Student t-test shows that there is no significant difference between the Fe concentrations obtained in steps 2 and 3. The data show that the Fe desorption pattern from the soil surfaces to be as follows: residual>oxidisable = reducible>ion-exchangeable.

Approximately 0.1%(18mg kg^{-1}), 12.5% (2525mg kg^{-1}), 14.4% (2920mg kg^{-1}) and 78% (15700mg kg^{-1}) of the total aqua regia soluble Fe in the **sample B1** was extracted in steps one, two, three and the residual digestion step respectively. 105% of the total aqua regia soluble Fe was mobilised during the sequential extraction process. One tailed Student t-test shows that there is a significant difference between Fe concentrations obtained in steps 2 and 3. The data show that the Fe desorption pattern from the soil surfaces to be as follows: residual>oxidising>reducible>ion-exchangeable.

Magnesium

Approximately, 27% (261mg kg^{-1}), 8.5% (81mg kg^{-1}) and 12.5% (119mg kg^{-1}) of the total Mg in **sample C1** was extracted in steps 1, 2 and 3 respectively. 49% of the total Mg was extracted in the first three steps. The remainder (51%) of the Mg in the soil was extracted in aqua-regia digests. The data show that the Mg desorption pattern from the soil surfaces to be as follows: residual>ion-exchangeable>oxidisable>reducible.

Approximately, 21% (163mg kg^{-1}), 5.5% (42mg kg^{-1}) and 24% (186mg kg^{-1}) of the total Mg in **sample C2** was extracted in steps 1, 2 and 3 respectively. 50.5% of the total Mg was extracted in the first three steps. The remaining (49.5%) Mg was extracted in aqua-regia digests. The data show that the Mg desorption pattern from the soil surfaces to be as follows: residual>oxidisable>ion-exchangeable>reducible.

Approximately 17% (97mg kg^{-1}), 4.6% (27mg kg^{-1}) and 19% (111mg kg^{-1}) of the total Mg in **sample B1** was extracted in steps 1, 2 and 3 respectively. The remaining Mg (59.4%) was extracted in aqua-regia digests. The data show that the Mg desorption pattern from the soil surfaces to be as follows: residual>oxidisable>ion-exchangeable>reducible.

Calcium

Approximately 59% (2310mg kg^{-1}), 28% (1110mg kg^{-1}) and 10% (386mg kg^{-1}) of the total aqua-regia soluble Ca in **sample C1** was extracted in steps 1, 2 and 3 respectively. The remaining 3% (124mg kg^{-1}) Ca was extracted in aqua-regia digests. The data show that the Ca desorption pattern from the soil surfaces to be as follows: ion-exchangeable>reducible>oxidisable>residual. It is useful to note that only a

fraction of the total Ca in the soil is extracted in aqua-regia, as the actual concentration of Ca in the sample C1 is approximately 21600mg kg^{-1}.

Approximately 63% (1640mg kg^{-1}), 29% (763mg kg^{-1}), 6% (163mg kg^{-1}) of the total aqua-regia soluble Ca in **sample C2** was extracted in steps 1, 2 and 3 respectively. The remaining 2% (163mg kg^{-1}) Ca was extracted in aqua-regia digests. The data show that the Ca desorption pattern from the soil surfaces to be as follows: ion-exchangeable>reducible>oxidisable>residual.

Approximately 63% (1860mg kg^{-1}), 23% (697mg kg^{-1}) and 10% (315mg kg^{-1}) of the total aqua-regia soluble Ca in **sample B1** was extracted in steps 1, 2 and 3 respectively. The remaining 2% (62mg kg^{-1}) Ca was extracted in aqua-regia digests. The data show that the Ca desorption pattern from the soil surfaces to be as follows: ion-exchangeable>reducible>oxidisable>residual.

3.2.8 Quality Control of the Sequential Extraction Procedure

The quality of the sequential extraction procedures was checked using the BCR certified reference sediment material CRM 601 (Table 13)[187]. This material was specifically developed as a quality control material for the original BCR sequential extraction procedure. However, another material CRM 701 was developed for the validation of the modified BCR sequential extraction procedure[187]. One-tailed Student t-tests (two-sample with unequal variance) were performed to compare experimental and literature values[187, 188]. The results show that there was no significant difference between the obtained and literature values for lead. This shows that the sequential extraction results obtained using the CRM 601 material are

valid[188]. This also suggests that the results obtained through the application of the modified three-step BCR sequential extraction procedure to the soil samples C1, C2 and B1 might have been accurate. Additionally, this also suggests that the quality of analysis procedures was good.

CRM 601	Step 1	Step 2	Step 3
Pb Obtained	2.1 ± 0.5	225 ± 6.3	22.4 ± 2.5
Pb published	2.3 ± 1.2	205 ± 11	19.7 ± 5.8
Zn Obtained	290 ± 17	273 ± 7	121 ± 13
Zn published	261 ± 13	266 ± 17	106 ± 11
Cu Obtained	10.6 ± 0.1	67.7 ± 4.7	88.7 ± 6
Cu published	10.5 ± 0.8	72.8 ± 4.9	78.6 ± 8.9
Cr Obtained	0.3 ± 0.1	8.8 ± 1.5	12.9 ± 1
Cr published	0.4 ± 0.1	10.6 ± 0.9	14.4 ± 2.6
Ni Obtained	8.9 ± 0.1	11.6 ± 1.5	7.7 ± 1
Ni published	7.8 ± 0.8	10.6 ± 1.3	6.0 ± 1.3
Cd Obtained	5.3 ± 0.3	4.9 ± 1	2.4 ± 0.5
Cd published	4.5 ± 0.7	4.0 ± 0.5	1.9 ± 1.4

Table 13: Data (mg kg^{-1}) obtained from sequential extractions performed on the BCR 601 certified reference material and values published in literature.

3.2.9 XRD Analysis of Residues

XRD analysis was performed on a portion of the residue from each step of the sequential extraction procedure. Prior to analysis the residues were washed in deionised water and centrifuged to remove residual reagents and air-dried at 105°C. The dried sample was ground in a pestle and mortar to reduce the particle size to 60μm. The ground samples were then subject to X-ray diffraction analysis. These analyses were performed to study the nature of the soil and the associated contaminants after completion of the sequential extraction process. The analyses were performed on residues from sample C1 only, as the total contaminant concentrations in other samples were below XRD detection limits.

The results presented in Figure 11 and Table 14 show that there were only slight differences between the peak intensities of the residues from the three steps. When the peaks were matched with the JCPDS database using Xpert Graphics software,

there was a noticeable lack of peaks of all lead minerals except lead phosphate in the first step. Iron was observed to be principally in the form of haematite, while the principal clay was albite. The XRD spectrum of the residue from step 2 showed peaks for calcium lead silicates, iron fluoride, quartz and albite. The XRD spectrum of the residue from step 3 showed peaks for albite, anorthite, quartz, iron sulphates and lead oxide carbonates.

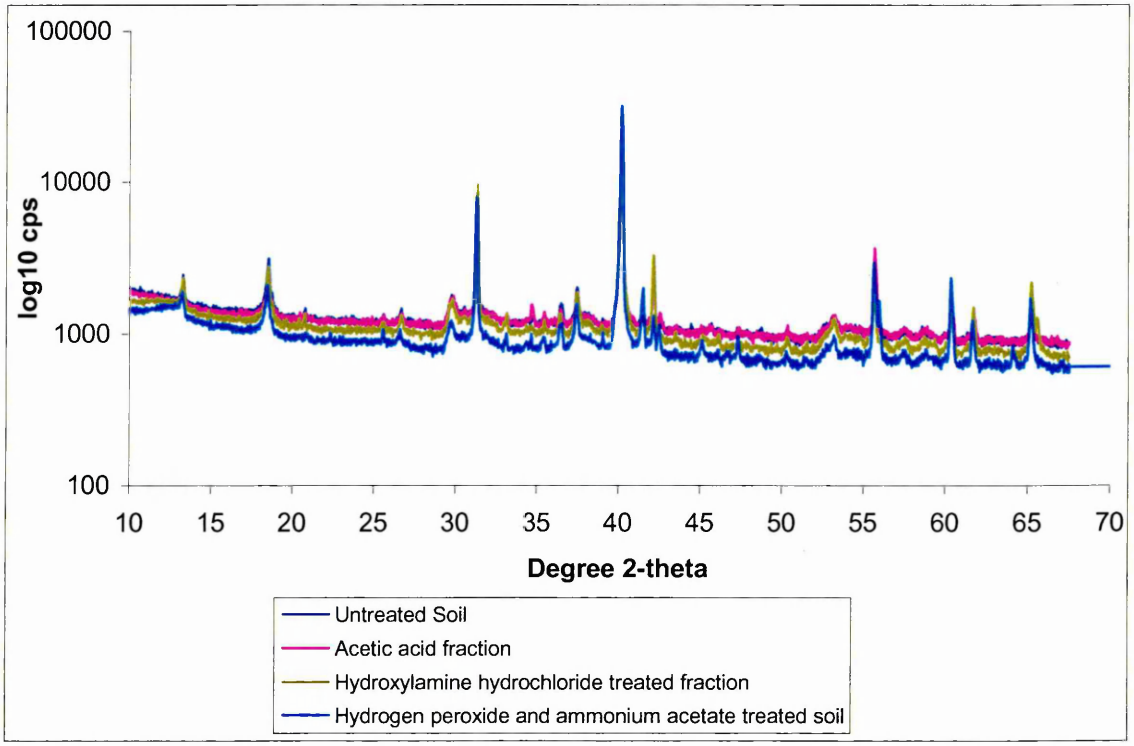

Figure 11: XRD analysis of the soil samples collected after each step of the sequential extraction process. Acetic (ethanoic) acid fraction – XRD spectrum of air-dried residue from step 1; hydroxylamine hydrochloride treated fraction – XRD spectrum of air-dried residue from step 2; hydrogen peroxide and ammonium acetate treated soil – XRD spectrum of air-dried residue from step 3. The residue from each step was washed in deionised water and the washings were discarded. Each of the residues were then air-dried at 105°C overnight, ground using a clean pestle and mortar and analysed using an XRD using the same program as that used for the untreated soil samples. See Table 14 for likely mineral assignments for the peaks observed in each of the spectra.

Peak (°2θ)	Possible Mineral Species			
	Original Soil	Step 1 Residue	Step 2 Residue	Step 3 Residue
13	Quartz, Goethite	Silicon oxide, Albite low ($NaAlSi_3O_8$), Hematite (Fe_2O_3)	Albite low, Albite ordered, Potassium Iron Fluoride	Lead oxide carbonate (PbC_2O_4), Anorthite ($Ca(Al_2Si_2O_8)$)
18	Quartz, Goethite, Lead silicate, Kaolinite-1Md, Lanarkite, Lead oxide carbonate	Quartz	Albite low, Albite ordered, Potassium Iron Fluoride	Albite ordered, lead oxide carbonate, quartz
30	Quartz, Goethite, Lead silicate, Lead sulphate	Hematite, Albite low	Albite low, Quartz	Albite ordered, lead oxide carbonate, quartz
32	Quartz, Lead oxide carbonate, Goethite, Lead silicate, Calcium lead silicate, lead sulphate	Silicon oxide, Hematite	Calcium lead silicate, Potassium Iron Fluoride	Albite ordered, lead oxide carbonate, quartz, iron sulphate
37	Quartz, Kaolinite-1Md Goethite, Lead silicate lead sulphate	Quartz, Hematite	Albite, kaolinite	Albite ordered, lead oxide carbonate, quartz
38	Quartz, Kaolinite, Lanarkite, Lead oxide carbonate, Goethite, Calcium lead silicate.	Quartz, Hematite	Albite, kaolinite	Albite ordered, lead oxide carbonate, quartz
40	Lanarkite, Quartz, Kaolinite-1A, Lead oxide carbonate, Illite Hydroxylapatite, Calcium Phosphate, Goethite, Calcium lead silicate, Muscovite	Illite, Quartz, Hematite	Albite, Quartz, Potassium Iron Fluoride	Albite ordered, lead oxide carbonate, quartz
42	Quartz , Lead phosphate, Iron lead phosphate, Lanarkite, Lead oxide carbonate, Goethite, Calcium lead silicate	Albite, lead phosphate ($Pb_2P_2O_7$)	Potassium Iron Fluoride, Albite, kaolinite, quartz, Calcium lead silicate	Albite ordered, lead oxide carbonate, quartz
52	Pyrophosphite, Lanarkite, Lead oxide carbonate, Quartz	Albite, lead phosphate	Potassium Iron Fluoride, Albite, kaolinite, quartz, Calcium lead silicate	Albite ordered, lead oxide carbonate, quartz
56	Quartz, Lanarkite, Lead oxide carbonate,	Hematite, Silicon oxide	Potassium Iron Fluoride, Albite, kaolinite, quartz, Calcium lead silicate	Albite ordered, lead oxide carbonate, quartz
60	Lanarkite, Lead oxide carbonate, Goethite, Lead silicate, Calcium lead silicate,	Hematite, silicon oxide	Potassium Iron Fluoride, Albite, kaolinite, quartz, Calcium lead silicate	Albite ordered, lead oxide carbonate, quartz

Table 14: XRD peak assignments for the residue from each step of the BCR SSE.

3.3 Discussion

The data described in this chapter allow the interpretation of results from the sequential extraction results in the context of soil mineralogy. Based on current land use pattern i.e. private gardens and agriculture, and historical records, it is safe to assume that there was no made-ground at the sampling location and the basic mineralogy of all three samples is similar i.e. concentration and nature of clays, mineral oxides etc[189,190]. The relatively low organic matter content of the soils (2-3%) suggests that this soil component does not have a major role to play in the retention of most metals by the soils[191]. The pH range of these soils, 5.6-5.9, suggests that most trace metals would be relatively immobile in the soil solutions[17]. Most cationic trace metals precipitate as hydroxides in this pH range e.g. lead precipitates as $Pb(OH)_2$[192]. These cationic metals can be remobilised and leached out of the soil sinks (i.e. from the surface of mineral fractions such as clays and oxides) when the pH is lowered[193].

XRF analysis of the sample C1 showed that the molecular ratios of SiO_2:Al_2O_3 was >2, both values are important indicators of the natural abundance of fire clay in the soil[10]. These are clays that are dominated by kaolinite and illite, with alumina contents varying between 25% and 40% (the composition was approximately 24% in these soil samples)[194]. Impurities such as quartz and titanium oxide minerals (TiO_2 content of this soil being approximately 1%) and their silica content were above expected levels i.e the silica content of pure kaolinite is 47% while that of the soil samples was approximately 65%. The high quartz content of the soil was exaggerated in the XRF data for the 'heavy' fraction, which show that 75% of the soil was composed of this mineral. A higher concentration of aluminium oxides in the 'light' fraction of the soil (23.59%) than those in the 'heavy' fraction (9.87%), suggests that

most of the clays and aluminium oxides/hydroxides might be concentrated in the former[195].

A higher concentration of iron oxide in the 'light' fraction (11.1%) than the 'heavy' fraction (6.10%) was either due to iron oxides being specifically adsorbed to the clays or more likely, iron oxides being lighter than quartz might have floated off with clays. This is probably because Fe and Al form structurally analogous oxides and hydroxides, which are derived from weathered or altered ferromagnesian and aluminosilicate minerals that include gibbsite ($Al(OH)_3$), diaspore (α-AlO.OH), boehmite (γ-AlO.OH), goethite (α-FeO.OH), lepidocrite (γ-FeO.OH), haematite (Fe_2O_3), limonite ($2Fe_2O_3.3H_2O$)[21].

The presence of sulfur in the soil (1.1%) and without any significant variations in its concentration in the different fractions suggests the presence of metal sulphates, sulphides, slag, gypsum etc[196]. The presence of phosphorus (0.86%) in the soil suggests the possible presence of phosphates notably heavy metal phosphates and apatite. It is interesting to note that concentration of lead was higher in the 'light' fraction (0.86%) than the 'heavy' fraction (0.32%). This provides preliminary evidence of preferential binding of metals to clays and iron oxides to silicates. Further confirmation of the concentration of lead in the 'light' fraction, was obtained by performing an ESEM/EDX analysis of the 100μm fraction of the soil (Figure 10), which showed a clear overlap between the iron, lead and aluminium distribution maps[24].

XRD analysis of soil C1 (fractions – 'light', 'heavy' and 100μm) (Figure 8; Table 8) confirmed that the major clay fraction in the soil was kaolinite with a minor contribution from illite and muscovite[197]. Iron was mainly found in the form of goethite although iron phosphates appeared to be present as well. Calcium was principally present as phosphates and calcium lead silicates, which might be part of the lead slag in the soil (also reported by Li & Thornton[198]). The geological profile of this area suggests an abundance of limestone; therefore it would be safe to assume that a majority of calcium in the soil was in the form of carbonates (not 'visible' in the XRD spectra due to lack of crystallinity).

The higher abundance of kaolinite and iron oxides/hydroxides in the soil has major implications for metal binding[28]. Kaolinite is a 1:1 clay with a low cation exchange capacity (CEC) and low swelling capacity[10]. Metal binding, if any, would have been to the surface of this clay rather than interlayer cation substitution as it happens in 2:1 clays such as montmorillonites and illites[10]. Most of the surface binding would be mainly due to 'edge effects', phenomena whereby a surface negative charge is produced on the clay, due to breakages in the clay layer. Furthermore, iron is the most frequently reported element that substitutes in kaolinite[199]. The structural substitution of Fe in the kaolinite has been demonstrated by data from ESEM/EDX mapping, which showed that there was a strong overlap between the aluminium fraction and the iron fraction of the soil.

The data obtained from the sequential extractions (Tables 10-12) suggest that a majority of the cationic trace and heavy metals were principally present in the soil in a

reducible form i.e., they were associated with Fe/Mn oxides and hydroxides (step 2). The relative percentage of Pb associated with the Fe/Mn oxyhydroxides increased in proportion to the total concentration of lead in the three soil samples (see Figs. 12 (a-c). Conversely, the relative proportion of Pb associated with the organic fraction (oxidisable) (step 3) of the soil increased with a decrease in the concentration of total lead in the soils. As shown in Figure 12, the proportion of lead present in an ion-exchangeable form (step 1) in the soils was highest in sample C1 followed by B1 and C2. This preference of Pb for Fe oxides and clays was demonstrated in the EDX map of the secondary electron image of the 100μm soil particle (Figure 10). However, this image does not provide comprehensive evidence proving the exclusive binding of Pb to Fe oxides and clays.

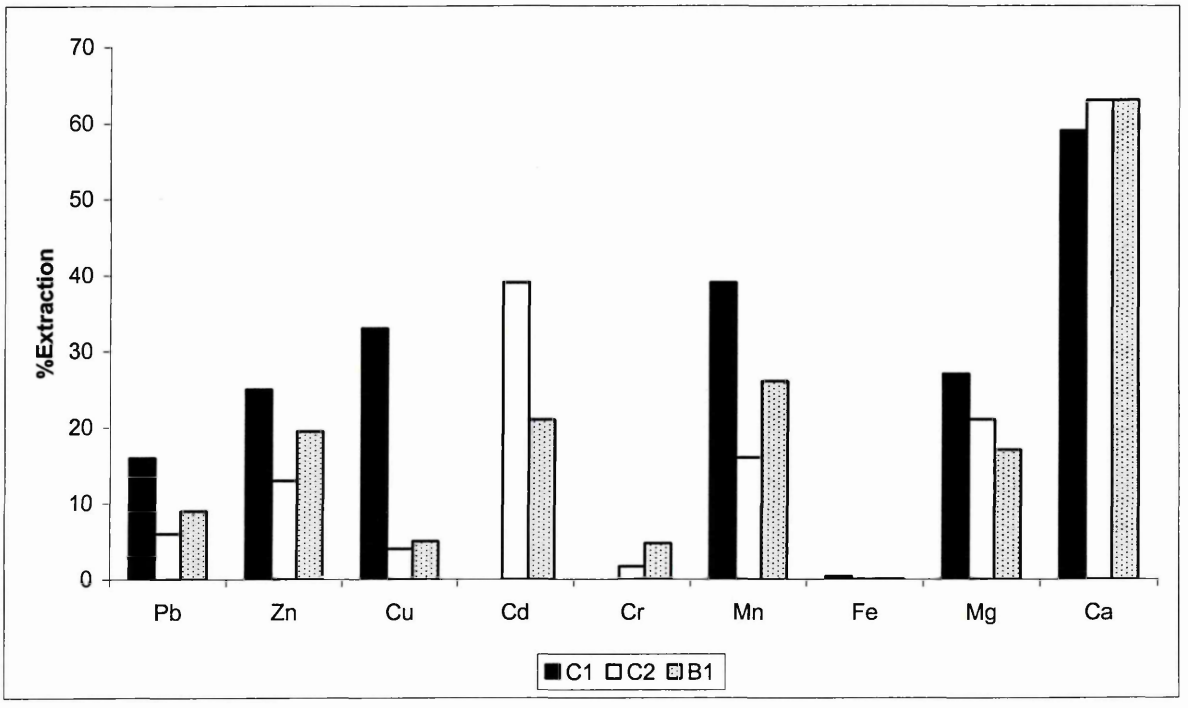

Figure 12 (a): Proportion (%)(mg kg^{-1}) of the pseudo-total metal concentration in samples C1, C2 & B1 extracted into 0.11 M ethanoic acid during the **first** step of the modified BCR procedure.

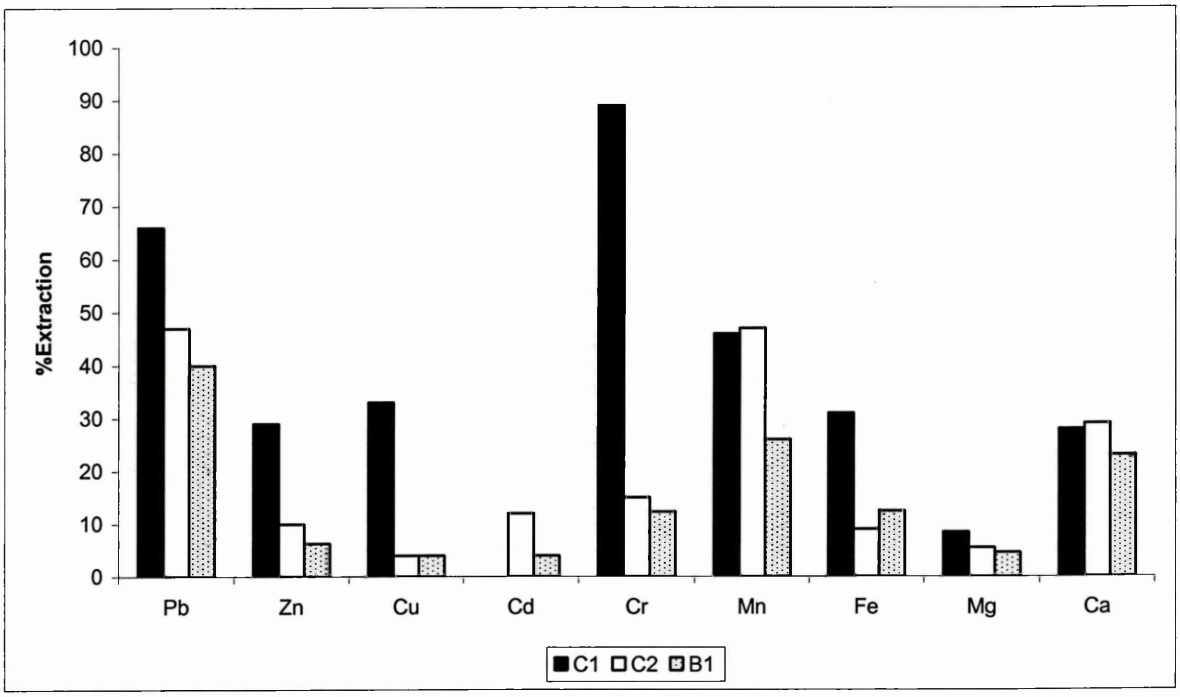

Figure 12 (b): Proportion (%)(mg kg^{-1}) of the pseudo-total metal concentration in samples C1, C2 & B1 extracted into 0.5 M hydroxylamine hydrochloride solution during the **second** step of the modified BCR procedure.

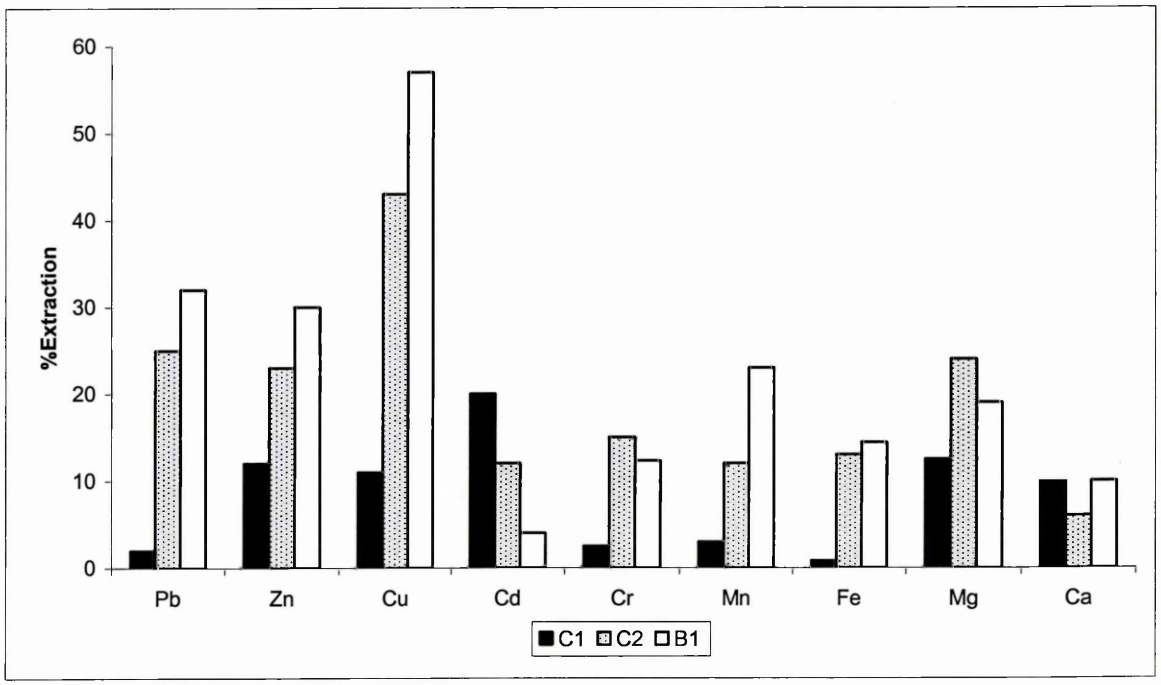

Figure 12 (c): Proportion (%)(mg kg^{-1}) of the pseudo-total metal concentration in samples C1, C2 & B1 extracted into 1 M ammonium acetate solution during the **third** step of the modified BCR procedure.

Li and Thornton[194] reported that most of the lead in soils at the old mining sites in the Derbyshire area was strongly associated with the carbonate phase. Evidence for preferential binding of Pb to the carbonate fractions comes from the XRD analysis performed on the residue (sample C1) from each step of the sequential extraction process. This did not reflect any significant changes in the concentration of lead minerals in the soil i.e. there were no perceptible differences in the peak heights of the crystalline lead minerals. This suggests that a majority of the lead in the soil C1, as a result of the high concentrations, might have been precipitated onto the surface of the soil particles as non-crystalline compounds such as cerussite ($PbCO_3$). XRD analysis of mine waste in Derbyshire by Cotter-Howells[200] showed that cerussite is one of the major Pb minerals. This is in agreement with the thermodynamic predictions that cersussite would be the dominant Pb mineral at the Eh-pH conditions in these soils[201]. Therefore, it can be concluded that a majority of Pb in the soil can be mobilised through ion-exchange mechanisms using reagents such as $CaCl_2$ and $MgCl_2$ solutions[202,203] or using complexing agents such as weak ethanoic acid[204] and EDTA[205]. Chapters 5 & 9 present results from soil washing studies performed using these reagents.

There was no perceptible pattern to the extraction of Cd and Cr from the three soils, although the most important observation would be the concentration of mobilisable Cd from soils C2 and B1 (see Table 12). Approximately 66mg kg^{-1} and 42mg kg^{-1} Cd were extracted in 0.11M acetic acid (step 1) from the samples C2 and B1 respectively. Approximately 20mg kg^{-1} and 49mg kg^{-1} Cd were extracted in 1.0M-ammonium acetate (step 3) from the samples C2 and B1 respectively. These values are several

times higher than the ICRCL recommended limit for Cd in soils, which is 10mg kg^{-1}. The relatively high extraction of Cr from sample C1 compared with that from samples C2 and B1 in step 2 is more likely related to the high concentration of Pb in soil, possibly a Pb chromate[199]. There was no conclusive evidence for this, it is only an assumption, and it could have been a hot spot. Therefore, it can be concluded from these results that similar to Pb, a majority of the Cd in these soils should be extractable by ion-exchange or through complexation[206]. Chromium was immobile in the soil and should not be extractable unless a harsh treatment technique is used[24].

The extraction patterns observed for essential metals such as Zn and Cu from the three soil samples were similar. There was no significant difference between the concentrations of Zn extracted in steps 1 and 2, as suggested by a one-tailed Student t-test. There was no significant difference between the concentration of Zn extracted from sample C2 either in steps 1 or 2 (see Figure 12). Another interesting observation is the concentration of Zn extracted from the three soil samples in step 3. One tailed Student t-test (assuming unequal variance) performed on the data does not show a significant difference between the concentrations of Zn extracted from the three soils in ammonium acetate (step 3) i.e. the concentration of Zn extracted from these soils in the oxidisable stage was equal. There was no significant difference between the concentrations of Cu extracted from all three samples in steps 1 and 2.

The leachability of another essential metal Mg was different to that of Zn and Cu. Approximately half of total Mg in all three soils was insoluble in the first three steps of the extraction process. Of the remaining 50% majority of the metal was extractable

in the ethanoic acid (step 1) followed by ammonium acetate and hydroxylamine hydrochloride. The high recovery of Mg in the residual stage was possibly due to the presence of magnesium carbonates associated with calcite in the soil[26]. A fraction of these carbonates was soluble in the first and third steps by ion exchange whilst the remainder stayed insoluble.

Heavy metals bound to Fe/Mn oxyhydroxides and carbonates could be 1:1 complexes with transition metal ions and soft ions like Pb[210]. Several authors[170] have reported the capacity of EDTA to extract metals that are complexed or adsorbed to carbonates in Fe-rich soils (similar to the type of soil used in this study). Furthermore, EDTA has the advantage of being a complexing agent whose chemical structure is similar to natural complexing agents such as L-cysteine, and has the added advantages of being able to form stable metal complexes and being non-biodegradable.

It is difficult to quantify or predict the concentration of metals that would be available for uptake by plants based on the information obtained from the sequential extraction procedure. There is insufficient guidance from regulatory authorities as to what fraction should be considered bioavailable. The Dutch Environment Protection Authorities use batch extraction data using 0.1M $CaCl_2$ to estimate bioavailability, while in the United Kingdom of 0.01M EDTA (pH = 4) is used for the same[207]. In France, availability of Cu, Zn and Mn is studied using solutions composed of 0.01M Na_2-EDTA, 1M CH_3COONH_4 at pH 7. In Italy bioavailability of Cu, Zn, Fe and Mn is studied using solutions composed of 0.02M EDTA and 0.5M CH_3COONH_4 at pH 4.6.

Metal extraction using $CaCl_2$ takes place by ion-exchange, while that using ammonium acetate and EDTA would take place principally through complexation. Since ammonium acetate has similar properties to that of ethanoic acid, extractions obtained in the first step of the sequential extraction procedure would be the bioavailable fraction i.e approximately 10-16% of the total Pb in the soils. However, as discussed previously EDTA is a lewis base and has the capacity to complex metals bound to clays, carbonates and Fe/Mn oxide fractions. This implies that approximately 80% of the total Pb should be available for uptake by plants. The presence of mobile Pb in the soils at such high concentrations would be not only phytotoxic, but would also have a great potential to harm controlled waters (and the resulting bioavailability implications). This brings into question the applicability of the BCR three-step procedure and the other procedures (used in various countries) as ecological risk assessment tools.

3.4 Conclusions

Industrially contaminated soil samples were characterised using mineralogical techniques such as XRD, XRF, ESEM/EDX, FT-IR and wet chemical techniques such as total digestion and the BCR sequential extraction procedure. The results showed that the soils were principally contaminated with Pb along with low levels of Cd, Cr, Zn and Cu. Isotopic analysis suggested that the Pb contamination was a result of mineral ore processing activities at the site. The mineralogical techniques showed that a majority of the lead in the soils were present as oxides, sulphates and phosphates, principally bound to the clays (mainly kaolinite) and Fe oxides.

Data from the application of the BCR sequential extraction procedure showed that a majority of the contaminant metals were present in ion-exchangeable, weak acid

soluble and reducible forms. This is additional evidence that the presence of metals in these soils was a result of human activity, rather than natural occurrence, as naturally abundant metals are generally bound to silicates[2]. Overall, there is broad agreement between the data obtained from the mineralogical techniques and the BCR procedure. The BCR procedure has provided some important pointers as to which remediation techniques to use for these soils, without radically altering the principal structure of the soils. Soil washing using complexing reagents such as EDTA should be an effective tool for the removal of a major fraction of the metals from the soil.

Chapter 4 Effect of Solution pH on Solid-Solution Partitioning of Metals

4.1 Introduction

The data obtained in the previous chapter have shown that a majority of the contaminant metals such as Pb are bound to the reducible fractions in the soil. As discussed before, pH is the most important factor dictating the soil-solution partitioning (K_d) of metals in soils. This is because the point of zero charge (PZC), which is the pH at which the net charge on the surface of minerals is zero, for different minerals is at different pH values as shown in Table 15. It can be assumed from the data in Table 15, that in the absence of complexing agents in solutions, a majority of contaminant metals in the soils used in this study, would only be mobile under alkaline conditions, as the PZC of Fe oxides and oxyhydroxides is in the pH range 7.7 - 9.

Mineral	PZC
γ-AlOOH	10.4
	9.3
α-FeOOH	9.0
	7.7
α-Fe_2O_3	8.5
Allophane:	
SiO_2/Al_2O_3 = 1.10	6.9
SiO_2/Al_2O_3 = 1.34	6.5
SiO_2/Al_2O_3 = 1.67	5.5
SiO_2	2-3
Mn(II) manganite	~1.8
δ-MnO_2	1.5

Table 15: PZC values for common soil minerals[208].

This chapter investigates metal desorption from soil surfaces into water over the pH range 2-12. A series of batch extraction experiments using pH adjusted deionised water (pH range 2-12) were conducted. The volume and extraction time were kept constant at 40mL and 16h respectively, in order to allow a broad comparison with the data obtained through the application of the BCR sequential extraction process. The principal aim of these experiments was to study the effect of solution pH on metal desorption and the consequent bioavailability of metals. Another aim of these

experiments was to obtain baseline values for soil-solution partition coefficients (K_d), against those obtained through the use of other complexing agents (i.e. other than those already present in the pH adjusted water solutions such as Cl^-) could be compared.

4.2 Results and Analysis

The pH of each of the soil solutions was measured at the beginning and end of each of the extractions. One-tailed Student t-test shows that there is a significant difference in the pH of the soil solutions before and after each of the extractions. This suggests that the soil has a poor buffering capacity.

At the conclusion of each extraction the soil solutions were immediately centrifuged and the supernatant filtered. The filtrate was immediately transferred to clean polyethylene centrifuge tubes and acidified with dilute nitric acid to prevent the precipitation of metals. These solutions were then stored in a cold room at 4°C prior to analysis.

pH	Ca	Al	Mg	Fe	Man	Pbe	Zn
2	3180±138	475±77	276±15	71±3	154±10	2220±222	36±1
3	333±10	73±4	51±3	74±2	10±1	43±6	8±0.8
4	214±15	128±6	35±2	71±3	7±1	53±5	6.2±0.2
5	175±27	163±16	55±12	150±15	7±1	70±5	5.5±0.8
6	149±16	184±21	30±3	159±15	7±2	94±5	4.2±0.7
7	132±22	56±29	22±4	91±5	2±1	129±3	<0.01
8	168±8	37±11	29±1	53±1	7±1	60±3	<0.01
9	163±5	20±1	32±1	45±1	7±1	72±7	<0.01
10	112±1	16±1	23±1	29±1	5±1	90±8	<0.01
11	121±6	206±27	22±2	209±28	9±1	147±24	<0.01
12	679±16	4280±207	219±14	2520±157	<0.0060	1450±93	<0.01

Table 16: Metal extractions (mg kg^{-1}) from the soil sample C1 into deionised water over the pH range 2-12.

Calcium

The data show that approximately 92% (3200mg kg^{-1}) of the total aqua-regia soluble Ca was extracted at pH 2 followed by a rapid decline at the subsequent pH values until pH 12, at which point there was a sharp increase in the extracted Ca to 680mg kg^{-1} (Table 16).

Magnesium

The extraction pattern for Mg was similar to that for Ca. Approximately 31% (276mg kg^{-1}) of the total aqua-regia soluble Mg was extracted at pH 2, followed by a sharp decrease until pH 12, at which point there was a sharp increase to 220mg kg^{-1}) (Table 2).

Aluminium

Approximately 10% (475mg kg^{-1}) of Al was extracted at pH 2 followed by a decrease at pH 3 (73mg kg^{-1}). This was followed by an increase in extraction until pH 6 (184mg kg^{-1}), after which there was a decrease until pH 11 (206mg kg^{-1}) and pH 12 (4280mg kg^{-1}).

Iron

There was no significant difference between the concentrations of Fe extracted in the pH range 2-3 (approximately 74mg kg^{-1}). This value doubled in the pH range 5-6 (150mg kg^{-1}), followed by a decrease until pH 10 (30mg kg^{-1}). There was a large increase in the concentration of Fe extracted in the pH range 11-12. The concentration of Fe extracted at pH 11 and pH 12 were 210mg kg^{-1} and 2500mg kg^{-1} respectively.

Manganese

The highest extraction of manganese was at pH 2 (154mg kg^{-1}), followed by a decrease to 10mg kg^{-1}. Thereafter the concentration of Mn extracted into solution remained constant at approximately 5mg kg^{-1}, until pH 12 where the concentration of Mn extracted into solution was below instrumental (ICP-AES) limits of detection.

Lead

The data show that the highest extraction of Pb was at pH 2 (2250mg kg^{-1}) followed by pH 12 (1500mg kg^{-1}) and pH 11 (150mg kg^{-1}). The extractions in the intermediate range were very low, in the approximate range 45 to 90mg kg^{-1}.

Zinc

Approximately 36mg kg^{-1} of Zn was extracted at pH 2, which is approximately in the same range as that extracted in the first step of the sequential extraction process (45mg kg^{-1}). These metal ions are possibly the ones bound to carbonates or silicates. The concentration of Zn extracted in the following pH range was very low to below limits of detection.

4.3 Discussion

There was a marked trend to the extraction pattern of metals at individual pH values. Overall, there is low mobility of metals ions in the pH range (5-6) of plant survival. The high extractions at each end of the pH scale, apart from other mechanisms, are possibly due to the displacement of M^{2+} ions from mineral surfaces through ion exchange mechanisms due to the presence of an excess of H^+ and OH^- ions (the potential determining ions (PDI)) in the solutions[209]. The metal ions released in the intermediate pH range are probably the ones bound to the soil surfaces by weak electrostatic forces[3]. Data obtained from these experiments were used to calculate K_d,

the solution-soil partition coefficient of metals in soil at different pH values (Table 17). This data do not provide information on the mobility of different metals in relation to the total metal concentration in the soils. Partition coefficients, detailed in Table 3 provide an estimate of metal leachability (i.e. desorption capacity) from soil surfaces at different solution pH values.

pH	2	3	4	5	6	7	8	9	10	11	12
Ca	40	400	680	800	1000	1000	800	800	1320	1000	200
Al	400	2000	1320	1320	1000	4000	4000	n/a	n/a	1000	40
Mg	120	680	1000	680	1320	2000	1320	1000	1320	2000	160
Fe	40000	40000	40000	4000	4000	4000	10000	13320	20000	4000	320
Man	120	2000	2000	4000	4000	4000	2000	2000	4000	2000	n/a
Pbe	120	4000	4000	4000	2000	2000	4000	4000	4000	2000	160

Table 17: Soil-solution distribution coefficient (K_d) (L kg^{-1}) data for the metals; these values were calculated by dividing the concentration of metals extracted into aqua-regia by the concentration of metals in deionised water (40mL) at different pH values. The higher the K_d value, the greater the binding of metals to the mineral surfaces (i.e. K_d α metal binding strength). n/a signifies that the concentration of metals were below the limits of detection.

Partition Coefficients of Metals at pH 2

The increasing order of partition coefficients of metals at pH 2 were as follows: Ca>Mn>Pb>Mg>Al>Fe. This data show that significant concentrations of contaminant metals such as Pb can be mobilised at this pH. The effectiveness of the leaching process could be enhanced through the addition of complexing agents such as EDTA and citric acid to the solutions.

The high extraction of Ca (K_d = 40) was probably because at very low pH, the rate of dissolution of calcite ($CaCO_3$) is so fast that the rate is limited by the transport of the reacting species between the bulk of the solution and the surface of the mineral[210]. Although a Student t-test comparison of this data with those from the first step of the BCR sequential extraction process (2310mg kg^{-1}) reveals a significant difference, it

can be assumed that the underlying principles behind the two extraction processes are similar i.e. ion exchange. The higher extraction is possibly because 10% HCl solutions were used to adjust the pH of the solutions (HCl is a stronger acid compared to CH_3COOH). The high level of extraction of Mn at pH 2 was possibly due to disproportionate of manganese oxyhydroxides such as manganite (Month) with the subsequent formation of higher oxides[211]. A typical reaction may be written as: $2MnOOH + 2H^+ = Mn^{2+} + MnO_2 + 2H_2O$. Additionally, the PZC of Mn oxides is in the range 1.5-1.8.

The extraction concentration of Pb at pH 2 was approximately twice that extracted in step 1 of the sequential extraction process (1030mg kg^{-1}). This higher extraction is possibly because HCl is a stronger acid than ethanoic acid, consequently there is greater metal release by ion exchange. The Pb ions released at pH 2 are probably those bound to the calcium carbonate fraction and the silicate fraction. Those bound to the carbonate fraction would have been released during calcite dissolution, while those attached to the surface of silicates would have been released due to the lack of a surface charge on silicates at pH 2 as the PZC of silicates is in the pH range 2-3[2].

The concentration of Mg extracted into solution at pH 2 was approximately the same as that in the first step of the sequential extraction process (165mg kg^{-1}). The magnesium extraction at this pH is possibly that associated with calcite, as Mg regularly substitutes for Ca in calcite. The relatively high extraction of Al at pH 2 is possibly due to Al^{3+}release due to the dissolution of kaolinite, muscovite and δ-Al_2O_3[212]. The Fe ions released in the pH range 2-3 are possibly the ones bound to the surface of silicates electrostatic ally.

Partition Coefficients of Metals at pH 4

This is a common pH of rainwater and the data obtained here can be used to a limited extent to understand the leachability of metals in rainwater (Table 17). This data cannot be used in its entirety because there are no rainwater constituents such as carbonates or bicarbonates in these solutions, which could have aided the dissolution of soil minerals and also allowed good buffering of the soil solutions. The increasing order of partition coefficients of metals at pH 4 were as follows: Ca>Mg>Al>Mn>Pb>Fe. Since, the partition coefficients were very low, the mobility of most of these metals is expected to be very low.

Partition Coefficients of Metals at pH 7

This is the pH at which most metal cations would have precipitated from the solution as hydroxides. However, the metals analysed in the solutions would have been those associated with colloids or organic matter[213]. The increasing order of partition coefficients of metals at pH 7 (neutral) were as follows: Ca>Mg>Pb>Al>Fe>Mn. The increase in the Fe extraction in the pH range 5-7 was probably due to the release of Fe ions bound electrostatically to allophanes (short chain aluminosilicates), whose PZC lies in this range[212]. It is noteworthy that the K_d for lead (2000L kg^{-1}) at this pH was close to the values (2500L kg^{-1}) used by other sources such as the CLEA model[112] and the Dutch National Institute of Public Health and the Environment[214].

Partition Coefficients at pH 12

This is pH at which a majority of the anions in the soil would be mobile. Most of the major metals in the soil were extracted at this pH. The increasing order of partition coefficient of metals at pH 12 were as follows: Al>Mg>Ca>Pb>Fe. The very high extraction concentration of Al at pH 12 was possibly due to the dissolution of

aluminium hydroxides and oxyhydroxides such as gibbsite ($Al(OH)_3$) or boehmite ($AlOOH$)[6]. It is unclear as to what causes the increase in Ca and Mg extraction, although an assumption can be made about the nature of the reaction. An excess of NH_4^+ ions in the solution at pH 12 (solutions' pH was adjusted using NH_4OH solutions) could have caused the replacement of Ca^{2+} and Mg^{2+} ions on with NH_4^+ ions by ion exchange. The large increase in the concentration of Fe extracted in the pH range 11-12 is due to the dissolution of iron oxyhydroxides such as goethite ($FeOOH$)[215]. The Pb ions released at pH 12 are probably those bound to goethite ($FeOOH$).

4.4 Conclusions

The leachability of the different metals from the soil sample (C1) was studied in the pH range 2-12. Of all the contaminant metals in the soils only Pb was leachable in concentrations measurable by ICP-AES. Relatively high concentrations of the major metals in the soil were leached out at each end of the pH scale. In the intermediate pH range, there was relatively low mobility of these metals, as shown by the partition-coefficient (K_d) calculations. This showed that under pH standard conditions (pH 4-7), most of the metals in the soil are not bioavailable or leachable. However, this can be changed through the addition of complexing agents to the solutions.

Chapter 5 Evaluation of Metal Desorption from the Soil through Ion Exchange

5.1 Introduction

Data obtained through the application of the BCR procedure has shown that a significant fraction of the metal ions in the soil samples were extracted in the first two steps. This is the step where the majority of the ion-exchangeable and bioavailable metals are mobilised. The data obtained from the batch extraction experiments using water have shown that significant concentrations of the metals in the soil were mobilised into solution in the pH range 2-3. Although assumptions were made as to the nature of the mechanisms dictating these mobilisations e.g., ion exchange, dissolution of carbonates and complexation with acetate ions, metal release due to PZCs on the surface of minerals etc., there has not been any conclusive proof so far for these inferences.

The Tessier sequential extraction scheme (step 1) and several other authors[216] have utilised 1mol L^{-1} $MgCl_2$ at pH 7 to mobilise metals that exist in soil in an exchangeable form[217,218]. The availability and mobility of heavy metals in polluted soils is studied in the Netherlands using 0.1 mol L^{-1} unbuffered $CaCl_2$[219]. Novozamsky et al.[220], working on a range of extractants and soil types concluded that 0.01M $CaCl_2$ was the most useful extractant to estimate plant bioavailability, as it had approximately the same salt concentration as a standard soil solution, and because Ca^{2+} is often the dominant cation competing for binding sites on mineral surfaces. Other authors have recommended the use of 0.05M $CaCl_2$ for extractions, as it has a similar pH, concentration and composition to soil solutions.

In order to assess the leachability and potential mobility of the metals in the soil sample C1, batch extractions were performed using 1, 0.5, 0.1, 0.05 and 0.01M $CaCl_2$ and $MgCl_2$ solutions. Further experiments were conducted using $CaCl_2$ and $MgCl_2$ solutions (at the optimum molarities) in the volume range 20-100mL at increments of 20mL, to observe the optimum soil-solution ratio (the term 'optimum' has been used here to signify the molarity, volume or pH at which there was maximum extraction of metals from soil surfaces). These experiments were conducted at pH 5.2±0.2 in order to prevent the precipitation of cations such as Pb^{2+} and Cd^{2+} as hydroxides. Additionally, this is the ideal pH range for optimal plant growth. Both calcium and magnesium chloride solutions were used in order to directly compare the relative efficiency of these reagents in extracting metals from the soil.

The aims of the experiments described in this chapter were three fold: (1) study the leachability of metals as a result of ion exchange using calcium and magnesium chloride solutions; (2) study the potential of using these two solutions as soil washing reagents; (3) compare the data obtained from these experiments with those from the first step of the sequential process i.e. to study if the metal ions extracted during the BCR process were result of ion exchange, dissolution of carbonates or complexation with ethanoate (CH_3COO^-) ions.

5.2 Results and Analysis

The pH of both solutions when measured before and after the extractions was observed to be within the pH range 5.5-6.0. The concentrations of Cd, Cu and Cr extracted into solution using both the $CaCl_2$ and $MgCl_2$ solutions were below instrumental limits of detection across the entire molar range (Tables 18(a-b) and 19(a-b)). The concentrations of Fe and Al mobilised into solution were minimal

compared to the total concentration of these metals in the soil (Tables 18(a-b) and 19(a-b)).

	Ca	Cd	Cu	Al	Cr	Mg	Fe	Mn	Pb	Zn
1M	n/a	<0.07	<0.05	112±2	<0.07	422±23	6±1	24±3	575±71	216±3
0.5M	n/a	<0.07	<0.05	58±1	<0.07	332±4	<0.003	32±1	901±113	244±29
0.1M	n/a	<0.07	<0.05	7.6±2	<0.07	257±5	<0.003	43±3	216±28	156±9
0.05M	n/a	<0.07	<0.05	<0.03	<0.07	257±24	<0.003	49±1	150±22	122±42
0.01M	n/a	<0.07	<0.05	<0.03	<0.07	235±20	<0.003	35±3	<0.15	26±2

Table 18(a): Effect of changing the molar concentration $CaCl_2$ extractant on amounts of metals leached from soil C1 (results in mg L^{-1}; 1g soil treated with 40mL extractant).

	Ca	Cd	Cu	Al	Cr	Mg	Fe	Mn	Pb	Zn
20mL	n/a	<0.07	<0.05	<0.0232	<0.07	378±16	<0.003	68±1	624±96	47±12
40mL	n/a	<0.07	<0.05	65±9	<0.07	394±5	<0.003	43±1	976±250	155±10
60mL	n/a	<0.07	<0.05	145±1	<0.07	639±18	8±1	53±6	827±253	190±7
80mL	n/a	<0.07	<0.05	288±56	<0.07	731±132	21±6	46±22	1130±65	219±41
100mL	n/a	<0.07	<0.05	277±67	<0.07	719±187	22±2.5	38±17	1050±94	241±38

Table 18(b): Effect of changing the soil: solution ratio on amounts of metal leached from soil C1 (results in mg kg^{-1}; 1g soil extracted with 0.5M $CaCl_2$).

Lead

The data show that 0.5M $CaCl_2$ solutions extracted the highest concentration (901±113mg kg^{-1}) of Pb from the soil (Table 18(a)). The optimum soil-solution ratio using this solution was observed to be 1:80 i.e. the extraction of Pb was highest using 1g soil in 80mL $CaCl_2$ (1130±65mg kg^{-1}) solution (Table 18(b)). The calculated soil-solution partition coefficient was 448L kg^{-1} (Table 20).

The data show that 1M $MgCl_2$ solutions extracted the highest concentration (885±169mg kg^{-1}) of Pb from the soil (Table 18(a)). The optimum soil-solution ratio using this solution was observed to be 1:80, with the extraction concentration being

1586±80mg kg^{-1} (Table 18(b)). The calculated soil-solution partition coefficient was approximately 320L kg^{-1} (Table 20).

Metals	Ca	Cd	Cu	Al	Cr	Mg	Fe	Mn	Pb	Zn
1M	1630±93	<0.07	<0.05	25±6	<0.07	n/a	13±1.7	29±3	885±169	51±2
0.5M	1750±50	<0.07	<0.05	23±0.5	<0.07	n/a	11±0.6	34±0.2	612±99	45±1
0.1M	1450±78	<0.07	<0.05	12±4	<0.07	n/a	5±2.7	29±1	79±2	27±0.4
0.05M	1670±139	<0.07	<0.05	10±2	<0.07	n/a	4±0.5	34±4	42±4	24±3
0.01M	1530±52	<0.07	<0.05	8±0.6	<0.07	n/a	5±0.5	31±1.4	<0.15	11±0.4

Table 19(a): Effect of changing the molar concentration $MgCl_2$ extractant on amounts of metals leached from soil C1 (results in mg kg^{-1}; 1g soil treated with 40mL extractant).

Metals	Ca	Cd	Cu	Al	Cr	Mg	Fe	Mn	Pb	Zn
20mL	2100±24	<0.07	<0.05	12±1	<0.07	n/a	7±1	50±2	1110±14	56±2
40mL	2080±28	<0.07	<0.05	17±1	<0.07	n/a	8±1	41±1	1280±16	68±1
60mL	2520±167	<0.07	<0.05	26±1	<0.07	n/a	15±1	83±5	1530±313	100±2
80mL	2690±94	<0.07	<0.05	31±1	<0.07	n/a	17±1	76±1	1590±80	112±3
100mL	2690±80	<0.07	<0.05	33±1	<0.07	n/a	17±1	73±2	1550±63	115±5

Table 19(b): Effect of changing the soil: solution ratio on amounts of metal leached from soil C1 (results in mg kg^{-1}; 1g soil extracted with 1M $MgCl_2$).

Metals	Al	Mg	Fe	Mn	Pb	Zn	Ca
0.5M $CaCl_2$	1336	104	80000	728	448	64	n/a
1M $MgCl_2$	8000	n/a	80000	448	320	128	104
0.11M CH_3COOH	1000	124	13332	84	505	200	60

Table 20: Soil-solution partition coefficients (K_d) (L kg^{-1}) for metals extracted from the soil using 0.5M $CaCl_2$ (80mL), 1M $MgCl_2$ (80mL) and 0.11M CH_3COOH (40mL) solutions.

Zinc

The data show that 0.5M $CaCl_2$ solutions extracted the highest concentration (244±29mg kg^{-1}) of Zn from the soil. The optimum soil-solution ratio was observed

to be 1:80, with the extraction being 219 ± 41 mg kg^{-1}. The calculated soil-solution partition coefficient was 64L kg^{-1} (Table 20).

The data show that 1M $MgCl_2$ solutions extracted the highest concentration (51 mg kg^{-1}) of Zn from the soil (Table 18(a)). The optimum soil-solution ratio using this solution was observed to be 1:80, with the extraction concentration being 112±3 mg kg^{-1} (Table 18(b)). The calculated soil-solution partition coefficient was approximately 128L kg^{-1} (Table 20).

Manganese

The molarity for optimum Mn extraction (49±1mg kg^{-1}) from the soil was observed to be 0.05M of $CaCl_2$ (Table 18(a)). The optimum soil-solution ratio using this solution was observed to be 1:10, with the extraction being 68 ± 1mg kg^{-1} (Table 18(b)). The calculated soil-solution partition coefficient was approximately 728L kg^{-1} (Table 20).

The molarity for optimum Mn extraction (34mg kg^{-1}) from the soil using $MgCl_2$ was observed to be 0.5M (Table 19(a)). The optimum soil-solution ratio using this solution was observed to be 1:60, with the extraction being 83±5 mg kg^{-1} (Table 19(b)). The calculated soil-solution partition coefficient (K_d) was approximately 448L kg^{-1} (Table 20).

Magnesium

The molarity for optimum Mg extraction (422±23mg kg^{-1}) using $CaCl_2$ was observed to be 1M (Table 18(a)). The optimum soil-solution ratio for Mg extraction using this

solution was observed to be 1:80, with the extraction being 731±132 mg kg^{-1}. The calculated soil-solution partition coefficient (K_d) was approximately 104L kg^{-1} (Table 20).

Calcium

The molarity for optimum Ca extraction (1750±50mg kg^{-1}) using $MgCl_2$ was observed to be 0.5M (Table 18(a)). The optimum soil-solution ratio for Mg extraction using this solution was observed to be 1:80, with the extraction being 2692 ± 94mg kg^{-1}. The calculated soil-solution partition coefficient (K_d) was approximately 104L kg^{-1} (Table 20).

5.3 Discussion

Ca and Mg ions being doubly positive actively exchange with metals bound to carbonates such as calcite and those bound to the surface of kaolinite by electrostatic bonding. Soil-solution partition coefficients for metals extracted from the soil using the $CaCl_2$ and $MgCl_2$ at the optimum molarities (0.5 and 1M respectively) were calculated and compared with those obtained using 0.11M ethanoic acid (Table 20). It is interesting to note that the K_d values obtained for extractions using $CaCl_2$ and CH_3COOH are in the same range (448 and 505L kg^{-1} respectively), which suggests that the BCR procedure might indeed have been effective in estimating the concentration of ion-exchangeable fraction of Pb in the soil. Similarly, the concentrations of Ca extracted from the soil using $MgCl_2$ and ethanoic acid were in the same range. The K_d values for other metals extracted using the three reagents were not comparable.

The data showed that 1M $MgCl_2$ solutions were the most effective of the three reagents for the extraction of Zn, Ca and Pb, while 0.11M ethanoic acid solutions were most effective at extracting Mn, Fe, and Al. The higher extraction of Pb and Zn by the $MgCl_2$ solution is probably due to the rapid saturation of calcite surfaces as a result of an excess of calcium ions in the calcium chloride solution. This suggests that the concentration of Pb and Zn available in ion-exchangeable forms might be greater than that predicted by the BCR procedure. This observation is in agreement with Li and Thornton[221] who observed that approximately 10-50% of the total Pb in smelter soils was associated with the carbonate phase, possibly as lead carbonates.

However, Foster and Lott[222] have shown that lead emissions from smelters consist of lead sulphate ($PbSO_4$), lead monoxide (PbO) and lead oxysulfate ($PbO.PbSO_4$), an observation similar to that from XRD analysis of the soil C1 (presented in Figure 8 and Table 8). Clevenger et al.[223] showed that 0.5M NH_4OAC could dissolve 81% of the PbO in the soil. The reagent used here (1M $MgCl_2$) has a similar ionic strength. Therefore, it can be assumed that the Pb and Zn extracted in this step may represent PbO and ZnO as well as sulphate. Further evidence for reduced Pb and Zn binding to Fe oxides and oxyhydroxides comes from the low partition coefficients for Fe extracted using all three reagents.

5.4 Conclusion

Batch extractions of metals from the soil were conducted using $CaCl_2$ and $MgCl_2$ and the data compared with those obtained using 0.11M ethanoic acid. These experiments were conducted in the pH range 5.2±0.2, as this is the pH of optimum plant survival and to prevent the precipitation of divalent cations. The data show that 1M $MgCl_2$ is the most effective reagent for the extraction of Pb and Zn. Approximately, 25% of

the total Pb in the soil was extracted using this reagent, which suggests that majority of the Pb was in an ion-exchangeable form or in the form of PbO, $PbSO_4$ and $PbO.PbSO_4$. A further observation was that the proportion of Pb, Zn, Mn and Mg mobilised into solution from the soil surfaces was dependent on the ionic strength of the extractants. Consequently, as shown in these experiments, the molarity of ethanoic acid used in the first stage of the BCR sequential extraction process might have been insufficient to accurately predict the concentration of ion-exchangeable metals in the soil. Another important conclusion that can be drawn from these studies, is that 0.5M $CaCl_2$ and 1M $MgCl_2$ solutions can be used as effective soil washing solutions for heavy metal contaminated soils.

Chapter 6 Batch Extractions using Ethanoic Acid

6.1 Introduction

The experiments in the previous chapter have shown that the proportion of ion-exchangeable lead and zinc (the major contaminants) extracted using calcium and magnesium chloride solutions in the pH range 5.0 - 5.5 was almost equal to that extracted using ethanoic acid in the pH range 2.4-2.8. However, the proportion of structural metals such as Al and Fe extracted using the former solutions was much lower than that mobilised by ethanoic acid. Two major inferences that can be drawn from these observations are: (i) Pb and Zn in the soil might not have been associated with any particular mineral phases in the soil i.e. they might have simply precipitated on to soil surfaces and exist in the form of sulphates and oxysulfates; (ii) they could have been potentially extracted at a more 'environment friendly' pH range i.e. 5-6, using complexing agents, without changing the structure and composition of the soils.

The greater extraction of metals in 1M $MgCl_2$ solutions compared with those in 0.5M calcium chloride and 0.11M ethanoic acid solutions suggests that the leachability of metals in the soil might also depend on the ionic strength of the solutions. This implies that an increase in the molarity of ethanoic acid solutions might result in a greater extraction of metals. In order to support this inference, batch extraction experiments were conducted to ascertain the effect of ethanoic acid molarity on metal extractions from the soil. The optimum molarity, pH and volume were noted and a set of extractions conducted under these conditions. XRF analysis of the residue from the extractions was performed to ascertain changes in soil mineral content. The speciation of Pb in ethanoic solutions in the pH range 2-6 was calculated using the geochemical modelling software MINEQL+.

The principal aims of this experiment were: (i) to develop a procedure customised to predict the fractionation of contaminant metals in heavily contaminated soils; (ii) to calculate the proportion of the total lead in the soils present in the form of oxides and sulphates, as lead oxides and sulphates are known to be easily soluble in dilute ethanoic acid[222]; (iii) to develop a soil washing procedure that can completely extract contaminant metals from the soils without affecting the structure and composition of soil minerals in a major way. This chapter will focus principally on the extraction patterns of lead, as this is the only contaminant metal present in significant concentrations in the soil.

6.2 Results and Analysis

Molarity Optimisations

The data presented in Table 21(a) shows that there was a progressive increase in the concentration of all metals extracted into ethanoic acid in the molarity range 0.001 – 3.0M (pH = 2.8±0.4), followed by a progressive decline. The concentration of Pb extracted into solution at the molar values 0.001, 1, 3.0, 3.5 and 6M were 25±2, 2870±250, 4420±95, 4420±39 and 2430±152mg kg^{-1} respectively. The concentrations of Zn extracted into solution at the same molar values were 2.5±1, 37±4, 40±2, 43±3, 10±2mg kg^{-1} respectively. The concentration of Fe extracted into the solutions were 1.2±0.3, 277±6, 1528±12, 1025±162 and 1085±10mg kg^{-1} respectively. The concentration of Ca extracted into the solutions were 25±5, 3200±66, 3700±11, 3000±89, 2270±35mg kg^{-1}.

Volume Optimisations

The soil-solution ratio for the extractions was optimised using 3M ethanoic acid (pH = 2.8±0.4) solutions (data in Table 21(b)). The data showed that extraction equilibrium was reached for all the metals in the volume range 70-80mL. The concentration of Pb extracted in 20, 40, 60, 80 and 100mL of 3M ethanoic acid solutions were 3640±335, 4770±1030, 4600±223, 5100±20, 5300±259mg kg^{-1} respectively. The concentration of Zn extracted in the same solutions were 43±3, 56±3, 64±1, 57±6, 59±1, 59±11mg kg^{-1} respectively.

pH Optimisations

The optimum pH for maximum metal extraction from the soil was measured using 80mL of 3M ethanoic acid solutions. The extractions were only performed in the pH range 2-6, as it was impossible to adjust the pH of the solutions beyond 7 using the NH_4OH solutions. There was no significant difference in solutions pH before and after the extractions. As the data presented in Table 21(c) show, the highest metal extraction takes place in the pH range 4-5.

As shown in Figure 13(a), there was a progressive increase in the concentration of Pb mobilised into solution in the pH range 2-4, until equilibrium was reached in the pH range 5-6. The soil-solution partition coefficients (K_ds) for Pb extracted into ethanoic acid solutions at pH 2, 3, 4, 5 and 6 were 168, 152, 112, 96 and 104L kg^{-1} respectively (higher K_d signifies lower extraction). Approximately, 48%, 52%, 73%, 81% and 75% of the total Pb in the soil were extracted at pH 2, 3, 4, 5 and 6 respectively. The high extraction of Pb using dilute ethanoic acid in the pH range 4-6 provides definitive evidence of the overwhelming presence of Pb in the soil as PbO, $PbSO_4$,

$PbO.PbSO_4$, as these compounds are known to be readily soluble in dilute ethanoic acid[222]. These lead oxides and sulphates are likely to be products of smelting of galena (PbS) and would have precipitated onto the surface of soil minerals.

The high extraction of Pb in the pH range 4-6 was due to a greater availability of CH_3COO^- ions for complexation, as the pK_a of ethanoic acid is approximately 4.8. The geochemical modelling software MINEQL+ was used to ascertain the speciation of Pb in these acetate solutions. Figure 14 is a graphical representation of the distribution of the Pb species in the solutions. The figure shows that at pH 2 approximately 20% of the total Pb in the solution was in the form of Pb^{2+}, 5% in the form of $Pb(CH_3COO)_2$ (pKa = 4.08), and 75% in the form of $(CH_3COO)Pb^+$ (pKa = 2.87). The proportion of Pb^{2+} in solutions almost reaches 0% at pH 3, while those of $(CH_3COO)Pb^+$ and $Pb(CH_3COO)_2$ are almost equal at 50% each. At pH 4 the proportion of $Pb(CH_3COO)_2$ is approximately 75%, while that of $(CH_3COO)Pb^+$ was approximately 10%, with the remainder being in the form of other lead acetate species such as $Pb(acetate)^{2-}$. At pH 5, the proportion of $Pb(CH_3COO)_2$ declines to approximately 40%, with a simultaneous increase in the concentration of other species such as $Pb(CH_3COO)_4^{2-}$, $Pb(CH_3COO)_5^{3-}$ and $Pb(CH_3COO)_6^{4-}$.

As shown in Table 21(c) and Figure 13(b), there were no significant differences in the concentration of Zn extracted (20-25%) over the entire pH range. There were no significant differences in the concentrations of Mg, Mn, Ca and Al extracted over the pH range 2-6. Approximately 80% of the total acid-soluble Ca was extracted in the pH range 4-6. There was a progressive increase in the concentration of Fe extracted in the pH range 2-4, at which point there was chemical equilibrium. MINEQL+

database suggests that approximately 100% of the Fe in the solutions was in the form of iron acetates in the pH range 4-6.

Molarity	Ca	Al	Mg	Fe	Mn	Pb	Zn
0.001	25±5	5.3±0.5	26±1	1.2±0.3	25±3	25±4	2.5±1
0.01	100±3	15.4±1.2	63±2	2.6±0.3	35±3	65±16	4.6±0.4
0.05	750±19	30.5±2.7	93±1	4±0.5	46±3	215±35	9.2±0.4
0.1	1080±20	40.4±3.3	105±1	5.5±0.2	54±3	1164±15	11±1
0.25	1250±15	65±5	125±1	12±0.5	66±2	1761±25	13.5±1
0.5	3280±25	200±9	256±1	63±0.3	198±2	2100±130	34±4
0.75	3020±1	220±10	265±1	95±0.6	190±2	2390±175	34±4
1	3200±66	240±10	245±1	277±6	206±6	2865±250	37±4
1.5	2980±52	270±12	262±1	326±6	225±5	3040±220	34±4
2	3140±58	290±12	257±1	708±15	224±6	3415±240	39±3
2.5	3360±30	325±16	277±1	1150±11	257±3	3840±155	40±2
3	3690±11	360±17	284±1	1530±12	274±2	4410±95	43±3
3.5	3000±89	451±69	249±15	1020±162	163±12	4420±39	37±4
4	2580±176	313±130	213±64	1190±288	122±56	3320±88	25±5
4.5	2060±183	272±59	176±25	1320±178	100±17	2810±124	17±2
5	2600±275	387±74	229±75	1310±120	145±8	2660±84	15±1
5.5	2150±490	306±151	184±50	1180±508	107±41	2360±602	12±1
6	2270±35	247±3	192±1	1090±10	108±1	2430±152	10±2

Table 21(a): Effect of changing the molar concentration ethanoic extractant on amounts of metals leached from soil C1 (results in mg kg^{-1}; 1g soil treated with 40mL extractant).

Vol. (mL)	Ca	Al	Mg	Fe	Mn	Pb	Zn
10	3330±68	397±16	287±6	888±130	219±5	2740±153	36±5
20	3710±109	514±45	298±4	1220±66	231±24	3640±335	43±3
30	4150±309	583±184	325±28	1410±473	240±43	4230±665	52±4
40	4180±233	572±172	308±7	1560±543	245±32	4770±1027	56±3
50	4460±56	534±16	310±6	1360±51	248±2	4890±32	64±1
60	4430±104	629±59	335±14	1510±196	248±14	4580±223	57±6
70	4480±67	773±15	321±3	2210±89	274±10	5000±21	55±2
80	4670±80	678±25	327±9	1680±117	260±5	5080±20	59±1
90	4720±43	698±25	319±1	1710±98	360±10	5110±100	55±1
100	4850±107	760±139	314±1	2340±685	303±21	5300±259	59±11

Table 21(b): Effect of changing the soil: solution ratio on amounts of metal leached from soil C1 (results in mg kg^{-1}; 1g soil extracted with 3M ethanoic acid).

pH	Ca	Al	Mg	Fe	Mn	Pb	Zn
2.00	2530±12	521±2	267 ± 2	1800±26	252±10	3085±56	64±3
3.00	2530±200	414±61	326 ± 26	2470±69	263±65	3280±378	60±1
4.00	4000±90	445±17	312±6	2720±90	276±2	4640±326	68±2
5.00	2700±288	418±12.	284±23	2340±150	329±35	5160±194	64±1
6.00	2850±36	320±30	273±34	2690±34	185±24	4820±124	68±5

Table 21(c): Effect of changing the pH on amounts of metal leached from soil C1 (results in mg kg^{-1}; 1g soil extracted into 80mL of 3M ethanoic acid solutions).

(a) Lead

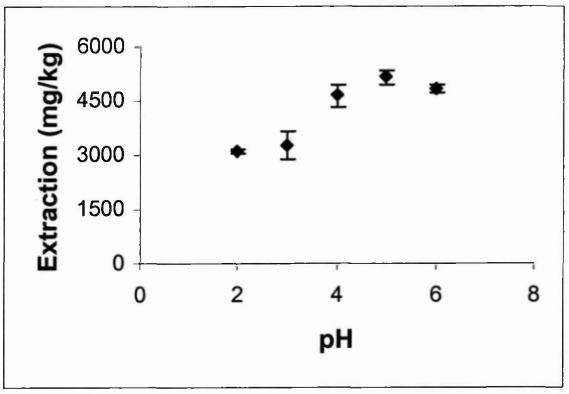

(b) Zinc

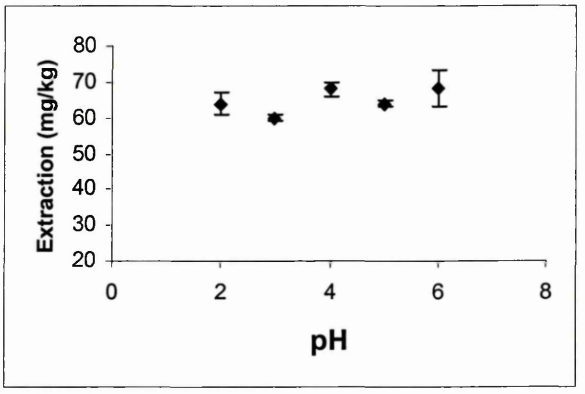

(c) Calcium

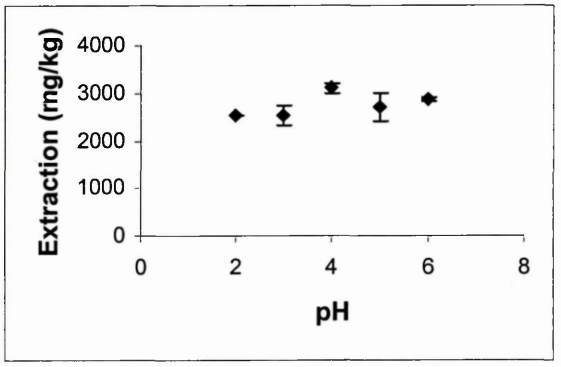

(d) Iron

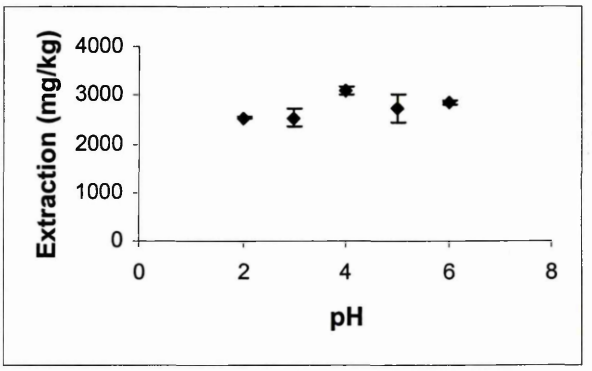

(e) Magnesium

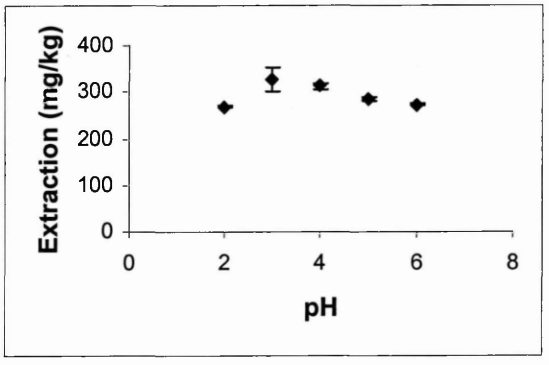

(f) Manganese

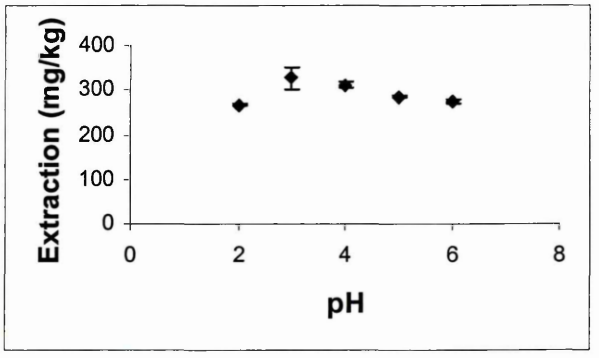

Figure 13: Desorption pattern for metals extracted using 3M & 70mL ethanoic acid in the pH range 2-6.

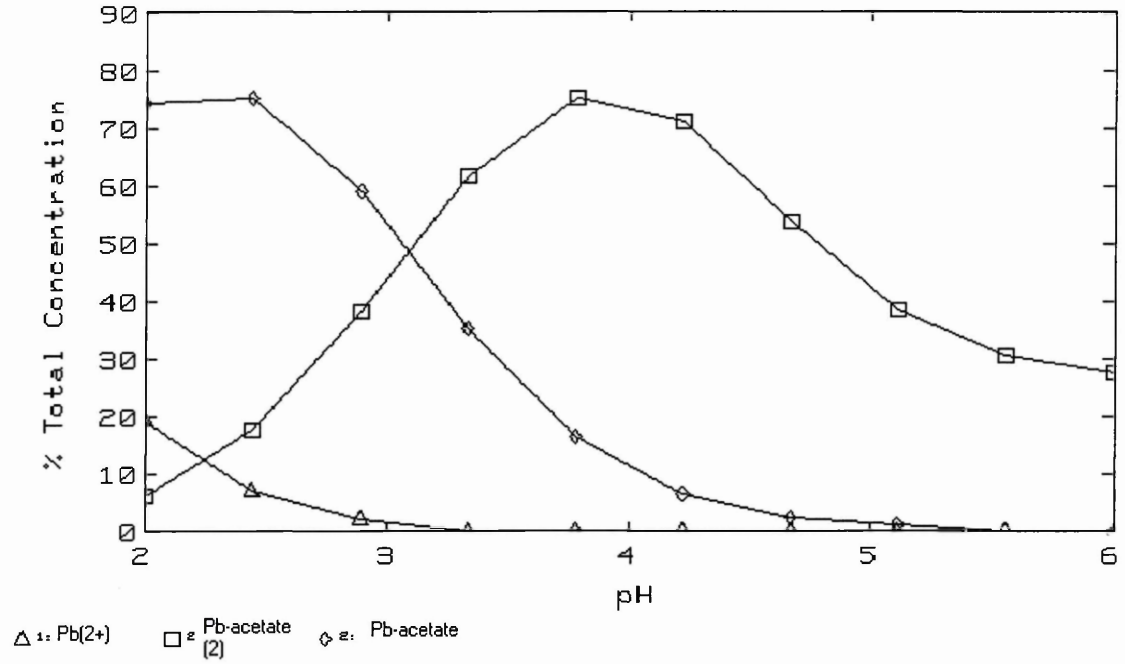

Figure 14: Speciation of Pb ions in 3M ethanoic acid solutions over the pH range 2-6, as derived using the MINEQL+ geochemical modelling software.

XRF Analysis of the Residue

XRF analysis of the residue from batch extractions using 3M ethanoic acid at pH 5 (presented in Table 22) shows that approximately 75% of the total Pb in the soil was mobilised into solution. The remainder of Pb in the soil was probably that associated with Fe/Mn oxyhydroxides and silicates. There was no significant change in the concentrations of Fe, Al, Si, K and Na oxides in the soil after the extractions, suggesting that the ethanoic acid does not target these minerals and that there might not be any significant association between these minerals and those of lead. The most important observation from these analyses is the lack of change in the concentration of sulphates and phosphates in the soil after the extractions. The concentration of sulphates before and after the extractions were 0.81% and 1.04% respectively, while those of phosphates were 0.71% and 0.79% respectively (the increase post-extraction signifies an increase in the proportion of these minerals in relation to the total mineral content in the soil). This lack of change indicates that the Pb minerals in the soil

might not have been present as sulphates or phosphates as the dissolution of these minerals would have resulted in changes in their respective concentrations in the soil. This means that lead oxides were the principal minerals in the soil, which explains the ease of lead dissolution in ethanoic acid.

Mineral composition	Untreated Soil (%w/w)	Acetate treated (%w/w)
SiO_2	59.3	64.7
Al_2O_3	21.3	19.8
Fe_2O_3	9.0	7.6
K_2O	2.2	2.1
CaO	1.6	0.4
MgO	1.1	0.9
TiO_2	1.0	0.9
PbO	0.7	0.2
P_2O_5	0.7	0.8
SO_3	0.8	1.0
Na_2O	0.5	0.4
MnO	0.2	0.1

Table 22: XRF analysis data for the residue from batch extractions using 3M ethanoic acid at pH 5.

6.3 Discussion and Conclusions

The main conclusions that can be drawn from the data are: (i) metal contaminants in *heavily* contaminated soils are not associated with specific mineral fractions in the soil, rather they would be present as precipitates, most likely in the form of separate mineral forms; (ii) dilute (3M) ethanoic acid solution in the pH range 4-6, can extract upto 80% of the total Pb from the contaminated soil and can be used as an effective soil washing reagent because as shown by XRF analysis (Table 22) it does not alter the principal soil properties; (iii) modifications to the BCR procedure are required, in order for the method to be more effective at predicting contaminant metal fractionation in industrially contaminated soils. It is important to note that this does not invalidate the bioavailability predictions obtained through the application of the modified BCR process. The validity of those predictions can only be ascertained by performing phytoextraction experiments.

Chapter 7 Customisation of the BCR Sequential Extraction Procedure

7.1 Introduction

One of the main conclusions that were drawn in the previous chapter was that the contaminant metal compounds in heavily contaminated soils exist mainly in the form of precipitates on soil surfaces or as independent mineral phases. This raises questions about the usefulness of the modified BCR procedure as a tool to characterise metal fraction in industrially contaminated soils. The experiments in chapter 6 demonstrated the ease with which lead can be mobilised into dilute ethanoic acid solutions, providing evidence for the fact that the metal was present in this soil principally as PbO. Approximately 80% of the total Pb in the soil was solubilised in 3M ethanoic acid, with the remainder presumably bound either to Fe/Mn oxyhydroxides or silicates. Assuming that there was extraction equilibrium in the pH range 4-6, metal desorption from mineral surfaces can possibly be explained using the Freundlich Model.

The Freundlich model suggests that a surface is comprised of a continuous series of binding sites. Adsorption to each of these sites occurs with a constant binding energy and limited by the formation of a monolayer of the solute on the surface of soil particles. The mathematical form of the model is $q = K_d C^{1/n}$; where q is the binding energy, where K_d is the soil-solution partition coefficient, C is the equilibrium concentration of an ion and n is a joint measure of the energies associated with a particular adsorption reaction. This means that the K_d is inversely proportional to the total concentration of the metals, C, i.e. greater the concentration of metals in the soil greater the potential for their desorption. This implies that subsequent to the formation of a monolayer on a surface (complete coverage), subsequent metal binding to the surface would take place principally as a result of precipitation, which means

that whilst the monolayer may be difficult to dissolve, the precipitate should be soluble with relative ease. This means that metals in low or marginally contaminated soils should be much more difficult to dissolve than those in heavily contaminated soils.

In order to test this hypothesis, a set of experiments was conducted, which involved modifications to the BCR sequential extraction process. These were performed on the soils C1, C2 and B1, with the first step of the BCR process changed to utilise 80mL of 3M ethanoic acid at pH 5, rather than 40mL of 0.11M ethanoic acid at pH 2.5. The conditions for hydroxylamine hydrochloride, hydrogen peroxide and ammonium acetate used in steps 2 and 3 were the same as those used for the modified BCR sequential extraction process. The principal aims of this experiment were (i) to compare the desorption pattern of metals from heavily (C1), moderately (C2) and marginally contaminated soils (B1) using the customised procedure; (ii) to develop a sequential extraction procedure that can characterise the fractionation of metals in soils heavily contaminated with metals and also function as a useful tool for the prediction of potential soil remediation techniques.

7.2 Results and Analysis

Lead

Approximately 57%, 29%, 10% and 4% of the total Pb in the sample B1 were extracted in steps 1, 2, 3 and 4 respectively (data presented in Table 23). Approximately 57%, 31%, 8.7% and 3% of the total Pb in the sample C2 were extracted in steps 1, 2, 3 and 4 respectively. Approximately 60%, 31%, 6% and 3% of the total Pb in the sample C1 were extracted in steps 1, 2, 3 and 4 respectively.

The K_ds for Pb extracted into 3M ethanoic acid solutions (the customised procedure) during step 1 from samples B1, C2 and C1 were 136, 136 and 136L kg^{-1} respectively. The K_ds for Pb extracted into 0.11M ethanoic acid solutions (the modified BCR procedure) during step 1 from samples B1, C2 and C1 were 464, 636 and 244L kg^{-1} respectively.

(a) Sample B1

Step	Cu	Ca	Al	Mg	Mn	Pb	Zn	Fe
1	14.5±3.7	5110±400	1175±121	198±10	189±26	909±99	46±6	5380 ±720
2	5.4±0.6	447±62	980±23	37±5	68±3	462±11	13.5±0.5	4580 ±104
3	15.2±0.6	211±64	3320 ±155	456±17	41±4	151±19	46±3	6150 ±288
4	5.5±0.4	92±72	7520 ±350	640±41	36±3	63±8	54±4	13000± 262
Sum	40	5857	12995	1330	334	1585	158	29200

(b) Sample C2

Step	Cu	Ca	Al	Mg	Mn	Pb	Zn	Fe
1	5.3±0.3	3360±60	953±18	241±14	267±9	1312±55	35±3	2370 ±88
2	2.5±0.1	316±12	1012±71	49±7	209±13	712±18	10±2	4000 ±410
3	12.4±1.5	118±14	2800±253	482±63	72±9	199±49	48±7	6910 ±66
4	8.9±0.3	162±6	6490±411	676±70	79±10	71±12	70±9	15300 ±307
Sum	27	3957	11300	1448	627	2294	163	28600

(c) Sample C1

Step	Cu	Ca	Al	Mg	Mn	Pb	Zn	Fe
1	10±0.4	5970±210	1570±76	179±10	333±11	6694±202	114±5	4280 ±181
2	3.6±0.1	3145±82	2480±96	248±15	156±22	3440±346	81±4	6590 ±242
3	23±2	2630±196	3900±338	1115±416	65±21	659±101	134±16	7325 ±820
4	7.1±3.2	183±16	5040±446	667±410	49±16	344±46	89±27	13300±505
Sum	43	11923	12646	2208	604	11136	418	31500

Table 23: Metal extraction (mg kg^{-1}) values using the customised sequential extraction procedure, where (a) soil B1 (b) soil C2 (c) soil C1. Step 1 – 3M ethanoic acid at pH5; Step 2 – 0.5M hydroxylamine hydrochloride at pH 2; Step 3- boil in hydrogen peroxide followed by extractions in 1M ammonium acetate at pH2; Step 4- digestion of residue from step 3 in aqua-regia. Each extraction was repeated five times (n = 5).

Copper

The extraction trends for Cu extracted from the soils were different to those for Pb. Approximately 36%, 13.5%, 38% and 14% of the total Cu in sample B1 were extracted in steps 1, 2, 3 and 4 respectively (data presented in Table 23). Approximately, 36.3%, 9.2%, 38% and 13.8% of the total Cu in sample C2 were extracted in steps 1, 2, 3 and 4 respectively. Approximately, 23.3%, 8.3%, 53.4% and 16.5% of the total Cu in sample C1 were extracted in steps 1, 2, 3 and 4 respectively. All the results showed moderate reproducibility with the average relative standard deviation being in the range ±8% - 15%.

The soil-solution partition coefficients (K_ds) for Cu extracted into the 3M ethanoic acid solutions during step 1 from samples B1, C2 and C1 were 224, 408 and 344L kg^{-1} respectively. The K_ds for Cu extracted into the 0.11M ethanoic acid solutions (*the modified BCR procedure*) during step 1 from samples B1, C2 and C1 were 1000, 2360 and 256L kg^{-1} respectively. This implies that the proportion of Cu desorbed from samples (μg mL^{-1}) B1 and C2 was higher in the 3M solutions at pH 5 (step 1 customised BCR procedure) than in 0.11M solutions at pH 2.5 (step 1 modified procedure). This increased desorption was either to a greater availability of acetate ions at pH 5 or due to a higher soil-solution ratio (80mL) used in the customised procedure.

Zinc

The extraction efficiency of Zn from all three soils during step 1 was higher using the customised procedure than those using the modified BCR procedure (data presented in Table 23). Approximately, 29.1%, 8.5%, 29.1%, and 34.2% of the total Zn in sample B1 were extracted in steps 1, 2, 3 and 4 respectively. Approximately, 21.5%,

6.1%, 29.5% and 43% of the total Zn in sample C2 were extracted in steps 1, 2, 3 and 4 respectively. Approximately, 27.3%, 19.4%, 32% and 21.3% of the total Zn in sample C1 were extracted in steps 1, 2, 3 and 4 respectively.

The K_ds for Zn extracted during step 1 of the customised procedure from soils B1, C2 and C1 were 272, 376, and 296kg L^{-1} respectively. The K_ds for Zn extracted from the same soils using the modified BCR procedure were 256, 316, 160kg L^{-1} respectively. This implies that it is easier to desorb Zn ($\mu g\ mL^{-1}$ solution) using the 0.11M ethanoic acid solutions than the 3M solutions. This might be possibly be due to the saturation of binding sites on the acetate ions by an excess of Pb ions in the 3M solutions.

Iron

The Fe extractions in step 1 of the customised procedure were much higher extraction than those using the modified BCR procedure (data presented in Table 23). Approximately, 18.4%, 15.7%, 21.1%, and 44.7% of the total aqua-regia soluble Fe in sample B1 were extracted in steps 1, 2, 3 and 4 respectively. Approximately, 8.3%, 14%, 24.2% and 53.5% of the total aqua-regia soluble Fe in sample C2 were extracted in steps 1, 2, 3 and 4 respectively. Approximately, 13.5%, 20.9%, 23.2% and 42.3% of the total aqua-regia soluble Fe in sample C1 were extracted in steps 1, 2, 3 and 4 respectively. This implies that a majority of the total Fe in the soil was associated with the silicate fractions of the soils.

The K_ds for Fe extraction during step 1 of the customised procedure from the samples B1, C2 and C1 were 432, 960 and 592L kg^{-1} respectively. The K_ds for Fe extraction during step 1 of the modified BCR procedure from the samples B1, C2 and C1 were

48300, 93300 and 10900L kg^{-1} respectively. This clearly shows that the 3M ethanoic acid (pH 5) solutions are more effective at the mobilisation of Fe than the 0.11M ethanoic acid solutions. This might have been due to a greater dissolution of iron oxides associated with lead oxides in the soil.

Calcium

Approximately, 87%, 7.6%, 3.6% and 1.5% of the total aqua-regia soluble Ca in sample B1 was extracted in steps 1, 2, 3 and 4 respectively (data presented in Table 23). Approximately, 84.9%, 7.9%, 2.9% and 4.1% of the total aqua-regia soluble Ca in the sample C2 was extracted in steps 1, 2, 3, and 4 respectively. Approximately, 50%, 26.3%, 22% and 1.5% of the total aqua-regia soluble Ca in the sample C1 was extracted in steps 1, 2, 3 and 4 respectively. The K_ds for Ca extractions during step 1 from the samples B1, C2 and C1 using the customised procedure were 88, 96 and 160L kg^{-1} respectively, while the K_ds using the modified BCR procedure were 64, 64 and 68L kg^{-1} respectively.

Magnesium

Approximately, 15%, 2.8%, 34.3% and 48.1% of the total Mg in the sample B1 were extracted in steps 1, 2, 3 and 4 respectively (data presented in Table 23). Approximately, 16.6%, 14.4%, 33.2% and 46.7% of the Mg in the sample C2 were extracted in steps 1, 2, 3 and 4 respectively. Approximately, 8.1%, 11.2%, 50.5% and 30.2% of the Mg in the sample C1 were extracted in steps 1, 2, 3 and 4 respectively. The K_ds for Mg extractions from the samples B1, C2 and C1 during step 1 using the customised procedure were 536, 480, 984L kg^{-1} respectively. The K_ds for Mg extraction from the samples B1, C2 and C1 during step 1 using the modified BCR procedure were 240, 188, 144L kg^{-1} respectively. This implies that the modified BCR

procedure is more efficient at desorption of Mg than the customised procedure during step 1.

Manganese

Approximately 56.6%, 20.4%, 12.2% and 10.8% of the total Mn in the sample B1 were extracted in steps 1, 2, 3 and 4 respectively (data presented in Table 23). Approximately 42.5%, 33.3%, 11.5% and 12.6% of the total Mn in the sample C2 were extracted in steps 1, 2, 3, and 4 respectively. Approximately 55.1%, 25.8%, 10.8%, and 8.1% of the total Mn in the sample C1 were extracted in steps 1, 2, 3, and 4 respectively. This data show that a majority of the metal was extracted in step 1 from all three soils, which implies that it exists principally in an ion-exchangeable form.

The K_ds for Mn extracted from samples B1, C2 and C1 during step 1 of the customised procedure were 144, 322, 144L kg^{-1} respectively. The K_ds for Mn extracted from samples B1, C2 and C1 during step 1 of the modified BCR procedure were 156, 252, and 100L kg^{-1} respectively. This implies that the modified BCR sequential procedure is more efficient at desorption of Mn than the customised procedure.

7.3 Discussion

The data presented above implies that an increase in molarity of ethanoic acid does have an effect on the total concentration of metals desorbed in each stage of the sequential extraction process. The data provides further confirmatory evidence that a majority of the Pb in all three soils was present in ion-exchangeable forms, rather than associated with Fe/Mn oxides, as suggested by the modified BCR procedure. The average increase in Pb extraction from the three samples in step 1 of the customised procedure was approximately 6-10 times that extracted during the same stage using the modified BCR procedure. The increased desorption was most likely due to a formation of lead acetates, as suggested by the MINEQL+ modelling data. It is unclear at this stage as to what fraction of the metal would be in a bioavailable form, as this can only be ascertained using phytoextraction studies.

Another important observation from this data is that the Freundlich isotherm cannot be used for the explanation of lead desorption from these soil samples. The Freundlich isotherm suggested that the efficiency of metal desorption is dependent on the concentration of metals in the soil i.e. the desorption efficiency being inversely proportional to the concentration. However, this trend was not observed in the three samples subjected to extractions using 3M ethanoic acid at pH 5 or to 0.11M ethanoic acid at pH 2.5. This is possibly because Pb might not have been associated with any specific mineral fractions; it was most likely in the form of PbO precipitated onto all the available soil surfaces.

A pattern similar to that for Pb was observed for Ca extractions from all three soils. A comparison of the total concentrations of Ca extracted in the first step of the modified BCR and the customised procedures, shows an average increase of approximately 2-3

times in the latter. This suggests that the Ca extraction in this stage might have been due to increased dissolution of calcium lead silicates identified using XRD. However, the soil-solution partition coefficients (K_ds) were higher for the Ca extracted using the customised procedure, than those using the modified BCR procedure, which suggests a lower mobility in the former. This suggests that the increase in extraction might be a product of the greater solution volume (80mL) used in the customised procedure rather than due to an increase in ethanoic acid molarity. As discussed in chapter 3, higher K_ds for Ca would be expected at low pH values due to the dissolution of calcite in the pH range 2-3.

Another important observation is the desorption pattern of Fe. A comparison of the total concentrations of Fe extracted in the first step of the modified BCR and the customised procedures, shows an average increase of approximately 80-300 times in the latter. A similar comparison of the K_ds shows an increase of approximately 20-100 times in the latter. This increase is possibly due to the co-dissolution of Fe oxides associated with lead oxides in the soil. Evidence for this association comes from the ESEM/EDX mapping data, which showed an overlap of Pb and Fe distribution patterns in the soil. This confirms that the extractants used in the sequential extraction process may not be phase specific. However, it is noteworthy that majority of the aqua-regia soluble Fe in the soils were extracted in steps 3 and 4, which indicates that most of the metal would have been associated with the soil silicates.

However, the data also show that the majority of Cu in all three soils was extracted during step 3 (hydrogen peroxide and ammonium) and therefore, would have been bound to the organic matter in the soil. Another noteworthy observation is that

proportion of Cu extracted in all four steps from soils B1 and C2 was approximately equal. This implies that most of the Cu in the soil would be unavailable for biological uptake or ion exchange. Furthermore, extractions using the BCR procedure follow the Freundlich isotherm suggested pattern, as the highest extractions were from the sample C1, followed by samples B1 and C2 (the total concentration of Cu was highest in sample C1 followed by samples B1 and C2).

Extraction patterns for Mg and Zn showed that the K_ds for these metals in the 0.11M solutions were higher than those in the 3M solutions. The concentrations of Mg and Zn extracted during step 1 of the customised procedure were higher than those in the same stage using the modified BCR procedure. However, a majority of the total metal in the soils were extracted in steps 3 and 4 using the customised procedure too. This implies that a majority of the metals in the soil would have been associated with either the organic or the silicate fractions and most of it would be unavailable for ion exchange and biological uptake.

7.4 Conclusion

The conclusions that can be drawn based on the data presented in this chapter are: (i) Pb in the soils was present principally in the form of PbO and readily available for ion-exchange or weak-acid dissolution. It was not principally associated with Fe/Mn oxides as suggested by the BCR sequential extraction procedure. It is difficult to predict the bioavailability of this metal, as this can only be ascertained using phytoextraction experiments; (ii) although there was an increase in the total concentration of all the other metals (except Fe) extracted in step 1 using the customised procedure, analysis of K_d for these metals in solution showed that the desorption efficiency of the customised procedure was lower than that of the modified

BCR process; (iii) this low desorption of all the other metals was probably due to the saturation of binding sites on acetate ions by Pb^{2+} and Fe^{2+} ions; (iv) although a majority of these metals were in an oxidisable form, the data shows that their concentration in ion-exchangeable or acid-soluble forms (probably those associated with calcite and kaolinite or found as 'free' phases) was higher than those predicted by the modified BCR procedure; (v) 3M ethanoic acid solution at pH 5 at a soil-solution ratio of 1:80 can be used effectively as a soil washing reagent without altering the basic structure of soils heavily contaminated with divalent metals; (vi) it is unclear as to what fraction of these metals are available for biological uptake. The bioavailability of these metals has been investigated and the data presented in the next two chapters.

Chapter 8 Phytoextraction of Metals from the Contaminated Soil

8.1 Introduction

The data obtained using the modified BCR procedure sequential extraction procedure has shown that a majority of the contaminant and essential metals in the soil were in reducible or oxidisable forms, while a small fraction was observed to be in ion-exchangeable forms. However, the customised BCR procedure has shown that a majority of Pb and Mn and a relatively higher proportion of total Mg, Zn, Cu and Fe in the soils were in ion-exchangeable or weak acid soluble forms (probably as 'free' mineral phases). Some authors[224] have suggested that the fractions desorbed in the first step of the sequential extraction process would be the bioavailable fraction. Using this argument, the majority of Pb, Ca and Mn and a significant fraction of Mg, Zn and Cu would be available for uptake, as suggested by the customised BCR procedure. It is useful to recall that the first step of the customised procedure used 3M ethanoic acid solutions at pH 5, which is within the pH range in which most plants would survive healthily. However, increase in metal uptake by plants is also facilitated by secretion of weak acids by their roots and by symbiotic microorganisms in their rhizospheres. Since, the properties of these acids are unknown, it is difficult to use the data from batch and sequential extractions to predict metal uptake by plants. The applicability of these procedures can only be ascertained by performing phytoextraction experiments.

In order to test this hypothesis, a set of experiments were conducted that involved the growth of *Helianthus annuus* plants in the three contaminated soil samples, C1, C2 and B1. *Helianthus annuus* was used because of its easy availability, quick turnover, good metal uptake capacity and widely available literature on its agronomy. In addition, *H. annuus* is a monocotyledonous plant similar to grasses and other agrarian

plants such as wheat, maize and rice. Therefore, phytoextraction data obtained for this plant could be potentially used for the prediction of bioaccumulation due to consumption of these edible plants. Experiments were conducted over a period of 8 weeks using pre-germinated seedlings (4 week old), with samples being taken at two-week intervals. Twelve plants growing in each soil type (i.e. C1, C2 and B1) were harvested after 4 weeks (harvest 1), 6 weeks (harvest 2) and 8 weeks (harvest 3). The harvested plants were washed using deionised water, separated into leaves, stems and roots, freeze-dried and ground. A known amount of the ground sample was digested in concentrated nitric acid. The aims of this chapter are as follows: (i) study the uptake of metals by plants; (ii) study the usefulness of the modified BCR and the customised procedure as a predictive tool for metal uptake by plants; (iii) observe the potential applicability of phytoremediation as a useful procedure for the remediation of metal contaminated soils.

8.2 Results and Analysis

Accumulation data for Fe and Ca has not been presented here, as the ICP-MS could not analyse these elements, because the atomic masses of Fe ions and that of CaO^+ in the argon plasma were in the same range as those of argon oxides such as ArO^+. The concentrations of these ions in solution were below the instrumental detection limits of the ICP-AES, which prevented this instrument from being used for the analysis of these two elements.

The biomass weight for the plants in soil C1 after 4, 6, and 8 weeks of growth was 154, 304 and 844mg respectively. The biomass weight for plants in soil C2 after 4, 6, and 8 weeks of growth was 151, 324 and 631mg respectively. The biomass weight for plants in soil B1 after 4, 6 and 8 weeks of growth was 146, 267 and 562mg

respectively. It is noteworthy that the leaves of plants growing in soils C1 turned yellowish brown after 8 weeks growth, which suggest partial necrosis (and hence the stunted growth).

Lead

The mean accumulation of Pb in the *roots* of plants grown in the sample B1 was 78±22, 114±6, 18±15mg kg^{-1} after 4, 6 and 8 weeks growth respectively. The mean accumulation of Pb in the *roots* of plants grown in soil C2 was 120±49, 150±35, 205±56mg kg^{-1} after 4, 6, and 8 weeks growth respectively. The mean accumulation of Pb in the *roots* of plants grown in soil C1 was 295±88, 720±60, 533±147mg kg^{-1} after 4, 6 and 8 weeks growth respectively.

The mean accumulation of Pb in the *stems* of plants grown in *soil B1* was 6.7±4.5, 14±4, 8.3±3.2 after 4, 6 and 8 weeks growth respectively. The mean accumulation of Pb in the *stems* of plants grown in *soil C2* was 28±11, 21±9, 43±16mg kg^{-1} respectively. The mean accumulation of Pb in the *stems* of plants grown in *soil C1* was 58±17, 91±6.4, 35±16mg kg^{-1} after 4, 6 and 8 weeks growth respectively.

The mean accumulation of Pb in the *leaves* of plants grown in *soil B1* was 2.6±0.6, 3.6±0.1, 2.9±0.8mg kg^{-1} after 4, 6 and 8 weeks of growth respectively. The mean accumulation of Pb in the *leaves* of plants grown in *soil C2* was 10.6±8.1, 4.2±2.9, 9.7±3.4mg kg^{-1} after 4, 6 and 8 weeks of growth respectively. The mean accumulation of Pb in the *leaves* of plants grown in *soil C1* was 24±11, 28±5, 27±11mg kg^{-1} after 4, 6 and 8 weeks of growth respectively.

The data for the total accumulation of metal in the biomass has been presented in Tables 24(a)-26(a) for plants growing in B1, C2 and C1 respectively. The percentage concentration (w/w) of the metal extracted from the soils was calculated by dividing the concentration of metals in the plants with their total concentration in soil and the data presented in Table 24(b)-26(b) for soils B1, C2 and C1 respectively. The *total* concentrations of Pb extracted by the plants from *soil B1* after 4, 6 and 8 weeks of growth were 95(9.4%), 132(13.1%) and 107(10.6%)mg kg^{-1} respectively. The values in parentheses are the % proportion of the total metal in the soil transferred to the biomass. The total concentrations of Pb extracted by the plants from *soil C2* after 4, 6 and 8 weeks of growth were 158(9.5%), 257(10.5%) and 175(15.4%)mg kg^{-1} respectively. The total concentration of Pb extracted by the plants from *soil C1* after 4, 6 and 8 weeks of growth were 377(5.9%), 840(13.2%) and 595(9.4%)mg kg^{-1} respectively.

The root to shoot translocation factors (TF) for the metals was calculated by dividing the concentration of metal in the shoot with the total concentration in the roots. The root-shoot *TFs* for plants growing in *soil C1* was 0.28, 0.17 and 0.12 after 4, 6 and 8 weeks of growth. The root-shoot *TFs* for plants growing in *soil C2* after 4, 6 and 8 weeks of growth was 0.32, 0.17 and 0.26 respectively. The root-shoot *TFs* for plants growing in *soil B1* after 4, 6 and 8 weeks of growth was 0.12, 0.16 and 0.13 respectively. This data show that a majority of the Pb in the plants was accumulated in the roots.

The total accumulated concentration of Pb was highest in the biomass of plants from harvest 2 (6 weeks growth), followed by a decline in harvest 3 (8 weeks growth).

This decline was most likely due to a large increase in the biomass of the plants in the final harvest, which would have caused a dilution in total concentration of the metals. However, there was a substantial increase in the actual mass (g) of Pb accumulated in the biomass. The actual mass of the metal accumulated in the plants was calculated by taking a product of the metal concentration ($\mu g\ g^{-1}$) with the biomass weight (g). The actual mass of Pb accumulated in the biomass of plants growing in soil B1, after harvests 1, 2 and 3 was 15, 40 and 91μg respectively. The actual mass of Pb accumulated in the biomass of plants growing in soil C2, after harvests 1, 2 and 3 was 24, 57 and 85μg respectively. The actual mass of Pb accumulated in the biomass of plants growing in soil C1, after harvests 1, 2 and 3 was 58, 101 and 212μg respectively.

Magnesium

The mean accumulation of Mg in the *roots* of plants grown in *soil B1* was 4020±458, 4940±347 and 4040±747mg kg^{-1} after harvests 1, 2 and 3 respectively 24(a)-26(a). The mean accumulation of Mg in the *roots* of plants grown in *soil C2* was 5070±435, 6770±387, 5600±544mg kg^{-1} after harvests 1, 2 and 3 respectively. The mean accumulation of Mg in the *roots* of plants grown in *sample C1* was 1280±612, 2700±446, 1985±74mg kg^{-1} after harvests 1, 2 and 3 respectively.

The mean accumulation of Mg in the *stems* of plants grown in *soil B1* was 3570±275, 6180±937, 4640±1590mg kg^{-1} after harvests 1, 2 and 3 respectively. The mean accumulation of Mg in the *stems* of plants grown in *soil C2* was 5000±604, 5320±837, 5440±775mg kg^{-1} after harvests 1, 2 and 3 respectively. The mean

accumulation of Mg in the *stems* of plants grown in *soil C1* 1330±475, 3560±312, 1610±263mg kg^{-1} after harvests 1, 2 and 3 respectively.

The mean accumulation of Mg in the *leaves* of plants grown in *soil B1* was 3690±502, 4770±627, 5660±387mg kg^{-1} after harvests 1, 2 and 3 respectively. The mean accumulation of Mg in the *leaves* of plants grown in *soil C2* was 4100±270, 4610±2816, 5320±582mg kg^{-1} after harvests 1, 2 and 3 respectively. The mean accumulation of Mg in the *leaves* of plants grown in *soil C1* was 2450±971, 3600±425, 3250±380mg kg^{-1} after harvests 1, 2 and 3 respectively.

The *total* concentrations of Mg extracted by the plants from *soil B1* after 4, 6 and 8 weeks of growth were 11290(2267%), 15900(3191%) and 14300(2879%)mg kg^{-1} respectively (Table 27). The values in parentheses are the % proportion of the total metal in the soil transferred to the biomass. The total concentrations of Mg extracted by the plants from *soil C2* after 4, 6 and 8 weeks of growth were 14200(1879%), 16700(2212%) and 16400(2168%)mg kg^{-1} respectively. The total concentration of Mg extracted by the plants from *soil C1* after 4, 6 and 8 weeks of growth were 5060(561%), 9900(1094%) and 6840(759%)mg kg^{-1} respectively. The concentration of Mg accumulated in the plants might be indicative of the health of the plants, as Mg is at the centre of the porphyrin rings in chlorophylls. This implies that the plants growing in the least contaminated soil were the healthiest.

Copper

The mean accumulation of Cu in the *roots* of plants grown in *soil B1* was 36±6, 56±8, and 53±11mg kg^{-1} after harvests 1, 2 and 3 respectively. The mean accumulation of Cu in the *roots* of plants grown in *soil C2* was 34±24, 12±7, and 7±2mg kg^{-1} after harvests 1, 2 and 3 respectively. The mean accumulation of Cu in the *roots* of plants grown in *soil C1* was 16±9, 24±5 and 23±4mg kg^{-1} after harvests 1, 2 and 3 respectively.

The mean accumulation of Cu in the *stems* of plants grown in *soil B1* was 9.4±4.1, 8.2±1.4 and 7.2±3.3mg kg^{-1} after harvests 1, 2 and 3 respectively. The mean accumulation of Cu in the *stems* of plants grown in *soil C2* was 11.3±1.8, 5.2±3.2, and 7±2.2mg kg^{-1} after harvests 1, 2 and 3 respectively. The mean accumulation of Cu in the *stems* of plants grown in *soil C2* was 10±5.8, 9.7±2.5 and 4.8±0.1mg kg^{-1} after harvests 1, 2 and 3 respectively.

The mean accumulation of Cu in the *leaves* of plants grown in *soil B1* was 53±19, 39±3 and 46±2mg kg^{-1} after harvests 1, 2 and 3 respectively. The mean accumulation of Cu in the leaves of plants grown in soil C2 was 48±4, 40±26, 39±12mg kg^{-1} after harvests 1, 2 and 3 respectively. The mean accumulation of Cu in the leaves of plants grown in soil C1 was 37±20, 34±3, 30±5mg kg^{-1} after harvests 1, 2 and 3 respectively.

The *total* concentrations of Cu extracted by the plants from *soil B1* after 4, 6 and 8 weeks of growth were 98(214%), 62(136%) and 170(148%)mg kg^{-1} respectively. The

values in parentheses are the % proportion of the total metal in the soil transferred to the biomass. The total concentrations of Cu extracted by the plants from *soil C2* after 4, 6 and 8 weeks of growth were 93(85%), 56(89%) and 52(76%)mg kg^{-1} respectively. The total concentration of Cu extracted by the plants from *soil C1* after 4, 6 and 8 weeks of growth were 64(162%), 67(168%) and 57(145%)mg kg^{-1} respectively.

The actual mass of metal accumulated in the biomass of plants growing in soil B1 was 15, 30, 83μg after harvests 1, 2 and 3 respectively. The actual mass of metal accumulated in the biomass of plants growing in soil C2 was 14, 30 and 31μg after harvests 1, 2 and 3 respectively. The actual mass of metal accumulated in the biomass of plants growing in soil C1 was 10, 20 and 36μg after harvests 1, 2 and 3 respectively. Cu like Mg is an essential element and is vital for several key physiological functions in plants, therefore the accumulation of Cu would be also be an indicator of plant health. This implies that the plants growing in soil B1 were the healthiest.

Zinc

The mean accumulation of Zn in the *roots* of plants grown in *soil B1* was 95±5, 56±8, 53±11mg kg^{-1} during harvests 1, 2 and 3 respectively. The mean accumulation of Zn in the *roots* of plants grown in *soil C2* was 82±20, 41±11, 37±10mg kg^{-1} during harvests 1, 2 and 3 respectively. The mean accumulation of Zn in the *roots* of plants grown in *soil C1* was 195±37, 60±4, 55±9mg kg^{-1} during harvests 1, 2 and 3 respectively.

The mean accumulation of Zn in the *stems* of plants grown in *soil B1* was 80±26, 108±19, 56±24mg kg^{-1} during harvests 1, 2 and 3 respectively. The mean accumulation of Zn in the stems of plants grown in *soil C2* was 100±39, 69±18, 76±13mg kg^{-1} during harvests 1, 2 and 3 respectively. The mean accumulation of Zn in the *stems* of plants grown in *soil C1* was 59±17, 91±7, 35±16mg kg^{-1} during harvests 1, 2 and 3 respectively.

The mean accumulation of Zn in the *leaves* of plants grown in *soil B1* was 47±1, 75±7, 69±6mg kg^{-1} during harvests 1, 2 and 3 respectively. The mean accumulation of Zn in the *leaves* of plants grown in *soil C2* was 69±6, 62±36, 79±4mg kg^{-1} during harvests 1, 2 and 3 respectively. The mean accumulation of Zn in the *stems* of plants grown in *soil C1* was 58±22, 85±3, 71±3mg kg^{-1} during harvests 1, 2 and 3 respectively.

The *total* concentrations of Zn extracted by the plants from *soil B1* after 4, 6 and 8 weeks of growth were 243(256%), 226(238%) and 188(198%)mg kg^{-1} respectively. The values in parentheses are the % proportion of the total metal in the soil transferred to the biomass. The total concentrations of Zn extracted by the plants from *soil C2* after 4, 6 and 8 weeks of growth were 251(244%), 172(167%) and 191(185%)mg kg^{-1} respectively. The total concentration of Zn extracted by the plants from *soil C1* after 4, 6 and 8 weeks of growth were 305(168%), 229(126%) and 157(153%)mg kg^{-1} respectively.

The actual mass of metal accumulated in the biomass of plants growing in soil B1 was 37, 74, 204μg after harvests 1, 2 and 3 respectively. The actual mass of metal

accumulated in the biomass of plants growing in soil C2 was 39, 81 and 83μg after harvests 1, 2 and 3 respectively. The actual mass of metal accumulated in the biomass of plants growing in soil C1 was 47, 93 and 172μg after harvests 1, 2 and 3 respectively.

Manganese

The mean accumulation of Mn in the roots of plants grown in soil B1 was 36±11, 34±5, 23±2mg kg^{-1} during harvests 1, 2 and 3 respectively. The mean accumulation of Mn in the roots of plants grown in soil C2 was 78±30, 72±13, 53±14mg kg^{-1} during harvests 1, 2 ad 3 respectively. The mean accumulation of Mn in the roots of plants grown in soil C1 was 16±7, 25±17, and 11±1mg kg^{-1} during harvests 1, 2 and 3 respectively.

The mean accumulation of Mn in the stems of plants grown in soil B1 was 30±22, 84±20, and 42±20mg kg^{-1} during harvests 1, 2 and 3 respectively. The mean accumulation of Mn in the stems of plants grown in soil C2 was 71±14, 138±31 and 161±28mg kg^{-1} during harvests 1, 2 and 3 respectively. The mean accumulation of Mn in the stems of plants grown in soil C1 was 7.5±3.5, 17.4±2.4 and 8.4±1.3mg kg^{-1} during harvests 1, 2 and 3 respectively.

The mean accumulation of Mn in the leaves of plants grown in soil B1 was 56±10, 118±10 and 118±25mg kg^{-1} during harvests 1, 2 and 3 respectively. The mean accumulation of Mn in the roots of plants grown in soil C2 was 74±11, 194±130 and 289±33mg kg^{-1} during harvests 1, 2 and 3 respectively. The mean accumulation of

Mn in the leaves grown in soil C1 was 22±8, 36±3 and 35±4mg kg^{-1} during harvests 1, 2 and 3 respectively.

The *total* concentrations of Mn extracted by the plants from *soil B1* after 4, 6 and 8 weeks of growth were 122(59%), 236(115%) and 184(89%)mg kg^{-1} respectively. The values in parentheses are the % proportion of the total metal in the soil transferred to the biomass. The total concentrations of Mn extracted by the plants from *soil C2* after 4, 6 and 8 weeks of growth were 222(44%), 403(79%) and 503(98%)mg kg^{-1} respectively. The total concentration of Mn extracted by the plants from *soil C1* after 4, 6 and 8 weeks of growth were 45(11%), 78(19%) and 54(13%)mg kg^{-1} respectively.

The actual mass of metal accumulated in the biomass of plants growing in soil B1 was 19, 37, 103μg after harvests 1, 2 and 3 respectively. The actual mass of metal accumulated in the biomass of plants growing in soil C2 was 34, 72 and 74μg after harvests 1, 2 and 3 respectively. The actual mass of metal accumulated in the biomass of plants growing in soil C1 was 7, 14 and 26μg after harvests 1, 2 and 3 respectively.

Chromium

The mean accumulation of Cr in the roots of plants grown in soil B1 was 3. ±1.1, 1.5±0.5, 0.1±0.02mg kg^{-1} during harvests 1, 2 and 3 respectively. The mean accumulation of Cr in the roots of plants grown in soil C2 was 4.2±1.5, 1.9±0.3, 0.1±0.02mg kg^{-1} during harvests 1, 2 ad 3 respectively. The mean accumulation of Cr

in the roots of plants grown in soil C1 was 1.9±0.9, 1.3±0.9, and 0.1±0.07mg kg^{-1} during harvests 1, 2 and 3 respectively.

The mean accumulation of Cr in the stems of plants grown in soil B1 was 0.4±0.05, 0.7±0.4, and 0.14±0.06mg kg^{-1} during harvests 1, 2 and 3 respectively. The mean accumulation of Cr in the stems of plants grown in soil C2 was 0.7±0.2, 0.2±0.1 and 0.1±0.1mg kg^{-1} during harvests 1, 2 and 3 respectively. The mean accumulation of Cr in the stems of plants grown in soil C1 was 1.5±0.9, 0.3±0.04 and 0.3±0.1mg kg^{-1} during harvests 1, 2 and 3 respectively.

The mean accumulation of Cr in the leaves of plants grown in soil B1 was 0.5±0.1, 0.5±0.3 and 0.07±0.03mg kg^{-1} during harvests 1, 2 and 3 respectively. The mean accumulation of Mn in the roots of plants grown in soil C2 was 0.5±0.1, 0.3±0.2 and 0.2±0.2mg kg^{-1} during harvests 1, 2 and 3 respectively. The mean accumulation of Cr in the leaves grown in soil C1 was 0.1±0.1, 0.2±0.07and 0.2±0.05mg kg^{-1} during harvests 1, 2 and 3 respectively.

The *total* concentrations of Cr extracted by the plants from *soil B1* after 4, 6 and 8 weeks of growth were 6.7(6.3%), 3.5(3.3%) and 0.3(0.2%)mg kg^{-1} respectively. The values in parentheses are the % proportion of the total metal in the soil transferred to the biomass. The total concentrations of Cr extracted by the plants from *soil C2* after 4, 6 and 8 weeks of growth were 5.3(6.8%), 2.4(3.1%) and 0.4(0.4%)mg kg^{-1} respectively. The total concentration of Cr extracted by the plants from *soil C1* after 4, 6 and 8 weeks of growth were 4.4(5.7%), 1.8(2.4%) and 0.3(0.4%)mg kg^{-1} respectively.

The actual mass of metal accumulated in the biomass of plants growing in soil B1 was 1, 2, 5.6μg after harvests 1, 2 and 3 respectively. The actual mass of metal accumulated in the biomass of plants growing in soil C2 was 0.8, 1.7 and 1.8μg after harvests 1, 2 and 3 respectively. The actual mass of metal accumulated in the biomass of plants growing in soil C1 was 0.7, 1.3 and 2.5μg after harvests 1, 2 and 3 respectively.

(a)

Metals	Harvest 1	Harvest 2	Harvest 3
Mg	11300	15900	14300
Al	666	563	289
Cr	6.7	3.5	0.3
Mn	122	236	184
Cu	98	62	67
Zn	243	226	188
Pb	95	132	107

(b)

Metals	Harvest 1	Harvest 2	Harvest 3
Mg	2270	3190	2880
Al	16.4	13.8	7.1
Cr	6.3	3.3	0.2
Mn	59	115	89
Cu	214	136	148
Zn	256	238	198
Pb	9.4	13.1	10.6

Table 24: Accumulation (mg kg^{-1}) of metals in the biomass of plants grown in soil B1. (a) total concentration of metals; (b) percentage (w/w) of the total metal in the soil.

(a)

Metals	Harvest 1	Harvest 2	Harvest 3
Mg	14200	16700	16400
Al	839	590	335
Cr	5.3	2.4	0.4
Mn	222	403	503
Cu	93	56	52
Zn	251	172	191
Pb	158	257	175

(b)

Metals	Harvest 1	Harvest 2	Harvest 3
Mg	1880	2210	2170
Al	17.8	12.5	7.1
Cr	6.8	3.1	0.4
Mn	44	79	98
Cu	233	142	132
Zn	244	167	185
Pb	9.5	15.4	10.5

Table 25: Accumulation (mg kg^{-1}) of metals in the biomass of plants grown in soil C2. (a) total concentration of metals; (b) percentage (w/w) of the total metal in the soil.

(a)

Metals	Harvest 1	Harvest 2	Harvest 3
Mg	5060	9870	6840
Al	493	370	169
Cr	4.4	1.8	0.3
Mn	45	78	54
Cu	64	67	57
Zn	305	229	157
Pb	377	840	595

(b)

Metals	Harvest 1	Harvest 2	Harvest 3
Mg	561	1100	759
Al	10.0	7.5	3.4
Cr	5.7	2.4	0.4
Mn	11	19	13
Cu	85	89	76
Zn	168	126	86
Pb	5.9	13.2	9.4

Table 26: Accumulation (mg kg^{-1}) of metals in the biomass of plants grown in soil C1 (a) total concentration of metals; (b) percentage (w/w) of the total metal in the soil.

(a) B1

Metals	Harvest 1	Harvest 2	Harvest 3
Mg	1740	3430	9480
Al	103	203	560
Cr	1.0	2.0	5.6
Mn	19	37	103
Cu	15	30	83
Zn	37	74	204
Pb	15	40	91

(b) C2

Metals	Harvest 1	Harvest 2	Harvest 3
Mg	2180	4320	11900
Al	129	255	705
Cr	0.8	1.6	4.5
Mn	34	68	187
Cu	14	28	78
Zn	39	76	211
Pb	24	57	85

(c) C1

Metals	Harvest 1	Harvest 2	Harvest 3
Mg	780	1540	4260
Al	76	150	414
Cr	0.7	1.3	3.7
Mn	7	14	39
Cu	10	20	54
Zn	47	93	257
Pb	58	115	317

Table 27: Actual total mass (μg) of metals accumulated in the biomass of plants growing in soil (a) B1 (b) C2 (c) C1 (a total of 12 plants were analysed for each harvest).

8.3 Discussion

The data presented in this chapter show that all the essential metals i.e., Cu, Zn, Mg, and Mn were accumulated by the plants at concentrations far higher than those present in the soils. This was especially so in case of Mg, the concentration of which was almost 25 times that present in the soil. This is not an unexpected trend, as all these elements are essential for normal functioning of the physiological mechanisms in plants. However, the most important observation from these experiments is the uptake pattern of Pb by the plants growing in the three soils. The proportion of Pb accumulated in the plants growing in all three soils was on average 10-12% of the total concentration of the metal in the soil. Furthermore, it is notable that the majority of the accumulated metal was sequestered in the roots of plants.

The data for metal uptake by plants was compared with those obtained from the modified BCR and the customised sequential extraction process. The comparison shows that there was no correlation between desorption pattern of essential metals during the BCR process and the pattern of their uptake by plants. However, a comparison of Pb extraction data from the modified BCR procedure and the metal uptake by plants shows a very *good correlation*. There was *no correlation* between the data obtained from the *customised* BCR procedure and Pb uptake by plants. The concentrations of Pb extracted during step 1 of the modified BCR process from soils B1, C1 and C2 were 95±10, 121±12 and 1030±43mg kg^{-1} soil respectively, while the Pb uptake by plants growing in the same soils during harvest 2 (point of highest uptake by plants) was 95, 257 and 840mg kg^{-1} plants respectively. Although there is a certain underestimation of the concentration of Pb extracted from soils B1 and C2, it does suggest that the data obtained from the first step of the BCR modified BCR sequential extraction process can be considered the bioavailable fraction. This

underestimation also suggests that the uptake of Pb by the plants might not be a simple passive process i.e., a result of ion-exchange. Other factors such as phytochelatins secreted by plant roots are also likely to be responsible for an increased uptake.

8.4 Conclusions

The principal conclusions that can be drawn from this chapter are: (i) the proportion of Pb accumulated by plants would be approximately 10-15% of the total concentration of the metals in these soils. These are high extractions, which implies that phytoremediation can be used as an effective technique for the remediation of heavy metal contaminated soil. Furthermore, since a majority of the metal is sequestered in the roots of the plants, there is no obvious risk to the food chain as a consequence of grazing; (ii) the customised procedure cannot be used for the bioavailability predictions for essential metals; (iii) however, the *modified BCR* procedure can be used for the bioavailability predictions for non-essential metals; (iv) the data obtained in this chapter suggest that in order to obtain effective bioavailability predictions, complexing agents such as EDTA would have to be used, as these have the potential to extract metals from all soil fractions; (v) the *customised* BCR procedure however, can be used for prediction of leachability of contaminant metals such as Pb using soil washing, especially when they are present at high concentrations. The rationale for this being that at high concentrations, these metals either precipitate onto the surface of minerals or exist as independent mineral phases.

Chapter 9 Influence of Complexing Agents on Metal Extractions in Soils

9.1 Introduction

The phytoextraction experiments have shown that the modified BCR sequential extraction procedure was only useful for the bioavailability predictions for contaminant metals such as Pb, as the essential metals are hyperaccumulated by plants. This accumulation of essential metals suggests the influence of an active transport mechanism in the rhizospheres of plants, possibly involving complexing agents such as citric acid and L-cysteine[225]. Evidence for this comes from the high uptake of the essential metals by the plants. Both the modified BCR and the customised processes, suggested that a majority of metals such as Cu, Zn and Mg were in oxidisable forms in soils, which according to the procedural theory should be unavailable for uptake. However, evidence suggesting to the contrary shows that plant roots secrete chemicals that actively seek out these metals.

Several authors have suggested that metal mobilisation by plants and microorganisms involves the use of metallothioneins and phytochelatins such as citric acid, which have the potential to dissolve Fe compounds[226,227]. These transporters are lewis bases because they possess electron rich atoms such as N and soft/medium acids such as –SH that prefer either to donate electrons or bind with transition metal cations. As a result they have the capacity to complex metals bound to clay, carbonate and Fe/Mn oxide fractions. Pb uptake can also be mediated by desferrioxamine-B, a siderophore that is produced by microorganisms for the uptake of Fe and other metals as nutrients[228]. Citric acid is an important precursor produced in all living organisms (citric acid cycle) and has been reported to play a role in metal detoxification in plant

cells[229,230]. Apart from its capacity to form complexes with soft metal ions, it is readily biodegradable; as a result it is an environment friendly soil-washing agent. Furthermore, citrate is widely used by metallogenic bacteria such as *Citrobacter*, to mobilise metals from soils. Therefore, this could be a potential solution for the bioremediation of soils, whereby most of the metals bound to the kaolinite and calcium carbonate and those bound to the Fe/Mn oxyhydroxides could be bioleached by *Citrobacter*.

Phytochelatins (PCs) are short-cysteine rich metal chelating peptides that are found in all plants and yeasts such as *Candida glabrata, Schizosaccharomyces pombe, Saccharomyces cerevisiae* and *Neurospora crassa*[231]. Cysteine is an important amino acid produced by most living organisms and is expected to have good heavy metal complexing capacity due to the presence of –SH groups[232]. The bulk of all the SH and SS groups in nature are contributed by the amino acids, L-cysteine, $HS.CH_2CH(NH_2)COOH$, (CySH) and L-cystine, $HOOC.CH(NH_2)CH_2.SS.CH_2CH(NH_2)COOH$, (CySSCy) in various combined forms. Free cysteine is stable either as the crystalline hydrochloride, $CySH.H_2O.HCl$ or in acid solution. In neutral solutions it oxidises to cystine: $2CySH \rightarrow CySSCy$. The latter may then precipitate because, though cysteine is freely soluble, cystine has a water solubility (pH 7.25) of only 110mg L^{-1} at 20°C. Cystine and cysteine are both unstable in alkali and undergo a complex desulfuration reaction. Metal complexes with cysteine are of interest because though several amino acids form metal complexes, those with cysteine have the highest metal binding constants and because the –SH group in cysteine may be a binding site in some metalloproteins. Ferrous ions form several complexes with cysteine, some of which are stable in acid solutions,

while others predominate at a high pH. Experimental observations by several authors have suggested that colloidal metal sulphides are relatively soluble in solutions of amino acids and that polypeptides containing SH residues react spontaneously with pyrite[233], which suggests thiol-biochemical groups could be involved in sulphide leaching by *T. ferroxidans* (sulfur bacteria)[234]. This suggests that cysteine based soil washing solutions could be used to leach out metals bound to Fe oxyhydroxides in the soils used in this study.

The data presented in this chapter are those from batch extractions performed to optimise the molarity, soil-solution ratio and pH of citric acid (pH 5±0.2), L-cysteine (pH 5±0.2) and EDTA (pH 5±0.2) for metal extractions from soil C1. Speciation of metals in solution was deduced using the geochemical modelling software MINEQL+. EDTA (ethylene diamine tetracetic acid) was also used as an extraction agent due to its high affinity for a wide range of cationic metals and popularity among researchers[235, 236]. EDTA is a tetraprotic acid (H_4Y) with four dissociation constants at pK_as of 2.00, 2.67, 6.16 and 10.26, which yield H_3Y^-, H_2Y^{2-}, HY^{3-} and Y^{4-}, respectively. At pH 7.0±0.5, the primary form of EDTA will be the mono-protonated acid (HY^{3-}). Below a pH of 6.16, the doubly protonated form of EDTA exists with stability constants that differ from that of the monoprotonated form by several orders of magnitude. Concentrations of EDTA at or below 0.1M have been extensively studied as a reusable resource for remediation and recovery of heavy metals from contaminated soils[81,237].

The aims of these experiments were as follows: (i) to assess the suitability of these complexing agents as potential soil washing reagents; (ii) compare the data obtained

from these extractions with those from the customised sequential extraction process i.e. to assess the suitability of this procedure as a predictive tool for soil washing; (iii) compare the data obtained from these extractions with those obtained using the phytoextraction experiments, in order to assess if carboxylic and amino acids secreted by the plant roots have a major role to play in the mobilisation of metals; (iv) study the effect of each of these reagents (and ethanoic acid) on the bulk mineralogical composition of the soils. It is noteworthy that all solutions were analysed within a few hours of completion of the extractions, in order to prevent the transformation of metal species in solutions, due to biological action.

9.2 Results and Analysis

Citric Acid

Data from batch extractions using citric acid, presented in Table 28(a), show that the optimum molarity for metal extractions was 0.75M. There was a progressive increase in the extraction of all metals in the molar range 0.001-0.75M, after which the extractions reached equilibrium. It is noteworthy that it was impossible to dissolve more than 1mol L^{-1} of the citric acid salt in water at room temperature (the temperature at which all the experiments were performed. The average extractions for Fe, Pb, Ca, Mg, Mn, Zn and Cu were 6690±115 (35%), 5300±243 (82%), 3520±240 (100%), 351±2 (37%), 419±25 (94%), 61±3 (34%) and 8.4±1 (11%) mg kg^{-1} respectively. The values in parentheses are the relative % proportions of the metals extracted into solution compared with their respective total concentrations in soils. Batch extractions performed to deduce the optimum soil-solution (0.75M citric acid) ratio showed that the optimum ratio was 1:60 (data not presented).

Data from batch extractions using 60mL of 0.75M citric acid, presented in Table 28(b) and Figure 15, show that the highest extraction of metals took place at pH 2 and that there was a progressive decline in the concentration of all the metals extracted into solution in the pH range 2-6. It is noteworthy that it was impossible to adjust the pH of the solutions beyond pH 6 using the NH_4OH solutions, without radically altering the solution composition, i.e. without causing a dilution of the solution by adding an excess of NH_4OH. The average extractions for Fe, Pb, Ca, Mg, Mn, and Zn were 10100±186 (53%), 5920±555 (91%), 5160±129 (147%), 595±50 (63%), 595±49 (134%) and 141±6 (78%) mg kg^{-1} respectively. This data was compared with those obtained using 3M ethanoic acid at an equivalent pH. The calculation of ratios of the average metal extractions using the two solutions, citric acid and ethanoic acid showed that approximately 6, 2, 2, 2, 2, and 2 times more Fe, Pb, Ca, Mg, Mn and Zn respectively, were extracted into 0.75M citric acid solutions than into 3M ethanoic acid solutions. However, even at normal pH i.e. pH 5, the average extractions of these metals was equal or higher viz., 4, 1, 2, 2, 2, 2 times more Fe, Pb, Ca, Mg, Mn and Zn respectively were extracted into the citric acid solutions. This shows that citric acid actively scavenges Fe and mobilises all the associated metals.

Speciation analysis using the geochemical modelling software shows that at pH 2 100% of Pb in solution existed as Pb^{2+} (schematic in Figure 16). Thereafter there was a rapid decline in the concentration of Pb^{2+} in solution, with a simultaneous increase in the concentration of Pb-citrate and other Pb-citrate species until pH 7, at which point there was a rapid precipitation of Pb as $Pb(OH)_2$. 100% of Fe in solutions at pH 2 existed as Fe^{2+} ions, thereafter there was a rapid decline in the their concentration, with a simultaneous increase in the proportion of Fe-citrate in solution, increasing to

100% at pH4. There was no change in the proportion of Fe-citrate ions in solution until pH 12.

(a)

Molarity	Cu	Ca	Al	Mg	Fe	Mn	Pb	Zn
0.01	< 0.0028	1600±46	819±79	260±45	1890±146	229±78	243±25	17±1
0.025	< 0.0028	2400±285	691±32	151±16	2440±134	46±19	230±36	16±2
0.05	< 0.0028	2830±200	792±17	272±12	2790±144	248±24	1590±100	44±2
0.1	< 0.0028	3150±309	938±34	295±12	3580±135	323±25	2630±309	44±2
0.25	2.4±2	3460±127	1160±63	323±8	4860±157	377±15	3840±326	53±8
0.5	6.4±1	3400±149	1290±117	323±9	6010±180	392±24	4900±399	54±9
0.75	8.4±1	3560±240	1420±198	351±2	6690±115	419±25	5330±243	61±3
1	7.6±3	3560±385	1300±35	340±41	5850±217	405±35	5120±378	53±7

(b)

Metals	Ca	Al	Mg	Fe	Mn	Pb	Zn
2	5160±129	1930±48	594±50	10100±186	595±49	5910±555	141±6
3	3440±780	1490±108	377±80	8290±162	461±66	5340±510	117±6
4	2940±134	749±140	263±19	5100±110	346±9	5140±172	78±4
5	2840±80	675±102	284±10	3900±36	283±3	4400±154	74±6
6	2890±80	712±40	274±10	4500±40	315±9	4770±230	76±2

Table 28: Concentrations of metals (mg kg^{-1}) extracted from the soil using (a) citric acid solutions (pH 5) over the molar range 0.005 –1 M; (b) 60mL of 0.75M citric acid solutions over the pH range 2-6.

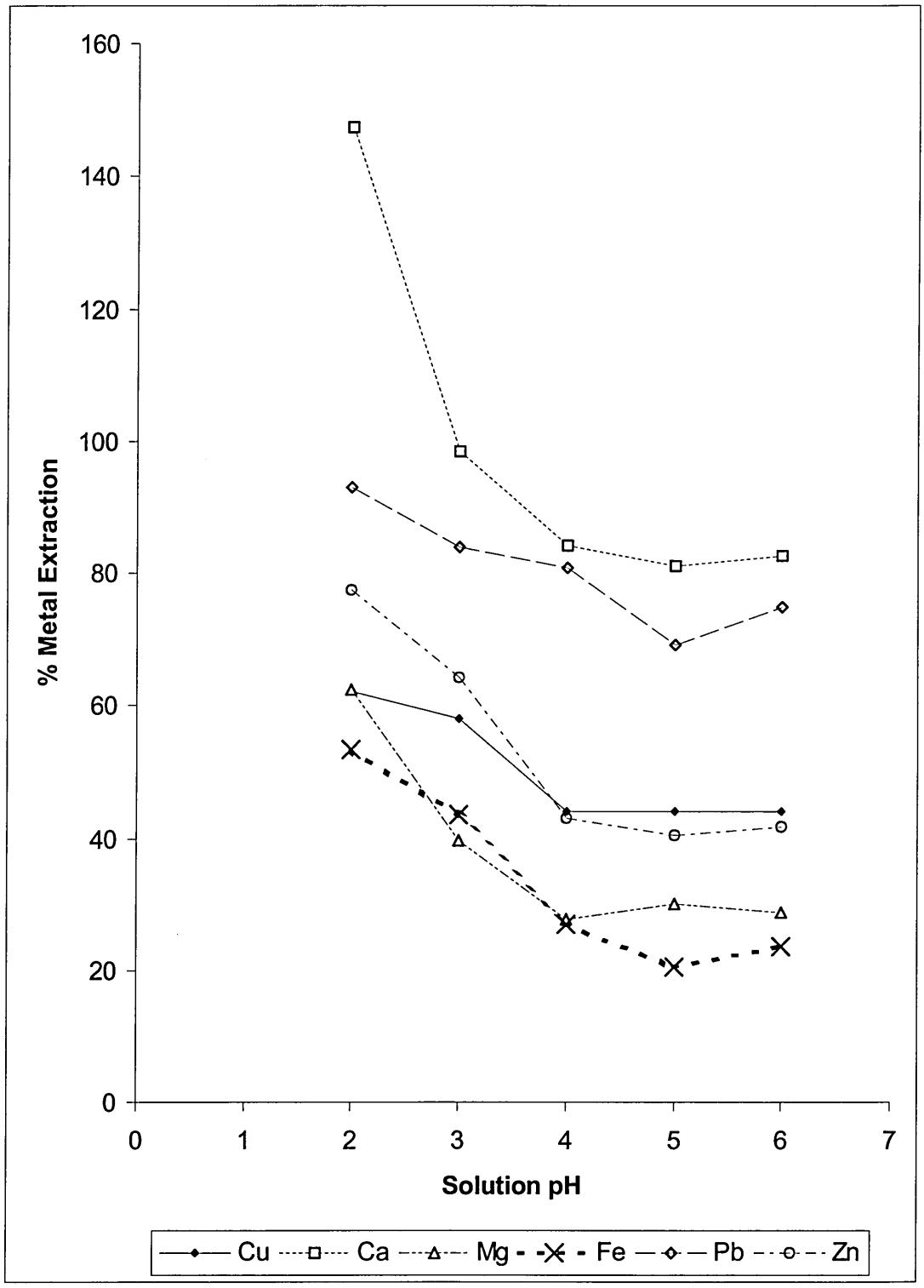

Figure 15: Extraction patterns for metal extractions using 0.75M citric acid over the pH range 2-6.

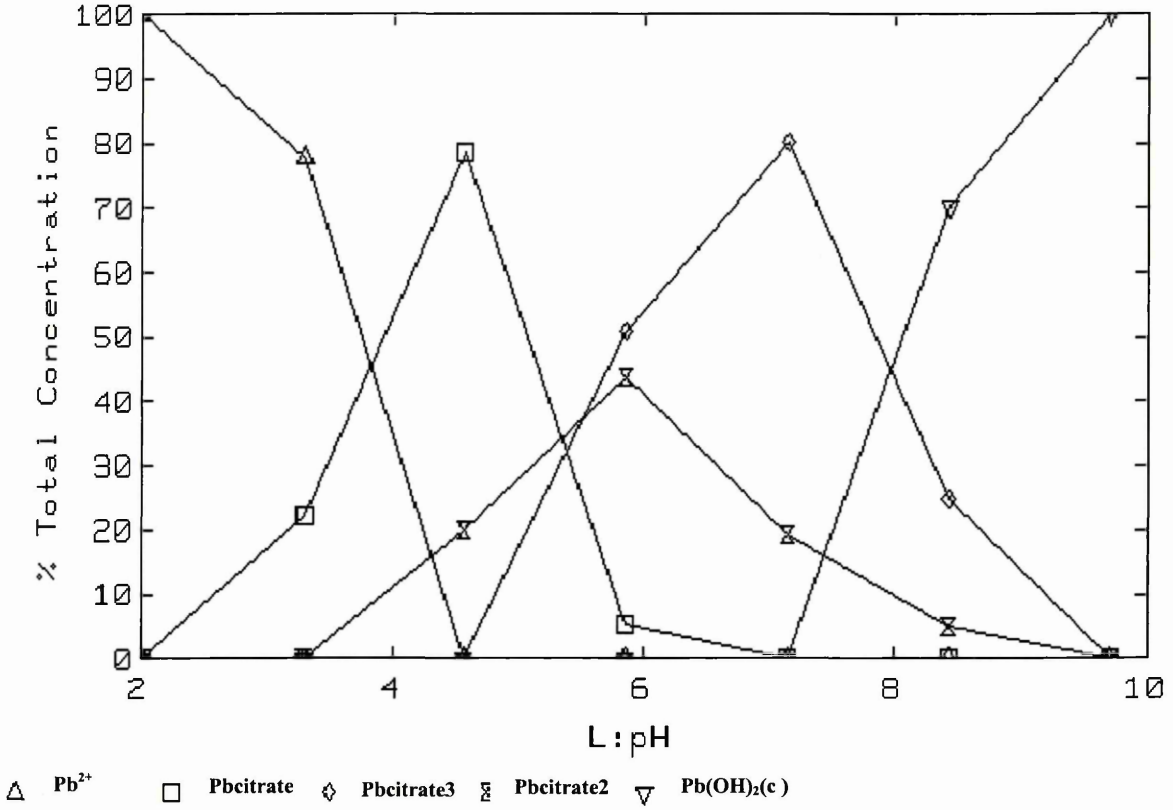

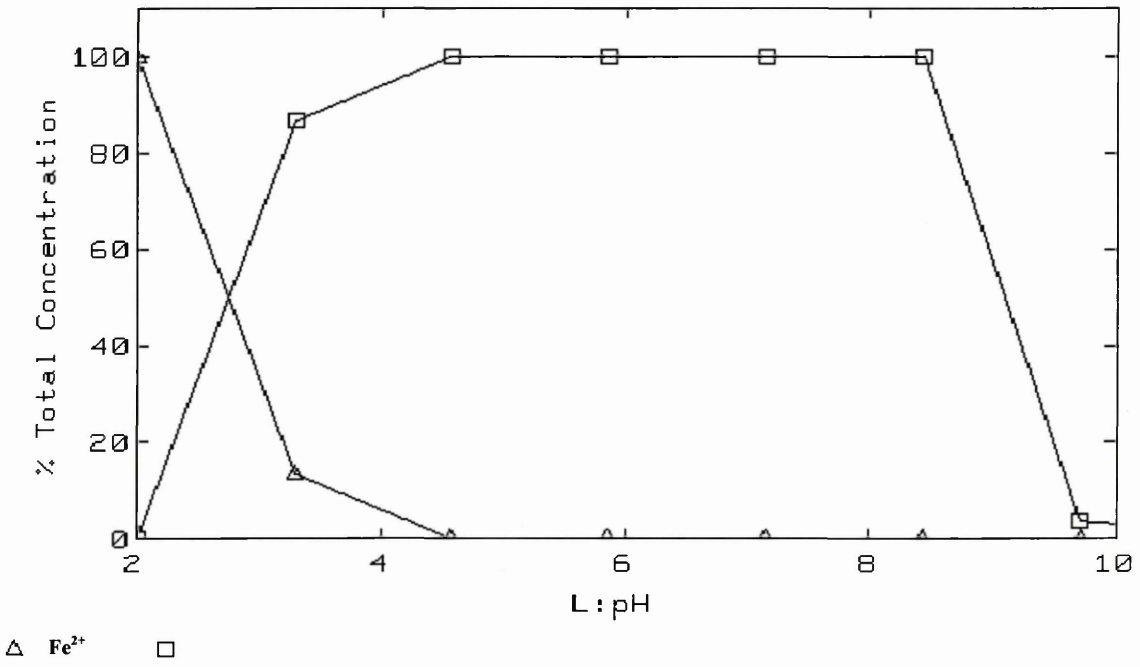

Figure 16: Speciation of (a) Pb (b) Fe in the 0.75M citric acid solutions as derived using the MINEQL+ geochemical modelling software.

Extractions using L-cysteine

The data obtained from batch experiments conducted using L-cysteine have been presented in Table 29(a), and show that the optimum molarity for metal extractions was 0.075M. It is noteworthy it was not possible to dissolve more than 0.1mol L^{-1} of the L-cysteine salt at room temperature. The average extractions for Ca, Al, Mn, Pb and Fe were 1250±27(36%), 94±3 (21%), 167±6(38%), 3930±83 (61%) and 6970±210 (37%)mg kg^{-1} respectively. The values in parentheses are the relative proportions of the metals extracted into solution compared with their respective total concentrations in soils. Batch extractions performed to deduce the optimum soil-solution ratio using 0.075M L-cysteine, showed that the optimum ratio was 1:40 (data not presented).

Batch extractions using 0.075M L-cysteine show that the optimum pH for Pb, Fe, Cu and Zn extractions using this solution was pH 8 (Table 29(b)). The highest extractions of Ca, Mg, Al and Mn into the solutions took place at pH 2. It is noteworthy that it was impossible to adjust the pH of the solutions above pH 9 without diluting the solutions. The data shows that there was a sharp increase in Pb extractions from the soils in the pH range 2-5, followed by equilibrium between pH 5-8, followed by a decrease at pH 9 (Figure 17). There was a sharp decline in the concentration of Fe extracted into solution in the pH range 2-5, followed by an increase in the pH range 6-8, which was followed by a decrease in the pH range 8-9. The average extractions of Cu, Ca, Mg, Fe, Mn, Pb and Zn at pH 8 were 46±3 (61%), 865±29 (25%), 150±3 (16%), 8910±210 (47%), 164±3 (37%), 5210±199 (80%) and 43±7 (24%)mg kg^{-1} respectively.

The most noteworthy observation from these experiments is the concentrations of metals extracted in pH range 5-7, which is the pH at which majority of plant growth takes place. The proportions of Pb extracted at pH 5 and 7 were 66% and 66% of aqua-regia soluble psuedo-totals respectively, while those of Fe extracted at the same pH values were 31% and 33% respectively. Similarly the proportions of Zn extracted at pH 5 and 7 were 29% and 29% respectively, while those of Mg extracted at the same pH values were 21% and 18% respectively. This implies that L-cysteine, a naturally produced amino acid, has the potential to actively solubilise heavy metals from soils in neutral and near-neutral pH conditions.

Speciation modelling data from the MINEQL+ database show that at pH 2, approximately 100% of the total Pb in solution existed as Pb^{2+} ions (Figure 17). Thereafter, there was a steady decline in the concentration of these ions, with a simultaneous rise in concentration of Pb-cysteine complex. The concentration of Pb^{2+} ions reached 0% at pH 5, at which the concentration of the Pb-cysteine complex reached 100%. The proportion of Pb-cysteine remained at 100% until pH 11. Modelling data for Fe in the cysteine solutions show that at pH 2, 100% of the metal existed as Fe^{2+} in solution. Thereafter, there was a steady decline in the concentration of Fe^{2+}, with a simultaneous rise in the concentration of Fe-cysteine complex, until pH 5. At this point the concentration of Fe-cysteine complex in solution reached equilibrium (at 50%) until pH 12.

(a)

Molarity	Ca	Al	Mn	Pb	Fe
0.001	165±16	71±42	8±3	25±3	61±3
0.0025	209±7	70±19	18±2	94±16	90±12
0.005	248±14	89±17	23±4	251±85	121±20
0.0075	469±3	105±60	60±2	1440±85	940±31
0.01	768±34	99±18	90±9	1980±31	2150±93
0.025	838±90	96±2	117±26	2200±408	2200±340
0.05	923±51	97±4	163±9	3400±214	5000±265
0.075	1250±27	94±3	167±6	3930±83	6970±21
0.1	1250±28	99±2	210±7	3970±298	7130±291

(b)

pH	Cu	Ca	Al	Mg	Fe	Mn	Pb	Zn
2	5.6±0.3	2950±210	564±4	275±3	8660±74	435±40	1540±48	46±3
4	6.7±0.1	1360±110	72±1	180±1	5130±300	221±20	3120±71	27±2
5	28±0.4	1240±60	66±4	201±4	5810±160	222±40	4290±244	52±6
7	29±3	960±30	100±2	172±4	6220±184	180±8	4300±244	52±6
8	46±3	865±30	84±6	150±3	8910±210	164±3	5210±199	43±7
9	43±3	714±141	119±28	123±19	8060±484	201±36	3920±576	51±5

Table 29: Concentrations of metals (mg kg^{-1}) extracted from the soil using (a) L-cysteine acid solutions (pH 5) over the molar range 0.001 –0.1 M; (b) 40mL of 0.075M L-cysteine solutions over the pH range 2-6.

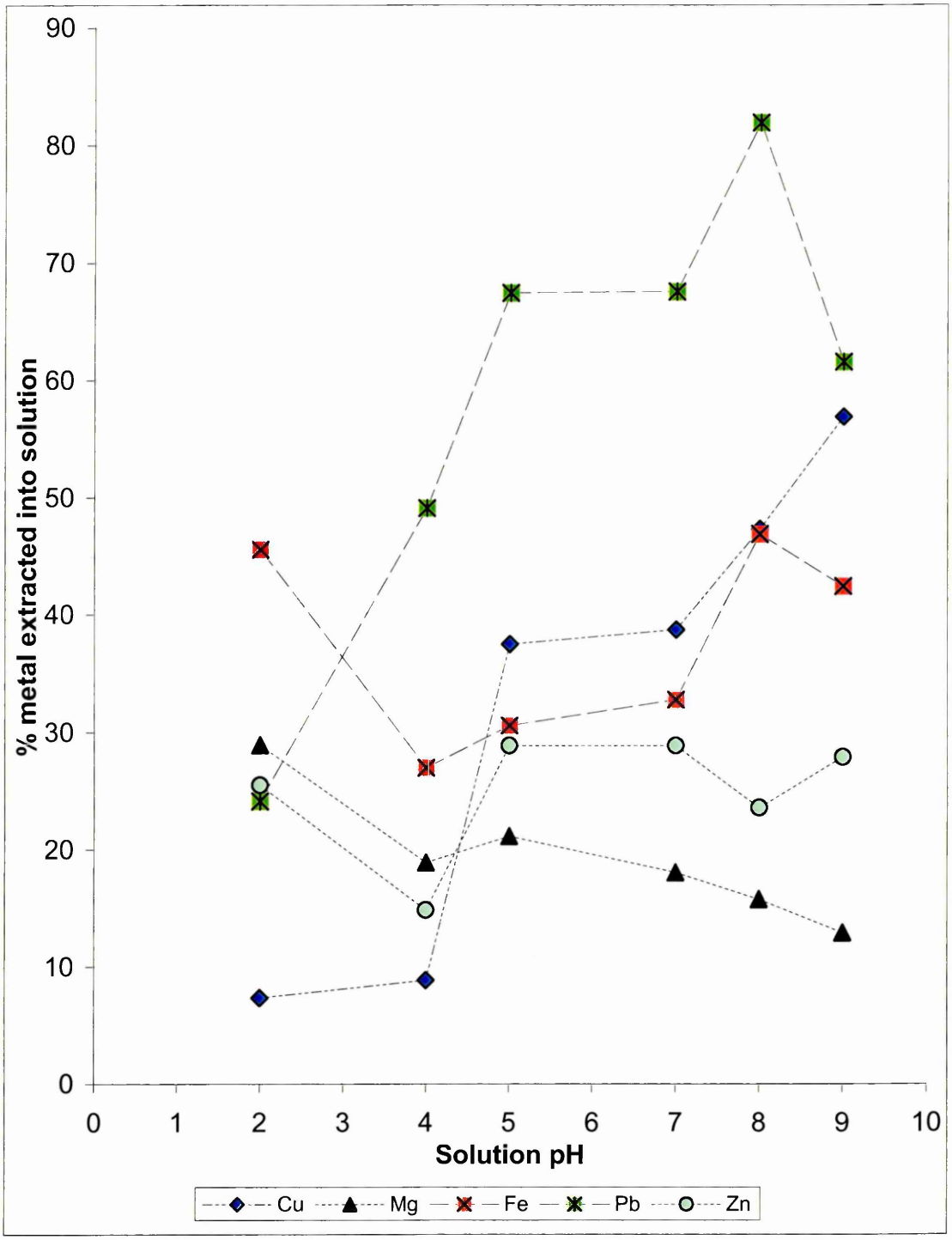

Figure 17: Extraction patterns for metal extractions using 0.075M L-cysteine over the pH range 2-9.

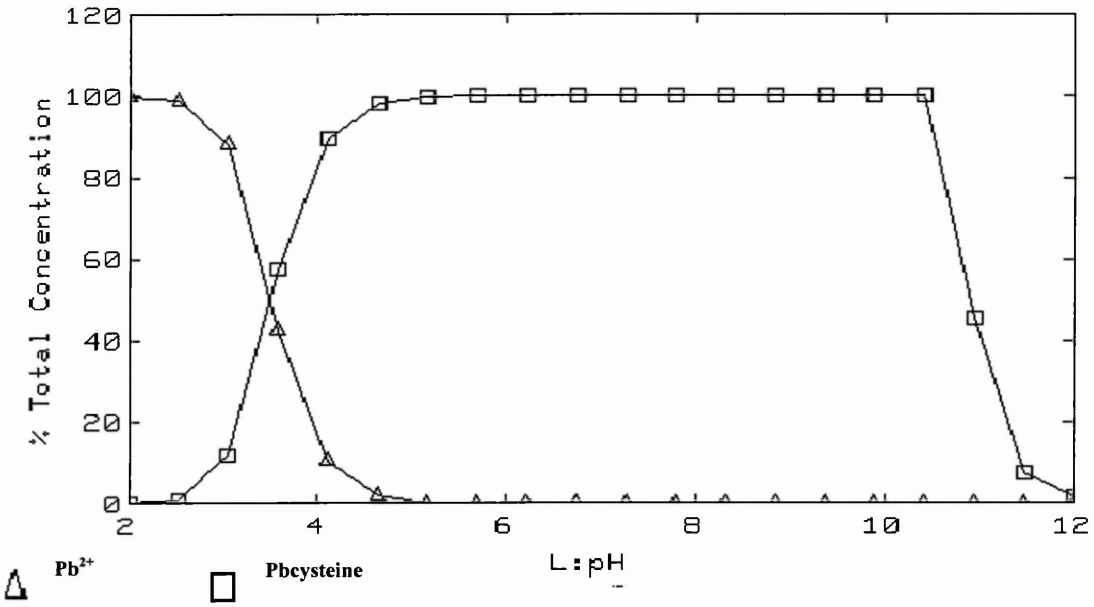

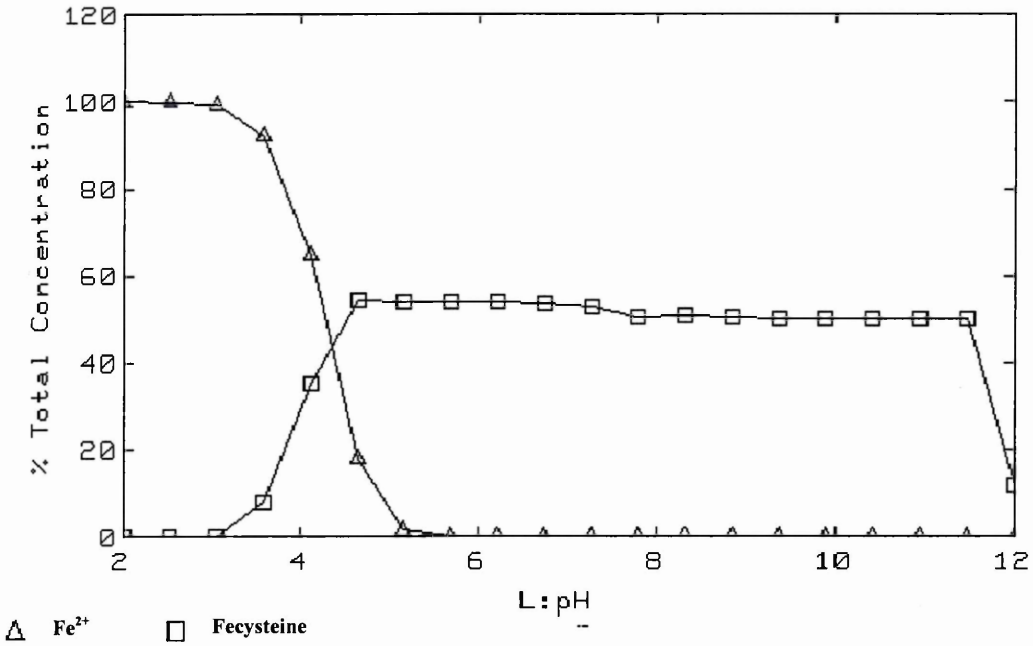

Figure 18: Speciation of Fe in the 0.075M L-cysteine solutions, as derived using the MINEQL+ geochemical modelling software.

Extractions using EDTA

Data obtained from batch extractions performed to deduce the molarity for optimum metal extractions using EDTA solutions (at pH 4) (presented in Table 30(a)), show that there was a linear increase in extractions of all the analysed metals apart from Cu, in the molar range 0.001-0.01M. Thereafter, there was a progressive decline in the concentration of metals extracted into solutions in the molar range 0.05-0.1. The extractions for Ca, Al, Mg, Fe, Zn, Mn and Pb in 0.01M EDTA solutions was 2560±89 (73%), 1160±50 (23%), 191±35 (20%), 4780±474 (25%), 39±5 (22%), 755±12 (170%) and 6870±32 (106%)mg kg^{-1} respectively. The highest concentration of Cu 94±3 mg kg^{-1} (124%) was extracted into 0.001M solutions. Batch extractions performed using 0.01M EDTA solutions show that the optimum soil-solution ratio was 1:30 (data not presented).

The most notable feature of the batch experiments using 30mL of 0.01M EDTA solutions was the desorption pattern of Fe, which showed that the Fe solubilisation remained constant in the pH range 3-5, followed by a decrease in the pH range 5-8 and an increase in the pH range 8-10 (Figure 18). The highest extractions of most of the metals took place in EDTA solutions at pH 5, wherein the extractions of Cu, Ca, Mg, Fe, Pb, Zn and Mn were observed to be 15±4 (20%), 2980±340 (85%), 245±12 26%), 9560±235 (50%), 6090±342 (94%), 79±6 (43%), 411±33 (92%)mg kg^{-1} respectively (Table 30(b)).

Speciation of Pb and Fe in the solutions was deduced via data input into the geochemical modelling software MINEQL+ (Figure 19). The distribution pattern of metals in the modelling output reflects a close overlap with the desorption pattern

obtained experimentally. The data show that at pH 2, approximately 60% of the Pb in solution existed as Pb-EDTA (K_s = 17.9) (where K_s is the metal-complex stability constant) while the remaining 40% was in the form of Pb^{2+} ions. There was a progressive increase in the proportion of Pb-EDTA to Pb^{2+} in solutions until pH 4, at which point almost 100% of the Pb in solution existed as Pb-EDTA. Approximately 100% of the Pb in solutions existed as Pb-EDTA in the pH range 4-6, followed by a rapid decline in the pH range 6-7, as majority of Pb precipitated out as $Pb(OH)_2$ (K_s = -8.2), due to a lack of binding sites on the EDTA. However, the concentration of Pb in solution progressively increased in the pH range 7-10, with the metal ions being in the form of Pb-EDTA.

Similarly, the modelling data obtained for Fe distribution pattern in 0.01M EDTA solutions over the entire pH range show an excellent overlap with the experimental data. The modelling data shows that in the pH range 2-6.5, 95% of Fe in solution was in the form of $Fe\text{-}EDTA^{4-}$ complex (K_s = 16.7), while the remaining 5% existed in the form of Fe^{2+}. There was a rapid decline in the concentration of Fe in solution in the pH range 6.5-7, at which point the total concentration of metal in solution decreased to 20% (of the total soluble Fe), with the Fe existing primarily as Fe^{2+}. The remaining 80% precipitated as haematite and manganite. The large stability constants of the chelated metals illustrate that the presence of EDTA can significantly increase metal solubility through the formation of soluble complexes.

(a)

Molarity	Cu	Ca	Al	Mg	Fe	Pb	Zn	Mn
0.001	94±3	1080±65	647±35	159±6	1580±28	5080±150	25±2	229±6
0.005	86±1	1980±104	931±64	139±6	3470±84	5760±161	31±1	684±24
0.01	79±8	2560±89	1160±50	191±35	4800±474	6870±362	39±1	755±15
0.050	15±9	3080±150	1170±64	267±15	4870±209	6970±187	44±4	755±12
0.100	30±4	2880±98	1090±57	251±10	4380±126	5400±98	41±15	744±33

(b)

pH	3	4	5	6	7	8	9	10
Cu	15±1	16±1	15±2	19±1	17±3	19±2	18±2	17±3
Ca	2570±110	2720±50	2980±340	3050±122	2820±310	2470±95	2600±121	2550±170
Al	1710±82	1340±27	1100±142	1305±74	1210±174	1010±209	1250±192	1260±272
Mg	325±16	177±10	245±12	261±12	278±28	488±23	547±24	538±52
Fe	9410±115	7960±214	9560±235	8860±258	5320±160	3820±190	4350±351	4380±153
Pb	5920±73	6530±307	6090±342	6000±238	5740±72	5470±100	5910±240	5850±175
Zn	86±5	88±20	79±6	51±5	33±4	61±4	77±10	63±15
Mn	357±9	370±20	411±33	446±12	434±45	432±45	408±34	296±11

Table 30: Concentrations of metals (mg kg^{-1}) extracted from the soil using (a) EDTA solutions (pH 5) over the molar range 0.001 –0.1 M; (b) 30mL of 0.01M EDTA solutions over the pH range 2-6.

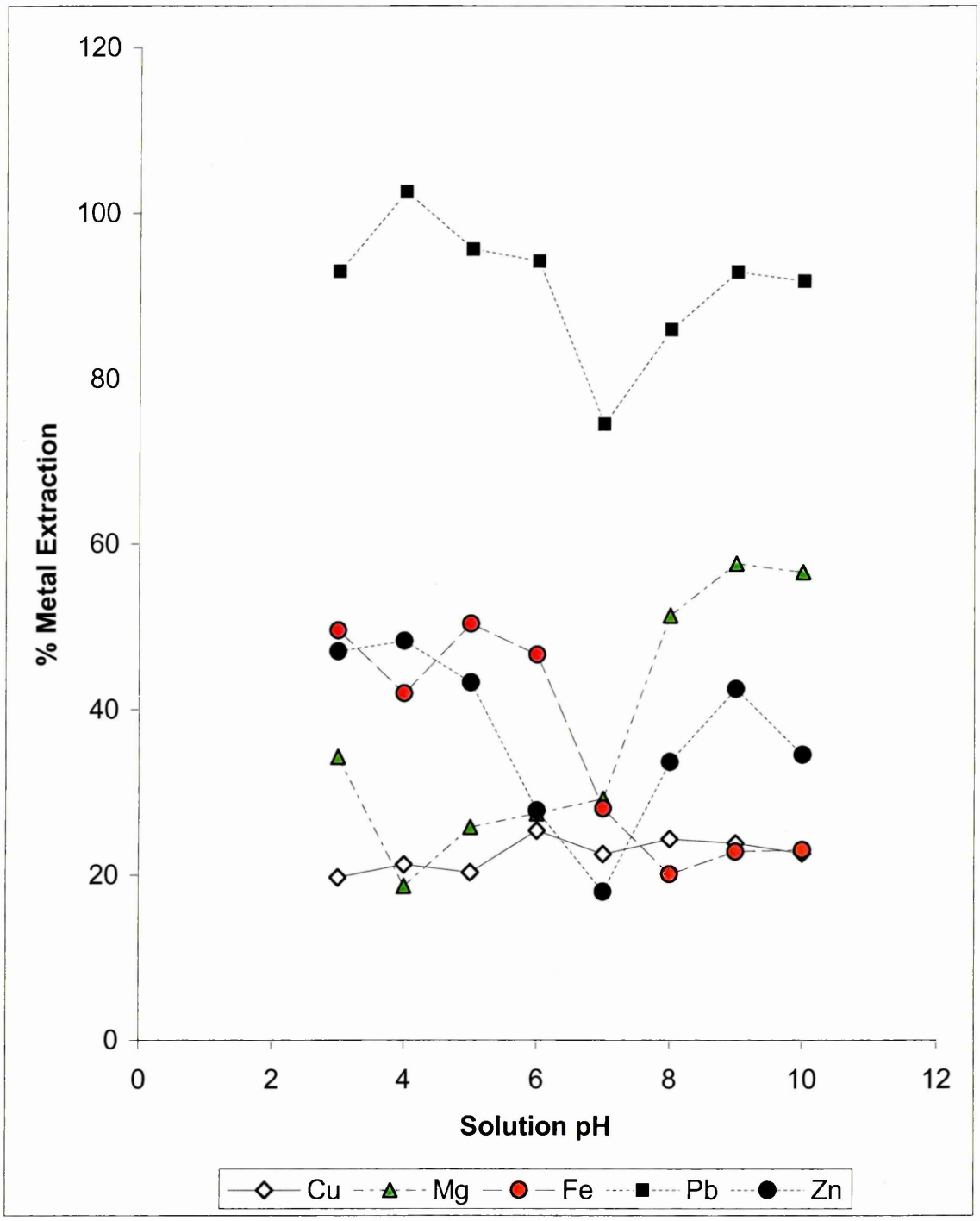

Figure 19: Extraction patterns for metal extractions using 0.01M EDTA over the pH range 2-10.

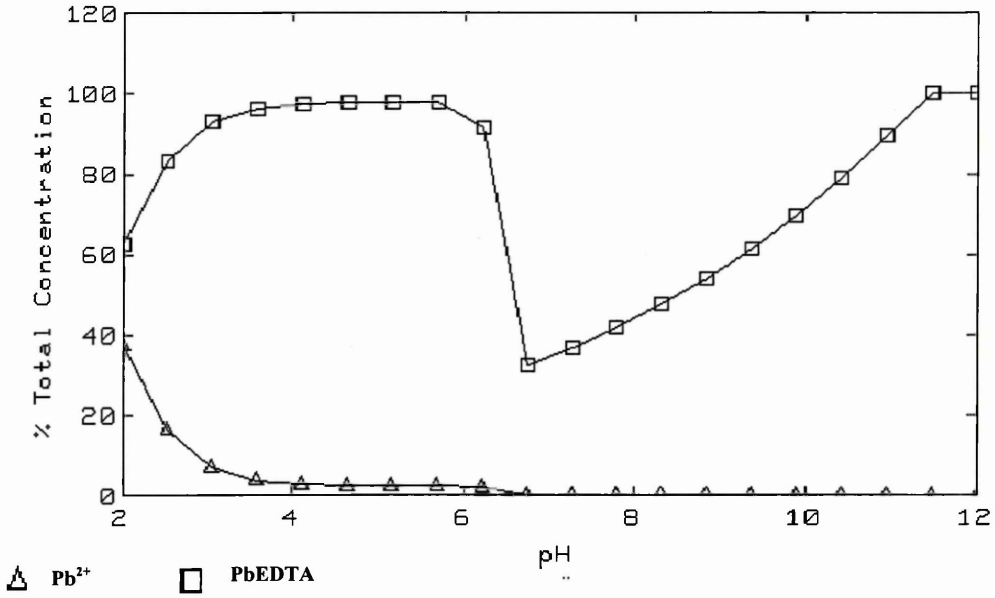

(b) Fe

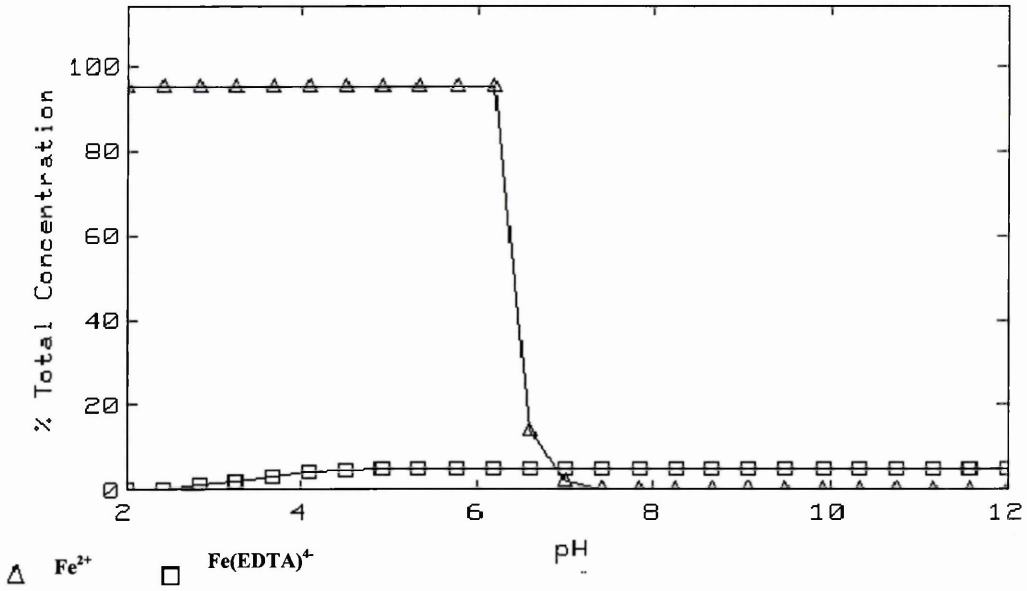

Figure 20: Speciation of (a) Pb and (b) Fe in 0.01M EDTA solutions, obtained by inputting the experimental data into the geochemical modelling software MINEQL+.

XRF Analysis

XRF analysis of the untreated soil and the residues from 3M ethanoic acid (pH 5), 0.01M EDTA (pH 5), 0.075M L-cysteine, 0.75M citric acid treated soils was performed and the data presented in Table 31. These experiments were performed to validate the data obtained from the batch extractions. The decreasing order of Pb extraction from the various samples were as follows: aqua-regia treated (95%) > EDTA treated (93%) > ethanoic acid (70%) > L-cysteine (57%) = citrate (57%). The values in parentheses are the fraction of aqua-regia soluble pseudo-total metal concentration in the soil sample C1. This data reflects an anomaly between these extraction patterns and those observed using the batch extractions, which showed that the proportion of metal extracted using the complexing agents was approximately 80 - >100% of the total metal in the soil. This difference highlights the inhomogeneities in distributions of metals in the soil, even in finely ground samples.

Mineral composition (%w/w)	Untreated soil	Aqua-regia digested soil	3M ethanoic acid treated soil (pH 5)	0.01M EDTA treated soil (pH 5)	0.75M citrate treated soil (pH 2)	0.075M L-cysteine treated soil (pH 8)
SiO_2	59.27	70.38	64.70	68.06	61.88	43.90
Al_2O_3	21.26	19.54	19.76	18.70	18.67	16.69
Fe_2O_3	8.97	2.39	7.61	5.84	9.41	6.75
K_2O	2.22	1.49	2.14	2.03	2.36	1.87
CaO	1.61	0.14	0.43	0.54	0.70	1.08
MgO	1.06	0.51	0.92	0.84	0.84	0.79
TiO_2	1.03	1.23	0.85	0.77	1.09	0.83
PbO	0.81	0.07	0.25	0.05	0.34	0.35
P_2O_5	0.71	0.09	0.79	0.67	0.54	0.50
SO_3	0.81	0.23	1.04	0.80	1.11	25.40
Na_2O	0.45	0.41	0.42	0.42	0.49	0.31
MnO	0.15	0.01	0.09	0.03	0.09	0.11

Table 31: A comparison of XRF data for untreated soil and residues from batch experiments using the various complexing agents.

Additionally, the data also show that apart from that of Ca and Fe, the concentration of none of the major metals in the various soil fractions was radically altered. The

decreasing order of Ca extraction from the various samples were as follows: aqua-regia treated (91%) > ethanoic acid (73%) > EDTA (66%) > citrate (57%) > L-cysteine (17%). The decreasing order of Fe extraction from the various soil samples were as follows: aqua-regia treated (73%) > EDTA (35%) > L-cysteine (25%) > ethanoic acid (15%) > citrate (0%). The high extraction of Fe by EDTA and L-cysteine was most likely due to the reduction of the Fe^{3+} to Fe^{2+} as a result of donation of electrons from the amino groups on these two compounds. The increases in concentration of the other metals in the various fractions (e.g. Si) was most likely due to the semi-quantitative instrumental software compensating for decreases in Pb and Ca content (in order for the sum of the compositions to be 100%).

9.3 Discussion

In this chapter the author has tested the feasibility of using citric acid (a tricarboxylic acid), L-cysteine (a natural amino acid) and EDTA (a synthetic amino acid) as potential soil washing reagents and compared with data obtained using a monocarboxylic acid, ethanoic acid. The data show that EDTA was the most effective of the four reagents in mobilising metals from the soil. One possible explanation for the higher release using EDTA is that the dilute chelant solution was aggressive enough to dissolve the entire fraction of lead oxides and a significant fraction of Fe oxides[238]. The large drop in the concentrations of Fe extracted into 0.01M EDTA solutions in the pH range 6-8 was possibly due to precipitation of Fe as hydroxides. A progressive decline in the concentration of Pb after pH 3, followed by an increase in the pH range 8-10 was most likely due to a greater availability of binding sites on the EDTA anions at the pH values 2.00, 2.67, 6.16 and 10.26. However, the most notable observation is the high dissolution of Pb over the entire range, which suggests that the Pb oxides in the soil could not have been in crystalline

forms (lack of crystallinity suggests contamination). This explains the lack of significant changes in the XRD spectra obtained on the residue from the first step of the BCR sequential extraction procedure (as XRD can only analyse crystals not amorphous materials) (Figure 11). This data also show that a majority of Pb in the contaminated soils was extractable using complexing agents at room temperature, without resorting to harsh techniques such as aqua-regia dissolution. However, MINEQL+ modelling data has shown that most of the divalent metals in the leachate solutions existed as metal-EDTA complexes, the ecological and human health effects of which are unknown. It is well known that EDTA at elevated concentrations is a potential carcinogen and its lack of biodegradability increases this toxicity.

Significant concentrations of Pb, Fe and Ca were mobilised into 0.75M citric acid solutions ($pK_a = 2.2$). The dissolution mechanism using citric acid would have been similar to that of ethanoic acid as their chemical structures are similar. The slightly higher dissolution of some of the metals in ethanoic acid is most likely due to the higher molarity of the latter solutions. The most important observation from this set of experiments was the high extraction of Pb in conjunction with Ca over almost the entire pH range. Speciation modelling data has shown that a majority of the metal in the citric acid solutions would have existed as metal-citrate ions. If citric acid were indeed a metal transporter in the rhizospheres to the plants, most metals would be transferred as metal-citrates rather than as divalent cations or as hydroxylated ions.

The high extraction of metals in 0.075M cysteine in the pH range 8-9, was most likely because the acid dissociation constant of cysteine is 8.5-8.7, as a result of which there is a greater availability of –SH, -COOH and $–NH_2$ amino groups in this pH range.

Rojas-Chapana and Tributsch[239] observed that in the absence of bacteria and presence of cysteine, pyrite (FeS_2) could be oxidised at a leaching rate comparable with that attained by bacteria (*Thiobacillus ferroxidans*) under normal leaching conditions. A similar dissolution process could have taken place in this study, whereby the amorphous Fe(III) oxides could have reacted with the sulfydril groups (-SH) groups, resulting in the release of iron-sulfur species. Evidence for this consumption of cysteine ions on the mineral surfaces comes from the large increase in the proportion of sulfur in the soil following batch extractions using L-cysteine (Table 31). If cysteine were indeed a phytochelatin and a transporter of metals from the rhizospheres to the plants, all the divalent metals would have been transferred in the form of metal-cysteine ions, rather than divalent or hydroxylated metal ions. Another noteworthy observation was the lack of significant differences in the proportion of sulphates and phosphates in the untreated soil samples and the residues left behind from batch extractions using the complexing agents. This suggests that the metals extracted into solutions did not exist in the soils as sulphates or phosphates.

9.4 Conclusions

The following conclusions can be drawn from the data presented in this chapter: (i) Pb was indeed in the form of PbO in the soil rather than sulphates and phosphates and would have been precipitated onto the surfaces of calcium carbonates and Fe oxides. This suggests that the customised BCR procedure could be a credible method for predicting the concentration of extractable metals using soil washing; (ii) soil washing using complexing agents such as EDTA, citric acid and L-cysteine could be used as a credible and efficient remediation procedure that would not radically alter the basic composition of soils; (iii) metals would be available for uptake by plants in the form of metal-phytochelatin complexes under normal soil conditions; (iv) there was a high

degree of mobilisation of essential metals such as Zn, Cu and Mn over the entire pH range in both citric acid and L-cysteine solutions, which provides a possible explanation for their accumulation in the above ground biomass of the plants; (v) however, the data also show that approximately 90-100% of the Pb in the soil would be available for uptake by plants. This was not in agreement with the observations obtained using the phytoextraction experiments, which showed that only 10-12% of the total Pb in the soils was available for uptake by plants. This suggests a detoxification mechanism in operation that actively excludes toxic metals from entering the main biomass of the plants. It is well known that cells control the type and reactivity of elements with which they associate by isolating heterogeneous aqueous compartments within hydrophobic cell membranes[240]. This is achieved by trapping molecules with hydrophilic ligands and by synthesising hydrophobic ligands that become trapped in the membrane itself. These form localised element sensing molecules containing elaborate structural ligands. Various elements become speciated with these ligands and thus segregated from the bulk phase to provide the organisational basis for effective survival of organisms.

Chapter 10 Hydroponics Experiments

10.1 Introduction

The data obtained from the soil washing experiments using citric acid and L-cysteine, two potential phytochelatins, showed that approximately 50-60% of the total Pb in the soil would have been available for uptake by plants. However, the data obtained from the phytoextraction experiments show that only 10-12% of the total Pb in the soils was actually taken up by the plants. This suggests that there might be mechanisms that actively prevent the excessive accumulation of toxic metals in the plants. Cotter-Howells et al[241], observed the formation of lead phosphate on the roots of the heavy metal tolerant grass, *Agrostis capillaris* grown on mine waste contaminated soils.

Some authors[242] have suggested that toxic metal immobilisation takes place on cell surfaces and was probably a result of biosorption on to negatively charged groups such as P-type heavy metal ATPases on the lipopolysaccharides (LPS)[243] of cell membranes[244, 245]. A good example is the precipitation of polycrystalline sodium uranyl phosphate ($NaUO_2PO_4$) on the cell surface of *Citrobacter* spp. *N14*[246]. The authors suggested that the initial nucleation for the polycrystalline compound was a result of UO_2^{2+} interaction with monophosphate groups on the LPS surface. The LPS also acts as an immobilisation matrix for phosphatase enzymes that catalyse the synthesis of more surface phosphate groups that bind with incoming metal ions resulting in the formation of polycrystalline sodium uranyl phosphate. In the event of a failure of the enzyme or if the metal ions diffused through the phosphate barrier, a second line of defence consisting of phospholipid groups on the membrane bilayer enveloping the cells in conjunction with phosphatases on periplasm and outer membranes is invoked. Both of these mechanisms are likely to occur in plants and could explain the binding of lead to root surfaces.

Furthermore, Keasling et al.[247] showed that a decrease in PO_4^{3-} in solution resulted in the precipitation of a uranium-phosphorus complex on *Escherichia coli* cell surface due to change in the concentration and behaviour of polymers called polyphosphates that store energy and phosphates. Under conditions of inorganic phosphorus (P_i) starvation, the sensory mechanisms on the cell surface trigger the induction of a gene known as *ppx* that encodes for polyphosphatase, an enzyme that cleaves the polyphosphates thereby causing the release of phosphate residues. In plants there is likely to be an increased release of these phosphate groups as a response to metal induced stress and P_i starvation as was the case in this study.

These mechanisms are key to the survival of plants in potentially phytotoxic conditions, such as solutions spiked with heavy metals. The wild legume *Sesbania drummondi* cultured in hydroponics solutions has been shown to accumulate 60000 and 40000mg kg^{-1} lead in the shoot and root respectively[248]. The results of these studies show that plants have the capacity to accumulate high concentrations of Pb in their biomass, but they do not explain the mechanism behind the very low root-shoot transfer coefficient. To gain an understanding of the mechanisms dictating the preferential accumulation of metals in the roots, experiments were performed using 4 week old *H. annuus* seedlings grown in nutrient solutions. Two sets of experiments were performed, one using lead nitrate spiked solutions without any essential nutrients and second, using spiked solutions with nutrients, in order to study the role played by nutrients on potential immobilisation of metals on root surfaces.

Initially lead nitrate solution was prepared by adding 1.64 mg L^{-1} of $Pb(NO_3)_2$ salt to 1L nutrient solution containing phosphates. This resulted in the rapid formation of a

dense white precipitate at the bottom of the volumetric flask, ostensibly, due to the formation of highly insoluble lead phosphates. Therefore, a set of nutrient free solutions i.e. in pure deionised water, containing 0 and 1000 mg L^{-1} of Pb were prepared for a first set of experiments. The second set of experiments involved the use of nutrient solutions free of phosphate spiked with 10, 100 and 1000 mg L^{-1} of Pb respectively.

10.2 Results and Analysis

Metal Speciation in Solution-Root System

The speciation of metals in deionised water and nutrient solutions with and without phosphate was modelled using the geochemical thermodynamic equilibrium software PHREEQC, with the thermodynamic data being obtained from the WATEQ4F database. The data show that in deionised water spiked with 1000mg L^{-1} Pb the majority of the metal would exist as *unhydroxylated* Pb^{2+} ions at an activity of 7×10^{-4}M. Assuming that the concentration of Ca, Cl and P (as these elements are constituents of ion-channels and ATPases on the cell membranes) on the surface of roots was 1.8×10^{-3}, 4.4×10^{-4}, 3.7×10^{-4}M respectively[243], the mass balance data show that there should be the formation of chloropyromorphite ($Pb_5(PO_4)_3Cl$), hydroxypyromorphite ($Pb_5(PO_4)_3OH$) and hydroxyapatite ($Ca_5(PO_4)_3OH$) on the root surfaces. The saturation indices for chloropyromorphite, hydroxypyromorphite and hydroxyapatite were calculated by the model to be 29.1, 16.4 and – 4.62 respectively.

Similar modelling was performed for the spiked nutrient solutions with and without phosphate, with the initial input being the concentration of the various nutrient constituents being that described in Table 3. The data showed that the metal ions in

both solutions would have existed principally in the form of *unhydroxylated* cations without any significant precipitation. Copper would have existed mainly in the form of Cu^{+} and Cu^{2+} at an activity of 1.8×10^{-6} and 4.8×10^{-5} respectively with the remaining metal in solution forming $CuCl_2^{-}$, $Cu(OH)_2(aq)$, $CuCl^{+}$, $CuOH^{+}$ etc. All the other divalent metals would have formed similar species. However, using assumptions made for phosphate and chlorine concentrations in the deionised water-root system, it was observed that whilst Pb would have precipitated onto the surface of roots in the form of chloropyromorphite, hydroxypyromorphite and hydroxyapatite, there was only limited mineralisation of the essential elements such as Cu, Zn, Ni, Fe and Mn. Cu^{2+} could have co-precipitated with Fe^{2+} due to the formation of cupric ferrite, which has a saturation index of 9.36.

Plants Growing in Deionised Water Solutions

The plants growing in the Pb spiked solutions showed signs of stress 24 hours after transplantation. The leaves and the stems of the plants growing in the spiked solutions lost their turgidity after 48h followed by yellowing of leaves (necrosis) after 72h. Plants growing in the control solutions did not lose as much turgidity and there were no visible signs of necrosis inspite of the lack of nutrients. The roots of the plants growing in the spiked solutions turned dull grey as opposed to the roots of control plants that remained milky white.

The concentration of the lead in the spiked deionised water solutions after 0, 12, 24 and 36 hours was observed to be 1010 ± 30, 384 ± 14, 358 ± 20 and 472 ± 18mg kg^{-1} respectively. The net solution concentration after 36 hours was higher than in the previous two samples as a result of solution evaporation. Multielemental analysis data, presented in Table 32, show that a majority of the Pb was sequestered in the

roots of the plants, with a relatively small fraction being transported to the stem and the leaves. Approximately 120,000mg kg^{-1} lead was accumulated in the roots, followed by approximately 6500mg kg^{-1} and 50mg kg^{-1} lead in the stem and the leaves respectively. However, the actual total weight of Pb accumulated in the biomass (weight 3.5±0.5g) would have been approximately 4.2mg. There was negligible accumulation of lead in the biomass of plants growing in the unspiked solutions.

The highest accumulation of Fe was observed in the roots (2740 ± 182mg kg^{-1}) followed by the leaves and stems. An equivalent accumulation pattern was observed in the biomass of the plants growing in the unspiked solutions (Table 32(b)). The highest concentration of Cu was observed in the roots followed by equal amounts in the stems and the roots, with the concentrations being approximately equal in plants growing in both spiked and unspiked solutions. The highest concentration of Ca and Mg was observed in the leaves followed by the stems and the roots. The concentration of Ca and Mg in the biomass of plants growing in the unspiked solutions was slightly higher than those in the spiked solutions, although still in the same data range.

(a)

Metals	Leaves	Stem	Roots
Cu	17 ± 1	17 ± 1	44 ± 2
Ca	13400 ± 95	6030 ± 280	3140 ± 180
Mg	5210 ± 208	3000 ± 325	820 ± 67
Fe	122 ±- 3	<0.001	2730 ± 105
Mn	64 ± 4	<0.001	<0.001
Pb	52 ± 2	6600 ± 135	111000 ± 25000
Zn	313 ± 3	604 ± 80	435 ± 56

(b)

Metals	Leaves	Stem	Roots
Cu	18 ± 1	17 ± 1	48 ± 2
Ca	12200 ± 95	7120 ± 280	4440 ± 180
Mg	5150 ± 288	3480± 375	850 ± 66
Fe	115 ± 3	<0.001	2690 ± 105
Mn	70 ± 4	<0.001	<0.001
Pb	2.3 ± 2	5 ± 1	10 ± 4
Zn	411 ± 3	585 ± 64	505 ± 56

Table 32: Mean metal accumulation in *H. annuus* roots grown in (a) 1000 mg L^{-1} lead spiked solutions (b) deionised water (control).

XRF analysis of the root samples from the plants growing in 1000mg L^{-1} was performed to confirm the wet chemical data (Table 33). The result showed that the %w/w concentration of lead accumulated in the roots was approximately 10% (100,000 mg kg^{-1}), which is in the same range as the data obtained from wet analysis. It was calculated that the ratio of lead (10.3%), phosphate (5.8%) and chlorine (1.1%) concentration in the root samples was 5:3:1 respectively suggesting the possible formation of chloropyromorphite [$Pb_5(PO_4)_3Cl$)]. Chloropyromorphite is a chemically and thermodynamically stable form of lead (log K = -84.43) and is known to be less soluble than widely abundant minerals such as cerussite ($PbCO_3$, log K = -13.13), or lead oxide (log K = -16.38).

Oxide	Mass %
PbO	10.3 ±0.2
P	5.8±0.1
K_2O	5.7±0.3
SO_4	2.4±0.2
CaO	1.3±0.1
Cl	1.1±0.1
Fe_2O_3	1.1±0.1
Na_2O	0.7±0.1
SiO_2	0.6±0.1
MgO	0.4±0.1
Al_2O_3	0.2±0.01

Table 33 – Accumulation (%w/w) data from XRF analysis of the roots growing in the 1000mg L^{-1} Pb spiked solution.

Speciation analysis using XRD show that Pb in the root biomass was principally in the form of calcium lead chloride phosphate ($Ca_{2.1}Pb_{7.9}Cl_2(PO_4)_6$) and chloropyromorphite($Pb_5(PO_4)_3Cl$) (Figure 20). Characteristic chloropyromorphite peaks were observed at 45, 47, 48, 64 and 68 degrees (the peaks from °2θ 45-50 were the most intense). Characteristic peaks for calcium pyromorphite [$Ca_{2.1}Pb_{7.9}Cl_2(PO_4)_6$] were observed at 32, 34, 40, 42 2θ-degrees. Clear visual evidence showing the association of lead, phosphorus and oxygen was obtained by ESEM/EDX analysis (Figure 21). EDX spot analysis shows a clear association between lead, phosphorus and oxygen maps. Evidence for the presence of phosphates on the surface of the roots was gathered through EDX analysis of the roots (Figure 22). Further evidence for pyromorphite formation was obtained by FT-IR analysis of the ground root samples. Characteristic pyromorphite bands at wavenumbers 1028.84 (1030), 974.84 (970), 572.75 (570) and 541.90 (542) cm^{-1} were identified in the FT-IR spectra (Figure 23). The values in brackets are wavenumbers for pyromorphite[249]. None of these bands were seen in the FT-IR spectrum for the control roots (Figure 23) indicating the absence of pyromorphite. The data obtained here is in good agreement with the thermodynamic predictions obtained from the PHREEQC model.

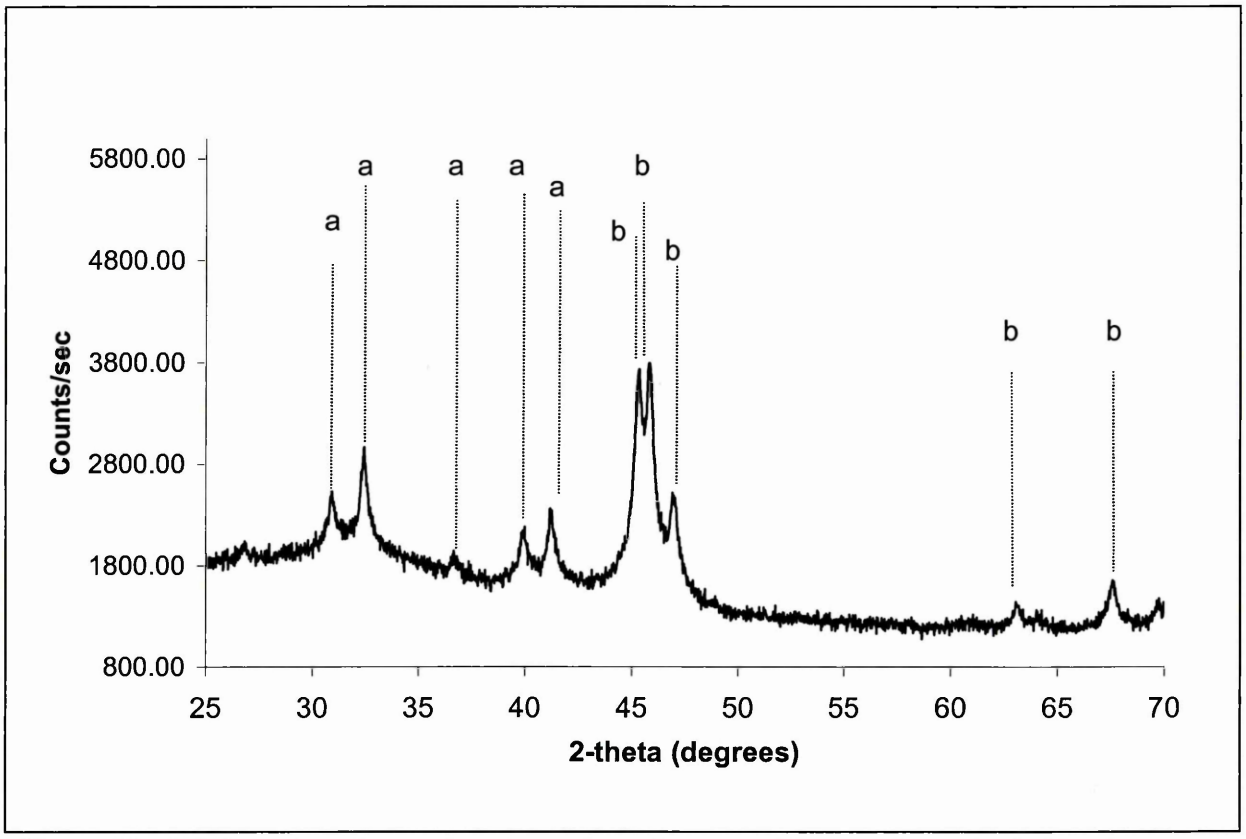

Figure 20 - XRD spectra of ground root samples, where **a** and **b** are calcium lead chloride phosphate [$Ca_{2.1}Pb_{7.9}Cl_2(PO_4)_6$] and pyromorphite [$Pb_5(PO_4)_3Cl$] peaks respectively.

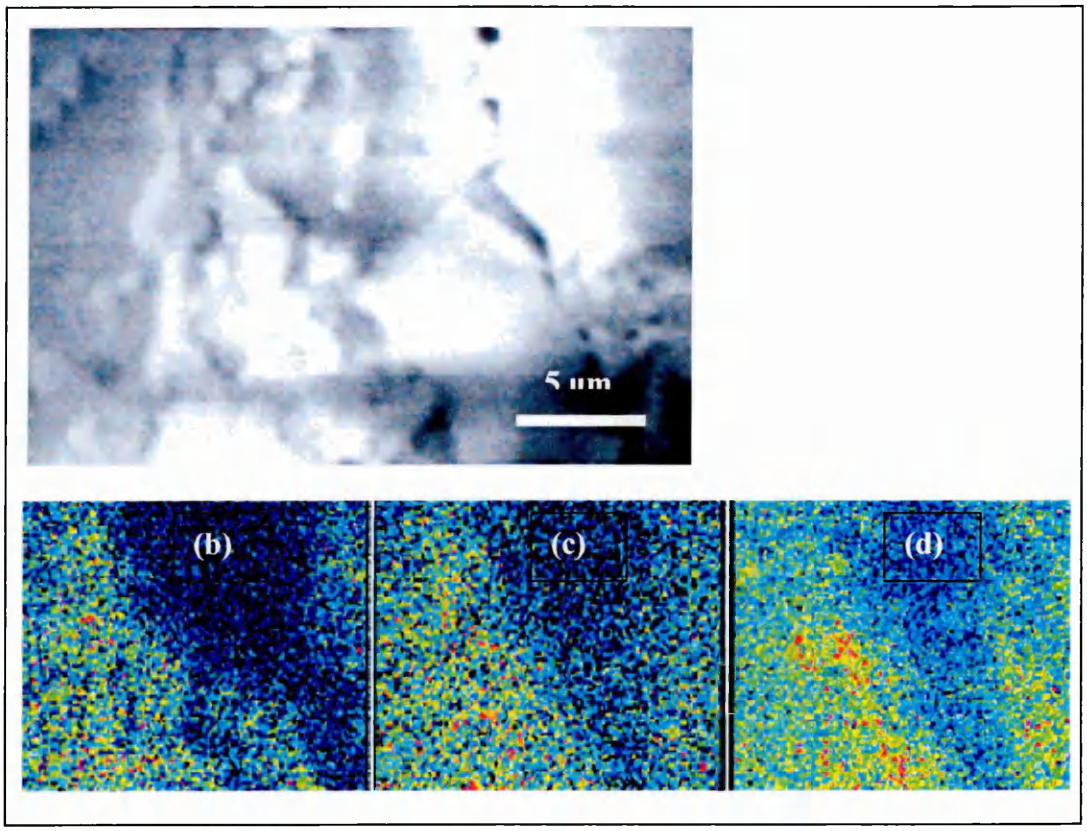

Figure 21 - (a) ESEM image of pyromorphite coated *H. annuus* root samples and EDX map of (b) Pb, (c) oxygen and (d) phosphorus.

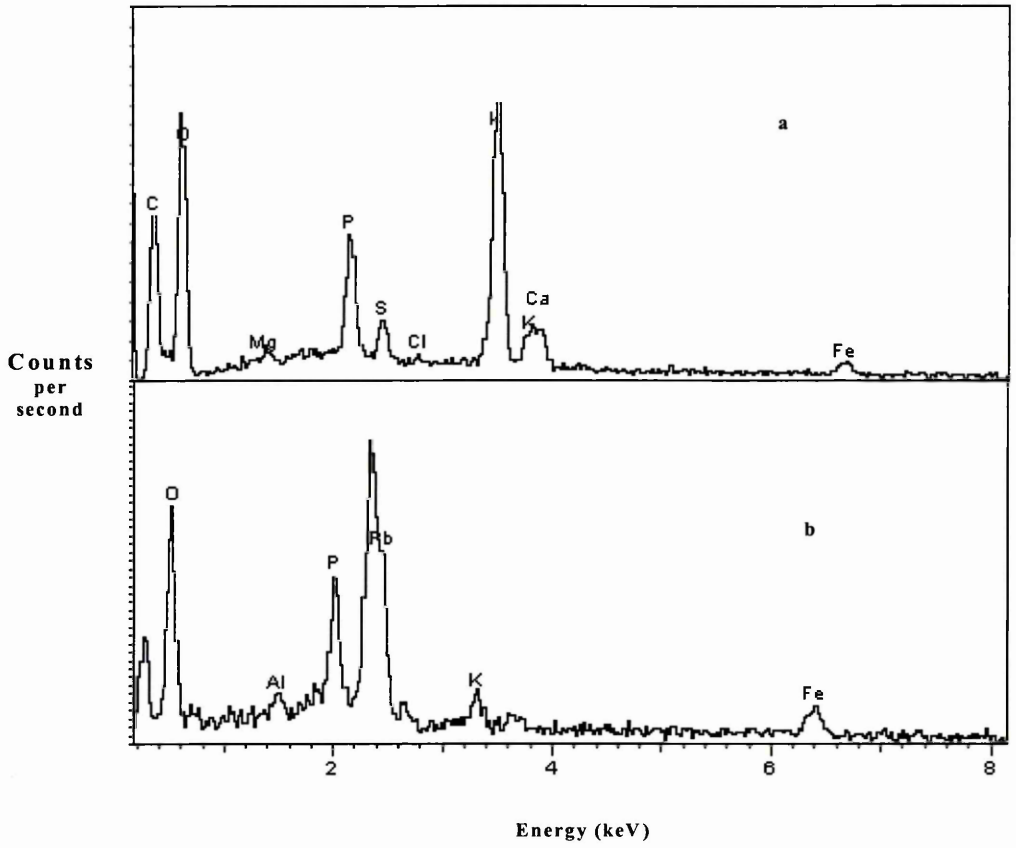

Figure 22 - EDX spectrum for H. annuus roots of (a) control roots and (b) pyromorphite.

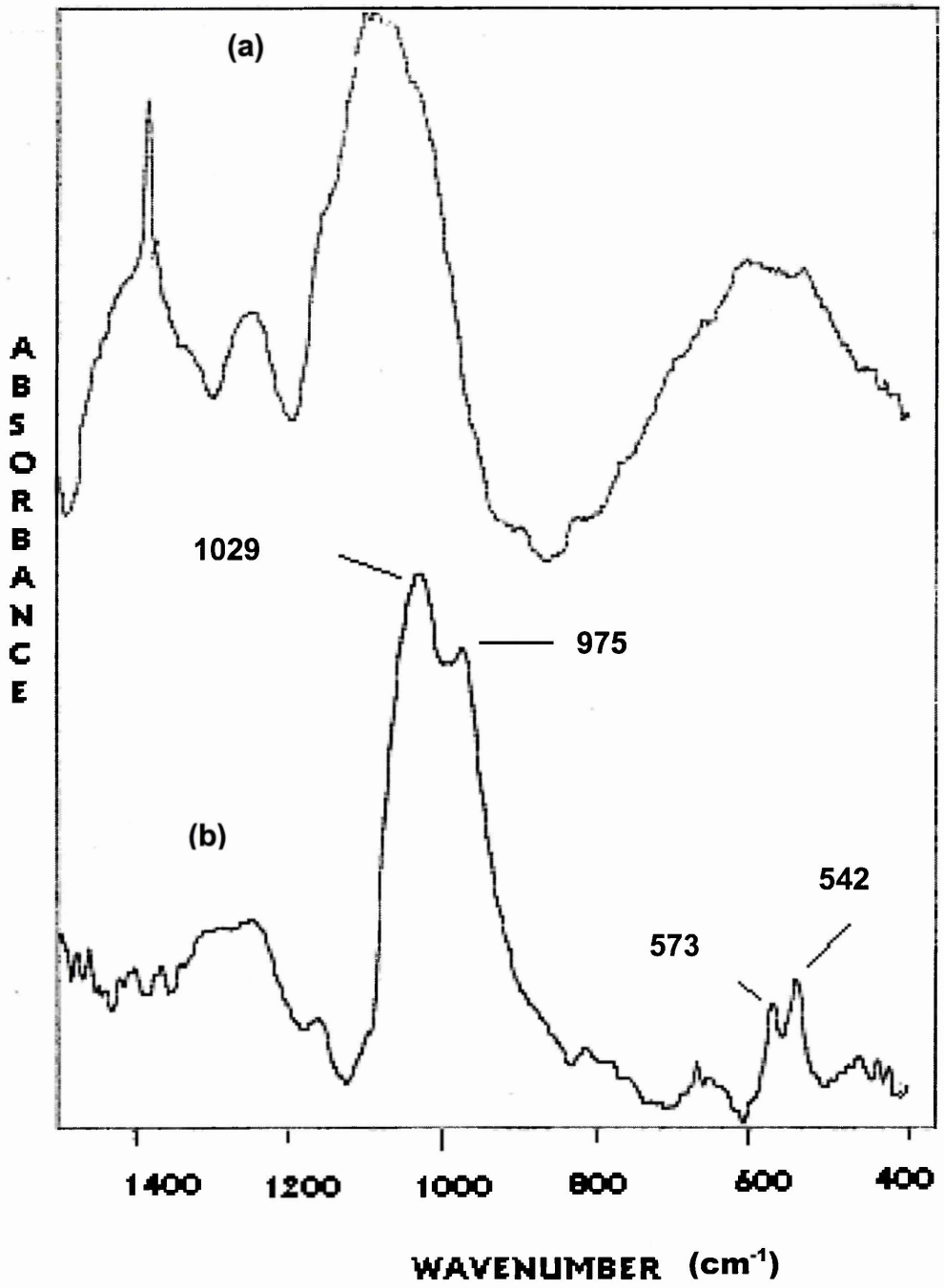

Figure 23 - FT-IR scan of the roots grown in (a) control and (b) spiked solutions, respectively.

Plants grown in Phosphate Free Nutrient Solutions

Plants growing in the spiked and unspiked phosphate free nutrient solutions did not show signs (after 24h) of stress, as there were no visible signs of necrosis. Therefore, the plants were allowed to grow for a further six days, with the solutions being replaced everyday to compensate for losses due to evapo-transpiration. At the end of the third day the plants growing in the unspiked solutions started drooping slightly whilst those in the control solutions looked healthy. At the end of fifth day, there was visible yellowing of plants growing in the spiked solutions with the roots turning a dull grey although not as dense as those growing in the deionised water. The colouring was much more visible for those growing in the 1000mg L^{-1} solution than those growing in the 10 and 100 mg L^{-1} solutions. At the end of a week the leaves of plants growing in 100 and 1000mg L^{-1} solutions turned visibly brown while the stems were flaccid. The shoots of plants growing in the control solutions turned yellow showing visible signs of chlorosis.

Analysis of the digested biomass showed that most of the lead was accumulated in the roots followed by the stems and the leaves (Table 34). The highest accumulation of Pb took place in the roots of plants growing in solutions spiked with 100 mg L^{-1} Pb^{2+}. The mean accumulation of Pb in the roots of the plants grown in blank, 10, 100 and 1000mg L^{-1} solutions was 418 ± 44.2, 42300 ± 205, 339000 ± 8200, 238000 ± 6670 mg kg^{-1} respectively. The mean accumulation of Pb in the stems of plants grown in blank, 10, 100 and 1000mg L^{-1} was 9.7 ±2.2, 179 ± 20.3, 107 ± 14.1, 68795 ± 3400mg kg^{-1} respectively. The mean accumulation of Pb in the leaves of plants grown in blank, 10, 100 and 1000mg L^{-1} was 20.3±2.1, 90±7, 118±2, 2320 ± 348mg

kg^{-1}. An interesting observation is the varying accumulation patterns of the essential metals in the biomass of the plants growing in the four solutions.

The accumulation of Fe was highest in the leaves and stems of plants growing in the control and 10mg L^{-1} spiked solutions, while the highest accumulation in roots took place in those growing in the 100mg L^{-1} spiked solutions. The lowest accumulation of Fe was in the biomass fractions of plants growing in the 1000mg L^{-1} spiked solutions. The highest accumulation of Cu was in the biomass fractions of plants growing in the control nutrient solutions. The concentrations of Cu in the roots growing in the control solutions was 20 times higher than those in the roots growing in solutions spiked with 1000mg L^{-1} Pb. The concentrations of Cu in the leaves of plants growing in the control solutions was 9 times higher than those in the leaves of plants growing in the 1000mg L^{-1} solutions.

The accumulation of Ca in the control roots was approximately 12 times that of the roots growing in the 1000mg L^{-1} solution. However, the differences in the concentrations of Ca in the stems and leaves of the plants growing in the various solutions were less pronounced. A similar accumulation pattern was observed for K and Na in the stems and leaves of plants growing in various solutions. However, the extraction of Na and K was highest in the roots of plants growing in the 1000mg L^{-1} solutions. The concentration of Mg in roots growing in the 1000mg L^{-1} solutions was approximately 17 times lower than that in the control solutions. The data show that presence of Pb in solutions plays a significant role in the inhibition of essential metal uptake by plants.

(a)

Solution	Control	10mg L^{-1}	100mg L^{-1}	1000mg L^{-1}
Fe	186±40	263±1	82±5	69±1
Cu	94±11	17±2	66±6	10±2
Zn	114±25	111±2	86±8	87±10
Ca	32100±3070	18200±3570	24100±4500	21400±5021
Mg	5820±320	5050±475	3980±760	5410±325
K	46260±3226	38500±7635	46300±4000	58400±4566
Na	213±27	193±6	178±26	527±38
Pb	20±2	90±7	118±2	2320 ± 348

(b)

Solution	Control	10mg L^{-1}	100mg L^{-1}	1000mg L^{-1}
Fe	57±11	52±13	22±4	37±6
Cu	5.5±1.2	5.1±1	3.2±1.1	7.3±1.6
Zn	103±17	65±8	50±9	99±9
Ca	13600±554	9720±989	10800±788	10300±668
Mg	5400±98	3490±656	3760±187	2310±297
K	65500±579	49300±356	53830±365	49300±468
Na	829±256	1030±86	791±64	824±23
Pb	9.7 ±2.2	179 ± 20	107 ± 14	68700 ± 3400

(c)

Solution	Control	10mg L^{-1}	100mg L^{-1}	1000mg L^{-1}
Fe	2270±90	1500±56	1800±65	710±87
Cu	107 ± 22	32 ± 9	32 ± 13	5 ± 2
Zn	266 ± 34	113 ± 23	175 ± 13	25 ± 7
Ca	10600±65	5020±34	7130±98	820±80
Mg	2870 ± 302	2120 ± 211	2610 ± 342	170 ± 89
K	34000 ± 737	48100 ± 3835	47600 ± 40	1075 ± 31
Na	2640 ± 333	1750 ± 134	1110 ± 78	124 ± 22
Pb	418 ± 44	42300 ± 205	339000 ± 8200	238000 ± 6600

Table 34- Mean metal accumulation (mg kg^{-1}) in the (a) leaves (b) stems (c) roots of plants grown in the nutrient-rich, phosphate-free solutions spiked with Pb.

XRF analysis of the leaves, stems and the roots of the plants growing in the 1000 mg L^{-1} confirm the data obtained from multielemental wet chemical data (Table 35). The values for lead in all three components of the biomass were within 10% of those

observed from ICP analysis. This suggests that the analytical procedures followed by the author during the course of the experiments were accurate.

% (w/w) metal composition	Leaves	Stem	Roots
K	16 ± 0.6	16 ± 1	1.1 ± 0.2
Ca	10 ± 0.2	7 ± 0.2	0.6 ± 0.1
P	1.3 ± 0.03	0.5 ± 0.03	6.3 ± 0.1
Pb	0.2 ± 0.03	5.5 ± 0.2	23 ± 0.2
Cl	0.5 ± 0.1	0.3 ± 0.04	1.3 ± 0.1
Sx	0.8 ± 0.2	0.2 ± 0.5	0.5 ± 0.1
Mg	0.4 ± 0.1	0.1 ± 0.03	0.03 ± 0.02
Zn	0.03 ± 0.01	0.04 ± 0.01	0.03 ± 0.01
Fe	0.1 ± 0.02	0.02 ± 0.01	1 ± 0.1

Table 35 – XRF analysis on the biomass of plants grown in the phosphate free Pb spiked 1000mg L^{-1} solution.

10.3 Discussion

The data obtained from these experiments clearly demonstrate the preferential accumulation of Pb in the roots over the stems and leaves of plants. The data also show that plants have a large capacity to accumulate Pb in their biomass, especially in their roots. There was clear evidence of the formation of lead phosphates on the root surfaces, with a preponderance of the phosphatic minerals pyromorphite and calcium pyromorphite. The presence of phosphates on the surface of roots growing in phosphate free solutions, as shown in the XRF analysis (Table 35), suggests a link between Pb uptake and increased secretion of phosphates on the root surfaces. Another interesting observation is the massively lowered uptake of the most essential metals such as Na, K, Mg and Ca into the biomass of plants growing in the spiked nutrient solutions when compared with those in control nutrient solutions. This is a classic demonstration of the phytotoxicity of Pb, as metals like Na and K are critical to the effective functioning of ion-channels. This suppression is possibly because the cell surface ligand groups such as –SH and $-P_x$ would preferentially bind class-B soft

cations over class-A hard cations. However, there were no significant differences between the concentrations of Ca, Fe, Mg and Zn in the biomass fractions of plants growing in the deionised water solutions. This is most likely due to the rapid cell death due to a lack of nutrients and an excess of Pb in the solutions. Evidence for necrosis in these plants comes from decreased spectral height of K in the EDX spectra obtained for the roots growing in the deionised water solutions spiked with 1000 mg L^{-1} Pb as shown in Figure 22.

Another notable observation was the differing distribution patterns of the various metals plants growing in the three spiked solutions (10, 100 and 1000mg L^{-1} Pb). The highest accumulation of Pb was observed in the roots of plants growing in the 100mg L^{-1} followed by those in 1000 and 10mg L^{-1} respectively. A similar accumulation pattern was observed for Fe, Cu, Zn, Mg and Ca, as all these were shown to exist in the growth media as M^{z+} species. Two models have been used to describe the suppression of essential ion-uptake and the higher metal uptake in the intermediate range spiked solutions. The former has been explained using the Biotic Ligand Model (BLM) and the latter using the Free Ion Activity Model (FIAM)[250,251].

The Biotic Ligand Model (BLM) explains the mechanism by which organic-metal complexes interact with the naturally occurring ligands on cell or tissue surfaces[252]. This model works on the assumption that it is always the free metals ions that are taken up by cells and that the biological response to presence of toxic metals in solution depends on their concentration. Increase in concentration of metal ions in solutions results in an increased secretion of biological ligands, until a saturation point is reached. Toxicity predictions through the application of the BLM model are

independent of the nature or location of the ligands and focus on the free ion, which is taken up at the membrane. The conditions for the application of this model are that the system has to be in equilibrium, including reversibility at the BL (biotic ligand) site, and that a crucial organ be identified, which allows the direct interface of an organism with the external environment e.g., plant roots. It is not absolutely compulsory for the BLM 'site of action' to be external or internal to a site, although if a site is internal, there cannot be equilibrium with the external medium.

Metal ions bound to complexing agents such as cysteine and citrate are exchanged at the cell surfaces, resulting in the release of free M^{z+} ions. This suggests that N and S rich phytochelatins and metallothioniens simply act as 'couriers' that pick up metals from soil surfaces and deliver them to the ligand on root surfaces. Soft metals bound to O ligands can dissociate, form the free ion, rapidly exchange onto cell surface BL site, and equilibrate with ease. When strongly bound to S atoms soft metal exchange proceeds by a strictly associative mechanism. The exchange rates are faster only if a surface BL site also bears a Cys-SH group and if neither the thiol-metal complex nor the surface BL site is sterically hindered. Failure to meet either of these conditions can result in a non-equilibrium situation. However, this model also suggests that an increased presence of complexing agents such as L-cysteine can also result in a higher accumulation of metals by plants. Several authors[253] have used EDTA to demonstrate this increased uptake, however, this approach is flawed for two reasons – it is not a naturally produced complexing agent, it is non-biodegradable and it destroys the agglomeration of cells in tissues. Therefore, EDTA application would have a limited application for the phytoremediation of metal contaminated soils.

The FIAM was developed to explain the 'the universal importance of free metal ion activities in determining the uptake, nutrition and toxicity of cationic trace metals'[54]. It has been used to explain key role of the activity of the free metal ion as a regulator of interactions (i.e. uptake or toxicity) between metals (M) and unicellular organisms[254]. The model is based on the assumption that the metal ions bind to the surface of cells in the form of M^{z+} rather than in the hydrated form $M^{z+}.nH_2O$. The model states that the free metal ion (M) is in rapid equilibrium with the cell surface binding sites and that the lowest activity range limits growth, in the intermediate range an optimum growth is obtained; and at higher concentrations toxic effects (reduction in growth) are observed. The FIAM cannot be used be used to explain the uptake of colloidal metals or metals complexed to strong organic ligands, as they are not able react to directly with the cell surface binding sites. The binding of metal-ligand complexes to cell surfaces can be explained using the biotic ligand model (BLM).

10.4 Conclusions

The data obtained in this chapter show that (i) phytoextraction of contaminated soils is a viable remedial option if there is an availability of metal ions in soil solutions in the M^{z+} form (in the free ion form); (ii) leachate from soil washing experiments can be effectively treated using *Helianthus annuus* plants in a hydroponics system; (iii) since a majority of the metal is accumulated in the roots as lead phosphates with a very low solubility product, ecological toxicity as a result of these plans being consumed by animals is limited; (iv) as the lifetime of the plants subsequent to introduction to the contaminated solutions is short and the metal accumulation rate is very high, quick crop turnover rates can be achieved.

Chapter 11 Additional Work - Column Washing Experiments

11.1 Introduction

The batch experiments described previously assumed that there was equilibrium in the soil-solution system. Although it is possible to achieve equilibrium using a small mass of soil (1g), this is rarely possible in real environments, due to the sheer heterogeneity of the soil matrices. As a result although the batch extraction data can be used to predict the conditions under which optimal metal extractions takes place, they do not provide any useful information about the kinetics of desorption in the real environments. Knowledge of kinetics is of great importance for the remediation of contaminated soils, as this allows practitioners to predict the clean-up time. Additionally, this also allows assessment of risk to controlled waters as a result of changes in soil conditions. Kedziorek and Bourg[248] have used batch extractions performed over a staggered period of time to study leaching kinetics. However, this approach is not indicative of the behaviour of chemicals in the real environment, where there are far more variables and rate limiting factors. In order to simulate the leaching of contaminants in-situ, albeit to a limited extent, other authors have used columns packed with soils. A major benefit of using column washing to study metal desorption kinetics, is that the concentration of metals in the leachates would be high enough for easy instrumental analysis, without the need to undertake complicated sample preparation procedures such as preconcentration.

In order to gain information on the interaction of Pb with soil and the kinetics and mechanisms of Pb transport in the near field environment, column washing experiments were conducted. These experiments were carried out by packing 50g of soil (2mm fraction) into a Pharmacia 76/40 chromatographic preparative column with cellulose filters (Figure 7). The columns were washed using 0.01M EDTA (pH

5±0.2) (after Kedziorek and Bourg)[255] and 0.11M (pH 2±0.3) and 1.75M (pH 5±0.5) ethanoic acid (as the column manufacturer prohibits the use of more than 10% (v/v) ethanoic acid). The data obtained from these experiments were compared with those obtained using the batch extractions. EDTA was used rather than L-cysteine and citric acid as it does not act as a substrate for microbial growth and is therefore non-biodegradable. Ethanoic acid at two concentrations was used to allow the comparison of the efficiency of the modified BCR and the customised sequential extraction processes, for the prediction of the rate of metal mobility.

11.2 Results and Analysis

Column Washing Experiments using EDTA

Column washing experiments using 0.01M EDTA solutions showed that a majority of Pb in the soil was extracted in the first three hundred minutes (Figure 24(a)). Approximately, 15% (825mg kg^{-1}) of the total lead in the soil was desorbed in the first two aliquots. The highest extraction was in the first aliquot, followed by a log-normal decline in the extraction until the thirty-fifth aliquot, after which there were no significant differences in the concentration of metal extracted into solution. A total concentration of 3500mg kg^{-1} Pb (54% of the total) was desorbed from the soil after 35 aliquots (950mL solution), while a total of 404mg kg^{-1} Pb was extracted in the remaining 35 aliquots. There were no significant differences between the pH of the influent solutions and the leachate. The area under the extraction curve was calculated and the total concentration of Pb extracted into 1775mL solution over a period of 8 hours was 4000mg kg^{-1}. This is approximately 60% of the total Pb concentration (6500mg kg^{-1}) in the soil. The extraction pattern of Zn was similar to that for Pb, which suggests that these two metals might have been in association,

(Figure 24(b)). However, the total concentration of the desorbed Zn was only 10% (20mg kg^{-1}) of the total metal in the soil.

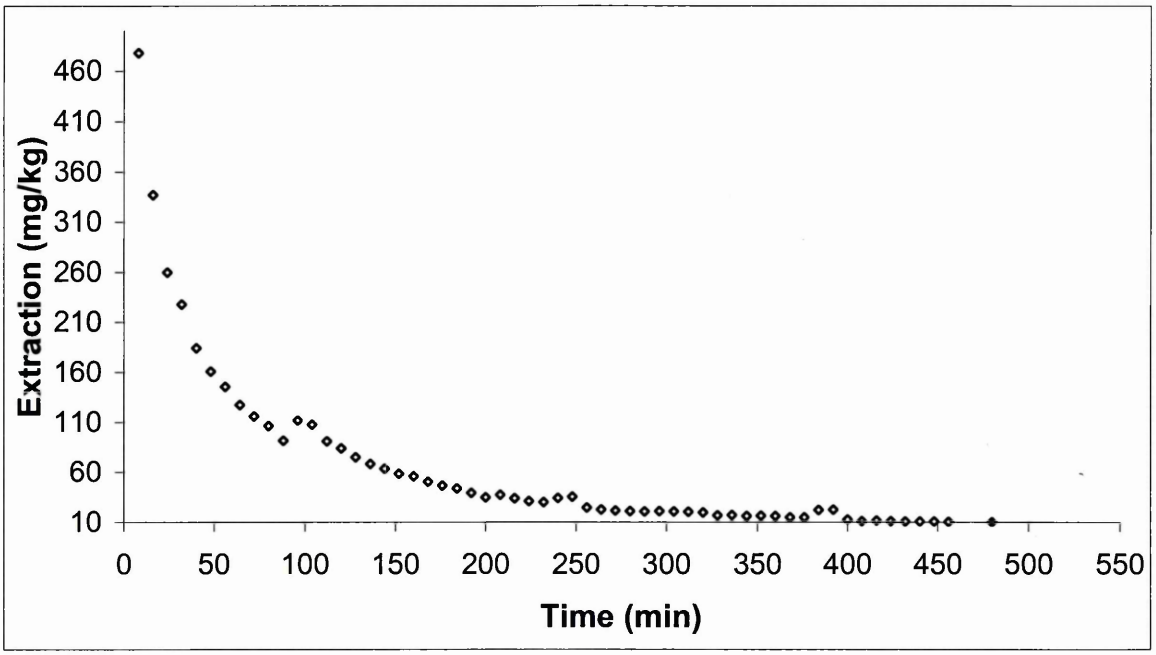

Figure 24(a): Desorption profile of lead using 0.01M EDTA (pH 5±0.5) from the soil C1.

The high extraction of Pb in the first few fractions was most likely due to the initial rapid dissolution of the first layers of PbO precipitated onto the surface of soil minerals. With a progressive decline in the concentration of the metal on the soil surfaces, the metal-soil surface binding strength would increase, resulting in decreased desorption. Another possible explanation is the formation of stagnant zones in the column due to soil inhomogeneities such as cementation of grains, or the clogging of pores by organic matter and oxides. However, the main observation from this data is that a majority of the Pb in the soil was easily desorbed, without the need for any mechanical forces.

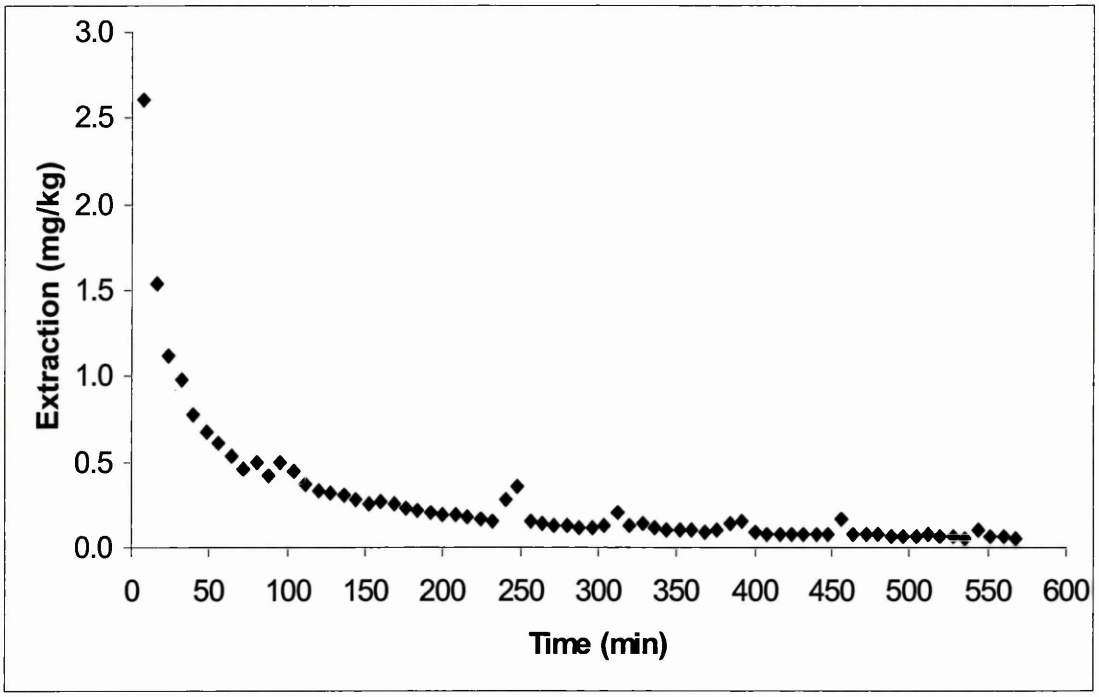

Figure 24(b): Desorption profile of zinc using 0.01M EDTA (pH 5±0.5) from the soil C1.

The highest extraction of Ca was in the first two aliquots followed by an exponential decrease (Figure 24(c)). Approximately 3% of the total aqua-regia soluble Ca was extracted in these aliquots. The total concentration of Ca extracted from the soil was 1820mg kg^{-1}, which is approximately 50% of the total aqua-regia soluble and 8% of the total Ca in the soil. The most important observation from this data is the relatively slow and limited desorption of Ca compared with that for Pb. This has two implications: (i) the Ca extracted into solution was associated with the Pb minerals or (ii) Pb exists as an independent mineral phase and the Ca in solution is a result of calcite dissolution. It is noteworthy that historical information suggests that it was common practice in the medieval times to add Ca to lead smelts. Evidence for this comes from XRD analysis, which showed Ca substitution in Pb minerals in various stoichiometric ratios.

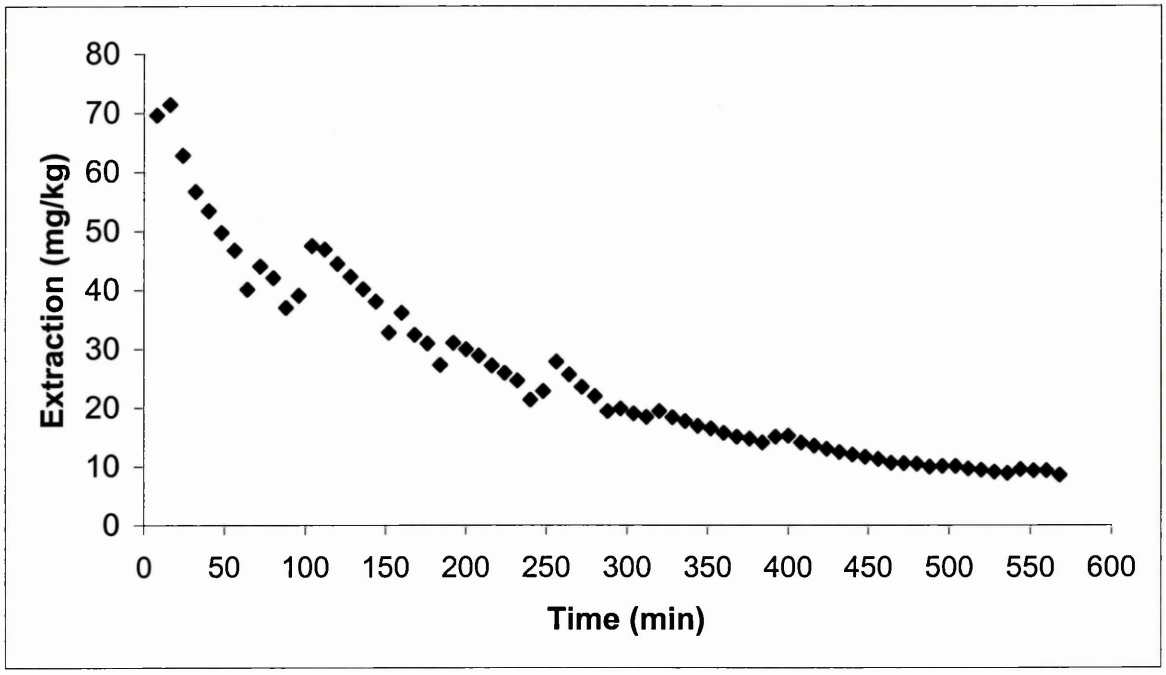

Figure 24(c): Desorption profile of calcium using 0.01M EDTA (pH 5±0.5) from the soil C1.

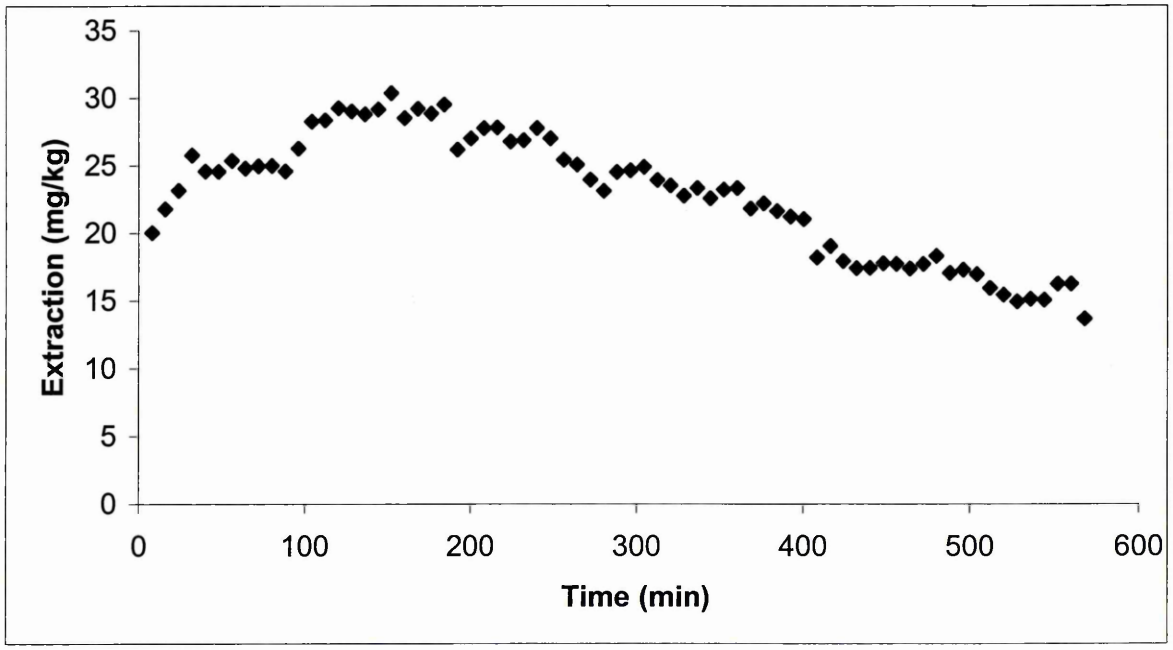

Figure 24(d): Desorption profile of iron using 0.01M EDTA from the soil C1.

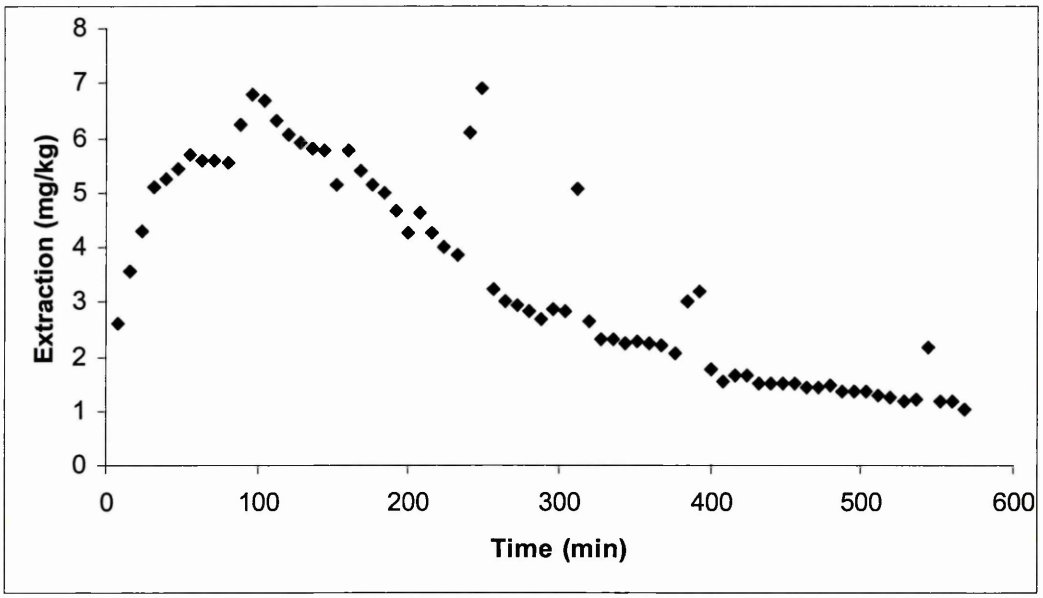

Figure 24(e): Desorption profile of manganese using 0.01M EDTA (pH 5±0.5) from the soil C1.

Approximately, 20mg kg^{-1} (0.0004% of the total) of Fe was extracted in the first aliquot, followed by a gradual increase until the 19th aliquot (152min; 485mL), where 30mg kg^{-1} of Fe was extracted (Figure 24(d)). This was followed by a gradual decline, without the system reaching equilibrium at any point. Approximately, 0.006% (2.5mg kg^{-1}) of the total Mn in the soil was extracted in the first aliquot, followed by a linear increase in concentration until the 12th aliquot (6.8mg kg^{-1}; 96mins; 300mL) (Figure 24(e)). This was followed by an exponential decrease in concentration to approximately 1mg kg^{-1} in the final (71st) aliquot. The lack of overlap of the extraction pattern of Pb with those of Fe, Mn and Ca coupled with the low desorption suggests that the Pb might indeed have existed as an independent mineral phase, most likely as PbO, without significant associations with Fe/Mn or Ca minerals.

Column Washing Experiments using Ethanoic Acid

The highest extraction of Pb using both solutions was in the first aliquot followed by a progressive decline in the desorption. The extractions in the first aliquot using 1.75M and 0.11M solutions were 268 and 107mg kg^{-1} respectively. The extractions did not reach equilibrium at any point in the extraction curves. A total of 4090 and 1640mg kg^{-1} of Pb was extracted from the columns using 1.75M and 0.11M ethanoic acid respectively (Figure 25(a)). The similarity in the shape of the extraction curves suggests that the source of Pb extracted in both sets of solutions was similar.

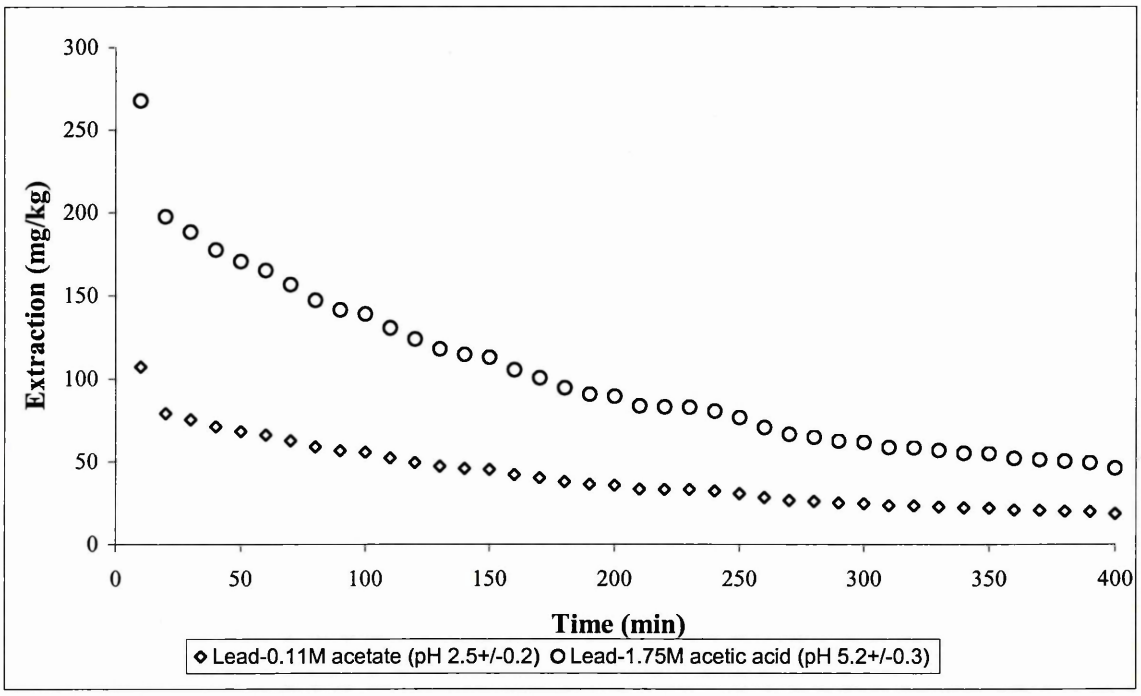

Figure 25(a): Desorption pattern of metals from the column using 1.75M and 0.11M ethanoic acid solutions.

The extraction pattern for Fe was different to other metals, wherein there was an initial short decline in desorption between the first and the second samples using both the solutions (Figure 25(b)). This was followed by a gradual increment in the concentration of the element in each aliquot, until the 37th aliquot (380mins; 925mL), at which point the system reached equilibrium. The total extraction of Fe from the

columns using the 1.75M and 0.11M ethanoic acid solutions was 331 and 132mg kg^{-1} respectively.

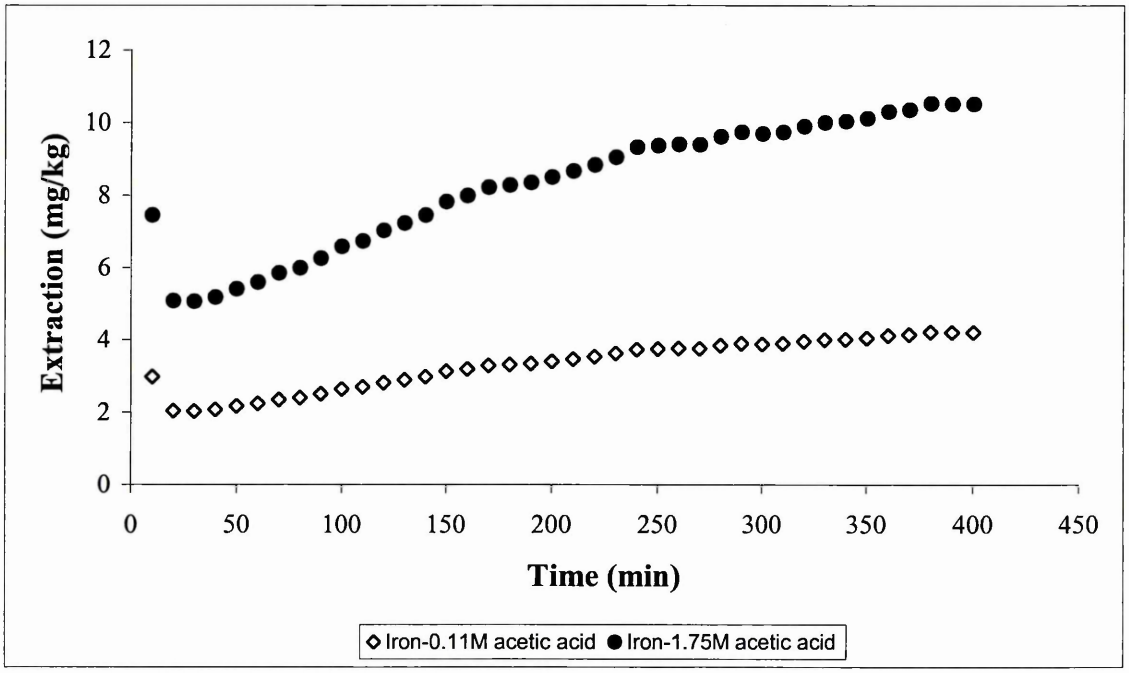

Figure 25(b): Desorption pattern of Fe from the columns using 0.11M and 1.75M ethanoic acid solutions.

The extraction patterns of calcium were different to those for Pb using both the ethanoic acid solution (Figure 25(c)). The highest extraction of Ca was in first two aliquots using both the solutions. Approximately 50% (1750mg kg^{-1}) and 20% (650mg kg^{-1}) of the total Ca in the soil were extracted using 1.75M and 0.11M ethanoic acid solutions respectively. Approximately 1800mg kg^{-1} of Ca was extracted using 1.75M ethanoic acid, whilst approximately 700mg kg^{-1} of Ca was extracted using 0.11M ethanoic acid. The extractions reached equilibrium after 160mins, at which point 34 and 12mg kg^{-1} Ca was extracted into 1.75 and 0.11M ethanoic acid solutions respectively. The total extraction of Ca using the 0.11M and 1.75M solutions was 1430 (41%) and 3570 (100%)mg kg^{-1} respectively. The extraction

pattern for Mn was similar to those for Ca. The highest extraction of Mn was in the first aliquots using both solutions. The extractions using both solutions reached equilibrium after 300mins (750mL solution volume), at which the extractions were 1.1 and 0.4mg kg^{-1} respectively. The total extraction of Ca using the 1.75M and 0.11M ethanoic acid solutions was 105 and 42mg kg^{-1} respectively.

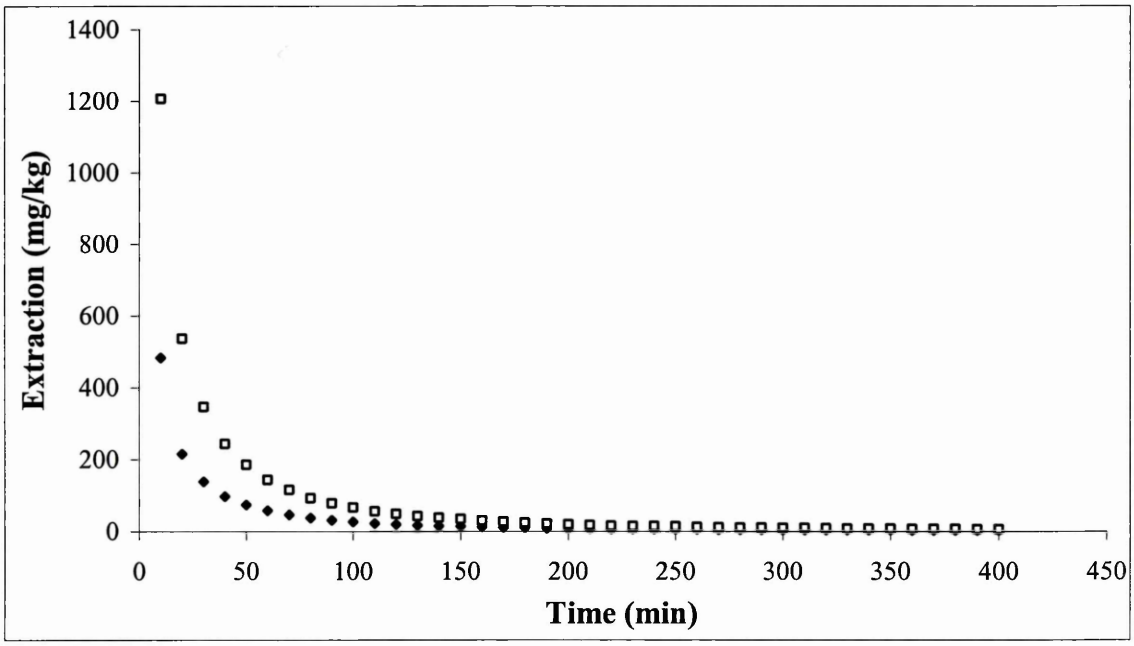

Figure 25(c): Desorption pattern of Ca from the columns using 0.11M and 1.75M ethanoic acid solutions.

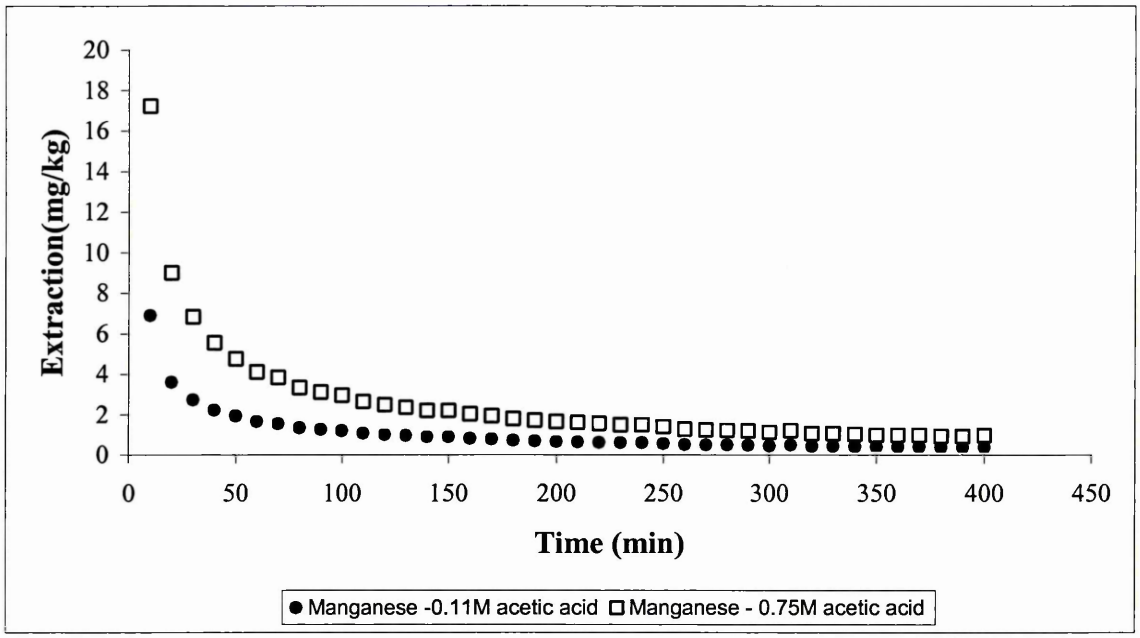

Figure 25(d): Desorption pattern of Mn from the columns using 0.11M and 1.75M ethanoic acid solutions.

The differences in the extraction patterns of Pb, Ca and Fe are probably due to the phenomenon of 'hysteresis'. Hysteresis is caused when the rate at which a solvent front moves across a mineral surface is faster than the dissolution rate of minerals i.e., there is disequilibrium. Slower solution flow rates would have probably produced a more normally distributed data i.e, equilibrium distribution. The first ethanoic acid wave front that came in contact with the soil surface must have dissolved the weakly bound metal ions and the metal compounds precipitated on mineral surfaces, as a result of which the very high desorption rates observed in the first few aliquots followed by a sharp decrease. The lack of overlap between the extraction patterns of Pb with those of other metals also suggests that Pb might not have been associated with these metal fractions in the soil.

11.3 Conclusions

The following conclusions can be drawn from the data obtained in this chapter:

(i) The desorption rate of metals from soil surfaces is not dependent on the contact time, rather it depends on their speciation in soils.

(ii) Metals such as lead in heavily contaminated soils can be easily leached out using weak complexing agents in a short time frame.

(iii) As the dissolution of structural metals such as Fe is very low, it can be safely assumed that the basic mineral composition of the soils does not alter under the influence of the complexing agents.

(iv) The concentrations of Pb extracted by the three reagents using the column washing experiments were approximately equal to those extracted in the batch mode.

Chapter 12 Additional Work - Gold Uptake Studies

12.1 Introduction

Nanoparticles of noble metals such as those of gold, silver and platinum are extremely useful for the miniaturisation of electronic devices, gas sensors, drug delivery systems, protein and DNA markers, catalysis and a host of other applications[256]. One of the key challenges in the field of nanoparticle research is the spontaneous self-assembly of nanoparticles into pre-determined ordered and complex structures. The fundamental requirements of this self-assemblage are uniform, stable building blocks. A range of ligands (e.g., thiols) and capping (C_6-C_{20} surfactants) agents are currently being used for the preparation of stabilised Au nanoparticles by chemical methods mainly from Au(I) and Au(III) compounds[257].

A new and exciting field of research is nanoparticle formation in living organisms because they possess stable building blocks in the form of various metal binding sites and other complexing agents in form of enzymes and co-factors[258]. Gardea-Torresday[259] reported the formation of pure gold nanoparticles inside the biomass of live alfalfa biomass. This is potentially an effective and cheap method of nanoparticle synthesis. During the hydroponics studies conducted to study the uptake of Pb by plants, a few plants surplus to requirements were left growing in the original nutrient solutions. The author in collaboration with his PhD supervisor, decided to perform a few trials to study the biomineralisation of gold. We report for the first time and present data obtained from studies conducted to study nanoparticle formation on the surface of roots.

Two sets of experiments were performed – (i) a preliminary experiment using 50mg L^{-1} of Au^{3+}; (ii) a second set of experiments using three solutions of concentrations –

50, and 150mg L^{-1} Au^{3+}. The colour of the potassium tetrachloroaurate solution was golden yellow, which gradually turned light brown when stored in a volumetric flask for several days. There was a noticeable blue colouration of the solution when the plants were inserted into the solution, which is a sign of possible colloid formation. Preliminary visual analysis at the end of the 7 days showed a visible brown colouration of the plant roots growing in the spiked nutrient solutions as opposed to the control plant roots that remained milky white. The pH of the solutions was checked to ascertain whether pH changes had any role to play in the brown colouration. The pH of the solutions was observed to be at 5.8 ± 0.2, which was the initial solution pH.

The optimum digestion time for the samples in nitric acid at 80°C on a hotplate was observed to be approximately 1h. The leaves and the stem samples digested without any significant problems. But the root samples on the other hand proved to be significantly harder to digest because all the samples left behind a dirty brown residue at the bottom of the containers. There was no residue in the containers that were used for the digestion of the roots grown in the control solutions. It was inferred that this might be a sign of possible formation of insoluble metallic gold either on the surface or inside the tissues of plants.

Total metal analysis on the plant biomass from the first set of experiments showed that the roots, shoot and leaves had accumulated 12300 ± 200mg kg^{-1}, 150±22 mg kg^{-1} and 100±12 mg kg^{-1} of Au respectively. No significant mean accumulation of Au was observed in the biomass of the control plants. Similar mean accumulation patterns were observed in the second set of experiments, wherein the concentration of gold in

the leaves, stems and the roots of plants growing in the 150 mg L^{-1} solution was 72.6, 133 and 13700 mg kg^{-1} respectively (Tables 36a-c). Gold unlike lead does not seem to affect the key physiological processes in the plants. The presence of gold in solution seems to have increased the uptake of key metals such as Mg, K, Na, Zn and Ca into the leaves, stems and the roots of the plants.

Solution	Control	50mg L^{-1}	150mg L^{-1}
Fe	125 ± 23.1	98 ± 27	118±22
Cu	10.6 ± 2.3	28±2	25
Zn	133 ± 20	114±16	151±9
Ca	27800 ± 882	27900±782	28600±674
Mg	4880 ± 441	5920±97	5650±35
K	15800 ± 1238	37800±766	35600±979
Na	145 ± 38	212±57	193±7
Au	14.2 ± 5.2	55±8	73±4

Table 36(a) – Total metal accumulation (mg kg^{-1}) in the leaves of plants growing in the Au spiked solutions.

Solution	Control	50mg L^{-1}	150mg L^{-1}
Fe	47±7	32±10	35±11
Cu	34±5	12±3	15±4
Zn	65±5	48±4	53±7
Ca	15600±657	16200±1020	13900±1225
Mg	6700±708	5200±878	4450±575
K	58100±779	65000±868	68400±858
Na	732±97	1160±87	1190±88
Au	11±4	60±7	132±8

Table 36(b) – Total metal accumulation (mg kg^{-1}) in the stems of plants growing in the Au spiked solutions.

Solution	Control	50mg L^{-1}	150mg L^{-1}
Fe	1375±57	1570±68	1500±98
Cu	1755±68	57±9	100±15
Zn	310±15	127±16	150±16
Ca	10500±686	14500±466	15700±757
Mg	4000±657	3190±325	2300±335
K	38100±657	28600±979	26800±468
Na	1410±46	2710±76	2810±53
Au	27±3	5890±75	13600±353

Table 36(c) – Total metal accumulation (mg kg^{-1}) in the roots of plants growing in the Au spiked solutions.

XRF analysis of ground root samples from the first set of solutions showed the percentage by mass of Au in the roots was 1.00 ± 0.04%, confirming the data obtained from total metal analysis using the ICP-AES (Table 37). The mean accumulation of Au in roots from the second set of solutions (150mg L^{-1} solutions) was significantly higher i.e. 20% of the total mass. This value is several times higher than that observed from the multielemental wet chemical analysis. This suggests that most of the gold from the roots might have been lost during the digestion process as a precipitate. This trend was repeated when the XRF values for Au in leaves and stems were compared with that obtained from the multielemental wet chemical analysis. This is an indication of the pure metal deposition on the surface of the roots rather than mineral formation because there were no significant discrepancies in the mean Au accumulation data.

Metal	Roots 1	Leaves	Stem	Roots 2
K	3.5	11.54	13.22	1.70
Ca	1.6	12.68	11.21	4.04
P	1.28	1.53	2.29	1.78
Au	1.00	0.04	1.91	20.01
Cl	0.166	2.31	0.29	0.35
Sx	0.955	0.97	0.47	0.45
Mg	0.291	0.42	0.31	0.07
Zn	0.02	0.05	0.02	0.02
Fe	0.251	0.11	0.11	1.13

Table 37– XRF analysis of biomass of plants grown in Au spiked solutions, where roots 1 are samples from the first set of experiments whilst root 2 are samples from the second set of experiments.

The oxidation state of gold in the roots was confirmed by powder XRD pattern (Figure 26) that showed relatively broad reflections for the (111), (200), (220), and (311) planes of metallic gold in a face-centered cubic lattice. The average particle

size of the metal nuclei **(6nm)** was calculated using the Scherrer equation, on the half width of the intense (111) reflection, which suggests these are *nanoparticles*. The images obtained from the STEM analysis showed that polycrystalline aggregates of Au *nanoparticles* were embedded on the root surface (Figure 27). This finding is supported by the XRD data. The average two-dimensional diameter of these polycrystalline *nanoaggregates* was 82-97 nm. Nanocrystals can be loosely defined as crystals with dimensions up to 100nm; above this size, they are more commonly termed microcrystals[257].

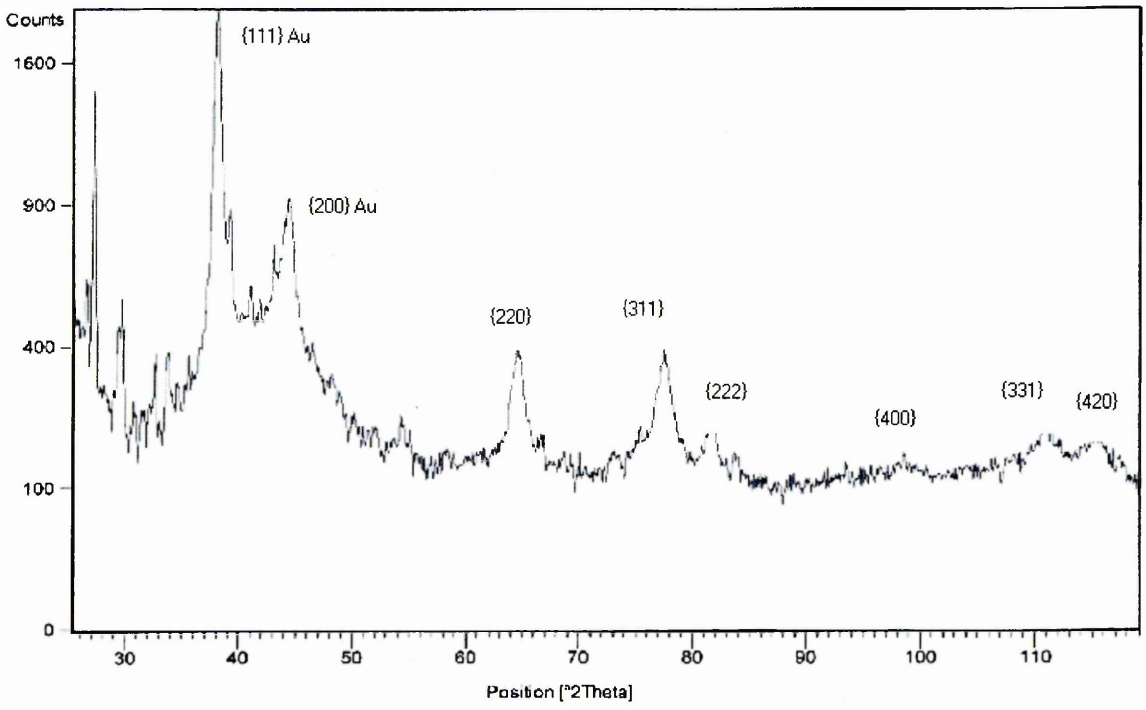

Figure 26 - XRD pattern of Au nanoparticles on the surface of *H. annuus* roots

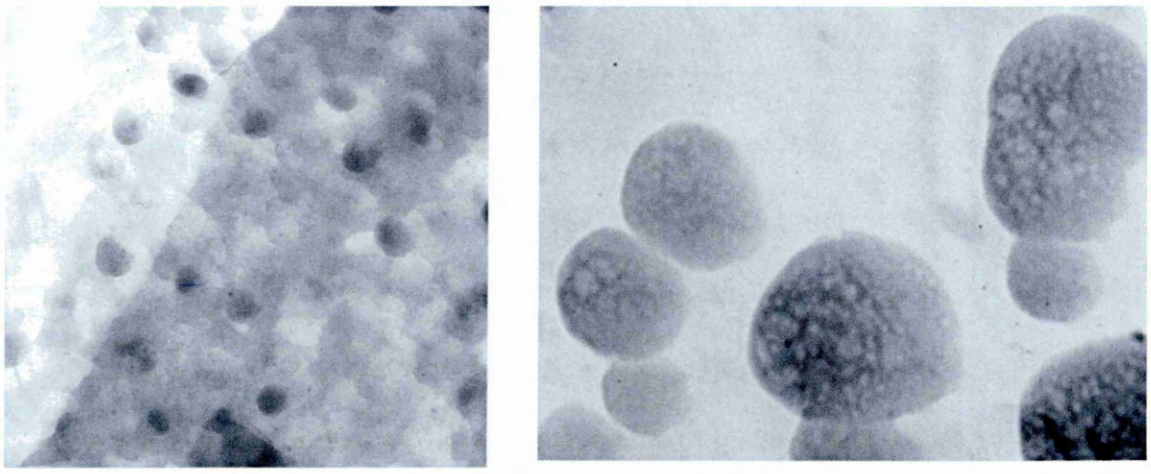

Figure 27 – TEM images 36k and 88K magnifications. TEM images of Au nanoaggregates in-situ on the *H. annuus* root surface.

The presence of Au nanoparticles was further confirmed using ESEM/EDX analysis of the ground root samples (Figs. 28 and 29). Sharp L and M shell Au peaks were observed in the EDX spectrum for the ground spiked root samples, as opposed to the EDX spectrum for control root samples that had no characteristic Au peaks. It is important to note the presence of sharp phosphorus peaks in the spectra of both the control and the spiked samples suggesting a possible role for phosphates in either nanocrystallisation of Au atoms or stabilisation of nanoparticles by phosphate ligand capping. Indeed, EDX spot mapping of the spiked roots showed excellent overlap between the distribution of Au, phosphorus and oxygen. ESEM images showed the average nanoaggregate size to be in the 80-100nm ranges. The distribution of the nanoaggregates on the root matrix was observed to be relatively homogenous although it is difficult to get an estimate of the three-dimensional distribution and size of the nanoparticles.

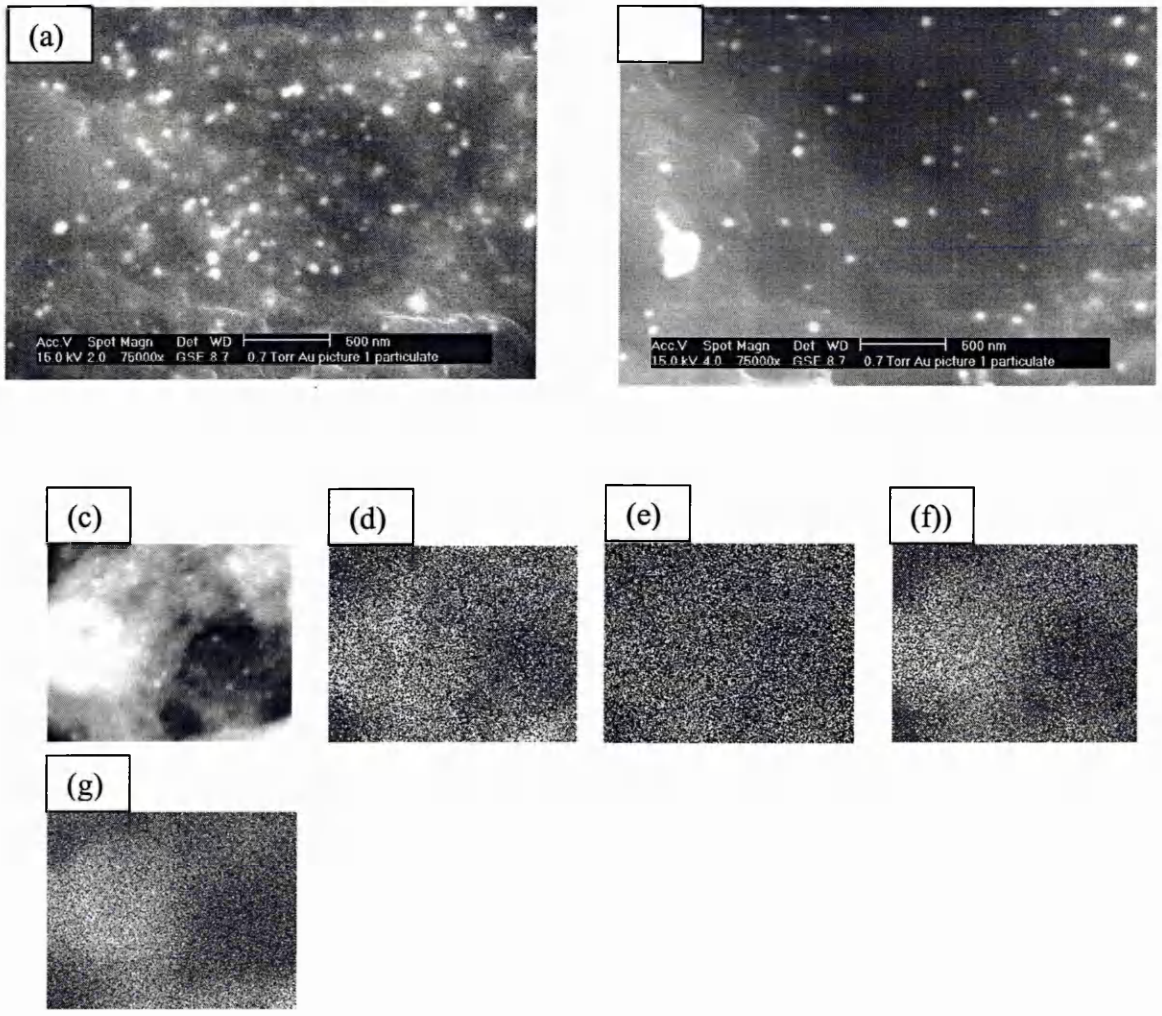

Figure 28 – EDX elemental mapping for a section of the *H. annuus* roots. (a) 500nm photo (b) 500nm photo (c) SE image (d) gold (e) sulfur (f) phosphorus (g) oxygen

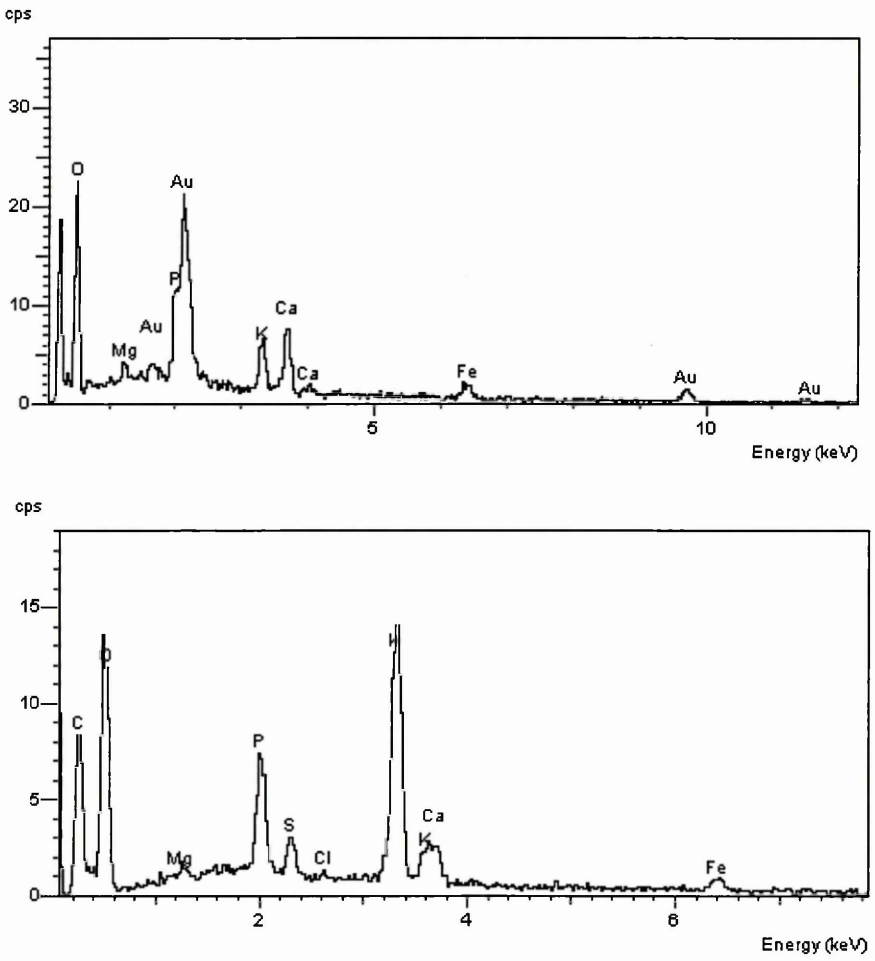

Figure 29– EDX spectrum of sample and control sample

In order to get an estimate of the three-dimensional distribution of the nanoaggregates atomic force microscope (AFM) analysis was performed. Ground root samples were suspended in acetone and sonicated for 30mins and the matrix allowed to sediment. This was done to dislodge the nanoaggregates from the root surface and suspend them into solution. The supernatant was separated and a few ml pipetted onto a clean, sterile glass slide followed by surface analysis using a DI Nanoscope IIIa AFM (Atomic Force Microscope) running in the tapping mode. The images obtained from the AFM showed capsule like structures stacked on top of each other (Figure 30).

This stacking is probably an optical illusion or most likely to have happened during deposition of the supernatant on to glass slide and subsequent drying. The average particle radius was observed to be 9.14 nm and the average height was 77.1nm. This data conclusively proves that the gold particles are in the nanoscale and are indeed nanoparticles.

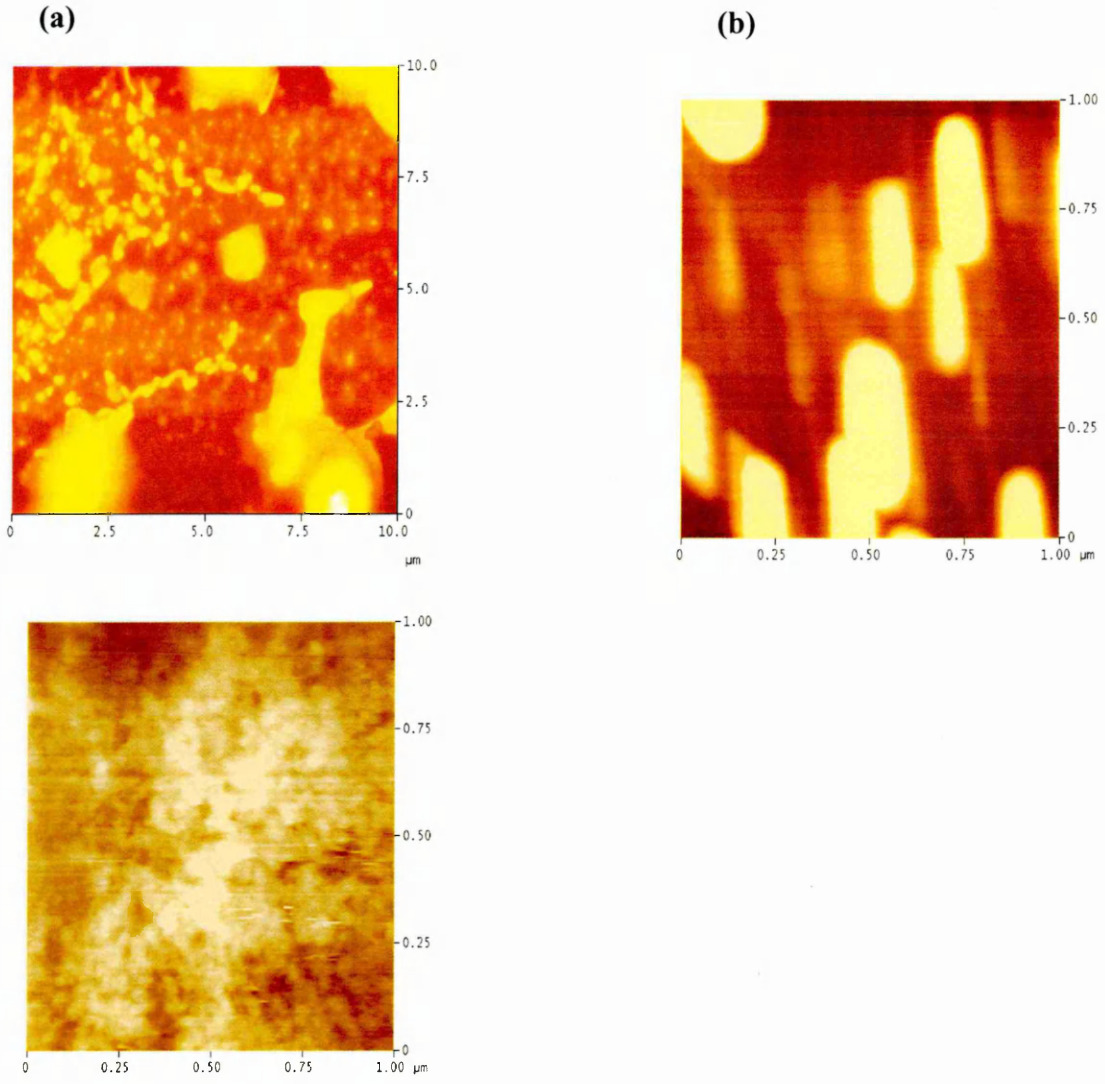

Figure 30 – 2-d AFM image of gold nanoparticles – (a)10 µm (b)1µm (c)control glass slide coated with acetone.

12.2 Discussion and Conclusion

The data presented in this chapter conclusively proves for the first time that Au forms nanoparticles on the surface of roots. A possible explanation for this can be obtained using the BLM model, which suggests that metals cannot form complexes with biotic ligands if they are in colloidal forms in solution. However, in order for the metal to nucleate and nanocrystallise on the surface of the roots, there must have been some kind of stabilising capping agents. These could have been the either the surface –SH groups or the surface metal ATPase binders. The nature of these ligands (possibly using extended X-ray absorption fine structure (EXAFS) has to be understood to get a clearer picture of the mechanism of nanoparticle formation on the surface of roots.

Chapter 13 General Discussion

As discussed previously, soils are composed of different types of minerals and organic matter, which present a variety of surfaces for metal sorption. These different surfaces display particular reactivities and consequently desorption of metals generally depends on their fractionation and speciation in soils. While speciation refers to the chemical form of a metal ion, fractionation can be defined as the distribution of metals among the various components of a soil matrix, irrespective of the valence state of the metals[26]. An understanding of the speciation and the fractionation of metals in soils is essential for the design of effective risk assessment and remediation schemes. Speciation of metals in soils is usually studied using mineralogical techniques such as XRD, XRF, ESEM/EDX, FT-IR, and XAFS etc. Fractionation of metals within a soil matrix is often studied using sequential extraction procedures such as the BCR developed methods.

The principal aim of this thesis was to study the applicability of the modified BCR sequential extraction procedure as a risk assessment tool and as a tool to predict the concentration of contaminant metals that can be extracted from contaminated soils using remediation techniques such as soil washing and phytoremediation. Soil samples were collected from a former lead smelting site in the outskirts of Sheffield with a known history of lead contamination. The mineralogy of these soil samples was analysed using XRD, XRF, ESEM/EDX and FT-IR.

Data from XRF analysis and pseudo-total soil digestions showed that the concentration of lead in the soil samples was several times higher than the CLEA soil guideline value (~750mg kg^{-1}), while those of all the other contaminant metals were

below the specified thresholds. Fractionation experiments using the modified BCR sequential extraction procedure showed that a majority of the lead in all three soil samples was in a reducible form. Data obtained using X-ray diffraction showed that a majority of the crystalline Pb in the soil was in the form of carbonates, oxides and sulphates. These Pb species would have been mainly associated with the Fe oxides in the soil as suggested by ESEM/EDX imaging and mapping (Figure 10).

XRD analysis was performed on the solid residues from each step of the modified BCR sequential procedure to study changes in the speciation of metals in the soils during the extractions, as some authors[260, 261] have reported that there is redistribution of metals in soils during the various extraction stages. Data from these studies showed that all the goethite (FeOOH) in the untreated soil sample C1 had been converted to hematite, which is a much more thermodynamically stable form of iron oxide (Fe_2O_3) (see Figure 11 and Table 14). However, this is unlikely to happen under the mildly acidic conditions in Step 1 as transformation of goethite to hematite generally occurs at temperatures of 600-900°C[262]. There could be two possible explanations for the presence of hematite in residue 1: (a) the result was an artefact of incorrect peak assignment ; (2) there was limited transformation of goethite to hematite during drying of the residues after the completion of step 1.

There was also a complete absence of kaolinite peaks in the spectrum for the residue from step 1, which could have been due to their 'masking' by hematite and quartz peaks in the XRD spectra. However, the kaolinite peaks reappeared in the spectrum for the residue from step 2, which provided limited evidence for the quartz masking inference. A number of peaks for albite were noticed in the spectra for the residues

from all the steps of the process. Albite ($NaAlSi_3O_8$) is a degradation product of kaolinite[13], the presence of which in the residue from step 1 is conceivable, given the progressively harsher nature of the reagents used in the extraction process[263].

As far as the changes in the speciation of Pb in the residues from each of the steps is concerned, XRD analysis failed to provide any conclusive information about the nature of the transformations of Pb compounds in the soil, which would have caused the release of Pb ions into solution. There was a complete absence of all Pb peaks apart from those of insoluble lead phosphates in the XRD spectra for the residue from step 1. There might be three reasons for this: (a) the masking of Pb peaks by stronger peaks of more abundant minerals; (b) a majority of soluble Pb (during steps 1 & 2) could have been in amorphous forms; (c) the concentration of Pb compounds in the samples could have been below the method detection limits of the XRD. The only significant Pb peaks in the XRD spectra for the residues from step 2 & 3 were those of calcium lead silicate and lead oxide carbonate, both of which would have been constituents of Pb slag[163].

A lack of quartz peaks subtraction and comparison with reference spectral data for standard materials for compounds[265] such as $PbCO_3$, PbO and $PbSO_4$ from the XRD spectra for the residues might have contributed to the limited usefulness of the data presented in Table 14[264]. This suggests that XRD is not an adequately sensitive technique that can be used to detect changes in oxidation state of metal ions present in soils at relatively low concentrations or if the compounds under study are present in non-crystalline forms. Several authors[265, 266] have studied changes in the speciation and mineralogy of soils during fractionation experiments using techniques such as X-

ray absorption fine spectroscopy (XAFS). Calamano et al.,[267] used XAFS to study the residues from each step of a sequential extraction procedure and observed serious changes in the speciation of Pb. These changes occurred due to the re-adsorption of Pb ions to soil minerals and the precipitation of Pb species with anions from the extractants. Knowledge of these kinds of processes is critical as sorption and desorption, physicochemical interactions between metal and minerals at the mineral-water interfaces are processes controlling the migration of toxic contaminants in soils[268].

Batch experiments using pH adjusted deionised water show that under normal pH conditions (conditions that are not phytotoxic) all the metals in the soils were virtually immobile. However, as shown in Table 12 a large fraction of the Pb in the soil was extracted in the pH ranges 2-3 and 8-10 respectively. The dissolution of Pb at both of these pH ranges raised doubts about the validity of the fractionation information obtained using the BCR procedure, as goethite (the major crystalline Fe mineral in the soil) should[13] only release metals in the pH range 8-10, because it's PZC is approximately 9.2. The release of significant concentrations of Pb in the low pH range is possibly due to the displacement of M^{2+} ions from mineral surfaces by ion exchange in the presence of an excess of H_3O^+ in the solutions[269]. The release of Pb ions in the pH range 9-12 was possibly due to the collapse of the platelet structure of kaolinite, resulting in the release of sorbed ions[268]. It is normally expected that Pb ions in solutions would have precipitated as hydroxides in this pH range, which is clearly not the case in this study. This lack of precipitation was most likely due to the presence of colloidal 'sinks' in solution such as Fe/Mn oxides and colloidal organic matter at high pH[13]. Field and laboratory experiments conducted by Bunn et al.,[270]

showed that the total mass of colloid release from soils increased with increasing pH and metal ions would have been bound to the surfaces of these colloids electrostatically.

Batch extraction experiments were conducted on soil sample C1 using magnesium and calcium chloride solutions at pH 5, to assess the fraction of ion-exchangeable metals in the soil sample C1 (see Tables 18 –20). The data showed that 1M $MgCl_2$ solutions were the most effective of the three reagents for the extraction of Zn, Ca and Pb from the soil surfaces, while 0.11M ethanoic acid solutions were most effective at extracting Mn, Fe, and Al. Metal cations bound to the surfaces of calcite and kaolinites are generally released by cationic exchange with Ca and Mg ions[13]. Soil-solution partition coefficients calculations show that the K_d values obtained for the batch extractions using $CaCl_2$ and 0.11M CH_3COOH were in the same range (448 and 505L kg^{-1} respectively), which suggests that the BCR procedure might indeed have been effective in estimating the concentration of ion-exchangeable fraction of Pb in the soils. Similarly, the concentrations of Ca extracted from the soil using $MgCl_2$ and ethanoic acid were in the same range. The K_d values for all the other metals extracted into solution using the three reagents did not show similar comparisons. Furthermore, the relatively high extractions of Pb and Zn into $MgCl_2$ solution compared with those into $CaCl_2$ solutions was probably due to the rapid saturation of calcite surfaces as a result of an excess of calcium ions in the calcium chloride solution, which could have caused the release of these metal ions. This suggests that the concentration of Pb and Zn available in ion-exchangeable forms might be greater than that predicted by the BCR procedure.

In order to test this inference, batch extraction experiments were conducted using ethanoic acid at varying pH, molarity and volume (see Table 21). The data showed that approximately 80% of the total Pb in the soil was extractable using 3.5M ethanoic acid at pH 5. This provided further evidence for the observation that a majority of the Pb in the soil samples would have existed in weak acid soluble, ion-exchangeable and potentially bioavailable forms rather than reducible forms. As suggested by the data from the XRD analysis, a majority of this Pb could have been in the form of Pb oxides or sulphates, both of which are easily soluble in dilute ethanoic acid[271] and might indeed have existed as independent phases. XRF analysis of the residue from the batch extractions did not show any significant changes in the concentration of sulfur in the soil, which effectively eliminated the possibility of the presence of lead sulfates in the soil.

The modified BCR sequential extraction process was changed to accommodate the observations and inferences described above. The molarity and pH of ethanoic acid used in the first step of the modified BCR procedure were changed to 3.5M and 5 respectively and extractions were performed on the low (B1), medium (C2) and heavily (C1) contaminated soil samples, with the remainder of the extraction procedure remaining unchanged. The data obtained from all three samples showed that a majority of the Pb was extracted in the first step (see Figs. 31 a-c). However, soil-solution partition coefficient calculations showed that the concentration of metals such as Zn, Mg, Mn and Cu extracted into solution during the first step of the customised procedure was lower than that extracted in the same step of the modified BCR procedure and were principally found to be associated with the Fe/Mn oxides, organic matter and silicates.

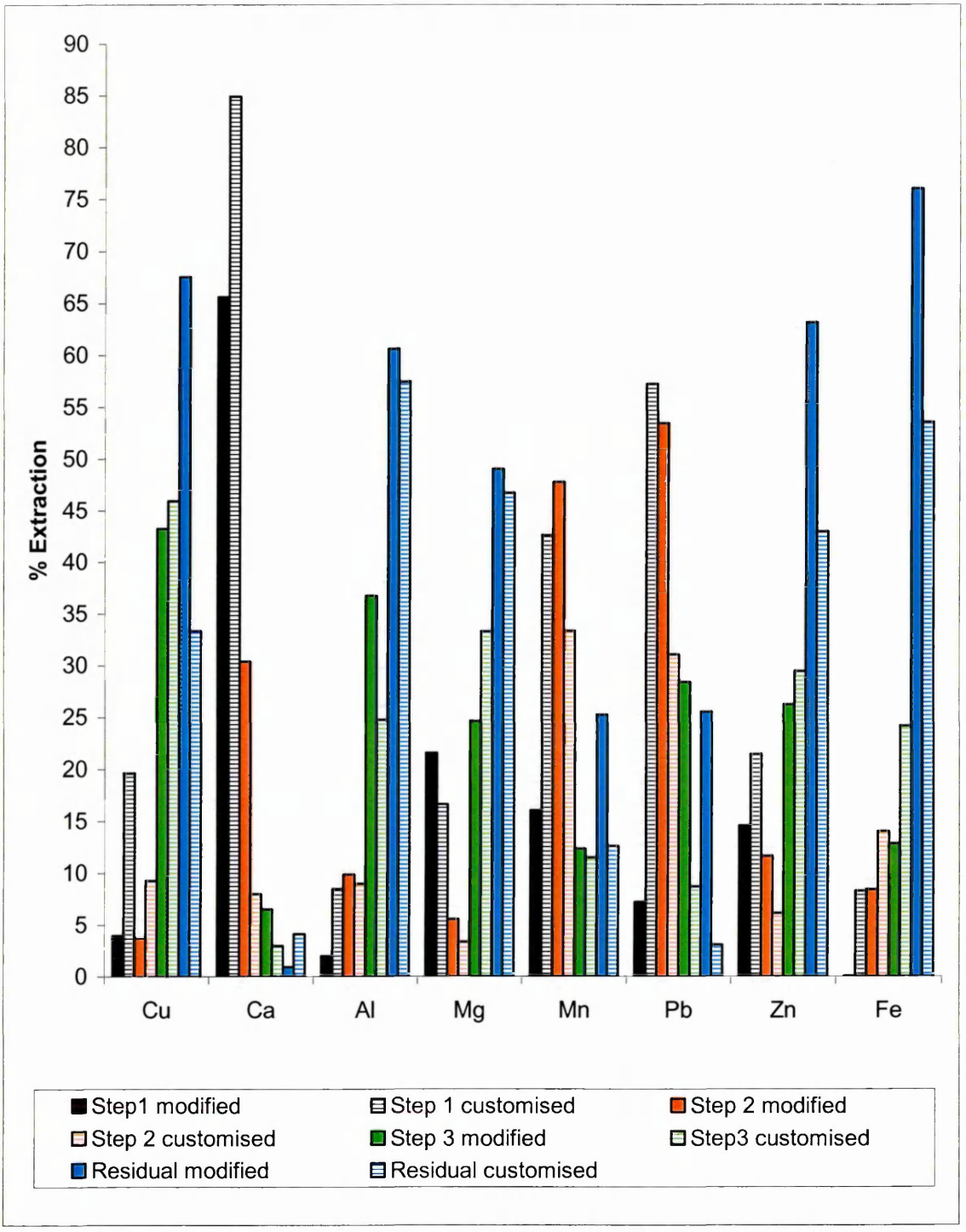

Figure 31 (a): A comparison of metal extractions from the soil sample C1 using the modified BCR procedure and the customised sequential extraction process.

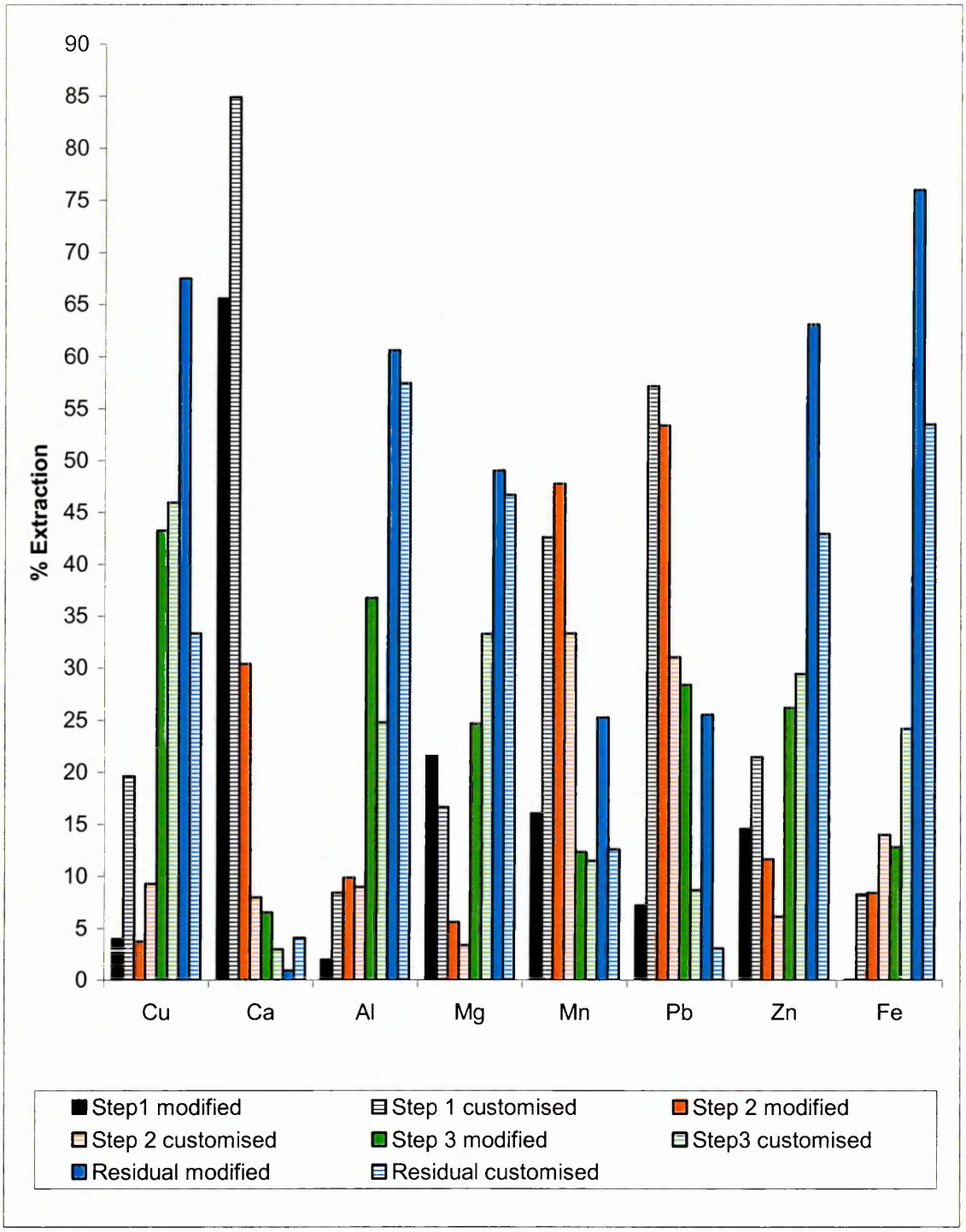

Figure 31 (b): A comparison of metal extractions from the soil sample C2 using the modified BCR procedure and the customised sequential extraction process.

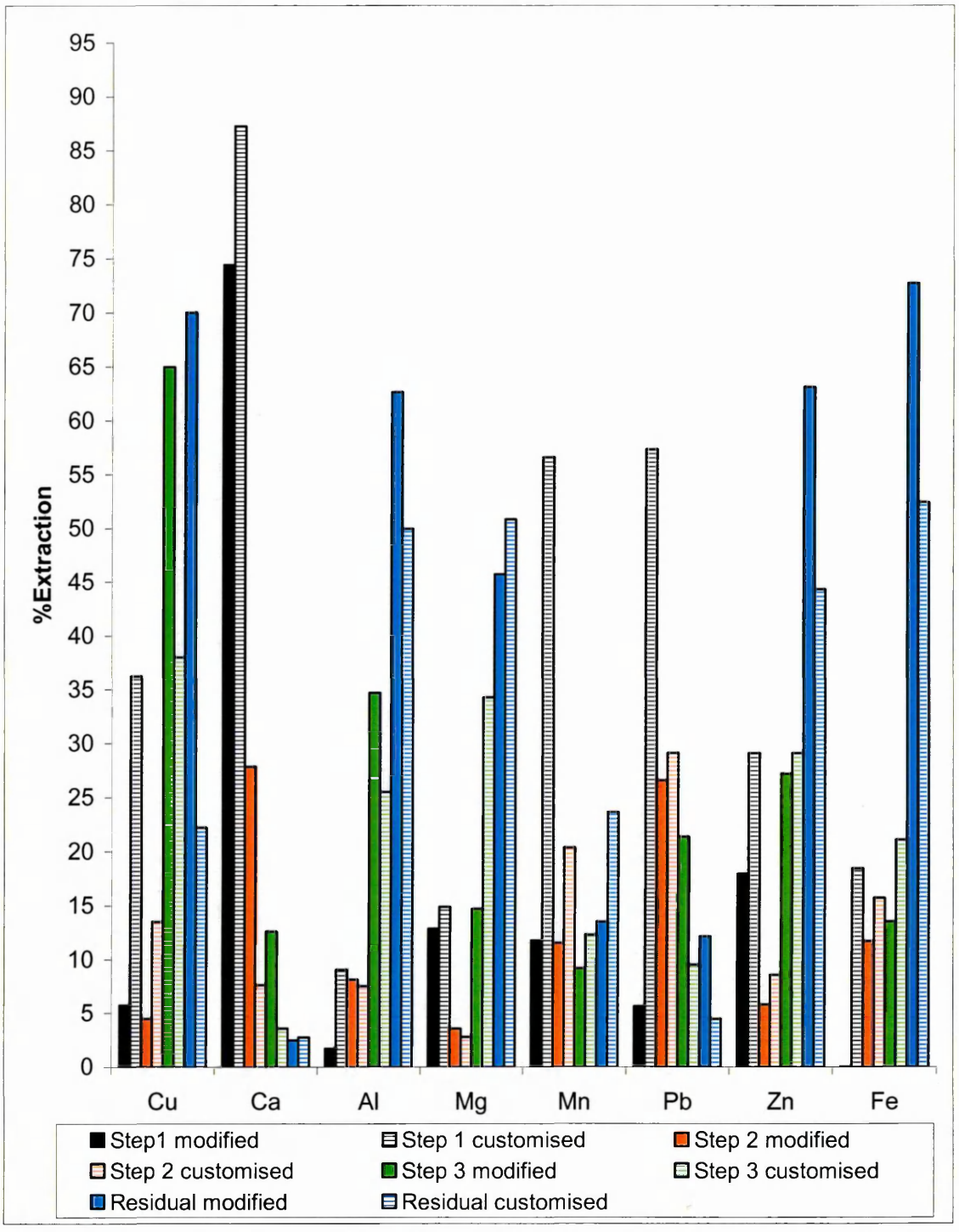

Figure 31 (c): A comparison of metal extractions from the soil sample B1 using the modified BCR procedure and the customised sequential extraction process.

An interesting observation from these customised sequential extraction experiments was the increased concentrations of Fe mobilised into 80mL of 3M ethanoic acid at pH 5 (see Figs. 31 a-c) solutions compared with those into 40mL of 0.11M ethanoic acid at pH 2.6. Approximately, 18, 8 and 23% of Fe was extracted into 3M ethanoic acid solutions from soil samples C1, C2 and B2 respectively into the 3M ethanoic acid solutions. There was a concurrent increase in the concentration of Pb and Ca, which suggests that a large proportion of Pb in all three soils would have been associated with Fe (hydr) oxides and Ca carbonates. Pb release from the surfaces of Fe (hydr) oxides would have been due to the dissolution of these minerals due to the reduction of Fe^{3+} to Fe^{2+}, whilst Pb release from calcite surfaces would have been due to cationic exchange with H^+ ions. The released metal ions would have formed Pb-acetate complexes in solutions such as Pb-$(acetate)^+$, Pb-$(acetate)_2$ and Pb-$(acetate)_3^-$ etc., at pH 5 as shown in Figure 14. Additionally, the relatively high extractions of Pb compared with those of the other metals provided further credence to the inference that a majority of the Pb in the soil would have existed as an independent mineral phases in the form of Pb oxides or sulphates, both of which are soluble in ethanoic acid. This also suggested a potential phytoavailability of Pb of approximately 80%, as plant roots secrete complexing agents capable of extracting metals from soil surfaces.

In order to compare the phytoavailability predictions of the modified BCR process and those of the customised process, phytoextraction experiments were performed using *Helianthus annuus* var. Dwarf Yellow plants. They were grown for a period of 8 weeks in the three soil samples, with harvests being obtained after 4, 6 and 8 weeks. The data showed that the highest accumulation of Pb and Mn in the biomass of plants

growing in all three soils was after harvest 2 (after 6 weeks of growth) (see Figs. 32 a-c). The highest accumulation of Cr was after harvest 1, following which there was a steep decline in uptake. The concentration of Mg, Cu and Zn accumulated by plants growing in all three soils, after each of the three harvests was approximately equal. These are interesting observations, as these results reflect the differences in uptake patterns of essential and non-essential metals. The decrease in accumulation of Pb and Mn after harvest 2 was most likely due to dilution effects in the plants as their biomass increased after the second harvest. Two tailed Student t-test showed that there was no significant difference between the concentrations of Pb accumulated by the plants growing in the soil samples C1, C2 and B1 and those solubilised into 0.11M ethanoic acid solution during the first step of the modified BCR process. This lack of difference could be a coincidence and further work needs to be done to assess the validity of these observations. The proportion of Zn, Cu and Mg accumulated by the plants during the three harvests remained more or less equal, as these are essential metals and their rate of uptake should be proportional to the rate of plant growth. There was no correlation between the concentrations of Zn, Cu and Mg extracted during the first step of the modified process and those accumulated in the biomass of plants growing in soil samples C1, C2 and B1. These observations suggest that the modified BCR procedure could only be used for the prediction of bioavailability of contaminant metals such as Pb, but not those of essential metals. This limited applicability of sequential extraction procedures for ecological risk assessments and prediction of bioavailability was also observed by Ahnstrom and Parker[272].

Root-shoot transfer factors (ratio of the concentration of metals in the roots to those in the shoots) showed that a majority of the lead was sequestered in the roots of the

plants, while the essential metals (Zn, Mg and Cu) and Mn were accumulated in the leaves and stems (see Tables 38 a-c). Another interesting observation from the results presented in Tables 24-26 and Tables 38 (a-c) was the uptake behaviour of Mg, which is a key constituent of chlorophyll. Under normal circumstances, it would be safe to assume that growth and metal uptake would be limited in plants growing in heavily contaminated soils such as sample C1. However, the data from these experiments show that the highest accumulation and root-shoot transfer of Pb & Mg were in plants growing in soil sample C1 followed by those growing in C2 & B1. A possible explanation for this trend can be found in the results from the modified BCR sequential extraction process (Figs. 31 a-c), which showed that the highest concentration of Pb released during step 1 was from soil C1 (16%) followed by samples C2 (7%) and B1 (6%). Similarly the highest concentration of Mg released during step 1 was from soil sample C1 (29%) followed by sample C2 (22%) and sample B1 (13%). The transfer factor data presented in Tables 38 (a-c) suggest the presence of a mechanism in the plant roots that allows accumulation of essential metals into the shoot biomass and actively sequesters toxic metals such as lead in the roots. Several authors[102-106] have suggested that this mechanism could involve the secretion of metallothioneins and phytochelatins, which are principally composed of carboxylic and thiolic acids (such as citric acid and L-cysteine), by the plant roots.

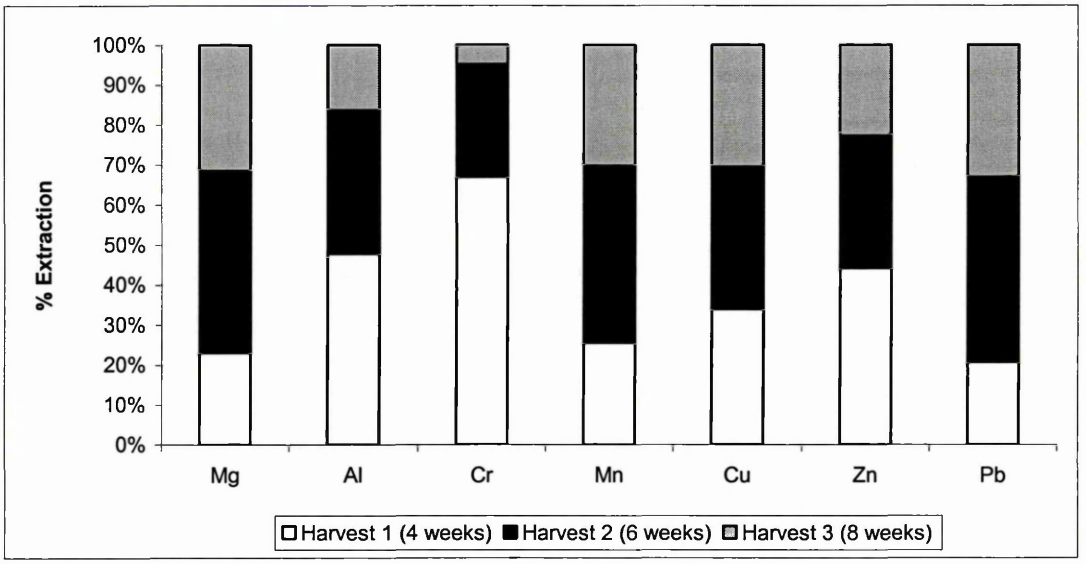

Figure 32 (a): Extraction patterns of metals by *H. annuus* plants growing in soil sample C1 after 4, 6 and 8 weeks growth.

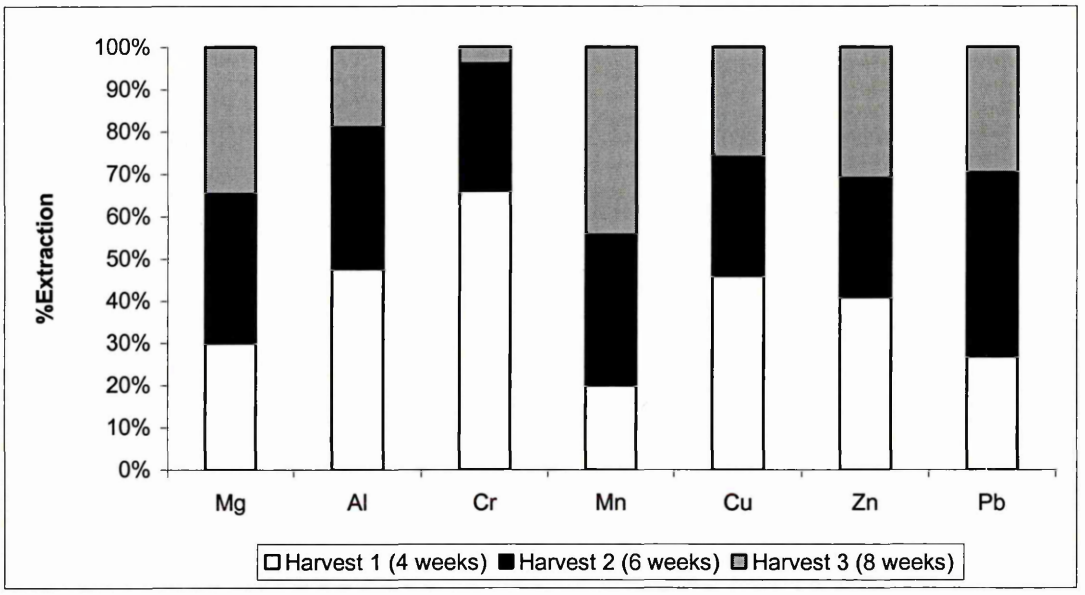

Figure 32 (b): Extraction patterns of metals by *H. annuus* plants growing in soil sample C2 after 4, 6 and 8 weeks growth.

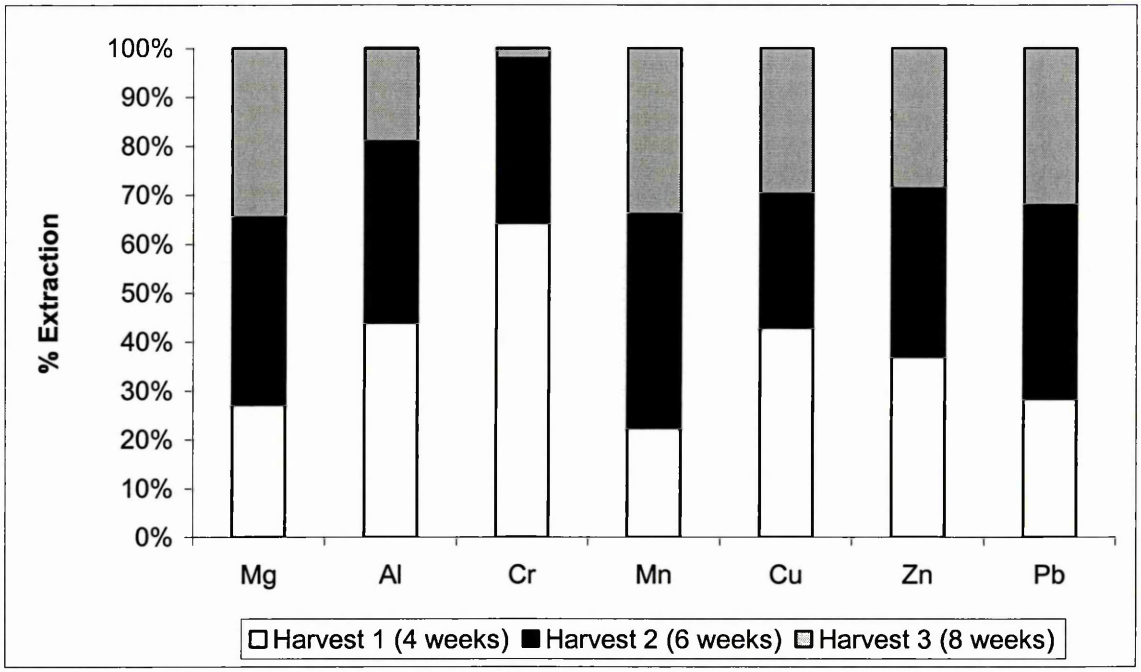

Figure 32 (c): Extraction patterns of metals by *H. annuus* plants growing in soil sample B1 after 4, 6 and 8 weeks growth.

Metals	Harvest 1	Harvest 2	Harvest 3
Mg	3.0	2.7	2.5
Al	0.2	0.1	0.1
Cr	1.3	0.4	2.2
Mn	1.9	2.2	3.9
Cu	3.0	1.9	1.5
Zn	0.6	2.8	1.9
Pb	0.3	0.2	0.1

Table 38 (a): Root – shoot transfer factors (ratio of concentration of metals in shoots to those in roots) of metals in plants growing in soil sample C1.

Metals	Harvest 1	Harvest 2	Harvest 3
Mg	1.8	1.5	1.9
Al	0.2	0.1	0.1
Cr	0.2	0.3	2.5
Mn	1.9	4.6	8.6
Cu	1.8	3.8	6.9
Zn	2.1	3.2	4.2
Pb	0.3	0.2	0.3

Table 38 (b): Root – shoot transfer factors (ratio of concentration of metals in shoots to those in roots) of metals in plants growing in soil sample C2.

Metals	Harvest 1	Harvest 2	Harvest 3
Mg	1.8	2.2	2.6
Al	0.05	0.06	0.08
Cr	0.3	0.8	2.3
Mn	2.4	6.0	7.0
Cu	1.7	2.2	2.5
Zn	1.3	3.3	2.4
Pb	0.1	0.2	0.1

Table 38 (c): Root – shoot transfer factors (ratio of concentration of metals in shoots to those in roots) of metals in plants growing in soil sample B1.

In order to understand the behaviour of these carboxylic and thiolic acids in the soils and assess their usability as potential soil washing reagents, batch extraction experiments were performed using these acids and EDTA (as this is non-biodegradable and popular amongst investigators). The data from these experiments show that approximately 60-100% of the total Pb in the soil was extracted using these acids, without a significant change in the composition of the soil as shown by XRF analysis (see Table 31). The high extraction of Pb and lack of significant changes in the soil composition suggest that these reagents can be used as soil washing reagents. However, the data also show that a majority of Pb in the soil could be phytoavailable, which is not in agreement with the phytoextraction data. Once again, this suggests the presence of an active toxic metal exclusion mechanism in plants.

In order to gain an understanding of this exclusion mechanism, experiments were performed wherein *H. annuus* plants were grown hydroponically in Pb^{2+} spiked solutions. The data showed that over a 3-7 day period of growth, the plants accumulated Pb at a concentration of approximately 10-30% (w/w). A majority of this Pb was sequestered in the roots, with those growing in spiked nutrient rich solutions accumulating three times more Pb than those in the spiked deionised water

solutions. ESEM/EDX and XRD analysis of the roots show that the Pb was mainly sequestered on the surface of the roots in the form of chloropyromorphite and calcium pyromorphite. This data matches the speciation data obtained using the PHREEQC geochemical model. However, this also raised questions about the high uptake of metals from the hydroponics solutions in comparison to uptake from contaminated soils. Almost all the Pb in the hydroponics solutions would have been available for uptake by the plants (assuming that uptake is a passive process and dependent only on speciation of metals in solutions). Data obtained from phytoextraction have shown a relatively low uptake (10-15%) of lead from the soils by the plants. It was hypothesised that this was most likely due to the varying speciation of metals in solutions and contaminated soils.

Assuming that all the Pb in soils mobilised by the plant roots was due to phytochelatins such as L-cysteine, the metal ions in soil solutions could have possibly be in the form of Pb-cysteine complexes (as suggested by MINEQL+), while all the Pb in hydroponics solutions would have been in the form of Pb^{2+} ions. The Free Ion Activity Model (FIAM) suggests that metal ions are taken up by cell surfaces mainly in the form of M^{z+} ions irrespective of what form they exist in (soil) solution (e.g., metal-EDTA complex)[273]. Sarret et al.,[274] observed that zinc and lead were accumulated in the roots and leaves of sweet pea (*Phaseolus vulgaris*) as zinc phosphate dihydrate and cerussite ($PbCO_3$) irrespective of what form they were present in solution, i.e. as free ions or as metal-EDTA complexes. The rate and quality of uptake slows down when the metals are bound to organic complexes (or found in the form of colloids) in solutions, which explains the lower uptake of Pb by plants growing in soils compared with those growing in solutions. The Biotic Ligand

Model (BLM) suggests that the metal-ligand response on the cell surfaces depends principally on the speciation and concentration of metals in solutions. These cell surface ligands such as ATPases are generally composed of phosphate and thiol groups, which explains the formation of pyromorphite on the root surfaces, as the Pb ions would react with the phosphates to form stable complexes[273].

Additional experiments were performed to study the leachability of metals from the soil sample C1 using column washing experiments. All the batch extraction experiments were performed using a small mass of soil (1g) over a period of 16hours, assuming that equilibrium conditions would have been reached during the experiments. However, in real field environments, equilibrium is seldom reached, especially over large volumes of soil. In order to gain an understanding of the kinetics of metal desorption, metals were leached out from soil samples packed in chromatography preparative columns using EDTA and ethanoic acid (0.11M and 1.75M). A majority of the Pb in the soil was extracted in the first few fractions and the proportions of metal extracted from the soils were approximately equal to those extracted in the batch mode. However, the concentrations of metals such as Ca and Fe extracted into the solutions were very low, providing conclusive evidence that the Pb in the soils would have existed independently as PbO. This also shows that the modified BCR sequential extraction might not be an effective procedure for the prediction of metal desorption from contaminated soils.

There was a surplus of *H. annuus* seedlings germinated in the rock wool; therefore some experiments were performed using solutions spiked with Au^{3+}. The data showed that similar to Pb, a majority of Au was sequestered in the plant roots.

However, analysis of the plant roots using XRD revealed that the deposition of pure gold on root surfaces. The average particle size of these gold deposits, as calculated using the Scherrer equation, was approximately 6nm, which is within the size range of a true nanoparticle[275]. Analysis using STEM and ESEM/EDX analysis showed that the particles had aggregated in the form of nanoaggregates, approximately 80nm in size. This is a classic demonstration of the Biotic Ligand Model (BLM) that suggests that metals do not form complexes with the surface ligands when they exist in solution in colloidal forms and also do not elicit a biological response. Consequently, in this case nanoparticle formation would have been a result of passive deposition of metal ions on the root surfaces. However, it is unclear as to what kind of capping agents would have stabilised the nanoparticles on the root surfaces. Some clues about the nature of these capping ligands comes from the EDX mapping data (Figure 28), which showed a strong overlap between the Au, P and O elemental distribution maps. Further work needs to be done using techniques such as EXAFS that can throw light on the true nature of the oxidation states and speciation of the elements.

Chapter 14 General Conclusions and Future Work

1. The modified BCR procedure could not accurately predict the operational (i.e. not the true) fractionation of contaminant metals in heavily contaminated soils. Further work needs to be done on a variety of soils from a variety of industrial sites contaminated with different metals to confirm this finding.
2. The customised sequential extraction procedure can be used for the fractionation of metals in soils heavily contaminated with lead.
3. However, phytoremediation experiments have shown that the modified BCR procedure can be used for the accurate prediction of phytoavailability of lead. Confirmation is needed using soils contaminated with metals other than lead and using plants other than *Helianthus annuus*, to study if the predictive capacity of the BCR procedure is limited to Pb and *H. annuus*.
4. Phytoextraction is a potentially effective and safe technique for remediation of heavy metal contaminated soils, as 10-15% of the Pb in the soil was extracted in a relatively short period of 8 weeks time. Additionally, since the majority of the metal was immobilised on the surface of roots in the form of extremely insoluble pyromorphite, the risk to human and environmental health as a result of ingestion of shoot biomass of the plants should be minimal.
5. Complexing agents such as citric acid, L-cysteine and EDTA are effective soil washing reagents as they extract a majority of the contaminant metal without altering the basic mineral composition of the soil. More work needs to be done to investigate if the contaminants in the leachate from these experiments could be extracted hydroponically by plants.

6. Column washing experiments have shown that contaminant metals can be leached out from soil surfaces rapidly without radically altering the basic properties (physical and chemical) of soils.

References

[1] DeSousa, C (2001). J. Environ. Management 62, 131-154.

[2] Nijkamp, P., Rodenburg, C. A., and Wagtendok, A. J. (2002). Ecological Economics, 40, 235-252.

[3] Environment Agency (2002). CLR 7. Assessment of risks to human health from land contamination: an overview of the development of guideline values and related research. The Environment Agency R&D Dissemination Centre, Swindon, UK.

[4] Environment Agency (1999). Guidance on the assessment and interrogation of subsurface analytical contaminant fate and transport models. National Groundwater and Contaminated Land Centre report. NC/99/38/1. The Environment Agency R&D Dissemination Centre, Swindon, UK.

[5] DEFRA and the Environment Agency (2002). Contaminants in Soil: Collation of Toxicological Data and Intake Values for Humans. Environment Agency, Bristol, UK.

[6] Peijnenburg, W.J.G.M and Jager, T. (2003). Ecotoxicology and Environmental Safety, 56, 63-77.

[7] Michalke, B. (2003). Ecotoxicology and Environmental Safety. 56, 122-139.

[8] Tipping, E., Riuwerts, J., Pan, G., Ashmore, M. R., Lofts, S., Hill, M. T.R, Farago, M. E., Thornton, I. (2003). Environmental Pollution, 125, 213-225.

[9] Shuman, L. M. (1991). Chemical forms of micronutrients in soils. In J. J. Mortvedt (ed.). Micronutrients in agriculture. Soil Sci. Soc. America Book Series #4. Soil Sci. Soc. America Inc., Madison, WI.

[10] Mattigod, S. V., Sposito, G., and Page, A. L. (1981). Factors affecting the solubility of trace metals. In D. E. Baker (Ed.). Chemistry in the soil environment. ASA Special Publication No. 40, Amer. Soc. Agronomy, Madison, WI.

[11] Weber, W. J. (1995). In Process Dynamics in Environmental Systems. John Wiley & Sons Inc.

[12] Weber, W. J., McGinley, P.M. and Katz, L. E. (1991). Water Research, 25, 499-528.

[13] Stumm, W and Morgan, J. J. (1995). Aquatic Chemistry: Chemical Equilibria and Rates in Natural Waters. John Wiley & Sons Inc.

[14] Stumm, W. (1992). Chemistry of the Solid-Water Interface. Processes at the Mineral-Water and Particle-Water Interface in Natural Systems. John Wiley & Sons, Inc.

[15] Jenne, E. A. (1968). Adv. in Chem. 7, 337-387.

[16] Dudley, L. M., McLean, J. E., Sims, R. C. and Jurinak, J. J. (1991). Soil Sci. 145, 207-214.

[17] Sposito, G., (1983). The chemical forms of trace metals in soils. *In* Applied Environmental Geochemistry. Academic Press, London, pp. 123-140.

[18] Sposito, G. (1989). The chemistry of soils. Oxford University Press. New York.

[19] Hendrickson, L. L. and Corey, R. B. (1981). Soil Sci. 131, 163-171.

[20] O'Connor, G. A., O'Connor, C., and Cline, G. R. (1984). Soil Sci. Soc. Am. J. 48, 1244-1247.

[21] Appelo, C. A. J. and Postma, D. (1993). Geochemistry, Groundwater and Pollution. A.A. Balkema.

[22] Cavallaro, N. and McBride, M.B. (1978). Soil Sci. Soc. Am. J. 42, 550-556.

[23] O'Connor, G. A., O'Connor, C., and Cline, G. R. (1984). Soil Sci. Soc. Am. J. 48, 1244-1247.

[24] Ure, A., Quevauvillier, P.H., Muntau, H. and Griepink, B., 1993. Int. J. Environ. Analyt. Chem. 51, 135-151.

[25] Loyland Asbury, S. M., Lamont, S. P., and Clark, S. B. (2001). Environ. Sci. Tech., 35, 2295-2300.

[26] (a) Shuman, L. M. (1985). Soil. Sci. 140, 11-22.
(b) Chao, T. T. (1972). Soil Sci. Soc. Am. Proc. 36, 764-768.
(c) Lindsay, W. L. and Norvell, W. A. (1978). Soil Sci. Soc. Am. J. 42, 421-428.
(d) Mehlich, A. (1984). Plant Anal. 15, 1409-1416.

[27] Fernández Alborés, A., Pérez Cid, B., Fernández Gómez, E., and Falqué López, E., (2000). Analyst, 1353-1357.

[28] Beckett, P.H.T. (1988). Advanced Soil Sci. 9, 144-175.

[29] U.S. Environmental Protection Agency (1986). Test methods for evaluating solid waste: physical/chemical methods SW-846. USEPA, Office of Solid Waste and Emergency Response. Washington D.C.

[30]Tessier, A., Campbell, P.G.C. and Bisson, M., 1979, Anal. Chem. 51, 844-851.

[31] Rapin, F., Tessier, A., Campbell, P.G.C. and Carignan, R. (1986). Environ. Sci. Tech., 20, 836-840.

[32] Schekel, K. G., Impelliterri, C. A., Ryan, J. A. and McEvoy, T. (2003). Environ. Sci. Tech. 37, 1892-1898.

[33] Jaunneau, J.M., Latouche, C. and Pautrizel, F. (1983). Environ. Tech. Lett. 4, 509-514.

[34] Fiedler, H.D., Lopez-Sanchez, J. F., Rubio, R., Rauret, G., Quevauviller, P. H., Ure, A. M. and Muntau, H. (1994). Analyst, 119, 1109-1114.

[35] Qiang, T., Xiao-Quan, S., Jin, Q. and Zhe-Ming, N., (1994). Anal. Chem., 66, 3562-3568.

[36] Quevauvillier, P., Rauret, G., Muntau, H., Ure, A.M., Rubio, R., Lopez-Sanchez, J.F., Fiedler, H.D. and Griepnik, B. (1994). Fresenius J. Anal. Chem. 349, 808-814.

[37] Ho, M. D. and Evans, G. J. (2000). Environ. Sci. Tech. 34, 1030-1035.

[38] Kheboian, C. and Bauer, C. F. (1987). Anal. Chem., 59, 1417.

[39] Rendell, R., Batley, G. E. and Cameron, A. J. (1980). Environ. Sci. Tech., 14, 314-318.

[40] Tipping , E., Hetherington, N. B., Hilton, J., Thompson, D. W., Bowles, E. and Hamilton-Taylor, J. (1985). J. Anal. Chem. 57, 1944-1946.

[41] Roger, B. (1986). Environ. Tech. Lett. 7, 539-546.

[42] Quevauvillier, Ph. (1998). Trends in Analytical Chemistry, 17, 632-641.

[43] Raksasataya, M., Langdon, A. G. and Kim, N. D. (1996). Anal. Chim. Acta. 332, 1.

[44] Ho, M. D. and Evans, G. J. (2000). Environ. Sci. Tech. 34, 1030-1035.

[45] Gardiner, P. H. E. (2001). Chemical speciation in reference materials. Conference Proceedings IAEA, Vienna.

[46] Lindsay, W. L. (1979). Chemical equilibria in soils. John Wiley and Sons, New York.

[47] Kramer, J. R. and Allen, H. E. (1988). Metal speciation: theory, analysis and speciation. Lewis Publishers Inc. Chelsea, MI.

[48] Kan, A. T., Fu, G., Hunter, M., Chen, W., Ward, C. H. and Tomson, M. B. (1998). Environ. Sci. Tech. 32, 892-902.

[49]Di Toro, D. M., Mahony, J. D., Kirchgraber, P. R., O'Byrne, A.L., and Pasquale L. R. (1986). Environ. Sci. Tech. 20, 55-61.

[50] Burgos, W. D., Novak, J.T. and Berry, D. F. (1996). Environ. Sci. Tech., 30, 1205.

[51] Barr, D., Bardos, R. P. and Nathanail, C. P. (2003). Non-biological methods for assessment and remediation of contaminated land - case studies. CIRIA.

[52] Allen, A. (2001). Engineering Geology, 60, 3-19.

[53] Burnley, S., (2001). Resources, Conservation and Recycling, 32, 349-358.

[54] Price, J.L. (2001). Resources, Conservation and Recycling, 32, 333-348.

[55] Virkutyte, J., Sillanpaa, M., and Latonstenmaab, P., (2002). The Sci. Tot. Environ., 289, 97-121.

[56] Darab, J. G., and Smith, P. A. (1996) Chem. Mater., 8, 1004-1021.

[57] Acar, Y.B.and Alshawabkeh, A.N. (1993). Environ. Sci. Tech. 46 2638–2647.

[58]Acar, Y.B. Gale, R.J., and Alshawabkeh, A.N. (1995). J. Hazard. Mater. 40 117–137.

[59]Lageman, R. (1993). Environ. Sci. Tech. 27, 2648–2650.

[60] NATO, June 1998, NATO/CCMS Pilot Study. Evaluation of Demonstrated and Emerging Technologies for the Treatment and Clean Up of Contaminated Land and Groundwater, Phase II, Final Report No. 219, EPA 542-R-98-001a.

[61] McBride, M. B., and Martinez, C. E. (2000). Environ. Sci. Tech. 29, 1318-1323.

[62] Lothenbach, B., Furrer, G., and Schulin, R. (1997). Environ. Sci. Tech., 31, 1452-1462.

[63] Roy, D. M. (1999). Cement and Concrete Research, 29, 249-254.

[64] Hettiarachchi, G. M., Pierzynski, G.M. and Michel, M.D. (2000). Environ. Sci. Tech. 34, 4614-4619.

[65] Mercier, L., and Detellier, C. (2000). Environ. Sci. Tech., 34, 4387-4391.

[66] Mulligan, C. N., Yong, R. N. and Gibbs, B.F. (2001). Engineering Geology, 60, 193-207.

[67] Richards, B.K., Steenhuis, T.S., Peverly, J.H. and McBride, M. B., (2000). Environmental Pollution, 109, 327-346.

[68] Singh, D., Wagh, A.S., Tlustochowicz, M. and Jeong, S.Y. (1998). Waste Management, 18, 135-143.

[69] Wang, Y.M., Chen, T. C., Yeh, K. J. and Shue, M. F. (2001). J. Hazard. Mater. 88, 63-74.

[70] Peters, R.W. (1999). J. Hazard. Mater., 66, 151-210.

[71] Evanko, C. R. and Dzombak, D. A. (1999). Technology evaluation report. Prepared for Ground-Water Remediation Technologies Analysis Center, Pittsburgh, PA.

[72] EPA (2000). 542-B-00-004. Innovative Remediation Technologies: Field-Scale Demonstration Projects in North America, 2nd Edition Year 2000 Report.

[73] Carey, M. A., Fretwell, B. A., Mosley, N G. and Smith, J. W. N. (2002). Guidance on the use of Permeable Reactive Barriers for Remediating Contaminated Groundwater. National groundwater and Contaminated Land Centre Report NC/01/51. Environment Agency, Solihull.

[74]Allen, H.E, and Chen, P-H. (1993).Environ. Progress., 12, 284-293.

[75]Benner, S.G., Blowes, D.W, Gould, W.D., Herbert, R.B, and Ptacek, C.J (1999).. Environ. Sci. Tech. 33, 2793-2799.

[76]Ganesh, R., Robinson, K.G., Reed, G.D. and Sayler, G.S. (1997). App. and Environ. Microbio. 63, 4385-4391.

[77]Brooks, S.C., Herman, J. S., Hornberger, G. M., and Mills, A. L. (1999). J. Contam. Hydrology. 32, 99-115.

[78] Ward, N. I., and Hare, R. J. (1999). The Sci. Tot. Environ. 235, 169-178.

[79] Gillespie, W. B., Hawkins, W.B., Rodgers, J. H., Cano, M. L., and Dorn, P.B. (2000). Ecological Eng. 14, 279-292.

[80] Lytle, C. M., Lytle, F. M., Yang, N., Qian, J., Hansen, D., Zayed, A., and Terry, N. (1998). Environ. Sci. Tech. 32, 3087-3093.

[81] Boopathy, R. (2000). Bioresource Tech. 74, 63-68.

[82] Mitchell, R. (1992). Environmental Microbiology. Wiley Interscience, 1992, 202-203.

[83] Fredrickson, J.K., and Gorby, Y.A. (1996). Curr. Opin. Biology. 7, 287-294.

[84]Barkay, T., and Schaefer, J. (2001). Curr. Opin. Microbio., 4, 318-323.

[85] Watanabe, K. (2001). Curr. Opin. Biotech. 12, 237-241.

[86] Gadd, G. M. (2000). Curr. Opin. Biotech. 11, 271-278.

[87]Kapoor, A., Viraraghavan, T., and Cullimore, D. R. (1999). Bioresource Technology, 70, 95-104.

[88] Kotrba, P., Doleková, L., de Lorenzo, V., and Ruml,.T. (1999). Appl. Environ. Microbiol. 65, 1092-1098.

[89] Diels, L., Pümpel, T., Ebner, C., Pernfuß, B., Schinner, F., Keszthelyi, Z., Stankovic, A., Finlay, F.A., Macaskie, L.A., Tsezos, M.A., and Wouters, H. (2001). Hydrometallurgy. 59, 383-393.

[90] Lovley, D.R ., and Coates, J.D. (1997). Curr. Opin. Biotech. 8, 285-289.

[91]White, C. and Gadd, G. M. (2000). FEMS Microbiology Letters, 183, 313-318.

[92] Zhou, J.L. (1999). App. Microbio.Biotech. 51, 686-693.

[93] Kapoor, A., Viraraghavan, T. and Cullimore, D. R. (1999) Bioresource Technology, 70, 95-104.

[94] Chen, S., and Lin, J. (2001). Chemosphere, 1093-1102.

[95] Baker, A.J.M., McGrath, S.P., Sidoli, C., and Reeves, R.D. (1994). Resources, Conservation and Recycling. 11, 41-49.

[96] Gall, U., Schlep, H., and Burned, C. (1994). Physiol. Plantarum. 92, 364-36.

[97] Blaylock, M.J., Salt, D. E., Dushenkov, S., Zakharova, O., Gussman, C., Banerji, L., Kapulnik, S., Ensley, B. D., and Raskin, I. (1997). Environ. Sci. Tech. 31, 860-865.

[98] Watanabe, M.E. (1997). Environ. Sci. Tech. 31, 182-185.

[99]Baker, A. J. M. (1981). Accumulators and excluders - strategies in the response of plants to heavy metals. J. Plant Nutrition. 3, 643-654.

[100] McGrath, S.P. and Fang-Jie, Z. (2003). Phytoextraction of metals and metalloids from contaminated soils. Curr. Opin. Biotech. 14, 277-282.

[101] Cunningham, S. D., Berti, W. R. and Huang, J. W. (1995). Trends in Biotech., 13, 393-397.

[102] Salt, D.E., Blaylock, M., Kumar, P.B.A.N., Dushenkov, V., Ensley, B.D., Chen, L., and Raskin, I. (1995). Biotechnology. 13, 468-478.

[103] Gall, U., Schlep, H., and Burned, C. (1994). Physiol. Plantarum. 92, 364-36.

[104] Chaudhry, T.M., Hayes, W.J., Khan, A.G., and Khoo, C.S. (1998). Australasian J. Ecotoxicol. 4, 37-51.

[105] Pawlowska, T.E., Blaszkowski, J., and Ruhling, A. (1996). Mycorrhiza. 6, 499-505.

[106] Tam, P.C., (2001). Mycorrhiza., 15, 181-187.

[107] Raman, N., Nagarajan, N., Gopinathan, S., and Sambandan, K. (1993) Biol. Fertil. Soil. 16, 76-78.
[108].Turnau, K (1998). Acta Soci. Bot. Poloniae. 67, 105-113.

[109]Cunningham, S.D., and Ow, D.W. (1996). Plant. Physio. 110, 715-719.

[110]Dushenkof, S., Vasudev, D., Kapulnik, Y., Gleba, D., Fleisher, D., Ting, K.C., and Ensley, B. (1997). Environ. Sci. Tech., 31, 3468-3474.

[111] Ebbs, S.D., and Kochian, L.V. (1998). Environ. Sci. Tech. 32, 802-806.

[112]Ebbs, S.D., Lasat, M.M., Brady, D.J., Cornish, J., Gordon, R., and Kochian, L.V.J. (1997). Environ. Qual. 26, 1424-1430.

[113] Bhargawa, S.C. (1991). Oilseed Brassicas in Indian Agriculture. Vikas, New Delhi. 1991, 161-197.

[114]Blaylock, M.J., Salt, D. E., Dushenkov, S., Zakharova, O., Gussman, C., Banerji, L., Kapulnik, S., Ensley, B. D and Raskin, I. (1997). Environ. Sci. Tech. 31, 860-865.

[115] Willey, N., Hall, S., and Mudiganti, A. (2001). Int. J. Phytoremediation. 3, 321-333.

[116] Bae, W., and Mehra, R.J. (1997). J. Inorganic Biochem. 4, 201-210.

[117] Maathuis, F.J.M., and Sanders, D. (1999) Curr. Opin. Plant Biol. 2, 236-243.

[118] Guerinot, M L., and Eide, D. (1999). Curr. Opin. Plant Biol. 2, 244-249.

[119] Eng, B. H., Guerinot, M. L., Eide, D., and Saier, M. H. (1998). J. Membr Biol. 66, 1-7.

[120] Karenlampi, S., Schat, H., Verkleij, J. A. C., van der Lelie, D., Mergeay, M., and Tervhauta, A.I., Environmental Pollution. 2000, 107, 225-231.

[121] Mejáre, M., and Bülow, L. (2001). Trends in Biotech. 19, 2, 67-73.

[122] Cohen, C. K., Fox, T.C., Garvin, D.F. and Kochian, L.V. (1998). Plant Physiol. 116, 1063-1072.

[123] Evans, K.M., Gethouse, J. A., Lindsay, W.P., Shi, J., Tomney, A.M., and Robinson, N.J. (1992). Plant Molecular Biology. 20, 1019-1028.

[124] Williams, L.E., Pittman, J.K. and Hall, J.L. (2000). Emerging mechanisms for heavy metal transport in plants. Biochimica et Biophysica Acta, 1465, 104-126.

[125] Tsuji, N., Hirayanagi, N., Okada, M., Miyasaka, H., Hirata, K., Zenk, M., and Miyamoto, K. (2002) Biochemical and Biophysical Research Communications, 293, 653-659.

[126] Piechalak, A., Tomaszewska, B., Baralkiwizc, D., and Malecka, A. (2002). Phytochemistry. 60, 153-162.

[127] Cobbett, C.S. (2000). Phytochelatin biosynthesis and function in heavy metal detoxification. Curr. Opin. Plant Biology, 3, 211-216.

[128]Morelli, E., and Scarano, G. (2001). Marine Environment Research, 52, 383-395.

[129] Bae, W., Mehra, R., Mulchandani, A., and Chen, W. (2001). Applied and Environ. Microbio., 67, 11, 5335-5338.

[130] Varga, A., Zaray, G., and Fodor. F. (2002). J. Inorg. Biochem. 89, 149-154.

[131] Bae, W., Mulchandani, A., and Chen. W. (2002) J. Inorg. Biochem. 88, 223-227.

[132] Satofuka, H., Fukui, T., Takagi, M., Atomi, H., and Imanaka. T. (2001) J. Inorgan. Biochem. 86, 595-602.

[133] Foyer, C.H., and Theodoulou, F. (2001). Trends Plant Sci., 6, 486-492.

[134]Cunningham S.D. and Ow, D.W. (1996). Plant. Physio. 110, 715-719

[135] Evanko, C. R. and Dzombak, D. A. (1999). Technology Evaluation Report 1999. Prepared for Ground-Water Remediation Technologies Analysis Center, Pittsburgh, PA. EPA 542-B-00-004. Innovative Remediation Technologies: Field-Scale Demonstration Projects in North America, 2nd Edition Year 2000 Report.

[136] Willard, H. H., Merritt, L. L., Dean, J. A., and Settle, F. A. (1988). Instrumental Methods of Analysis. 7th edition. Wadsworth Publishing Company. Belmont, California.

[137] Clement, R.E., and Yang, P.W. (2001). Anal. Chem. 56, 212-215.

[138] Hoenig, M. (2001). Talanta, 54, 1021-1038.

[139] Ph. Quevauvillier (1995). Quality assurance in environmental monitoring: sampling and sample pre-treatment, VCH, Weinheim.

[140] Montaser, A. (1998). Inductively Coupled Plasma Mass Spectrometry. Wiley-VCH.

[141] Rouessac, F. and Rouessac, A. (2000). Chemical Analysis: modern instrumental methods and techniques. Wiley Interscience.

[142] Ure, A.M.,.Butler, L.R.P, Scott, R.O. and Jenkins, R.(1999). Preparation of Materials for Analytical Atomic Spectroscopy and other Related Techniques (IUPAC Recommendations 1988). Spectrochimica Acta Part B, 52, 409-420.

[143]dos Anjos, M.J., Lopes, R.T., de Jesus, E.F.O., Assis, J. T., Cesaro, R. and Barradas, C.A.A. (2000). Spectrochima Acta Part B, 1189-1194.

[144] Moore, D.M., and Reynolds, R.C. (1997). X-Ray Diffraction and the Identification and Analysis of Clay Minerals. Oxford University Press.

[145] Crooks, J. E. (1978). The Spectrum in Chemistry. Academic, New York.

[146] Taylor, H.E. (2001). Inductively Coupled Plasma Mass Spectrometry. Academic Press.

[147] www.agilent.com (Accessed January 2004).

[148] Griffiths, P.R., and DeHasser, L. (1986). Fourier Transform Infrared Spectroscopy. John Wiley & Sons.

[149] Colthup, N. B., Daly, L. H., and Wiberley, S. E. (1975). Introduction to Infra-red and Raman Spectroscopy. 2nd Edition. Academic, New York.

[150] Ferraro, J. R., and Basile, L. J. (eds.) (1982). Fourier Transform Infrared Spectroscopy, Academic, New York.

[151] Keyse, R. J. (1998). Introduction to scanning transmission electron microscopy. BIOS Scientific Publishers.

[152] Oxford Instruments. (1990). Energy dispersive X-ray microanalysis: An Introduction.

[153] Crossley, D. (ed) (1989). Water power on the Sheffield Rivers. Sheffield Trades Historical Society and University of Sheffield, Division of Continuing Education.

[154] Rhodes, J.(1973). Derbyshire lead mining in the eighteenth century. University of Sheffield Institute of Education.

[155] Sparham, K. (1988). A study of the possible environmental legacies from the sites of lead smelting between the valleys of Cordwell and Totley. BSc Dissertation. Sheffield City Polytechnic.

[157] British Standard Methods of Test for Soils for Civil Engineering Purposed. Part 3. Chemical and Electrochemical Tests. British Standards Institution. BS 1377: Part 3: 1990.

[158] Cotter-Howells, J.D. (1993). The Sci. Tot. Environ. 132, 93-98.

[159] (a) Delves, H.D. (1988). Chemistry in Britain. (September), 1009-1012.
(b) Whitehead, K., Ramsey, M. H., Bacon, J. (1997). Applied Geochemistry. 12, 75-81.

[160] Rauret, G., Lopez-Sanchez, J.F., Sahuquillo, A., Rubio, R., Davidson, C.M., Ure, A. M. and Ph. Quevauvillier, (1999). J. Environ. Monit. 1, 57-72.

[161] Quevauvillier, Ph., Rauret, G., Lopez-Sanchez, J. F., Rubio, R., Ure, A.M, and Muntau, H.. (1997). The Sci. Total Environ. 205, 223-227.

[162] Rauret, G., Lopez-Sanchez, J.F., Sahuquillo, A., Barahona, E., Lachica, C., Ure, A. M., Davidson, C. M., Gomez, A., Luck, D., Bacon, J., Yli-Halla, M., Muntau, H., and Ph. Quevauvillier (2000). J. Environ. Monit., 2., 228-235.

[163] Hillier, S., Suzuki, K. and Cotter-Howells, J. (2001). Applied Geochemistry, 16, 597-608.

[164] Garrabants, A.C. and Kosson, D. S. (2000). Waste Management, 20, 155-165.

[165] Kedziorek, M.A.M.and Bourg, A. C. M. (2000). J. Contaminant Hydrology, 40, 381-392.

[166] Schiewer, S., and Volesky, B. (1995). Environ. Sci. Tech. 29, 3049-3058.

[167] Parkhurst, D. L. and Appelo, C. A. J. (1999). User's guide to PHREEQC (version 2). A computer program for speciation, batch reaction, one-dimensional transport and inverse geochemical calculations. U. S. Geological Survey, Denver, USA.

[168] Dzombak, D. A., and Morel, F. M. M. (1990). Surface Complexation Modelling. Hydrous Ferric Oxide. John Wiley and Sons. New York.

[169] Appelo, C. A. J., and Postma, D. (1996). Geochemistry, Grounwater and Pollution. AA Balkema, Rotterdam.

[170] Schecher, W. D., and McVoy, V. C. (1994). MINEQL+ User's Manual. Environmental Research Software. M. E. Hallowel, USA.

[171] Gleyzes, C., Tellier, S., and Astruc, M. (2002). In Sequential Extraction Procedures for the Characterisation of the Fractionation of Elements in Industrially Contaminated Soils. *In* Methodologies for Soil and Sediment Fractionation Studies. Editor: Ph Quevauvillier. Royal Society of Chemistry. Cambridge, UK.

[172] Environment Agency (1999). Methodology for the derivation of remedial targets for soil and groundwater to protect water resources. R&D Publication 20.

[173] National Rivers Authority (1994). Leaching tests for the assessment of contaminated land. NRA R&D Note 301. Prepared by WRc.

[174] Loyland Asbury, S. M., Lamont, S. P., and Clark, S. B. (2001). Environ. Sci. Tech., 35, 2295-2300.

[175] Quevauvillier, Ph. (1998). Trends Anal. Chem., 17, 289.

[176] Templeton, D.M., Ariese, F., Cornelis, R., Danielsson, L.G., Muntau, H., Van Leeuwen, H. P., and Lobinski, R. (2000). Pure Appl. Chem. 72, 1453.

[177] Jeng, A. S. and Singh, B. R. (1993). Soil Science, 156, 240.

[178] (a) Ure, A.M., and Davidson, C.M. (2002). Chemical speciation in soils and related materials by selective chemical extraction. A.M. Ure, C.M. Davidson (Eds). In Chemical Speciation in the Environment, 2nd ed., Blackwell Scientific Publications, Oxford.
(b) G. Rauret, J. F. Lopez-Sanchez, A. Sahuquillo, E. Barahona, M. Lachica, A. Ure, H. Muntau, Ph. Quevauvillier, Indicative values for extractable contents (mass fractions) of Cd, Cr, Cu, Ni, Pb and Zn in a sewage sludge-amended soil (CRM 483) following the modified BCR-sequential extraction (three-step) procedure, Report EUR 19503 EN, European Commission, Brussels, 2000.

[179] Whalley, C., and Grant, A. (1994). Anal. Chim. Acta 291, 287

[180] Department of Environment Food and Rural Affairs(2003). Soil Guideline Values for Lead. Environment Agency, Bristol.

[181]Department of Environment Food and Rural Affairs(2003). Soil Guideline Values for Cadmium. Environment Agency, Bristol.

[182] Department of Environment Food and Rural Affairs(2003). Soil Guideline Values for Chromium. Environment Agency, Bristol.

[183] Guidance on the assessment and redevelopment of contaminated land, Guidance Note 59/83, ICRCL, Department of the Environment, London, 1987.

[184] Manning, D. A. (1995). Industrial Minerals. Wiley Interscience.

[185] International Centre for Diffraction Data (2002). JCPDS database.

[186] van der Marel H.W.and Beutelspacher, H., in collaboration with E. Rietz and P. Krohme. (1976). Atlas of infrared spectroscopy of clay minerals and their admixtures. Amsterdam, Oxford (etc.) : Elsevier.

[187] Lopez-Sanchez, J.F., Sahuquillo, A., Fiedler, H. D., Rubio, R., Rauret, G., Muntau, H. and Quevauvillier, Ph. (1998). Analyst, 123, 1675–1677.

[188] Mossop, K. F. and Davidson, C. M. (2003). Anal. Chim. Acta. 478, 111-118

[189] Soult, Graham A. (1998). - Off the rails or on the right track? : an analysis of mixed-use development. CIRIA.

[190] http://www.defra.gov.uk/environment/statistics/land/ (Accessed February 2004).

[191] Brady, N.C., and Weil, R. R. (2002). The nature and property of soils.13th Edition. Upper Saddle River, NJ : Prentice Hall.

[192]Baes, C. F., and Mesmer, R.E. (1976). The hydrolysis of cations. Wiley Interscience, New York. London.

[193] Selim, H.M.and Amacher, M.C. (1996). Reactivity and transport of heavy metals in soils. CRC/Lewis, Boca Raton, Fla. London.

[194] Minerals in soil environments / co-editors, J.B. Dixon and S.B. Weed , 2nd edition - Madison, Wis. Soil Science Society of America, 1989.

[195] Cotter-Howells, J.D. (1993). The Sci. Total Environ. 132, 93-98.

[196] Dahlin, C. L., Williamson, C. A., Keith Collins, W., and Dahlin D. C. (2002). Environmental Forensics, 3, 191-201.

[197] Hillier, S., K. Suzuki and Cotter-Howells, J. (2001). Applied Geochemistry, 16, 597-608.

[198] Li, X., and Thornton, I. (2001). Applied Geochemistry, 16, 1693-1706.

[199] Schwertmann, U., and Taylor, R. M. (1989). Iron oxides. J. B. Dixon, S. B. Weed (1989). In Minerals in Soil Environments. Soil Science Society of America, Madison, Wiconsin, USA.

[200] Cotter-Howells, J. and Thornton, I. (1991). Environ. Geochem. Health, 13, 127-135.

[201] Garrels, R. M. and Christ, C. L. (1994). Minerals, Solution and Equilibria. Harper & Row, New York.

[202] Kheboian, C., and Bauer, C. F. (1987). Anal. Chem. 1987, 59, 1417.

[203] Li, X. D., Coles, B. J., Ramsey, M. H., and Thornton, I. (1995). Chem. Geol. 124, 109-123.

[204] Chang, A.C., Page, A. L., Warneke, J. E. and Grgurevic, E. (1984) J. Environ. Qual., 13, 33.

[205] Kennedy, V. H., Sanchez, A. L., Oughton, D. H. and Rowland, A. P. (1997). Analyst, 122, 89R–100R.

[206] Tessier, A., Campbell, P. G. C., and Bisson, M. (1979). Anal. Chem., 51, 844.

[207] Lopez-Sanchez, J. F., Sahuquillo, A., Rauret, G., Lachica, M., Barahona, E., Gomez, A., Ure, A. M., Muntau, H., and Quevauvillier, Ph., (2002). Extraction Procedures for Soil Analysis. In

Methodologies in Soil and Sediment Fractionation Studies – Single and Sequential Extraction Procedures. Editor: Ph. Quevauvillier. Royal Society of Chemistry, Cambridge, UK.

[208] Kramer, J. R. and Allen, H. E. (1988). Metal speciation: theory, analysis and speciation. Lewis Publishers Inc. Chelsea, MI.

[209] McBride, M. B. (1989). Surface Chemistry of Soil Minerals. *In* Minerals in Soil Environments. Editors: Dixon, J. B. and Weed, S. B. Soil Science Society of America. Madison, Wisconsin, USA.

[210] Stumm, W, and Morgan, J. J. (1995). Aquatic Chemistry - Chemical Equilibria and Rates in Natural Waters. John Wiley and Sons, Inc.

[211] McKenzie, R. M. (1989). Manganese oxides and hydroxides. *In* Minerals in Soil Environments. Editors: Dixon, J. B. and Weed, S. B. Soil Science Society of America. Madison, Wisconsin, USA.

[212] Hsu, P. H. (1989). Aluminium hydroxides and oxyhydroxides. *In* Minerals in Soil Environments. Editors: Dixon, J. B. and Weed, S. B. Soil Science Society of America. Madison, Wisconsin, USA.

[213] Di Toro, D. M., Mahony, J. D., Kirchgraber, P. R., O'Byrne, A. L., Pasquale, L. R. and Piccirill, D. C. (1986). Environ. Sci. Tech., 20, 55-61.

[214] Lijzen, J. P. A., Baars, A. J., Otte, P.F., Rikken, M. G. J., Swartjes, F. A., Verbruggen, E. M. J., and van Wezel, A. P. (2001). Technical evaluation of the intervention values for soil/sediment and groundwater – Human and ecotoxicological risk assessment and derivation of risk limits for soil, aquatic sediment and groundwater. National Institute of Public Health and the Environment. RIVM report 711701 023.

[215] Schwtermann, U. and Taylor, R. M. (1989). Iron Oxides. *In* Minerals in Soil Environments. Editors: Dixon, J. B. and Weed, S. B. Soil Science Society of America. Madison, Wisconsin, USA.

[216] Quevauvillier, Ph. (ed.) (2002). In Methodologies in Soil and Sediment Fractionation Studies. Single and Sequential Extraction Procedures. Royal Society of Chemistry, Cambridge, UK.

[217] Chang, E., Page, A. L., Warneke, J. E., and Grugerevic, E. (1984). J. Environ. Qual. 13, 33.

[218] Rigol, A., Vidal, M., and Rauret, G. (1996). J. Radioanal. Nucl. Chem. 208, 617.

[219] Houba, V. J.G., Lexmond, Th. M., Novozamsky, I., and Van der Lee, J. J. (1996). The Sci. Total Environ. 178, 21.

[220] Novozamsky, I., Lexmond, T. M., and Houba, V. J. G. (1993). Int. J. Environ. Anal. Chem., 51, 47.

[222] Foster, R. L., and Lott, P. F. (1980). Environ. Sci. Tech., 14, 1240-1244.

[223] Clevenger, T. E., Saiwan, and Koirtyoham, S. R. (1991). Environ. Sci. Tech., 25, 1128-1133.

[224] Emerson, R. H.C. , Birkett, J. V., Scrimshaw, M. and Lester, J. N. (2000). The Sci. Tot. Environ. 254, 75.

[225] Williams, L. E., Pittman, J. K., and Hall, J. L. (2000). Biochimica et Biophysica Acta, 1465, 104-126.

[226] (a) Ostberg, T. (1995). The origins of metal ions occurring in living systems. In: Berthon G (ed.). Handbook of Metal Ligand Interactions in Biological fluids. New York: Marcel Dekker, 10-28.
(b) Rojas-Chapana, J. A.and Tributsch, H. (2000). Process Biochemistry, 35, 815-824.
(c) Bae, W., and Mehra, R. K. (1997). J. Inorg. Biochem. 68, 201-210.

[227](a) I. Maiz (1997). The Sci. Tot. Environ., 206, 107.

(b) Oven, M, Grill, E., Golan-Goldhirsh, A., Kutchan, T. M., Zenk, M.H.(2002). Phytochemistry, 60, 467-474.
(c) Williams, L. E., Pittman, J. K., Hall, J. L. (2002). Biochimica et Biophysica Acta, 1465, 104-126.

[228] Templeton, A. S., Trainor, T. P., Spormann, A. M., Newville, M., Sutton, S. R., Dohnalkova, A., Gorby, Y., and Brown, G. (2003). Environ. Sci. Technol. 37, 300-307.

[229] Oven, M, Grill, E., Golan-Goldhirsh, A., Kutchan, T. M., and Zenk, M.H. (2003). Phytochemistry, 60, 467-474.

[230] Williams, L. E., Pittman, J. K., and Hall, J. L. (2003). Biochimica et Biophysica Acta, 1465, 104-126.

[231] Bae, W., and Mehra, R. K. (1999). J. Inorg. Biochem. 82, 451-462.

[232] Jocelyn, P.C. (1972). Biochemistry of the SH group. The occurrence, chemical properties, metabolism and biological function of thiols and disulphides. Academic Press, London and New York.

[233] Ostberg, T. (1995). The origins of metal ions occurring in living systems. In: Berthon G (ed.). Handbook of Metal Ligand Interactions in Biological fluids. New York: Marcel Dekker, 10-28.

[234] Rojas-Chapana, J. A., and Tributsch, H. (2000). Process Biochemistry, 35, 815-824.

[235] Cheng, T-C., and Hong, A. (1995). J. Hazardous Materials, 41, 147.

[236] Linn, J. H., and Elliott, H. A. (1988). Water, Air and Soil Pollution, 51, 844.

[237] (a) Elliott, H. A., and Brown, G. A. (1989). Water, Air, and Soil Pollution, 62, 157.

(b) Yu, J., and Klarup, D. (1994). Water, Air, and Soil Pollution, 75, 205.

[238] Slavek, J. and Pickering, W. F. (1985). Water, Air and Soil Pollution, 28, 151.

[239] Rojas-Chapana, J. A., and Tributsch, H. (2002). Process Biochemistry, 47, 164-172.

[240] Simkiss, K., and Taylor, M. G. (2001). J. Environmental Monitoring, 3, 15-21.

[241] Cotter-Howells JD, Champness PE, and Charnock JM (1999) Mineral. Mag. 63: 777-789.

[242] Nunan N, Ritz K, Crabb D, Harris K, Wu K, Crawford JW, and Young IM (2001) FEMS Microbiology Ecology 36: 67-77.

[243] Axelsen, K. B., and Palmgren, M. G. (1998). J. Mol. Evol. 84-101.

[244] Clarkson, D. T., and Luttge, U. (1989). Prog. Bot. 51, 93-112.

[245] Meharg, A. A. (1994). Plant Cell Environ., 17, 989-993.

[246] Harris K, Young IM, Gilligan CA, Otten W, and Ritz K (2003) FEMS Microbiology Ecology 44, 45-56.

[247] Keasling, J. D., Van Dien, S. J., and Pramanik, J. (1998). Biotechnol. Bioeng. 58, 231-239.

[248]Sahi, S. V., Bryant, N. L., Sharma, N. C., and Singh, S. R. (2002). Environ. Sci. Tech., 36, 4676-4680.

[249] van der Marel, H.W. and Beutelspacher, H.(1976). In collaboration with E. Rietz and P. Krohme. Atlas of infrared spectroscopy of clay minerals and their admixtures. Amsterdam , Oxford (etc.) : Elsevier.

[250] Paquin, P. R., Gorusch, J. W., Apte, S., Batley, G. E., Bowles, K. C., Campbell, P. G. C., Delos, C. G., Di Toro, D. M., Dwyer, R. L., Galvez, F., Gensemer, R. W., Goss, G. G., and Wu, K. B. (2002). The biotic ligand model: a historical overview. Comparative Biochemistry and Physiology, Part C, 3-35.

[251] Slaveykova, V. I., and Wilkinson, K. J., (2003). Environ. Sci. Tech. 36, 969-975.

[252] Bianchini, A., and Bowles, K. C. (2002). Comparative Biochemistry and Physiology Part C 133, 51-64.

[253] (a) Epstein A.L., C.D. Gussman, M.J. Blaylock, U. Yermiyahu, J.W. Huang, Y. Kapulnik and C.S. Orser. (1999). Plant Soil 208, 87–94.
(b) Chen, H., and Cutright, T. (2001). Chemosphere, 45, 21-28.
(c) Romken, P., Bouwman, L., Hapenga, J. and Draaisma, C. (2002). Environmental Pollution, 116, 109-121.
(d) Meyer, J.S., Santore, R.C., Bobitt, J.P., DeBrey, L.D., Boese, C.J., Paquin, P.R., Allen, H.E., Bergman, H.J., and DiToro, D.M. (1999). Environ. Sci. Tech. 33, 913-916.

[255] Kedziorek, M.A.M., and Bourg, A. C. M.. (2000). J. Contaminant Hydrology, 40, 381-392.

[256] (a) Brust, M., and Kiely, C. J. (2002). Colloids and Surfaces A: Physicochemical and Engineering Aspects, 202, 175-186.
(b) Wohltjen, H., and Snow, A.W. (1998). Anal. Chem. 70, 2856.
(c) Evans, S.D., Johnson, S.R., Cheng, Y.L., Shen, Y.L., and Shen, T. (2000). J. Mater. Chem., 10, 183.
(d) Pasquato, L., Rancan, F., Scrimin, P., Mancin, F., and Frigeri, C. (2000). Chem. Commun. 2253 - 2259.

[257] Nakamoto, M., Yamamoto, M., and Fukusumi, M. (2002). Chem. Comm.,1622-1623.

[258] Mukherjee, P., Ahmad, A., Mandal, D., Senapati, S., Sainkar, S., Khan, M.I., Parischa, R., Ajaykumar, P.V., Alam, M., Kumar, R., and Sastry, M. (2001). Nano Letters, 10, 515-519.

[259]Gardea-Torresdey, J.L., Parsons, J.G., Gomez, E., Peralta-Videa, J., Troiani, H.E., Santiago, P., and Jose Yacaman, M. (2002). Nano Letters, 2, 397-401.

[260]Raksasataya, M.; Langdon, A. G. and Kim, N. D. (1996). Anal. Chim. Acta., 332, 1-7.

[261]Ho, M. D., and Evans, G. J. (2000). Environ. Sci. Tech. 34, 1030-1035.

[262]Sorensen, M. A., Koch, C. B., Stackpoole, M. M., Bordia, R. K., Benjamin, M. M., and Christensen, T. H. (2000). Environ. Sci. Technol. 34, 4620-4627

[263]Chernyshova, I. V., Rao, K. H., Vidyadhar, A., and Shchukarev, A. V. (2001). Langmuir. 17, 775-785.

[264]Van Herck, P., Vandecasteele, C., Swennen, R., and Mortier, R. (2000). Environ. Sci. Tech. 34, 380, 3802-3808.

[265]Kim, C. S., Bloom, N. S., Rytuba, J. J. and Brown, G. E. (2003). Environ. Sci. Tech. 37, 5102-5108.

[266]Cao, X., Ma, C. Q., Chen, M., Singh, S. S., and Harris, W. G. (2002). Environ. Sci. Tech. 36, 5296-5304.

[267]Calamano W., Mangold, S., and Welter, E. (2001). Fresenius J. Anal. Chem., 371, 6, 823-880.

[268]Um, W., and Papelis, C. (2004). Environ. Sci. Tech., 38, 496-502.

[269] McBride, M. B. (1989). Surface Chemistry of Soil Minerals. *In* Minerals in Soil Environments. Editors: Dixon, J. B. and Weed, S. B. Soil Science Society of America. Madison, Wisconsin, USA.

[270] Bunn, R. A., Magelky, R. D., Ryan, J. N., Elimelech, M. (2002) Environ. Sci. Tech. 36, 314-322.

[271] Windholz, M., Budavari, S., Blumetti, R. F., and Otterbein, E. S. (eds.). (1983). In The Merck Index – An Encyclopaedia of Chemicals, Drugs and Biologicals. 10th Edition. Merck & Co., Inc. Rahway, N. J., U. S. A.

[272]Ahnstrom, Z. A. S. and Parker, D. (2001). Environ. Sci. Tech. 35, 121-126.

[273](a) Morel, F. M. M. (1984). Principles of Aquatic Chemistry; John Wiley: New York.
(b) Playle, R. C. (1998). The Sci. Total Environ. 219, 147.

[274] Sarret, G., Vangrovsveld, J., Manceau, A., Musso, M., Haen, J. D., Menthonnex, J., and Hazemann, J. L. (2001). Environ. Sci. Tech., 35, 2854-2859.

[275] Fendler, J. H. (Ed.). (1997). Nanoparticles and Nanostructured Films – Preparation, Characterization and Applications. Wiley-VCH.

Appendix 1

Maps of the Totley and Old Hay Areas

Figure 1: Historical Map of the Old Hay Area, 1891 (1:10,000).

Figure 2: Historical Map of the Old Hay Area, 1891 (not to scale) with sampling locations C1, C2 and B1 marked.

Figure 3: Current Map of the Old Hay Area, 2004 (1:50,000) with sampling locations C1, C2 and B1 marked.

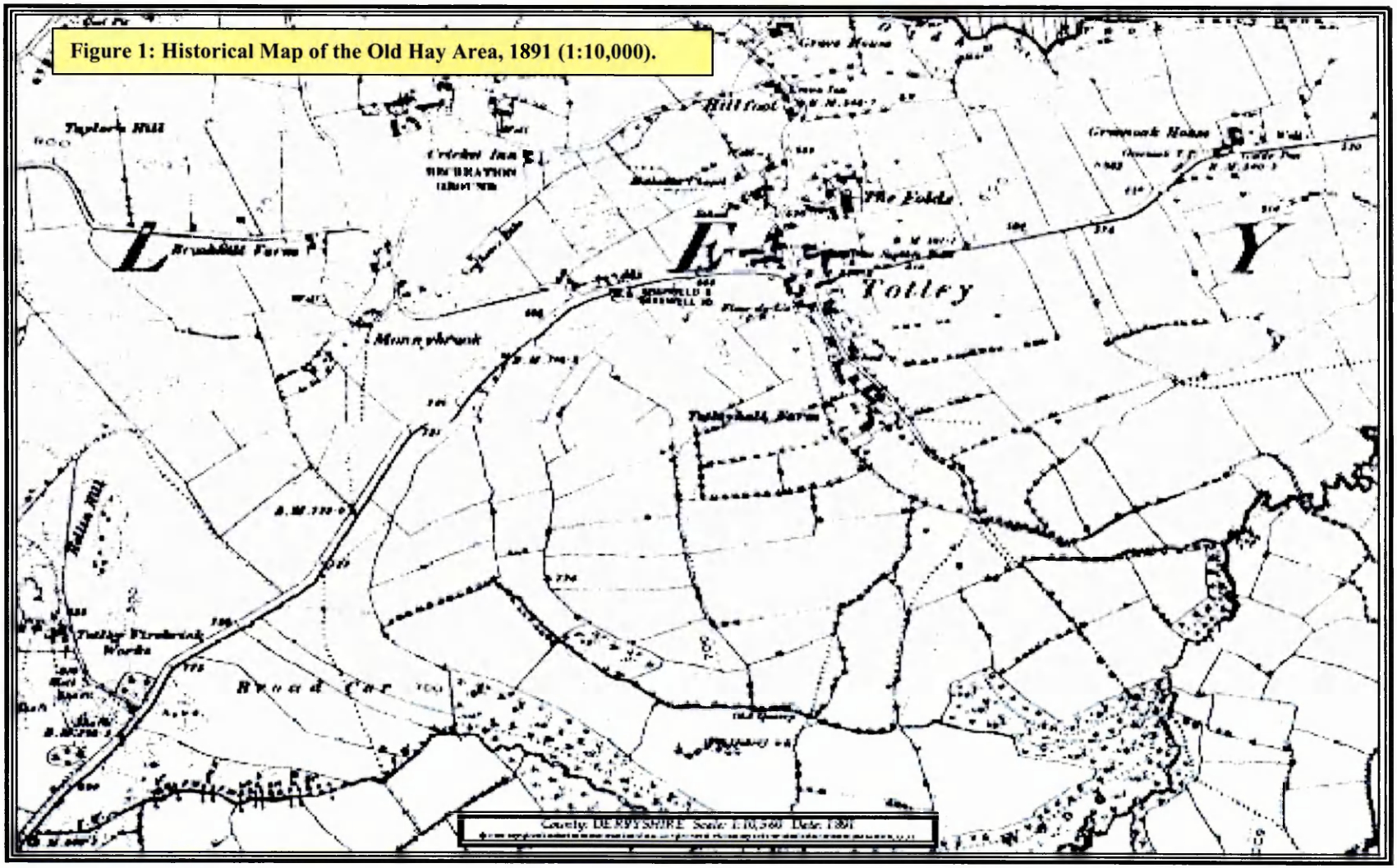

Figure 1: Historical Map of the Old Hay Area, 1891 (1:10,000).

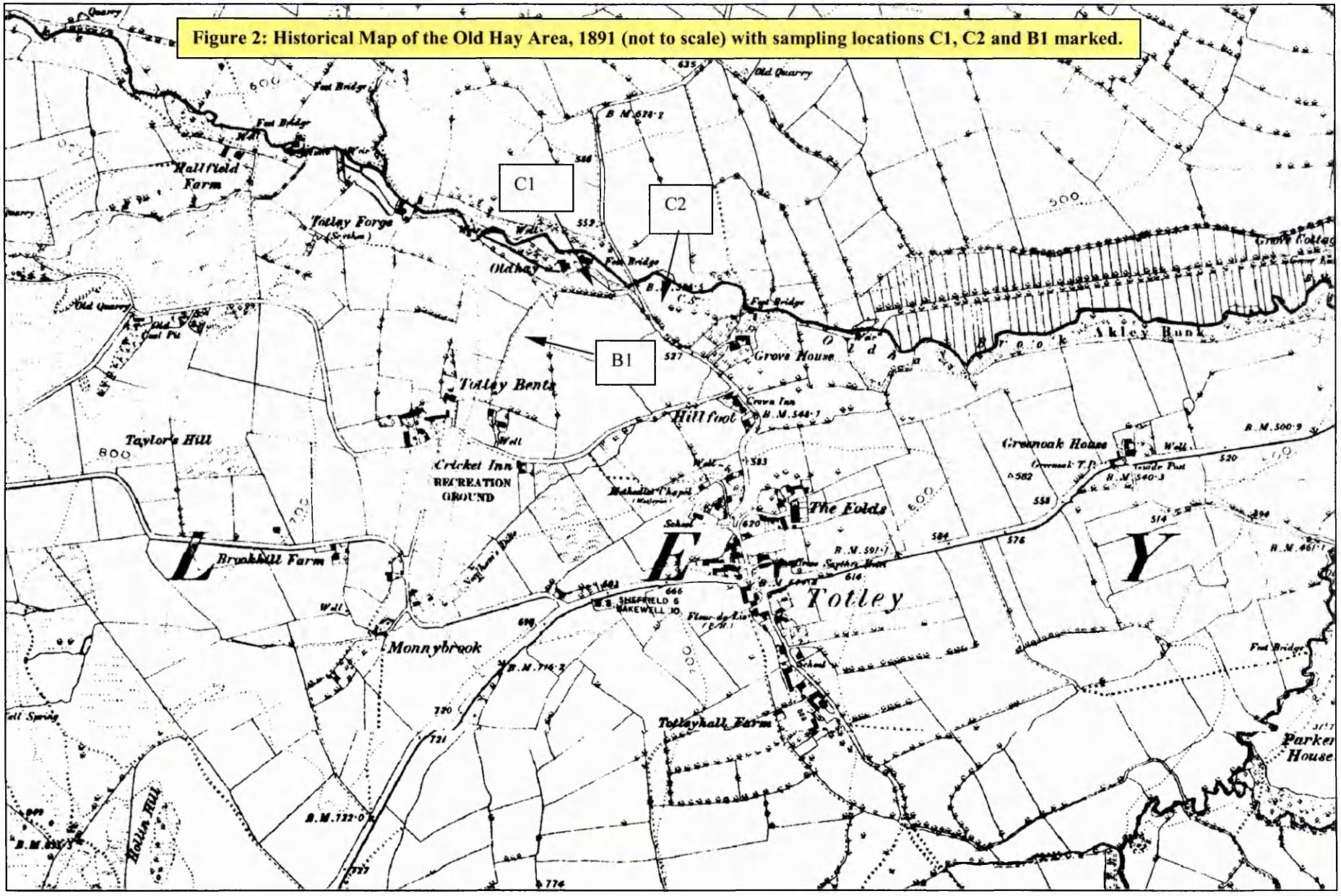

Figure 2: Historical Map of the Old Hay Area, 1891 (not to scale) with sampling locations C1, C2 and B1 marked.

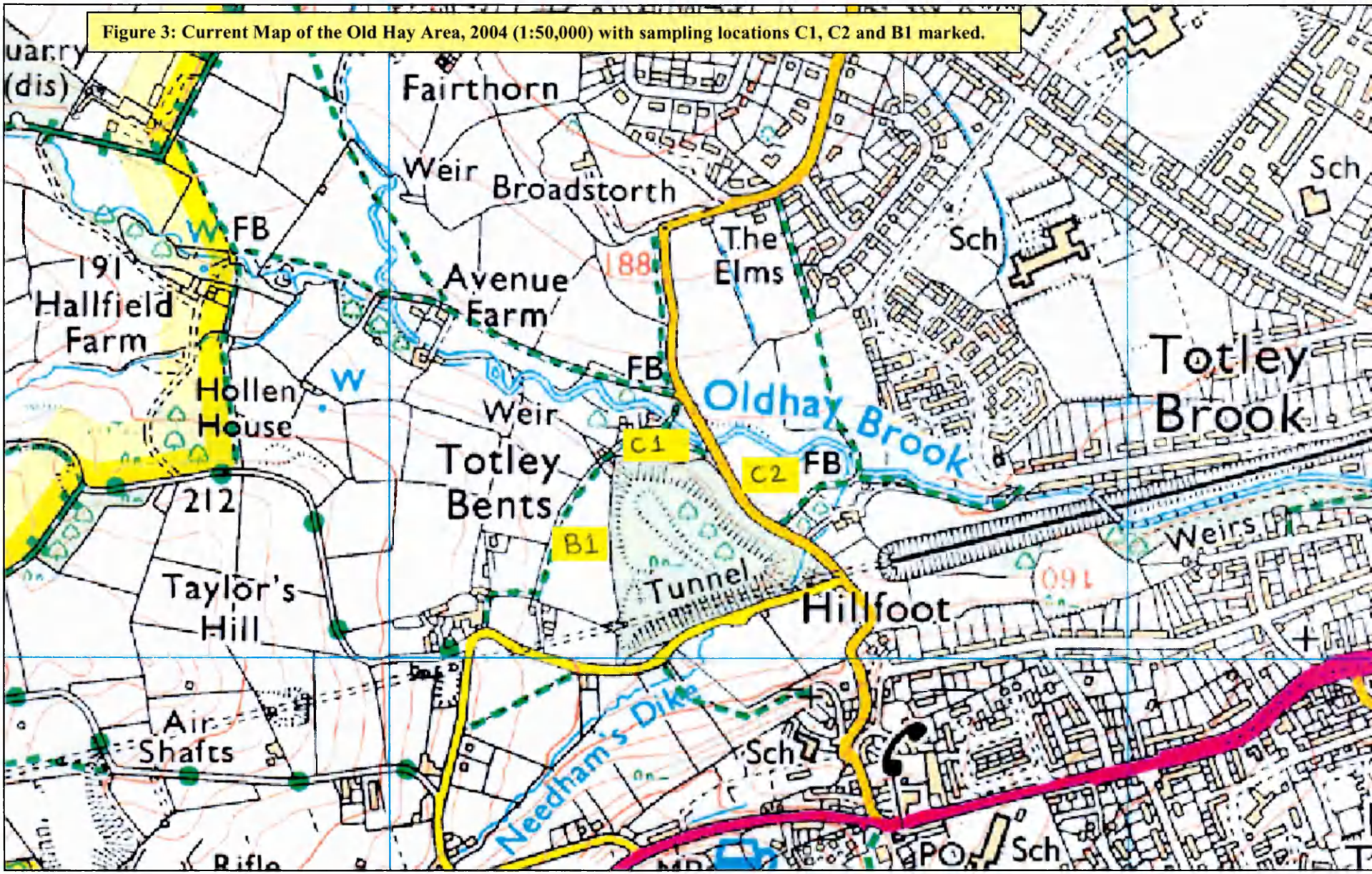

Figure 3: Current Map of the Old Hay Area, 2004 (1:50,000) with sampling locations C1, C2 and B1 marked.